Melting and Aggregation Behaviour of Novel Bio-Compatible Anionic, Cationic and Catanionic Surfactant Systems

Dissertation Presented for the Degree of Doctor of Natural Science

(Dr. rer. nat.)

University of Regensburg

Natural Science Faculty IV

Chemistry and Pharmacy

Eva Maurer

Regensburg 2011

Official Registration: 01.03.2011

Defense: 24.03.2011

Ph.D. Supervisor: Prof. Dr. Werner Kunz

Adjudicators: Prof. Dr. Werner Kunz

Prof. Dr. Thomas Zemb

Prof. Dr. Joachim Wegener

Chair: Prof. em. Dr. Dr. h. c. Josef Barthel

For Peter, my succour for so many years,

now!

Preface

The work described in this PhD thesis has been carried out at the Institute of Physical and Theoretical Chemistry at the Faculty of Chemistry and Pharmacy, University of Regensburg, between October 2006 and December 2010 under the supervision of Prof. Dr. W. Kunz.

Acknowledgements

Many thanks to all staff members for the pleasant atmosphere at the institute. I particularly appreciate the gummy bears of W. Simon, the good-morning-chat with R. Röhrl and S. Beutler and the relaxing and amusing atmosphere at the coffee club during lunch break. It was a nice contrast program to the scientific, "intellectual" work. Thanks to my lab-mate S. Dengler for bridging boring and frustrating hours with an open ear.

Apart from that I am grateful to S. Berzl for her friendship and her support. Thanks for the conductivity measurements!

Last but not least my infinite thanks to the most important persons in my life: My parents, my sister and my fiancé Peter, always giving me strength to reach my aims.

Table of Contents

I. Introduction

*Surf*ace *act*ive *agent*s (or short: surfactants) can aggregate into a multitude of microstructures, such as micelles or bilayer structures, like vesicles [1-2]. Mainly due to these properties such molecules became omnipresent in our every day life. Their potential to encapsulate hydrophobic compounds and stabilise those in an aqueous environment renders them most valuable tools in a variety of applications [3]. Nowadays, surfactants are indispensable. They stabilise and compartmentalize immiscible components in paints, varnishes or agricultural products. They are utilized in the petro-chemical industry as flotation agents [4]. Yet, they also come in much closer human contact, as they present the major components in detergents or personal care commodities [4-5]. Additionally, they even can enter the digestive system, since they are used as vehicles for active agents in galenic pharmacy [6] and cosmetic products; or as stabilizers in modern food formulations [1, 4]. The demands on surfactants systems have increased over the last decades. On the one hand, their performance should be perfectly adapted to the respective tasks. Yet, this comprises the least possible effort concerning complexity and affordable costs for the particular requirement. On the other hand, legal requirements enforce the utilization of compounds with the least possible toxic and environmental impact [7].

Therefore, two main ideas were followed within the scope of this thesis.

First, the implementation of Ionic Liquid-like properties in amphiphilic compounds was tested by exploiting the knowledge on ion affinities [8], acidities [9] and alkylchain flexibilities [10]. For that purpose, carboxylate ions of varying chainlength, with and without ether functionalities, were combined with a diversity of ammonium bases, yielding anionic, cationic or even catanionic surfactant systems. Bases were chosen with regard to their low toxicity (choline), to their accustomed utilisation in common processes (triethanolamine, long-chain primary amines) [11] or to their improvable performance in concrete applications (Lidocaine) [12]. The synthesised compounds were characterised with respect to their potential Ionic Liquid - and surfactant-features. Concretely, melting, thermal stability and partially

conductivity were evaluated. Likewise, the aggregation and the solution behaviour in diluted and concentrated mixtures with water were deduced.

The second main idea was the design of low toxic catanionic surfactant systems. This aim was tried to be accomplished in two steps:

- First, low toxic cationic surfactants with natural osmolyte headgroups, such as choline [13] and ectoine [14], were synthesised and characterized according to their physico-chemical, cytotoxic and biodegradation features.

- Second, these surfactants were combined with long-chain- and alkylether carboxylates with known/or approved biocompatibility [15].

Adjacently, the resulting mixtures were investigated with respect to their aggregation behaviour in dilute aqueous solution and their potential to form vesicles – one of the most used carrier systems for pharmaceutically active agents. Further, their efficiency to stabilise emulsions according to the Pickering mechanism [16-17] was elucidated.

The present thesis comprises a variety of studies ranging from Ionic Liquid features to aggregation behaviour of surfactants and cyto toxicity studies. For this reason, the thesis was subdivided into chapters, which follow the conventional layout: Introduction, materials and methods, results and discussion and finally conclusion. The bibliography is given at the end. A list of scientific contributions is given in the appendix.

II. Fundamentals

II.1 Ionic Liquids

For centuries, most of the scientific understanding of chemistry has been based upon the behaviour of molecules (and salts) in the solution phase in molecular solvents. A while ago, however, a new class of solvent has emerged – Ionic Liquids (ILs). These solvents are often fluid at room temperature, and consist entirely of ionic species. They have many fascinating properties because of which they are of fundamental interest to all chemists.

Over the years, the field of Ionic Liquids has been reviewed by several authors, including Welton [18], Holbrey [19], and Seddon [20]. The first room-temperature Ionic Liquid $[EtNH_3^+][NO_3^-]$ (melting point. 12 °C) was discovered in 1914 [21], but interest did not develop until the discoveries of Hurley and Wier twenty years later. They reported the properties of these mixtures as bath solutions for electroplating of aluminium [22]. However, systems composed of organic chloride salts and $AlCl_3$ were not studied further until 1968. Osteryoung and Wilkes then reported, room temperature liquid chloroaluminate melts for the first time [23-24]. Ionic Liquid research was mainly focused on electrochemical applications. In the early 1980s, the workgroups of Seddon and Hussey began to use chloroaluminate melts as non-aqueous, polar solvents for transition metal complexes [25-26]. However the Ionic Liquids used at that time persisted to be highly water sensitive. In this context Wilkes *et al.* described in 1992 the synthesis of ILs, incorporating the 1,3-dialkyl imidazolium cation and the tetrafluoroborate anion with significantly reduced instability against hydrolysis [27]. These molten salts were not only more stable against water but also a variety of functional groups that showed high reactivity with the former

chloroaluminate salts. Research in the field of Ionic Liquids as solvent substituents or reaction media began. A few years later, the investigation of long-chain Ionic Liquids in binary mixtures with water started and hence first publications discussing their super-structuring and their surfactant properties were released [28-30].

In recent years, the interests in Ionic Liquids are manifold. One focus is the exploration of the possible applications of Ionic Liquids, ranging from reaction media for nano-particle synthesis [31] to lubrication [32]. On the other hand the potential toxicity of these substances has been elicited in diverse approaches starting from bacteria constraining tests and ending with viability tests on cells and even higher organisms[33]. These results accelerated research in the synthesis of new low toxic Ionic Liquids [34].

II.1.1 General Aspects

Ionic liquids can be categorized in three main groups, namely simple salts (made of a single anion and cation), protic and binary Ionic Liquids (salts where an equilibrium is involved).Whereas, for example, 1,3-dialkylimidazolium chlorides are simple salts, $[EtNH_3][NO_3]$, a protic IL, and mixtures of aluminum(III) chloride and 1,3-dialkylimidazolium chlorides (a binary Ionic Liquid system) contain several different ionic and neutral species and their melting point and properties depend upon the mole fractions of the components present.

Nowadays, the most commonly used ions in recent Ionic Liquid research are based on imidazolium, ammonium, pyridinium, pyrrolidinium and phosphonium, combined with anions varying from simple halides to organic counterions like acetate (Table II-1).
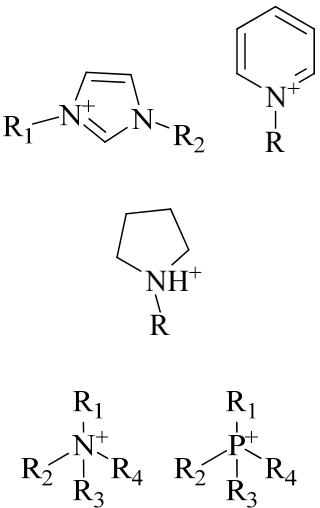
In general, Ionic Liquids are salts where one or both of the ions are large, and the cation has a low degree of symmetry [18, 35-37]. These factors tend to reduce the lattice energy of the crystalline form of the salt *E*, and hence lower the melting point which is described in Equation II-1.

$$E = M \cdot \frac{z^+ \cdot z^-}{d_{sep}}$$
II-1

Where M is the Madelung constant reflecting the packing efficiency, z^+ and z^- are the charges of the ions, and d_{sep} is the inter-ionic separation. With increasing ion-radii of cation and anion d_{sep} becomes effectively larger resulting in a smaller lattice energy and therefore in a lower melting point. Hence, lattice energy and with that melting points are low with single charged, big ions[38]. Table II-2 summarizes the melting points of Ionic Liquids with different ion diameter.
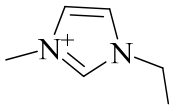
Table II-1: Classical cations and anions for Ionic Liquids.

Cations	*Anions*
	BF_4^-, PF_6^-, $EtSO_4^-$, Cl^-, Br^-, I^-, NO_3^-, CO_3^{2-}, SO_4^{2-}, CH_3COO^-, CF_3COO^-, $CF_3SO_3^-$, $(CN)_2N^-$, $(CF_3SO_2)_2N^-$

Furthermore the symmetry as well as the charge delocalisation within the ions strongly influences the melting behaviour. While fusion starts at 125 °C in case of 1-methyl-3-methyl-imidazolium chloride, this point is reduced to 65 °C for the non-symmetric 1-butyl-3-methyl-imidazolium derivative [24]. However, if the number of carbons in the alkylchain increases further, van der Waals interactions gain impact leading to local structuring and hence a

more favoured crystalline state. Therefore, melting points of the 1-alkyl-3-methyl-imidazolium Ionic Liquids show a minimum between six and eight C-atoms in the alkylchain [39].

Table II-2: Ion size dependent melting points.

Cation	Anion	Melting point [°C]
	Cl^-	$87^{[24]}$
	NO_2^-	$55^{[27]}$
	NO_3^-	$38^{[27]}$
	$AlCl_4^-$	$7^{[40]}$
	BF_4^-	$6^{[19]}$
	$CF_3SO_2^-$	$-9^{[41]}$
	$CF_3SO_2^-$	$-14^{[41]}$
[NMe₄]	Br^-	>300
[NEt₄]	Br	284
[NBu₄]	Br^-	124 – 128
[NHex₄]	Br^-	99 – 100
[NOc₄]	Br^-	95 - 98

II.1.2 Physical and Chemical Properties

As they are made up of at least two ions, which can be varied (the anion and cation), Ionic Liquids can be designed with a particular end use in mind, possessing a particular set of properties. Hence, the term "task-specific solvents" have come into common use [42]. Their properties can be adjusted to suit the requirements of a particular process. Properties such as melting point, viscosity, density, and hydrophobicity can be varied by simple changes to the structure of the ions.

II.1.2.1 Phase Transitions and Thermal Stability

The melting point together with the decomposition temperature of Ionic Liquids defines the liquid state, *i.e.* the range of temperature within it is possible to apply the salt in its molten form. The theoretical correlation between structure and melting point has been examined in many research studies. Unfortunately, the exact experimental melting point determination of ILs yet is, very difficult, since many of them undergo super-cooling. Hence, the temperature of the phase-transitions can differ significantly depending on whether the observations take place while heating or cooling [41, 43-45]

Beside the already discussed asymmetry [44], size [40] and charge delocalization [39] of the single ions, another important characteristic having considerable influence on the melting behaviour is the potential hydrogen bond formation between the present ions. Commonly, this effect can be detected between a basic anion and an acidic cation. Hydrogen bonding is observed, *e.g.* in the case of imidazolium-ILs, when basic anions such as halides, polyhalogenated metals, fluorinated organic anions, NO_3^-, BF_4^- or PF_6^- are present. Particularly, imidazolium chlorides exhibit high melting points (between 40 and 80 °C) as they form intra-molecular networks, or layered structures[46-47]. The higher the charge density of the ions the stronger intra-molecular interactions and H-bonds can be expected. Intra-molecular H-F interactions in BF_4^- or PF_6^--ILs are considered to be very weak because of

the lower charge-densities of these types of anions in contrast to H-Cl interactions due to the localized charge at the chloride ion [48].
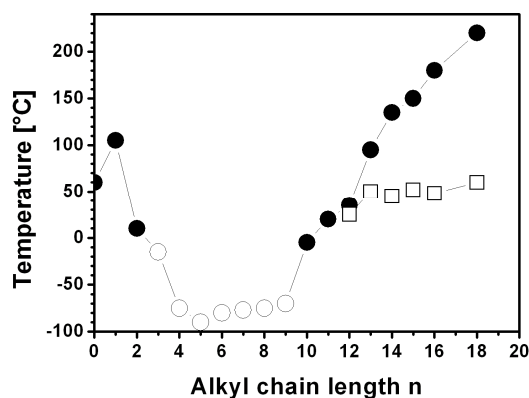
Figure II-1: Melting points of 1-alkyl-3-methylimidazolium tetrafluoroborates as a function of chainlength, showing true melting points ●, glass transitions ○, and the formation temperature of a smectic phase □ [39].

Glass formation, sometimes in addition or instead of crystal formation, is a common characteristic associated with many, but not all, of the Ionic Liquid salts. It is the result of the extremely unfavourable packing-efficiency of some ILs in the solid state. Consequently, the glass transition temperature (T_g) is found at outstandingly low temperatures, mainly below -50°C [41, 49].

Long-chain IL salts (n ≥ 10) have attracted some interest due to their thermotropic liquid crystalline (LC) state occurring below 100 °C. The origin for this characteristic can be explained by the formation of local structuring where the ionic headgroups interact with the counterions by means of Coulombic forces. Thus, layers are built from (anti) parallel stacking of the long alkyl-chains through van-der-Waals attraction. The melting to isotropic liquids usually occurs at rather high temperatures (Figure II-1) [19, 43].

The average thermal stability of Ionic Liquids is higher than 300 °C. The constricting points of the IL stability are the H-bonds and the covalent hetero-atom carbon bonds. Usually, the decomposition temperature of protic ILs is

much lower than that of simple salts, due to the tendency of protic Ionic Liquids to deprotonate at elevated temperatures (between 200 °C and 300 °C) [50-51]. Hence, these ILs easily evaporate. Further, protic ILs having carboxylate anions and ammonium cations tend to form amides through condensation reaction (Reaction II-1), especially at higher temperatures. Therefore, salts with these anions exhibit only low thermal stabilities [52].

$$R\text{-}NH3 + R'\text{-}COO\text{-} \quad \longrightarrow \quad R\text{-}NH\text{-}OCH\text{-}R' + H2O$$

Reaction II-1

In contrast, simple salt Ionic Liquids provide high decomposition temperatures, in special cases up to 450 °C. However, such ILs with long alkyl-chains in the cations are vulnerable to elimination and therefore show significantly lower decomposition temperatures (between 150 to 300 °C) [39]. The thermal stability of simple salts is also affected by the type of the anion. Relative anion stabilities have been suggested as $PF_6^- > (CF_3SO_2)_2N^- (= Tf_2N^-)$ ~ $BF_4^- >$ halides. In general, the temperature stability is higher when weak coordinating anions are used [19, 41, 44].

II.1.2.2 Viscosity

The viscosity of Ionic Liquids is essentially determined by their tendency to form hydrogen bonds and by the strength of their van-der-Waals interactions. The ability of hydrogen bond formation is mostly influenced by the present anions. Low viscosities are usually obtained by using large fluorinated asymmetric anions with good charge delocalization and by a weakening of the hydrogen bonds. Therefore, the viscosity decreases in the order $Cl^- > PF_6^-$ $> BF_4^- > Tf_2N^-$

Another factor considered to affect the viscosity is the structure of the cation: Cations substituted by long alkylchains show higher viscosities caused by

stronger van-der-Waals interactions [41, 53]. Values for some common ILs are given in Table II-3.

The temperature dependence of the viscosity can often be expressed by the empiric Vogel-Fulcher-Tammann Equation (Equation II-2) which describes the viscosity decrease of a liquid (fundamentally, of a glass forming liquid) with increasing temperature [54].

$$\eta = \eta^0 \cdot \exp\left(\frac{B}{T - T^0}\right) \qquad \qquad \textbf{II-2}$$

In Equation II-2, η is the viscosity at a given temperature T in K, η^0, B^0 and T^0 are fitting parameters depending on the investigated system.

Table II-3: Viscosities of common Ionic Liquids.

Cation	Anion	Viscosity at 298K [cP] [39]
$EMIM^+$	BF_4^-	41
$BMIM^+$	BF_4^-	115
$BMIM^+$	CH_3COO^-	440
$BMIM^+$	I^-	1110
$BMIM^+$	Cl^-	40890 (293K)
$OMIM^+$	BF_4^-	439
$OMIM^+$	Cl^-	33070
$(CH_3)_2(C_2H_5)(CH_3OC_2H_4)N^+$	BF_4^-	135
$(CH_3)_3S^+$	HBr^-	20.5

Shear-rate dependent measurements of the viscosity show that ILs can be classified in terms of being Newtonian-, whose viscosities remain constant with increasing shear rate, or pseudo-plastic-fluids, whose viscosities decrease as the shear rate increases

Only a few Ionic Liquids reach viscosities in the order of magnitude of water or the most common organic solvents. Usually, their values can be compared with those of paraffin oils [9]. In many cases their viscosities thwart a variety of applications. For example, a high viscosity may lead to a reduction in the rate of many organic reactions or in the diffusion of redox species [55].

It should be noted that present impurities remaining from the synthesis influence viscosity drastically. A viscosity reduction in the case of remaining solvents is observed, whereas a viscosity increase in the case of halide impurities by 30 to 600 % depending on the concentration is found [56-57].

II.1.2.3 Vapour Pressure

One of the most widely known features of Ionic Liquids is their negligible vapour pressure due to their salt character. This feature is an advantage from a engineering viewpoint, since separation by distillation of a reaction mixture becomes more effective as a method of product isolation, because solvent-product azeotropic formation cannot occur [58]. However, some ILs exhibit a boiling point before decomposition upon heating and can thus be distilled. Well-known examples, in this context, are the protic derivatives. Upon supply of energy the equilibrium is shifted and a simple back-protonation of the anion reforming the original, acid, neutral species takes place. During condensation, the charged species are reformed. The requirement for the distillation of a protic Ionic Liquid is a low proton-transfer energy [49, 59]. Very few simple salt ILs can be distilled as well, but in contrast to protic ILs, rigorous conditions, very low pressure and high temperature are necessary to prevent decomposition [60].

II.1.2.4 Polarity and Solubility

Generally, Ionic Liquids can be classified as dipolar, protic or aprotic, solvents. Polarity of molecular solvents can be quantified and compared by their dielectric constant ε. As this classification is not entirely useful in case of Ionic Liquids other scales, like the assignation via sovatochromic or fluorescent dyes, find application. Established dyes in this context are Nile red (neutral dye) and Reichardt´s dye (betaine dye) [61-62]. However, each dye shows sensitivity towards special interactions, *e.g.* hydrogen bonds or polarizability. Nile red (Figure II-2) is sensitive to solvent polarizability, whereas the Reichardt´s dye (Figure II-2) reflects the solvents ability to form hydrogen bonds. For Nile red, polarity values of Ionic Liquids similar to short-chain alcohols were found. The range of the values is narrow. Depending on the chainlength of the cation, the type of anion shows, in case of longer-chains, more or less impact on the total polarity. The polarity decreases with the effective charge density of the anion and hence its size [61]. Cations synthesised from protonation in general lead to higher polarities compared to simple salt ILs, sometimes similar to water.[62].
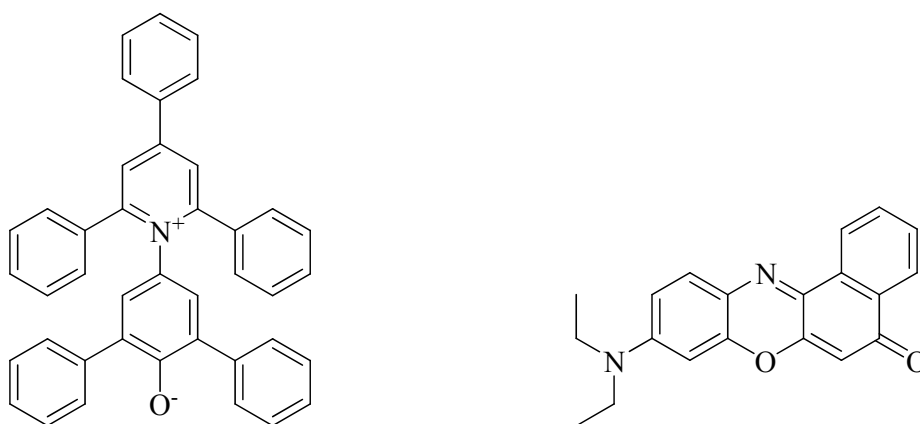
Figure II-2: Solvatochromic dyes; Reichhardt´s dye (left) and Nile red (right).

As ILs can be modified task-specifically, the polarities and thus the solvent properties can be adjusted by the cation-anion combination. A stepwise variation from hydrophilic to hydrophobic is possible which enables the solubilisation of either polar or non-polar substances [58]. Thus, *e.g.* the solubility of water in Ionic Liquids or the other way round changes with structure. For example, 1-alkyl-3-methylimidazolium tetrafluoroborate salts are miscible with water at 25 °C where the alkylchainlength is less than six, but at or above six carbon atoms, they form a separate phase when mixed with water. This behaviour can be of substantial benefit when carrying out solvent extractions or product separations [55].

II.1.2.5 Surface Tension

In general, liquid/gas surface tensions of ILs are slightly higher than those found for conventional solvents, but still lower than that of water. The surface tension is a measure of the cohesion force of liquids, and depends on the liquid structure and orientation. Structural changes on the cat- or the anion show similar impact on the surface tension [52, 63-64]. Usually both ions are present at the surface and hence affect the surface tension [65-66]. Cations with long alkylchains increase the amount of hydrocarbons situated at the surface, and therefore decrease the surface tension. In contrast, the exchange of the anions with larger derivatives causes high surface tension values. This suggests that as the anion radius is increased, the cations are pushed further apart, and the surface tension increases due to the reduction in the amount of hydrocarbon present at the liquid/ gas interface [64]. Hence, the surface tension of ILs is strongly connected to length and packing efficiency of the hydrocarbons of the ILs at the surface [52].

Long-chain ILs consist of a charged hydrophilic headgroup and one or more hydrophobic tails. Due to their structure and inherent charge, they can self-assemble not only in pure form leading to the formation of thermotropic liquid crystals, but also in binary mixtures with water. Hence, long-chain ILs resemble conventional surfactants and can form aggregates [28]. It was found

that the cmc values of long-chain imidazolium based ILs were lower than those of typical cationic surfactants, the alkyltrimethylammonium bromides. These results demonstrated that the surface activity of the long-chain imidazolium ILs is somewhat superior to that of conventional ionic surfactants and might be explained by a favoured packing and a higher hydrophobicity of the planar aromatic headgroup [29-30, 67].

II.1.3 Toxicity and Biological Activity

Ionic Liquids have been widely promoted as "green solvents" over the last decades. Mainly two major facts are the basis of that argumentation [68]:

Generally, their vapour pressure can be neglected, and thus inhalative exposure of workers is reduced as compared to conventional molecular solvents. Thus, no volatile organic compounds (VOCs) can be emitted.

They are claimed to be relatively non-toxic. Only a few Ionic Liquids have found their application in industry in large scale, as barely toxicity data are available. During the last three years more and more investigations attending this topic have been made, starting with viability tests of bacteria and ending with higher organisms like sweet water snails[69-71]. Toxicity standards reported in literature are mainly comparisons to commonly used molecular solvents such as tert-butyl ether (MTBE), tetrahydrofuran (THF), dichlormethane (CH_2Cl_2), Methanol (MeOH) and acetonitrile (AN). Another set of reference substances that are not always functionally analogous to ILs, but have structural analogies, are ionic surfactants including mostly cationic but also anionic ones. In summary, Ionic Liquids are often compared to organic solvents and ionic surfactants regarding five risk indicators: (i) release, (ii) spatiotemporal range, (iii) bioaccumulation, (iv) biological activity and (v) uncertainty. The structural variability of Ionic Liquids provides substances that have a low risk regarding each of the five risk indicators. However, the Ionic Liquids commonly used to date in applications (especially the imidazolium-ILs) are toxic in nature, which has been proven

by various toxicological data collections [72]. Several studies have been published trying to relate the structure of ILs with their biological action leading to the assumption of higher toxicity with rising overall hydrophobic character [69, 73-76]. For this reason, the term "green solvents" is a varnished sight often given by chemists and engineers who work in the field of Ionic Liquids as these substances indeed are not completely harmless for the environment.[72]. Ionic Liquids are described as designer solvents. Thus, a huge variety of ions is available to adjust the toxicological impact [77], while other properties can be kept. Recent investigations focused on this topic offering solutions with Ionic Liquids basing on compounds with biological origin, like choline carboxylates [34].

II.1.4 Applications

Ionic Liquids are predominantly considered as substitutes of organic solvents for industrial applications. The reasons for such interest in this area are due to several factors:

- synthetic chemists are limited by the available molecular solvents in which they can conduct chemistry;

- the solvents chemists like to use are increasingly banned by international protocols determined to reduce pollution, of which volatile organic compounds represent a significant part; and

- the prospect of discovering new chemistry or the ability to design a solvent that facilitates a specific reaction;

- Ionic Liquids not only offer new opportunities of performing known reactions, but can even be tailored to meet specific synthetic needs [39, 55].

Table II-4: Different features of organic solvents and Ionic Liquids.

Feature	Organic solvents	Ionic Liquids
Number of solvents	> 1000	> 1000000
Cost	Normally cheap	Normally 2 to 100 times of organic solvents
Tune ability	Limited range of solvents available	Virtually unlimited
Polarity	Conventional polarity concepts apply	Polarity concept questionable
Vapour pressure	Obey Clausius-Clapeyron Equation	Usually negligible vapour pressure
Catalytic ability	Rare	Common and tuneable
Solvation	Weakly solvating	Strongly solvating
Flammability	Usually flammable	Usually non-flammable
Applicability	Single function	Multifunction
Recyclability	Green imperative	Economic imperative
Viscosity [cP	0.2 – 100	22 – 40000
Density [g/cm^3]	0.6 – 1.7	0.8 – 3.3
Refractive index	1.3 – 1.6	1.5 – 2.2

Table II-4 shows the main differences of ILs and organic solvents. Beside the usage of ILs as solvents for organic reactions, the application as electrolytes in lithium batteries [78], in electroplating processes [79], and solar cells [80] reflects the applicability in electrochemistry. Great efforts have also been made utilizing Ionic Liquids as solvents for biopolymers. Especially, cellulose, presenting one of the most important bio-renewable resource, can be dissolved up to high concentrations (25 wt.%), which is not possible in conventional solvents [81].

Noteworthy are also the investigations of Ionic Liquids with regard to their advantages in formulation technology and in colloid science, leading to their usage *e.g.* as additives in paintings [82], templates in nano technology [83]or as innovative lubricants for steel on aluminium applications [84].

Currently, the most popular and well established example of an industrial process involving an Ionic Liquid is the BASIL™ (Biphasic Acid Scavenging utilizing Ionic Liquids) process, which was introduced by BASF AG in 2002. This process is used for the production of alkoxyphenylphospines [35].

II.2 Surfactants and Colloidal Systems

Surfactants are amphiphilic molecules. The term amphiphilic is composed of the two Greek words: "*amphi*" (both sides) and "*philia*" (love). It is used to describe molecules composed of two covalently bound parts with different affinities. The hydrophilic, water-soluble part of the surfactant is usually called the head and the hydrophobic part the tail (Figure II-3.).

hydrophobic tail   **headgroup**   **counterion**
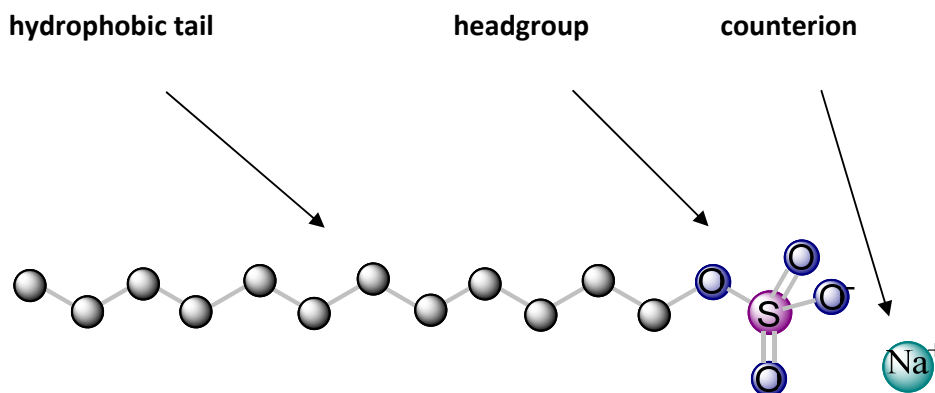
Figure II-3: Schematic representation of a charged surfactant molecule (SDS in this case).

Surfactants usually are classified depending on the charge of their headgroup, either in ionic or if uncharged, non-ionic amphiphiles. If the head is wearing a positive charge the surfactants are called cationic or respectively anionic and zwitter-ionic in case of a negative or both charges. Some common examples for the classification of surfactants are given in Table II-5 [4, 85-86].

Table II-5: Classification of surfactants [4, 85-86].

Classification	Headgroups	Examples
anionic		Alkylsulfates, Alkylcarboxylates
cationic		Alkyltrimethylammonium halogenides
zwitter-ionic		Alkylphosphatidylcholines Alkylbetaines
non-ionic		Alkylpolyethyleneglycols

II.2.1 Adsorption and Aggregation

Due to their amphiphilic character adsorption at interfaces and aggregation in various solvents are elementary features of surfactant molecules. Dissolved, the amphiphilic nature of surfactants leads to an increase of free energy, which is overcome by adsorption of the molecules at the interface or surface, respectively of the solvent and/or aggregation in the bulk. In the case of a polar solvent, the molecules arrange at the air/solvent interface by orientation of the hydrophobic alkyl-chains towards the air [4, 85-86].

For the purpose of comparing the performance of surfactants in changing interfaces, as in adsorption or aggregation, it is necessary to distinguish between the efficiency of the surfactant and its effectiveness. The efficiency describes the bulk phase concentration of surfactant required to change the interface properties by some significant amount, while effectiveness menas the maximum change of the interface property that can be observed, regardless of bulk phase concentration of the adsorbate. Usually, these two parameters are inversely proportional. In dilute surfactant solutions, the magnitude of change in any interfacial phenomenon related to the adsorption of a surfactant molecule to the surface is a function of concentration. Thus, efficiency is determined by the ratio between the surfactant concentrations at the interface and in the bulk phase [86-87]. In practice, a commonly used concept in this context is the negative logarithm of the concentration of surfactant in the bulk phase required to produce a surface tension reduction of 20 mN/m compared to the pure solvent. This concept bases on the following assumptions:

- The ideal measure of the efficiency of a surfactant at the interface is a function of the minimum concentration of amphiphile in the bulk phase necessary to produce maximum surface tension reduction.

- From investigations of surface tension as a function of *-log concentration* plots in the literature it was concluded that as soon as

the interfacial tension of the pure solvent has decreased about 20 mNm^{-1}, the surface is nearly completely saturated (85.0 – 99.9 %) and thus it can be a reference point for the comparison of surfactants concerning their efficiency.

The surface tension of a solution of a surfactant decreases steadily as the bulk concentration of surfactant is increased until the concentration reaches a nearly constant value known as the critical micelle concentration (cmc) above which the tension remains virtually unchanged. The surface tension at the cmc is therefore very close to the minimum tension that the system can achieve. Hence, it reflects a suitable measure of the ''effectiveness'' of a surfactant [4, 86, 88-89].

II.2.1.1 Adsorption Theory

The adsorption of amphiphilic molecules at the interface results in a reduction of its the free energy. The amount of component i at the interface in excess of the amount of the same species in the bulk, is the so-called surface excess concentration and can defined as:

$$\Gamma_i = \frac{n_i^z}{A} \qquad\qquad \textbf{II-3}$$

Where n_i^z is the concentration of the species i at the interface. The Gibbs concept relates the changes of interfacial energy (interfacial tension) $d\sigma_i$ to the adsorption of a species at the interface compared to the bulk composition under constant temperature and pressure as:

$$d\sigma_i = -\Sigma\Gamma_i d\mu_i \qquad\qquad \textbf{II-4}$$

with μ_i being the chemical potential of i in the bulk-phase. Hence, changes of the free energy dG of a system are given by:

$$dG = -SdT + Vdp - \sigma dA + \Sigma\mu_i dn_i \qquad\qquad \textbf{II-5}$$

Where S is the entropy, p is the pressure, V is the volume, A is the interfacial area, and T is the temperature. Under the assumption of constant conditions of T and a dilute system, as well as a clever choice of the dividing surface, so that the surface excess of the solvent is zero, the final Gibbs Equation for a two component system can be written as:

$$\Gamma_2 = -\frac{1}{RT}\frac{d\sigma}{d \ln c_2}$$
II-6

With c_2 being the molar concentration of component *2*. This Equation is true for un-charged species. In case of dissociation, the Equation has to be adjusted considering the equilibrium state of dissociation reaction and the degree of association [85-86].

II.2.1.2 Surfactant Self-Assembly

Like already mentioned, the second way to reduce free energy of a surfactant solution in a polar solvent is the formation of aggregates. The molecules arrange in clusters, so-called micelles, with their hydrophobic groups directed towards the interior and their headgroups towards the polar solvent.

Micelle formation can be explained by the "hydrophobic effect" [90-92]. This effect is triggered by two main contributions:

- The influence on the structure of water molecules (for commonly water being the solvent) around a dissolved molecule, leading to a state with less degrees of freedom.

- The energy needed to create a cavity in the solvent for the solute, which disturbs the inter-solvent cohesion forces.

Thus, the hydrophobic effect is proportional to the area between water and the apolar part of the solute[92]. Geometry dependent of the solute molecule a variety of different selfassembly structures appears, starting with simple spherical and ending in vesicular structures, which consist of surfactant

bilayers arranged in one or more concentric films (compare chapter II.2.1.2.3).

II.2.1.2.1 *Critical Micelle Concentration (cmc)*

A balance between forces promoting and those hindering micelle formation arises leading to an exactly defined concentration for each surfactant at which aggregate formation starts, the so-called critical micelle concentration (cmc). The concentration dependent aggregation behaviour of surfactants can well be monitored by measuring physical parameters of the solution, which undergo an abrupt change with micelle formation and hence indicate the cmc. For that purpose adequate physical properties and their surfactant concentration dependant developing are depicted in Figure II-4 [2, 4, 86, 88].

As the chemical structure of the amphiphile has a major impact on the cmc value. Some basic conclusions can be drawn [4, 93]:

- The cmc decreases with increasing hydrocarbon chainlength of the amphiphile. The factor of reduction is approximately two for ionic and three for non-ionic surfactants on adding one -CH_2- group to the alkylchain.

- The cmc of a non-ionic surfactant is generally lower than that of ionics with the same alkyl-chainlength.

- Cationic surfactants have slightly higher cmcs than equivalent anionics.

- In the case of ionic amphiphiles the valency as well as the polarizability of the counterion and the headgroup has a great influence.
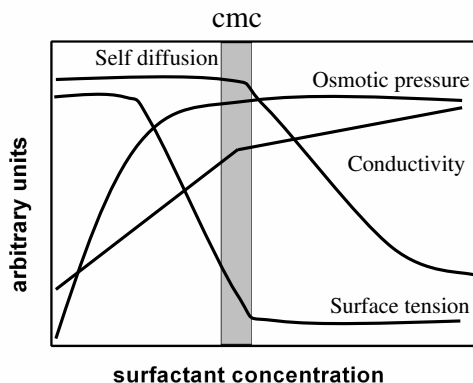
Figure II-4: Schematic developing of some concentration dependent physical properties of an amphiphile in water.

Especially the chainlength dependence of the cmc has been extensively investigated and can be expressed in the Klevens Equation [94]:

$$\log(cmc) = A - Bn \qquad \qquad \text{II-7}$$

where *A* and *B* are constants specific to the homologous surfactant series under the same micro-environmental conditions (*i.e.* temperature, pressure *etc.*) [95]. Generally, the value of *A* is approximately constant for a particular headgroup, whereas *B* is constant and approximately equal to 0.30 for all paraffin chain surfactants solubilised in water having a single-charged ionic headgroup. For a non-ionic amphiphiles *B* becomes 0.5.

II.2.1.2.2 *Solubility*

The solubility of ionic surfactants in water shows strong temperature dependence. The solubility generally is low at low temperatures and it increases rapidly in a narrow temperature range. This phenomenon is generally denoted as the "Krafft boundary" [1-2, 4, 86, 88]. In fact, the Krafft point is defined as the intersection of the solubility curve and the cmc curve (Figure II-5). In literature, the Krafft temperature is the temperature of the

Krafft boundary at an arbitrary concentration above the cmc, conventionally 1 wt% of ionic amphiphile in water.
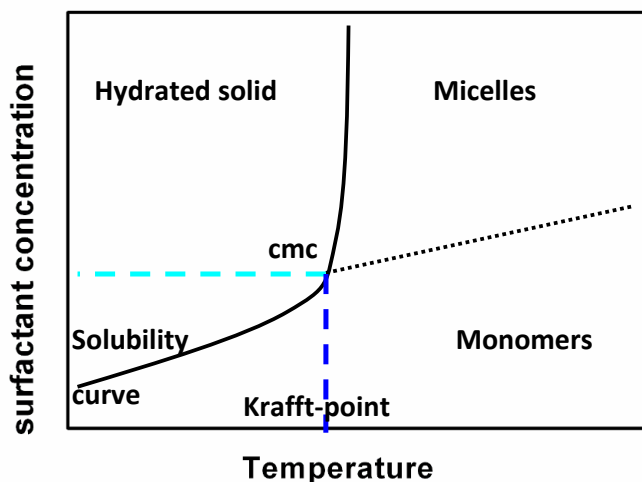
Figure II-5: Phase diagram of a surfactant at the Krafft-point region.

The Krafft point/temperature is ruled by the energetic relationship between the solid crystalline state (melting point) and the heat of hydration of the system [96]. Lower Krafft points/temperatures are generally obtained by making the packing of the surfactant in the solid state more unfavourable and by using highly hydrated polar headgroups or counterions, respectively [2, 4, 86, 97]. An unfavourable crystal packing can be achieved by an introduction of double bonds, polar segments or branching in the hydrophobic chain. In contrast to that, the increase in the linear alkylchainlength leads to higher Krafft-temperatures [98]. Resent investigations on surfactants proofed the Collins concept of "matching water affinities" [8, 99-100], which relates the solubility of salts to the size and polarizability of their ions and hence their affinity to form contact ion pairs or to dissociate in water, respectively. It was concluded, that the combination of large polarizable headgroups with the same type of counterion as well as small headgroups and counterions lead to less soluble ionic amphiphiles than the cross combination of large and small species [101].

On the other hand common non-ionic surfactants do not exhibit a lower solubility limit. Additionally to the hydration of the hydrophilic part, non-ionic amphiphilic molecules are further stabilized by the formation of hydrogen bonds between the ether units and water. The strength of these H-bonds is strongly temperature dependent and decreases with elevated temperature. Hence, non-ionic surfactants also show a characteristic temperature–solubility relationship in water that causes them to become less soluble as the temperature increases. In some cases, phase separation occurs, producing a cloudy solution of surfactant. The temperature (usually a range of temperature) at which the phases separate is referred to as the ''cloud point'' of that non-ionic surfactant [1-2, 86-87].

II.2.1.2.3   *Molecular Structure – Aggregate Correlation*

The most common structures of surfactant self assembly are:

- the spherical micelle with an interior composed of the hydrocarbon chains and a surface of polar headgroups towards the bulk water phase,

- elongated cylindrical micelles with a similar structure to that of spherical aggregates, but a highly variable length,

- bilayer structures, which are expressed in platelet like micelles, vesicles or lamellar structures and

- reverse micellar aggregates having a water core surrounded by the amphiphile headgroups and the alkylchains forming the continuous phase.

The formation of the different micellar aggregation types strongly depends on the geometry of the single amphiphile. The packing parameter P gives a measure to estimate the micelle form depending on molecular features [1-2, 86-87, 102-103].
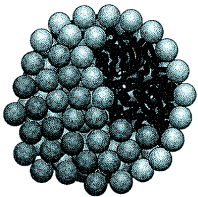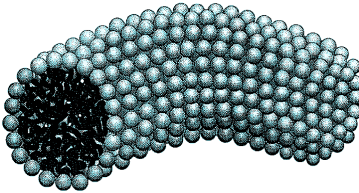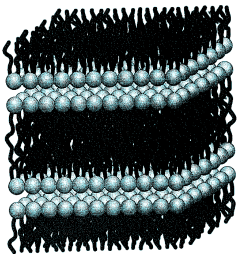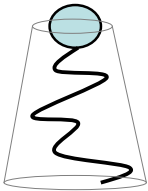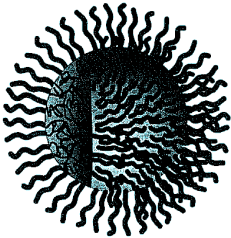
$$P = \frac{v}{al}$$
<div align="right">**II-8**</div>

where v is the volume of a single surfactant hydrocarbon chain, a is the cross-sectional area of one surfactant molecule in the aggregate, and l is the length of the fully extended hydrocarbon chain. The values of v and l can be estimated by the Equations of Tanford [104]:

$$v = 27.4 + 26.9 n_c \qquad [\text{Å}^3]$$
<div align="right">**II-9**</div>

$$l = 1.5 + 1.265 n_c \qquad [\text{Å}]$$
<div align="right">**II-10**</div>

Table II-6: Correlation between packing parameter and form of the expressed aggregate [2].

$P < \frac{1}{3}$	
$\frac{1}{3} < P < \frac{1}{2}$	
$P = 1$	
$P > 1$	

The surfactant packing parameter range and the various surfactants aggregate shapes are compared in Table II-6. The spherical micelles can be considered to be built from the packing of cones (large difference between the cross-sectional area of the headgroup and tail group), meeting the packing parameter requirement $P < \frac{1}{3}$. Other aggregate types, *e.g.* cylindrical micelles, are preferably formed by surfactants with truncated cones (with

packing parameters ⅓ < *P* < ½). The flexible bilayers, platelets or discs, respectively and vesicles result from a packing of surfactants with almost equal cross sectional areas of headgroup and alkylchain (½ < *P* ≤ 1). For *P* ≈ 1, planar extended bilayered structures can be expected. When *P* exceeds 1 (*P* > 1), reversed micelles are the favoured aggregates.
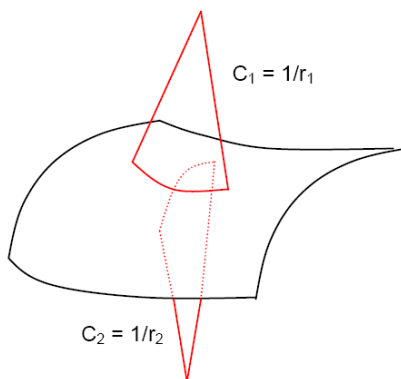
Figure II-6: The principle curfvatures C₁ and C₂ of a bended membrane.

Another important approach to the description of self aggregating systems is based on the theory of Helfrich [105]. The differential geometry of surfaces is applied to the model of interfacial curvature of a continuous surfactant film. A surface can be described by two fundamental types of curvature, mean and Gaussian. Both can be defined in terms of the principal curvatures $C_1 = 1/r_1$ and $C_2 = 1/r_2$. The mean curvature is

$$H = \frac{1}{2}(C_1 + C_2)$$
II-11

Whereas the Gaussian curvature is defined as

$$K = C_1 C_2$$
II-12

Conventionally the signs of the radii of curvature are defined to be positive if the surface points outwards (Figure II-6).

Additionally to the geometrical considerations, several further factors influence the aggregation behaviour of surfactants. Amongst others these parameters are the pH and the ionic strength (both influencing the area of a single surfactant molecule), the branching of the alkylchains as well as the number of the double bounds (influencing the length of the hydrophobic chain as well as the molecular volume), the temperature and additives in the solution (influencing the intra-molecular interactions as well as the salvation and hence the structure of the solvent) [4].

II.2.1.2.4 *Kinetics and Thermodynamics of Micelle Formation*

One approach to describe micellisation is the mass-action-model [2, 4]. It enables the consideration of a fraction of counterions bound to the micelles and thus is suitable for the description of ionic surfactants. At equilibrium the micelle formation of an ionic surfactant can be written as:

$$nS + mC \longleftrightarrow S_n C_m^z \cong M^z \qquad\qquad \textbf{II-13}$$

where S represents the surfactant ions, C the surfactant counterions, and S_n the formed aggregate with the bound counterions C_m , abbreviated as M^z . z is the micellar charge, m is the number of counterions bound to the micelle, and n is the aggregation number (also abbreviated as N_{agg}). The molar standard free energy of micellisation $\Delta_{mic}G^0$ can then be expressed as:

$$\Delta_{mic}G^0 = -\frac{RT}{n}\ln K = -RT(\frac{1}{n}\ln X_{M^z} - \ln X_S - \frac{m}{n}\ln X_C) \qquad \textbf{II-14}$$

with K being the equilibrium constant and X_i representing the molar fraction of species i. For surfactants of the symmetric electrolyte type and the assumption of large aggregation numbers as well as the awareness that at the cmc $X_c \approx X_s = X_{cmc}$ this Equation simplifies to:

$$\Delta_{mic} G^0 = (1 + \alpha)RT \ln X_{cmc}$$ **II-15**

Where

$$\alpha = \frac{m}{n}$$ **II-16**

is the degree of counterion adsorption on the micelle surface.

The aggregation number is not a constant value and only can be given as an average number. During the micelle formation initially dimers, trimers, *etc.* are formed. However, the actual concentration of these small aggregates is negligible. Thus, the size distribution in the case of spherical micelles usually can be estimated with 10 % [4].

Once formed, micelles have a large but finite lifetime. The exchange rate between micelles and monomers as well as the rate of formation/breakdown of micelles can be determined by various methods for diluted solutions. Typical exchange rates for the monomer-micelle exchange are in the range of $10^3 - 10^6 \, \text{s}^{-1}$. The formation/breakdown rates are typically between 10^{-1} and $10^2 \, \text{s}^{-1}$. Therefore a micelle lifetime of about $10^{-1} - 10^{-2} \, \text{s}^{-1}$ can be deduced. Due to the continuous exchange of monomers between the micelles and the bulk solution micelles are very mobile, disordered aggregates. Surfactants are permanently moving through the surface, inwards as well as outwards. The fast self diffusion is manifested in an average coefficient of approximately $10^{-10} \, \text{m}^2\text{s}^{-1}$. The exchange between the various possible conformations of the alkylchain is likewise fast ($\tau_C \approx 10^{-9} - 10^{-10} \, \text{s}$). 70 - 80 % of loosely bound counterions of ionic surfactants remain in direct vicinity of the micelles (within 10 Å),. The time-scale for the exchange between free ions and bound ions is approximately $10^{-9} \, \text{s}$ [2, 4].

II.2.2 Liquid Crystals

Crystalline solids can be transformed into a liquid state either by increasing the temperature up to the melting point or by dissolution of the substance in a solvent. Liquid crystals can be produced similarly, either on heating or dissolution. Those produced via heating are termed thermotropic, while those achieved with the help of a solvent are termed lyotropic. The liquid crystal order of the former arises from the anisotropic molecular shape and a short-range, intermolecular attraction. The latter generally occur with substances where the solutes (molecules or aggregates) have a much larger molecular size than the solvent. The liquid crystalline order arises from the repulsive interactions between solute entities at high concentration. The free energy change arising from the loss of entropy in forming an ordered structure (a liquid crystal) is less than the gain in free energy from dissolution of more solute [4, 106].

Generally, there are six classes of liquid crystal phases known, most of which now have well-established structures. These are the lamellar, hexagonal, cubic, nematic, gel and intermediate phases. In all of the stated phases, except the gel phases, both surfactant and water have a high molecular mobility, *i.e.* short-range diffusion on a time-scale of 10^{-12} s. They differ in the long-range symmetry and in the curvature of the surfactant aggregates. Except for the phases with flat aggregate surfaces, each class can occur with, either the polar regions or the non-polar regions representing the continuous medium. The former is referred to as normal, while the latter are reversed phase. As will be described later, the phases generally occur in a particular composition sequence. Each class of mesophases is usually labelled by a particular letter (see below) with the symbols having subscripts of "1" or "2" to distinguish between the normal or reversed forms, respectively [4, 106].

The micelle shape is determined by the molecular structure as described in the previous section. There is a critical volume fraction above which random, disordered solutions cannot occur for each of the shapes, *i.e.* spheres, rods

and discs. An ordered state (liquid crystal) must form at concentrations exceeding those critical fractions, if the surfactant is sufficiently soluble. The effective volume fraction of a surfactant is determined by the actual volume occupied by tails, headgroups and bound water. It further includes the effects of soft-core inter-micellar interactions such as repulsions due to overlap of headgroup conformations (as with EO surfactants) [10], electrostatics, hydration (solvation) forces and specific adsorption/desorption of solutes such as ions, polarizable organics, and polymers. The general behaviour is mostely close to that of an "effective hard-wall" particle[1, 4]. The general scheme of micelle shape- liquid crystal correlation is depicted in Table II-7.

Table II-7: Correlation of micellar shape and type of liquid crystal with increasing concentraion.

Micelle	*Liquid crystal*
Sphere	Cubic
Rod	Hexagonal
Disc	Lamellar

The maximum volume fraction of spherical and rod-like micelles without a morphology-change is approximately 0.74 and 0.91, respectively. The lamellar bilayers can, of course, pack to fill the total available volume (1.0). As soon as the available volume is occupied for a given shape, then more surfactant can only dissolve with a reduction of aggregate curvature to a shape with a higher packing limit. Figure II-7 depicts the mesophase behaviour of a surfactant as a function of its concentration. No explicit care was taken on the inclusion of the role of the headgroup size and hence its

type and the degree of counterion binding. Only few surfactants express more than two of the shown reverse phases at a certain temperature. Additionally, a direct transition of a lamellar to a reverse hexagonal phase is frequently observed without an intermediate phase like a V_2 [4].
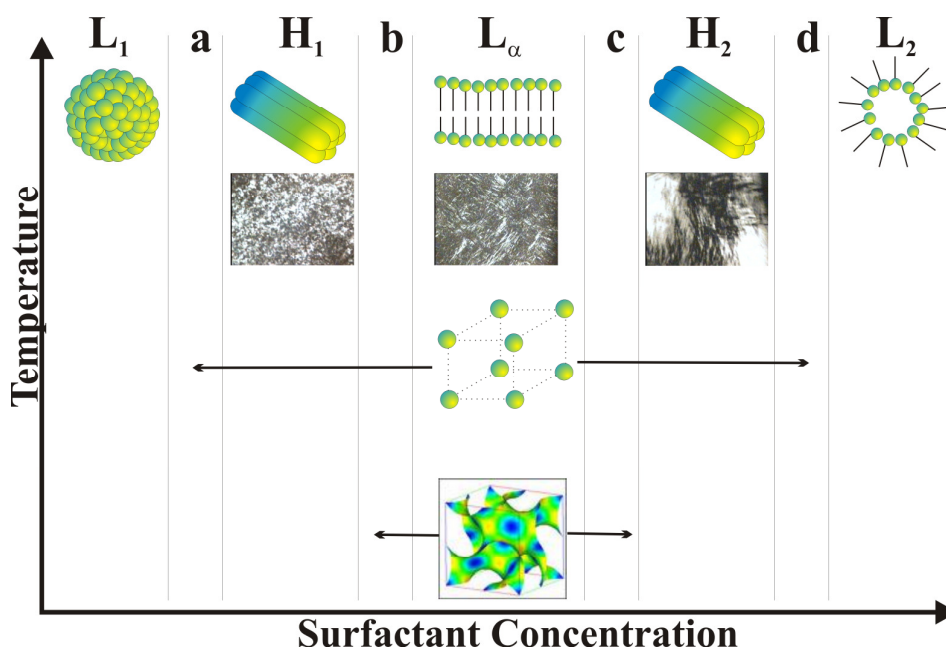
Figure II-7: Schematic illustration of the mesophase sequence with increasing surfactant concentration as a function of temperature [107].

The most important technique to identify mesophases, thermotropic as well as lyotropic, is their observation via polarizing microscopy. Birefringent phases express typical textures, while the isotropic cubic phases have none – however, their extremely high viscosity allows them to be distinguished from micellar solutions.

II.2.2.1 Lamellar Phase L_α

The most common surfactant mesophase is the lamellar phase (L_0,), also known as the "neat phase" from its occurrence during soap manufacturing. In this phase, the surfactant molecules are arranged in bilayers separated by water, which frequently extend over large distances (a micron or even more) [10, 108-112]. Such bilayers are the structural backbone of biological membranes [2, 106, 113]. The viscosity of a lamellar phase is comparatively low. Although it does not flow under gravity it can be easily poured. It can unambiguously be identified by its characteristic textures under crossed nicols. The surfactant bilayer thickness can vary from ca. 1.0 - 1.9 times of the all-trans conformation of its tail. With longer-chain surfactants, the maximum thickness is reduced to less than 1.7. The difference in layer thickness originates from differences in headgroup areas and gives rise to differing degrees of disorder within the alkylchain region. Hence, for large bilayers thicknesses the disorder usually is large. Thus, the alkylchains generally are in a fluid-like state. The water layer thickness is constant throughout the whole sample. Its value varies over a large range depending on the type of surfactant, ($\sim 8 - 200\,\mu\text{Å}$) [4]. The minimum water content is often that one, which is required to hydrate the polar groups, but very low or zero water content can occur with surfactants that form thermotropic lamellar phases, which are commonly called smectic phases [114].

II.2.2.2 Hexagonal Phases H_1, H_2

A further common lyotropic liquid-crystal phases is the hexagonal mesophase. There are two alternative types: the "normal" hexagonal phases (H_1), or "middle" phase in the soap manufacturing, and the "reversed" hexagonal phases (H_2). In the normal phases water is the continuous medium whereas it is composed of the alkylchains in the reversed hexagonal phases. The surfactants aggregate into indefinitely long circular aggregates (rods or worms) packed on a hexagonal lattice (Figure II.8).

The diameter of the normal hexagonal phase is approximately 1.3 - 2.0 times the all-trans alkylchainlength r_{max}. The typical inter-micellar separation is between 8 and 50 Å. The polar region diameter of the reversed hexagonal phases ranges in the same order of magnitude but values above 30 Å are rare. The thickness of the reversed phase is approximately 1 -1.5 r_{max}.
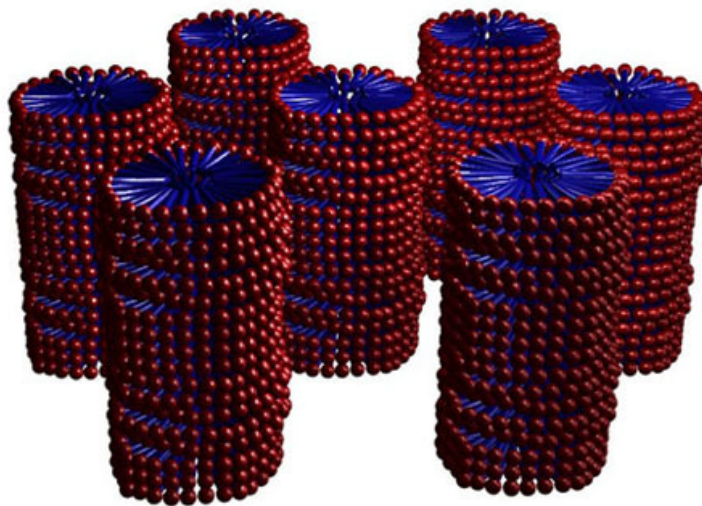
Figure II-8: Scheme of a H$_1$ phase.

Both types of hexagonal phases are comparatively viscous, much more than the L$_\alpha$ phases. The optical texture of these anisotropic phases, observable under the microscope is the same for both and can clearly be distinguished from the texture of the lamellar phases [4].

II.2.2.3 Cubic Phases I$_1$, I$_2$, V$_1$, V$_2$

Cubic phases are high viscous and isotropic. These structures base on one of the generally possible cubic lattices (primitive, face-centred and body-centred). Two different arrangements can occur in the cubic phase. The first one comprises small spherical micelles, normal or reversed and the other is based on three-dimensional "bicontinuous" networks. Both can occur as

normal or reversed phase, respectively. Consequently, four classes of cubic phases exist. The micelle-based, discontinuous ones are denoted as "I" and the bicontinuous network is termed as "V" (Figure II-9) [4].
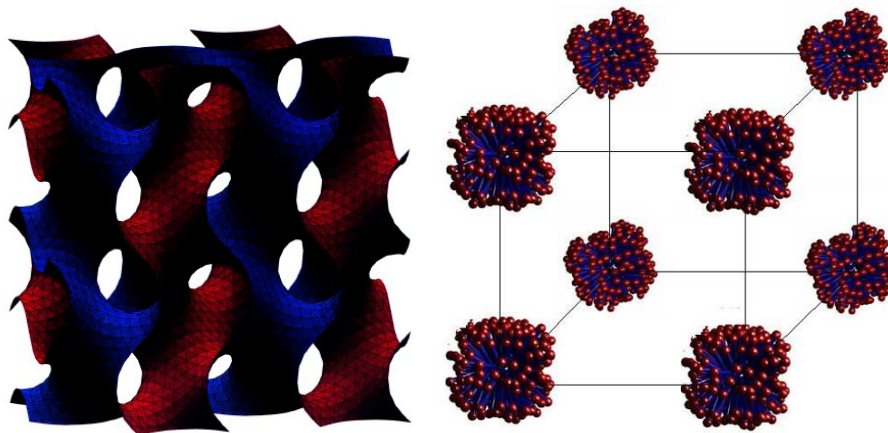
Figure II-9: Scheme of a biscontinuous V (left) and a discontinuous I_1 (right) cubic structure.

The I-type cubic structures are the simplest ones. For I_1 phases with water as continuous medium primitive as well as body-centred and face-centred lattices were found [113]. Not infrequently, several of these types are found coexisting in the phase diagram of one surfactant. A schematic illustration of I_1 with primitive lattice is shown in Figure II-9. The diameters of the aggregates are the same like in normal solutions and the separations are similar to those found in H_1.

For the Im3m and the Fm3m cubic lattices, only one micelle type, a quasi-spherical structure, is proposed. However, the aggregates structure of the Pm3n phase is still discussed. It is most probable, that two slightly different, short rod micelles are coexistent [4].

The existence of the reversed I_2 structure of spherical aggregates packed in a cubic array was questioned for several years. Meanwhile they are examined more and more [115-117]. The cubic phase with Fd3m symmetry is by now well known [117]. The joined micelles are spherical but there seem to be two different sized ones involved. In the case of reversed phases the alkylchain

packing constraints is no longer limiting the micellar radius. Hence, the coexistence of different sized micelles is more probable than for I_1 phases.

The second type of cubic phases (V), consisting of three-dimensional bicontinuous aggregate structures exhibit three main space groups: the Pn3m, Im3m and Ia3d [4, 106]. Most of the points on the surface of this structure are saddle points, having local curvatures compensating each other to a mean curvature of zero. The cubic phases V can be differentiated regarding to the net curvature. In case of a positive net curvature towards water the phase is labelled as V_1, for a positive net curvature towards oil it is denoted as V_2. The values of the curvatures of cubic phases are typically between those of hexagonal and lamellar phases. Thus, the cubic phases are located in the phase diagram in the domain between the hexagonal and the lamellar one [4]. The first reported biscontinuous cubic phase (Luzzatti *et al.*). was of the body-centred lattice type, Ia3d [118]. In contrast to the proposed structure by Luzzatti the structure today is described by periodic minimal surfaces [119].

There is a distinction between the V_1 and V_2 concerning the occurring symmetries. In the case of V_1 merely the Ia3d phase has been reported while for V_2 all three forms have been detected.

The two types of cubic phases I and V can be distinguished by their position in the binary phase diagram with water (Figure II-7). The discontinuous phases I generally occur as a result of their high mean curvature between the micellar and the hexagonal phases. The biscontinuous phases V can be found, because of their manifestly lower curvature, between the hexagonal and the lamellar phases [4].

II.2.2.4 Nematic Phases
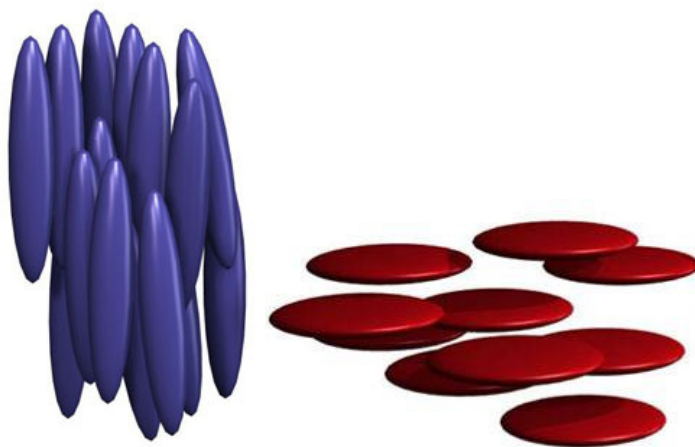
Figure II-10: Scheme of the Nematic phases N$_c$ and N$_d$.

Nematic phases are less common than the lyotropic mesophases discussed so far. They form at the boundary between an isotropic micellar and a hexagonal or a lamellar phase, respectively. They have similar micellar order to that of the molecules in a thermotropic nematic phase. The orientational and translational order in this phase is lower than in the other phases. These anisotripic phases, identifiable due to their characteristic "schlieren" texture under the polarizing microscope, have comparatively low viscosities. However, if highly disordered, the texture appears under the microscope just upon alignment of the structure by *e.g.* magnetic field or pressure and vanishes after force removal within milli-seconds. Either cylindrical micelles, related to the hexagonal phase, or disc micelles, related to the lamellar phase, are found for the Nematic phases N$_c$ or N$_d$ respectively. Details of their structure are not yet fully established. The suggested order of their structure are shown in Figure II-10 [4, 114, 120].

II.2.2.5 Gel Phases L$_\beta$

The gel phase has a closely related structure to the lamellar phase, as it is comprised of surfactant bilayers. However, their viscosity is much higher.

Within the gel phase, the bilayers are in a rigid state, with mostly all-trans conformation of the surfactant tails. The transition heat on melting is relatively high, with approximately 25 – 75 % of the pure crystalline surfactant fusion heat. This indicates restricted chain motions, mostly limited to solely rotation around the long axis. In contrast, the water phase is in a "liquid-like" state, with fast rotational and translational mobility [121].
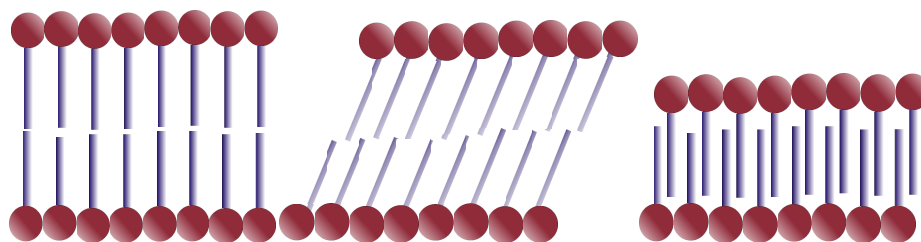
Figure II-11: Schematic presentation of the three different gel phase structures: From left to right: normal, tilted and interdigitated.

There are three different structures of the gel phase reported in literature (Figure II-11) [4, 122]. Most commonly found for dialkyl lipids is the first structure in Figure II-11, with the bilayer normal to the crystal [123]. In this case, the alkyl layer thickness is found to be approximately twice the all-trans alkylchainlength of the surfactant. Another structure expresses tilted bilayers and is found in systems where the polar headgroup is significantly larger than the width of the alkylchain. This structure has for instance been reported for monoglyceride systems. The interdigitated form is found for long-chain monoalkyl systems. The area of the hydrated headgroup determines structures occur. The perpendicular bilayers occur upon headgroup areas *(a)* of *ca.* 22 Å^2, while the tilted bilayer require $a = 22\text{-}40$ Å^2, and the monolayer interdigitated structure $a > 44$ Å^2 [4, 121].

L_β phases show high flexibility towards the structure of the surfactant as well as the total composition of the system. Like just mentioned, gel phases are observed for long-chain dialkyl amphiphiles just like for monoalkyl surfactants. Due to the lower packing order of the chains compared to that in a normal crystal, surfactants with a chainlength difference of up to four

carbons can be mixed without destroying the structure. Additionally, various headgroups can also mix within a gel phase [4, 121].

The melting temperature of an alkane of the chainlength n represents an approximate upper temperature limit for the hydrated gel phase of surfactants with equal chainlength, since the headgroups pack less effectively than a methyl group. Usually, a even lower melting temperature is found, because the headgroup is more hydrated in the molten state, which gives a higher free energy contribution than the chain packing [4, 121].

II.2.3 Catanionics

Many biologically relevant structures consist of amphiphilic bilayers, like the cell membranes. Therefore, these structures received a lot of scientific interest. All types of bilayer structures, mainly vesicles, present in biologically relevant processes consist of double chained amphiphiles like phospholipids. However, in the past years lots of research projects proved that bilayers can also be formed from single chain surfactants, under special conditions. For instance, this is the case for mixtures of anionic and cationic surfactants, whose association through their interactions can mimic the type of structures originated by phospholipids. The term 'catanionic', which consists of the words cationic and anionic, and describes the spontaneous self-assembly that occurs by mixing both types of surfactants, is now commonly accepted to qualify such structures, which were already mentioned in the literature [124] before this term was introduced. In the case of equimolar amounts of both types of surfactants due to strong van der Waals interactions between their chains and the intense electrostatic attraction of their heads, the surfactants commonly arrange pair-wise. That association leads to a strong reduction of the surface per head, which induces the formation of bilayers at quite low concentrations. This pair-wise aggregation of two single chained amphiphiles results in a type of surfactant, which can be considered as pseudo double-chained, as the two alkylchains are not attached to the same headgroup. The hereby formed pseudo-molecule has a cylinder-like shape, which evidences the assumption of bilayer formation, by considering the geometrical estimation of the packing parameter. Thus, the similarity of these surfactants to those really being double-chained and zwitter-ionic becomes obvious, as both are composed of two alkylchains and contain a headgroup bearing two opposite charges, which therefore leads to overall neutrality. Yet, the important difference to the classical zwitter-ionic surfactant type is the tuneability of the properties of the catanionic system. By slightly varying factors like the mixing ratio of anionic and cationic component, the chainlength of the surfactants or the degree of saturation of the alkylchains,

the properties of the system can be shifted immensely. The phase- and aggregation behaviour of a catanionic mixture in water is strongly dependant on a variety of factors and can be modified in any desired direction.
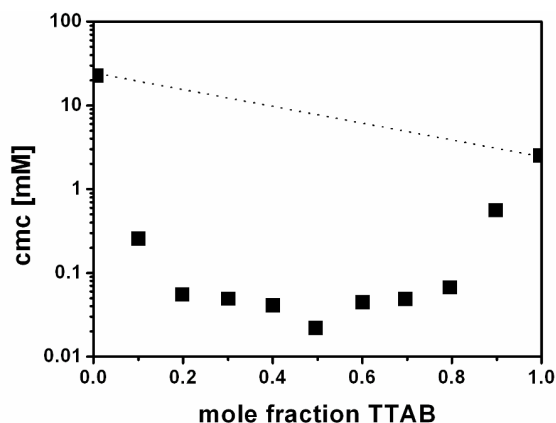
Figure II-12: cmc of the mixture tetradecyltrimethyl-ammonium bromide (TTAB) and sodium laurate versus the mole fraction of TTAB at 25°C [125].

For instance, the critical micelle concentration (cmc) of the mixture of two contrarily charged surfactants can differ a lot from the cmc of the pure surfactants [126]. If no net interaction between the amphiphiles exists, the cmc of a mixture of surfactants generally is the average of the cmc of the pure surfactants. Yet, between anionic and cationic amphiphiles a strong interaction, about 5 to 10 times higher than for non-ionic and anionic type ones, is present, which leads to the result of strongly reduced cmc values compared to the ideal mixing case without interactions (compare Figure II-12). Consequently, catanionics are of high industrial interest regarding their cleaning efficiency [127-128].

A diversity of microstructures, amongst others rod-like and spherical micelles [129-130] as well as lamellar phases [131-132] and vesicles [133-135], can be obtained depending on the ratio and nature of both surfactants. If one of the two surfactant types is in slight excess, the assemblies generally formed are

vesicles. Vesicle formation in that case is usually described as a spontaneous process [135].

In literature a distinction between "simple" cationic – anionic mixtures where each surfactant still is accompanied by its counterion, and so-called "Ion Pair Amphiphiles" (IPA) (equimolarity of both surfactants) [124, 135-141]], or "true" catanionics, is made. In true catanionic systems the initial counterions are replaced by protons and hydroxide ions respectively. At equimolar ratio of both surfactants these counterions can combine and form water molecules. In this case each of the surfactants acts as counterion of the oppositely charged one [142-145] and the system is called Ion Pair Amphiphile.

II.2.3.1 Phase Behaviour and Vesicle Composition

Phase diagrams of catanionic mixtures are delicate to derive. A rigorous phase analysis in such systems is complicated since five species, the two surfactant salts, the ion pair Amphiphile, the non-surfactant salt and water, are present. In the pure Ion Pair Amphiphile system the number of species is reduced since the excess salt was removed. Regardless of this multitude of components simplified ternary phase diagrams are used in literature. The corners of these phase diagrams represent the anionic surfactant, the cationic surfactant and water (Figure II-13).

The vesicular domains are usually situated in the dilute region of the phase diagram[146]. Under these conditions, vesicles are either represented by two lobes [135-136, 140], in the case of two types of vesicles with positive or negative excess charge respectively, or only one lobe if only one type of vesicle can be detected [137, 142].

A fact that one faces regularly during literature studies is that in equimolar composition of these surfactant mixtures precipitation can be observed [137-140, 147]. Yet, a few exceptions have been reported [148]. In true catanionic systems however, a precipitate is not frequently reported. Due to the lack of excess salt less screening occurs in this case and the electrostatic repulsion between

the charged double layers is much higher, which prevents precipitation. The fact of precipitation in simple systems is supported by the instance that *e.g.* the lobes of the vesicle domains are never crossed by the line of equimolarity but are commonly situated on either side of it, which implies the stability of catanionic vesicles being ensured by one of the surfactant being in excess.
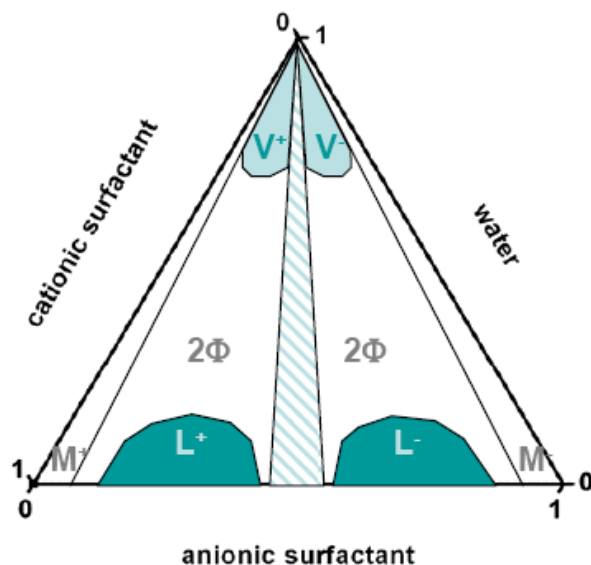
Figure II-13: Schematic phase behaviour encountered in catanionic surfactant systems. V- and V+: regions of negatively and positively charged vesicles; 2Φ: two-phase regions. L- and L+: lamellar phase with excess of respectively anionic and cationic surfactants; M- and M+: mixed micellar solutions with an excess of respectively anionic and cationic surfactants. Precipitate region around equimolarity.

This observation is not in agreement with the fact that vesicle formation was observed in true catanionic systems around equimolarity. Several explanations can be given for this inconsistency:

Some true catanionic systems showed only short time stability and were therefore reported not to be thermodynamically stable [143].

The apparent composition of the vesicles appeared to differ a lot from the initially implied ratio of the anionic and cationic surfactants and was much closer to equimolarity than could be expected. This was demonstrated by *e.g.* Brasher and Kaler [141] in SANS experiments of the system CTAB (Cetyltrimethylammoniumbromide) and SOS (Sodiumoctylsulfate).

Most true catanionics contain carbon acids or organic bases, which can be reprotonated and deprotonated, respectively. At equimolarity, not only the charged species are present, but a great amount of uncharged neutral derivatives [131]. Thus, one of the charged species might be present in excess. This seems to be the requirement for vesicle formation in the simple catanionic case [149].

The classical topology of a catanionic phase diagram is represented in Figure II-13 [146].

II.2.3.2 Thermodynamic Modeling

The thermodynamic description of catanionic systems has been a topic of interest in a couple of research projects in the past. Several groups developed approaches towards thermodynamic description of the formation of catanionic aggregates, especially vesicles. Various contributions need to be taken into account when considering the free energy of vesicle formation.

For instance the work to form a planar catanionic bilayer and the work to bend this bilayer into a closed vesicle were compared with the result that no vesiculation should occur around equimolarity as the bending work is too large [150].

A further theory considering the contributions of the surfactant tail packing, the surfactant head steric repulsion and the electrostatic interactions between oppositely charged heads, to the free energy was developed [151]. Details on

the vesicle size, the composition distribution and the effect of added salt can be derived from this theory. The model shows that the ratio of both surfactants is more narrowly distributed around equimolarity in vesicles than the initial composition would suggest. Furthermore the alkylchain asymmetry between the two surfactant types was evidenced to have an energetically stabilizing effect for vesicles.

The concept of curvature elasticity of the surfactant bilayer as a contribution to spontaneous vesicle formation was studied by Safran *et al.* [152]. This theory predicts a drastic change in bending modulus by the addition of short chain surfactants to an interface composed of long-chain molecules. A result is that the interactions between the surfactant molecules can stabilize spherical vesicular structures, whereas with a single surfactant the frustration of one of the layers has a destabilizing effect.

II.2.3.3 "Simple" Catanionics and "Ion Pair Amphiphiles"

Only a few studies exist about the comparison of the properties of special structures, like vesicles, formed by mixtures of cationic and anionic surfactant still bearing their counterions, with the true catanionic system, where all residual salt is removed.

Simple catanionics describe mixtures of anionic and cationic surfactants with excess salt. Both surfactants still have their counterions, like halogenides or alkali ions, respectively. These counterions form excess salt by combination. In the 1990s Kaler et al. studied several of these simple cationic - anionic - surfactant mixtures, in detail [135-137, 140]. One of the important results was that the formed catanionic vesicles showed long range stability and appeared to be in equilibrium and therefore thermodynamically stable. Furthermore the influence of the chainlength was examined. Equal chainlength in catanionics leads to the preference of lamellar phases or crystalline precipitate, whereas different chainlength or branched chains enhance the formation of vesicles. Further investigations dealt with the stability of catanionic vesicles against changes in temperature, salinity and pH [101, 153].

True catanionics or Ion Pair Amphiphiles have been investigated by Jokela et al. in the 1980s [142, 144-145]. In true catanionics the initial counterions are replaced by hydroxide ions for the positively charged surfactant and respectively protons in the case of the negatively charged surfactant. To obtain this replacement the initial surfactant counterions are removed. This removal is generally achieved by ion exchange resins, which need to be strongly basic for the cationic and strongly acidic for the anionic surfactant.

The removal of the low molecular weight salt is expected to modify the electrostatic interactions between the two surfactants by strongly increasing the Debye screening length. As a result the ion pair interaction between the polar heads of oppositely charged surfactants should be stronger than in case of simple catanionics with excess salt. This leads to a shift in the total area occupied by the polar headgroups [131, 134].

At mixtures of 1:1 of each surfactant only water instead of excess salt should be released. This means that in this case the surface charge density is assumed to be very low and the way is open to investigate hydration forces. Several of these systems, which form bilayers in equilibrium with almost pure water, have been analyzed and it was discovered, that not only electrostatic repulsion of the double layers but also the size of the polar headgroup has influence on the swelling of the phases. The bigger the head, the larger is the interlamellar distance [142].

Even by comparing the stability with time of some structures, differences between simple and true catanionics were reported. This is for example the case for vesicular structures. The vesicles formed by true catanionics showed less stability than those built up of catanionics still carrying their counterions. This has been proven by investigations of Fukuda et al. [143], who examined several true catanionic systems of the composition: alkylcarboxylic acid and alkylammonium hydroxide with equal chainlength. In the case of catanionics with excess salt, the formed vesicles showed long term stability up to several years. Hence, these vesicles seemed to be in the equilibrium state of aggregation. On the other hand true catanionics formed vesicles only around equimolarity with a stability of one hour to at maximum two days. It needs to be underlined that the comparison between true and simple catanionic systems is not always straight forward, as in the latter case vesicles usually are obtained if one of the surfactants was present in excess, in contrast to that, true catanionics seem to require equimolarity for vesicle formation.

A big variety of true catanionic systems has been investigated in the past some of which are quite sophisticated. For instance, multiple chain true catanionics have been designed to improve membrane tightness or to mimic archaebacterial membranes, which can sustain extreme physiological conditions [154]. Some catanionic systems have been examined on the basis of multiple chain structures like gemini surfactants, which are composed of two single chain amphiphiles being covalently attached to each other by a spacer between their headgroups [155]. The chain melting temperature was found to be strongly dependent on the size of this spacer.

To develop new surfactants originating from natural products, sugar-based true catanionics have been synthesised [156]. Their biological activity as well as their property to form vesicles was evidenced.
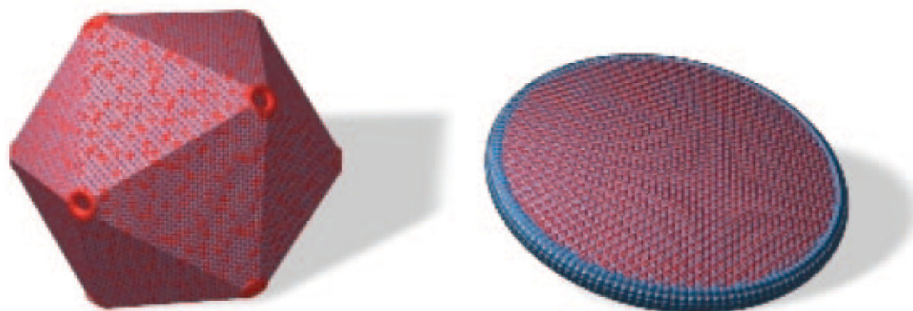
Figure II-14: Scheme of an icosahedron (left) and a nanodisc (right) composed of CTAOH and myristic acid [157].

An Onion Phase in Salt-Free Zero-Charged Catanionic Surfactant Solutions has been detected for the mixture of trimethyltetradecylammonium hydroxide and oleic acid [158].

Control of size and shape of a true catanionic system was met with success by Zemb *et al.* [159-162]. The system investigated was composed of myristic acid and cetyltrimethylammoniumhydroxid (CTAOH). By varying either the molar ratio of the surfactants or their concentration respectively, different forms of aggregation could be realized, like nanodiscs or icosahedra like, facetted, hollow objects in the form of frozen bilayers (Figure II-14) [159-161]. These structures are formed by segregation of excess charge into pores and towards the edges, respectively. Such special types of catanionic aggregates, icosahedra formation, have so far been reported only in the case of true catanionics. In a wide domain of the concentrated region lamellar phases of different effective charge are formed, depending on the ratio of anionic and cationic component. These lamellar phases have some interesting swelling properties. Earlier studies showed for example that the distances between the bilayers can reach approximately 1000 Å [159], which means that this system shows a very high swelling property. This is an important property for

industrial applications. For a large number of creams and gels, used as delivery medium after application on the skin in cosmetics or pharmaceutical industry, the capacity of retaining moisture is crucial.

II.2.3.4 Thermotropic Phase Behaviour of Neat Catanionics

Despite this strong interest in the phase behaviour of catanionic surfactants, several aspects deserve even further investigation, in particular the relation between geometry and self-assembly, with the goal of designing more efficient, task specific surfactants. Besides the lyotropic mesophases, catanionics also display fairly interesting thermotropic structrues, which frequently exhibit a stepwise melting from the solid crystalline to the liquid phase [163-166]. The thermotropic liquid crystalline phases of certain classes of amphiphiles have been investigated for some time. Lipids [167-172] and metallic soaps [173-174] are prominent examples for polymorphic and mesomorphic, amphiphilic compounds. The lyotropic as well as the thermotropic phase behaviour of surfactants are directly correlated to molecular chemistry and geometric shape [170, 175-176]. Catanionics frequently possess a greater number of thermotropic liquid crystalline phases than other amphiphiles. This observation is a consequence of the more complex chain packing and headgroup interactions. These surfactant mixtures crystallize in such a way that molecules are arranged in bilayers, where the highly ordered hydrocarbon chain double layers are covered by the polar headgroups. Molecular motion within the hydrocarbon chains increases gradually as the temperature increases until, at characteristic temperatures, a state with a higher rotational freedom is taken. This causes the formation of various mesomorphic phases (as observed for lipids). Several liquid crystals, mainly of the smectic type, have been observed so far [164-166]. With respect to chainlength, the asymmetric catanionics have been reported to express a thermotropic phase behaviour with a higher diversity compared to symmetric ones [165]. This might probably be due to the more unfavourable crystalline packing and hence the stabilization of liquid crystalline mesophases. Further, it has been observed for a series of double chained catanionics that headgroup

chemistry as well as volume constraints might determine the melting behaviour [166].

II.2.3.5 Applications

The field of nano-structured materials is of high industrial interest, for example catalysts or drug delivery media are important applications. An approach to synthesize these materials is by template guided reactions [177]. Since the properties of catanionic vesicles, like the diameter or the bilayer thickness, can be easily adjusted by varying *e.g.* the type of hydrophilic headgroup or the chainlength of the surfactant, they display ideal templates for certain synthesis of nanoparticles with defined size. Catanionic vesicles already found application as templates in the synthesis of hollow nanometer sized polymeric [178] and silica spheres [179], respectively.

A further important application of catanionic vesicles is the encapsulation of active molecules, as they hence can be protected of undesired reactions. Those vesicles thus can play a role as *e.g.* drug delivery media[6]. The spontaneous formation of the closed vesicular shapes bears an ideal way for encapsulation [180-181]. The properties of catanionics for encapsulation processes have been well investigated [135]. If the molecule is hydrophilic it can be encapsulated in the centre of the vesicle, if it is hydrophobic it will be retained in the bilayer. A detailed study about glucose entrapment in SDBS/CTAT systems was for instance made by Tondre *et al.* [182]

II.2.4 Toxicity and Biodegradability of Surfactants

Surfactants are omnipresent. Their applications range from simple household products over personal care, cosmetic, pharmaceutical additives to performance chemicals in industrial processes. Since they are used in products or processes that directly impact on human health or on the environment, there are concerns regarding their effect, particularly their toxicity to marine organisms as well as to humans.

II.2.4.1 Toxicity

In many applications surfactants are indispensable. Especially in their function as additives to human care or pharmaceutical products the main requirements to surfactants are: constant quality, chemical and physical inactivity, microbiological purity and over all a good physiological tolerance. Although, the oral toxicity of surfactants generally is assumed to be low, they are known to originate skin-, mucous- and eye irritancy. Hence, they consistently are in the focus of toxicological investigations [183].

II.2.4.1.1   Methods to determine the Potential of Irritancy

The determination of the potential of irritancy of surfactants can be realized with a huge diversity of methods. Generally, it should be distinguished between in-vivo and in-vitro methods. *E.g.* the skin-irritancy can be evaluated with the help of voluntary probands or patients. However, the most prevalent methods are based on animal experiments. Benefit-cost analyses of such studies commonly reveal a bad relation. Frequently, animal tests are invasive and give feebly reproducible results [184-185]. The Draize test, determination of irritancy potential in the rabbit eye, is a popular method with questionable conclusion as significant differences between mammals

eyes are fact. Due to its insufficient validity and its poor reproducibility in combination with the ethical questionability the research for adequate and efficient test methods began.

Table II-8: Common methods for the determination of cytotoxicity.

Principle		Method	
Determination of physiological performance	Active absorption of substances	Neutral red absorption[186-193] [³H] Uridin-absorption[188]	photometric or radio-detection after dye absorption
	Ability of reduction	MTT assay[186-187, 189-190, 194-195] Bindschedler green leucobase test[192]	photometric detection after dye reduction
	DNA and protein content	[³H] Thymidin test[196] Hoechst 33258[194]	fluorimetric or radio detection of DNA
		Kenacidblue[189, 197] [³H] Prolin test[198] Bio-Rad-Coloration[189, 191]	photometric or radio detection of total protein content
	Enzyme-activity	Intracellular ATP[199]	luminometric detection
		Lactate production[197]	photometric detection
		Glucose consumption[190]	detection via auto analyzer
Determination of membrane integrity	Liberation of intracellular substances, dyes and membrane components	LDH liberation[186, 189-190] β-NAG liberation[190]	detection via auto analyzer
		hemolysis[200-201] neutral red liberation[189]	photometric detection
		[³H] arachidonic acid[202]	radio detection
	absorption of dye by dead cells	Trypanblue[191]	counting
		Janusgreen[195]	photometric detection
Observations	morphological cell modification	Agar-Overly test[189]	visualisation of cell lysis
		Microscopy[193, 203]	
		coloration[187]	microscopy
		cell number[203]	*e. g.* crystal violet, counting chamber
		cell adhesion[189, 196] cell volume[196]	

A key role of irritancy seems to be the cell death (cytotoxicity) [204], hence, the in vitro investigations of cells and the impact of drugs on cell functions was intensified [185, 205].

Cytotoxicity can be induced by a variety of mechanisms. Important points of action for toxic substances thus are the disruption of membrane function, the disturbance of redox-homeostasis and the ATP- and macromolecule synthesis, as well as the damage of genetic material [206]. Toxic cell transformations can be reversible, *e.g.* the binding to receptors, complex formation with enzymes or the variation of permeability of the cell membrane. Though, several cell modifications are irreversible, like massive membrane disruptions or reactions like oxidations, hydrolysis or the formation of covalent bonds. Hence, factors of impact leading to effects which exceed the physiological range of variations always lead to cell death. Cell death can be necrotic or apoptotic. Whereas the apoptosis is a physiological process where the cell dies after a coded mechanism, the necrosis is triggered by external impacts and induces inflammations [206]. The possible action modes of toxic substances are just as numerous as the methods to determine cell death are diverse. Thus, to be able to draw unambiguous conclusions concerning the overall toxicity of a substance and its mode of action, a test array which covers various key parameters has to be accomplished. During most of those tests a special parameter, which is designated to a typical cell function being essential for cell viability, is determined after a defined period of time. Table II-8 gives an overview of the most common methods to determine cytotoxicity.

II.2.4.1.2   *Modes of Action*

For a while now, surfactants are known to cause membrane disruption. Already in 1967 this property was investigated in the system of sodium dodecylsulfate in ciliates [207]. Several further studies suggest the following operation sequence of membrane toxicity: primarily, time and concentration dependent an increase in membrane permeability occurs followed by a

disintegration of the membrane and finally ending in a total dissolution of the membrane. For instance, it was found out, that sodium dodecylsulfate and Triton X-100 cause cytotoxicity below the cmc in B16-melanoma cells, which was evaluated by Trypanblue tests. Close to the cmc cell lysis occurred, which was photometrically detected as cell dissolution. In this work, the membrane disruption was called the primary key impact for cytotoxicity [208]. In tests with human keratinocytes and skin models at low surfactant concentrations, effects, like the binding to the membrane and feeble variations in membrane permeability, were detected. At higher concentration, investigated were sodium dodecylsulfate and Triton X-100, membrane lysis and membrane fusion followed by total membrane destruction occurred. Mixed micelles, protein and lipoprotein complexes could be detected. [202] A similar sequence, namely, binding of the surfactants to dermal keratin, increasing of protein- and cholesterol-solubility and dissolution of phospholipids and membrane proteins followed by cytolysis was already discussed in an article of 1974 [209]. In a review article of Helenius and Simons the correlations of the cell membrane surfactant interactions are analyzed in detail. Below the cmc, surfactants show a strong affinity to membrane proteins. Due to those interactions, the protein conformation is changed leading to an increase in total membrane surface, in such a way as to enable a stabilization of the membrane against osmotic stress. Membrane bound enzymes are immensely affected. Due to the conformational changes, their activities are modified either towards inhibition or on the other hand even activation. At higher concentrations, the lysis of the cell happens. It begins, as soon as proteins and macromolecules start passing the membrane. The lysis is accompanied with a massive increase in surfactant binding to the membrane. Hemolysis, however, does not mean the total destruction of the lamellar order of the membrane, but the adsorption of surfactant monomers, penetration of those through the membrane and hence changes of molecular organization and permeability of the membrane. The osmotic equilibrium is shifted and hemoglobin is liberated. With the total breakdown of the liposomal structure, mixed micelles are formed and proteins and lipoproteins are released. [210].

The disruption of mitochondria seems to be closely correlated to the membrane toxicity of surfactants. The function of mitochondria is sustainably affected by the interaction with surfactants. Swelling of the mitochondria as well as modification of membrane bound enzymes in combination with disruption of their interactions has been reported several times. An increase in phosphorylation rate has been demonstrated. For instance, sodium dodecylsulfate leads to an increase in the membrane potential of the mitochondria and a shift of the ATP/ADP ratio [207, 210-211].

Almost all surfactants induce apoptosis at low concentrations which is shifted to necrosis with increasing concentration. In addition to the theory of enhanced membrane transport of toxic methabolites of the cell culture medium by increasing membrane permeability the apoptosis seems to be strongly correlated to direct membrane toxicity. Also the impact on mitochondria which is a result of membrane disruption, appears to correlate with apoptosis [212]. Although, the mechanisms of the induction of programmed cell death by various surfactants seem to be alike, differences in the way of toxicological action cannot be dismissed. Observations of the morphology changes of cells in contact with anionic, cationic or non-ionic surfactants lead to clear differences, especially the speed of action [213].

Several studies discussing the correlation between surfactant structure and property, like the hydrophilicity (HLB), the cmc, the charge, the number of ethoxy units *etc.* and toxic action appeared in the past. [208-210, 214-215] In some of these works a global classification of surfactant toxicity was made, commonly: cationic > anionic > non-ionic. [186]. Furthermore it was postulated, that the toxicity of surfactants to cells and their concentration in them depends upon their tendency to adsorb onto them and their ability to penetrate their cell membranes [216]. Concretely, the fraction of standard free energy of adsorption of the surfactant at the solution air interface and its minimum cross sectional are at that interface was found to correlate well for several anionic, cationic and non-ionic surfactants. Thus, toxicity rises with an increase in the length of the hydrophobic group and for isometric materials, decreases with branching or movement of *e.g.* the phenyl group to

a more central position in the linear alkylchain. In linear polyoxyethylene alcohols the toxicity increases with the decrease in the number of oxyethylene units in the molecule, also due to the expected changes in the adsorption energy – area fraction [217]. Scott Hall *et al.* found out that the general structure of a surfactant, whether highly branched, linear, aromatic or aliphatic, did not determine toxicity to the mysid shrimp Mysidopsis bahia, but observed that toxicity could be predicted by calculating the surfactant's ethylene oxide (EO) molar ratio. An EO ratio of <15 was common to the most toxic surfactants, while those chemicals with an EO ratio of 30-50 were consistently of very low toxicity. This observation applied both for a given series of homologues and across various surfactant types [218]. Wildish suggested a number of possible explanations for the longer-chain/lower toxicity observation: for example, uptake rate across biological membranes is the limiting factor in the ultimate toxic mechanism of longer-chain, less lipid-soluble surfactants. Alternatively, the number of surfactant molecules at the same weight per unit volume decreases with increasing chainlength. If a critical number of molecules must accumulate at the active site for lethal poisoning to occur, then surfactants with a longer-chain will exhibit less toxic effects. Another possible explanation is that surfactant binding to proteins may be less efficient when the chain is longer, resulting in a slower acting toxic mechanism [219]. And last but not least, long-chain surfactants often are less soluble than their shorter chain derivatives which lead to a lower total surfactant concentration than the expected one. Consequently, it appears that some chemical structures in the surfactant molecule that promote biodegradability (such as increased length and linearity of the hydrophobic group or decreased oxyethylene content) increase its toxicity [87]. Further, it is well known, that via combination of different surfactants the toxicity of the single components can be reduced [220]. The reduced toxicity usually is explained by a diminished monomer concentration due to the formation of mixed micelles, as only the monomer is discussed as being responsible for the toxic action [221]. However, several studies reported reduced toxicity at concentrations far below the cmc [222]. The lower cmc seems not to be a sufficient explanation so that *e.g.* protein binding is consulted as assertion [223]. Though, each study commonly highlighted the mode of action of only a

small number of different surfactants. Furthermore, several investigations found contradicting results [222, 224].

Every single surfactant seems to induce specific and highly complex processes in cells and tissue. They bind to proteins as well as to phospholipids influencing (stimulating or inhibiting) enzyme activity and membrane permeability. Hydrophilic and hydrophobic forces are simultaneously involved in the binding, and the effects observed are the result of the interplay of the various interacting forces. The toxicity does not simply originate from the cell membrane dissolution as a result of the interfacial properties of amphiphiles. Many different factors influence the toxic effect of surfactants, starting from their property as surfactant and their amphiphilic character, going to very specific affinities and interactions with proteins and ending in some of them being mimicries of hormones [225-228]. As recent research indicates, the biological effects strongly depend on the structure of surfactants. We need additional data for the more profound elucidation of the relationship between molecular structure and biological efficiency. With the exact knowledge of this relationship, it will be possible to select for each purpose a surfactant with minimal toxicity and maximal benefits.

II.2.4.2 Biodegradation

The changes required when machine-washing was introduced, especially problems with water hardness, caused that soap was replaced gradually by synthetic surfactants. The first practical substitute for soap was fatty-alcohol sulfate. In the 1950´s new, stable surfactants were introduced by the petrochemical industry, especially tetrapropylenebenzenesulfonate. The high washing power, widespread availability, and low price, led to these surfactants meeting about 50 % of the surfactant-demand in the Western world [229-230]. It was then that the biodegradability of surfactants was discovered to be an important, additional criterion for evaluating these products. Insufficient biodegradation led to the development of great masses of foam in streams and rivers in vicinity of dams or other obstructions, *e.g.* in

Germany in the 1960´s [229]. The discovery, that surfactants could pass essentially undegraded through modern wastewater-treatment plants, and thus enter the surface waters, led to both legislation and voluntary agreements between industry and government, at least in Western countries, which effected the transition to the use of biodegradable surfactants in household detergents. In Germany by 1964, the branched-chain alkylbenzenesulfonate (ABS) surfactants, *e.g.* tetrapropylenebenzenesulfonate, which resisted biodegradation, were replaced by linear alkylbenzenesulfonate (LAS) surfactants, which, if pure, are completely biodegradable [231-232]. From the microorganisms´ viewpoint, surfactants represent a potential source of carbon and energy for heterotrophic growth, despite the fact that these chemicals can be toxic. Bacteria use essentially two strategies to access the carbon in surfactants [231, 233], the bulk of which (at least in ionic surfactants) is generally present in the hydrophobic moiety. The first strategy involves an initial separation of the hydrophilic from the hydrophobic (hydrophile attack), which is then oxidatively degraded. In the second mechanism, the hydrophobe is initially oxidised, while still attached to the hydrophile. Both strategies lead to immediate loss of amphiphilicity in the molecule, which therefore no longer behaves as a surfactant. Residues of this primary degradation of surfactants may still contain much carbon to support microbial growth. The subsequent breakdown of these residues to biomass H_2O, CO_2, and mineral salts, represents the complete degradation of surfactants (mineralization). For both mechanisms, hydrophilic attack and hydrophobe attack, the oxidation of the alkyl-chain hydrophobe follows the pathway of chain-shortening through fatty-acid β-oxidation, and for the second mechanism, the surfactant molecule has to be initially activated as corresponding fatty-acid derivative, via ω-oxygenation and oxidations (Figure II-15).

Swisher [231] pointed out, that biodegradability increases with increased linearity of the hydrophobic group and is reduced, for isomeric materials, by branching in that group, particularly by terminal quarternary carbon branching. A single methyl branch in the hydrophobic group does not change the biodegradation rate, but additional ones do.

Cleavage/Oxidation I

II ω-Oxidation

COO-

COO-

β-Oxidation

COO-

β-Oxidation/
Cleavage/
Oxidation/
Desulfonication etc.

Cleavage/
Oxidation/
Desulfonication etc.

CO_2, H_2O, SO_4^{2-}
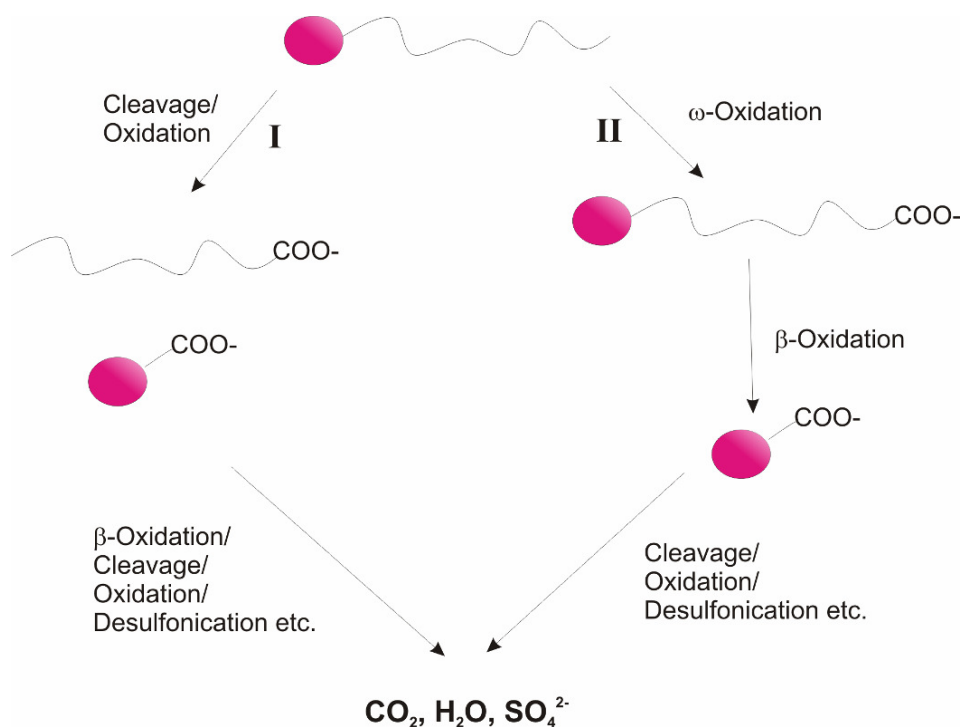
Figure II-15: Schematic mechanisms of surfactant biodegradation: I) direct cleavage of hydrophilic and hydrophobic part. II) degradation via oxidation of the alkylchain.

For example, the extensive methyl-branching of the non-linear chain of common alkylbenezenesulfonates (ABS) hinders these reactions, and explains their slow disappearance from the environment. In isomeric alkylbenzene and alkylphenol derivatives degradation decreases as the phenyl group is moved from a position near the terminal end of a linear alkyl group to a more central position [231]. In polyethylene non-ionics, biodegradation is retarded by an increase in the number of oxyethylene groups. The inclusion of oxypropylene or oxybutylene groups in the molecule tends to retard biodegradation. Secondary ethoxylates degrade more slowly than primary ethoxylates even when both have linear hydrophobic groups. In cationic quaternary ammonium surfactants, compounds with one linear alkylchain attached to the nitrogen degrade faster than those with two, and these degrade faster than those with three. The replacement of a methyl group attached to the nitrogen by a benzyl group retards the rate of degradation slightly.

II. Fundamentals

Pyridinium compounds biodegrade significantly more slowly than the corresponding trimethylammonium compounds, while imidazolium compounds generally degrade rapidly [87, 231].

II.2.5 Emulsions

Emulsions are omnipresent. They can be met in a wide variety of applications: ranging from cosmetic products, over foods (*e.g.* mayonnaise salad cream), cleaning products to colours or tarmac and chemical processes. Thus, they are still in the focus of research. Additionally to the search for improved stabilisation mechanisms, hence, emulsifiers with better biodegradability or lower toxicity than the commonly used ones, the breaking of emulsions is a field of sophisticated investigations [1-2, 4, 234].

II.2.5.1 Definition

Generally the term emulsion describes a system of a liquid saturated phase which is dispersed as drops in another saturated phase.[235-236] The official IUPAC definition of an emulsion is: "In an emulsion liquid droplets and/or liquid crystals are dispersed in a liquid" [237].

Depending on the phasing one has to differentiate between oil-in-water (o/w) emulsions, where oil drops are dispersed in water and water-in-oil (w/o) emulsions, with oil as the outer phase [2-3, 234]. The classification of the two phases either as outer, bulk phase or as dispersed one depends on two factors: On the one hand there is the volume fraction of the phases which commonly cannot exceed a certain value before the emulsion breaks, and on the other hand the type of the used emulsifier and its hydrophilicity or hydrophobicity is crucial. The phase ,in which the emulsifier is more soluble, will become the outer phase (Bancroft´s rule) [238-239].

Emulsions are basically thermodynamically instable, due to the surface energy *ΔE* between the two phases. The interfacial tension γ between the phases is related to the surface energy and the increase of the interface along the following Equation:

$\Delta E = \gamma \Delta A$ <div style="float:right">**II-17**</div>

ΔE is the surface energy, γ is the interfacial tension and ΔA is the increase of the interface.
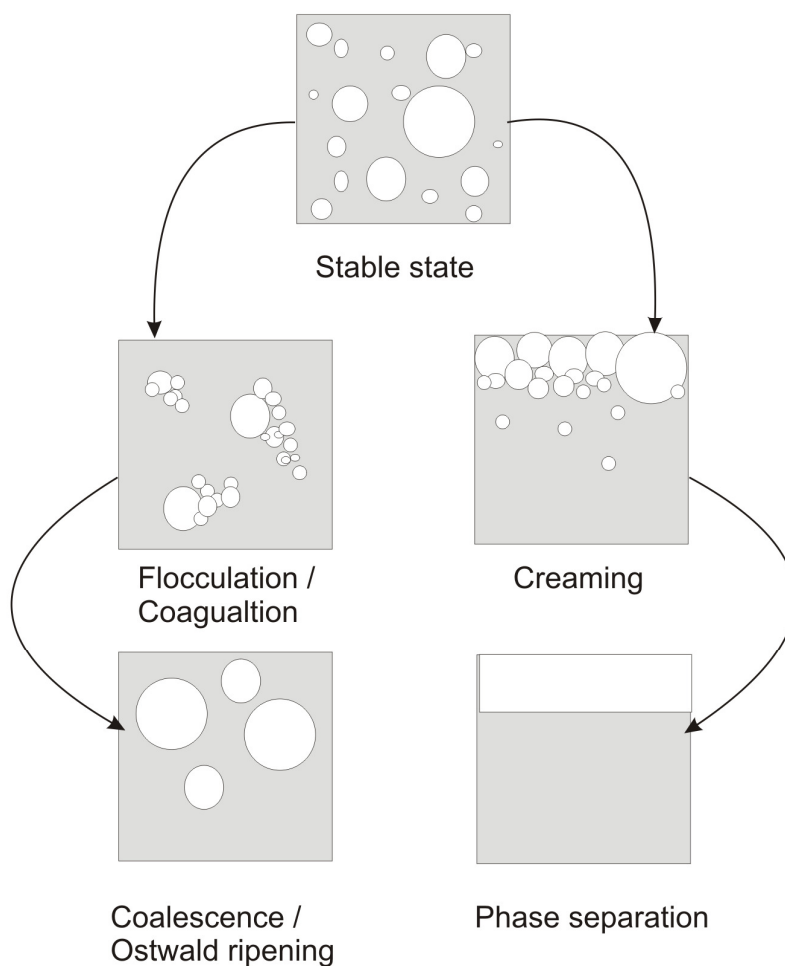
Figure II-16: Destabilisation phenomena in emulsions.

Equation II-17 reflects the fact that emulsions are not formed spontaneously, since a defined amount of energy is necessary to disperse one phase in the other and to build the interface between both, which entails an increase of total energy of the system. The interfacial tension between both phases is the driving force of the tendency of the system to decrease its interfaces. Since the ideal state of an interfacial tension of zero between the oil- and water-phase generally cannot be achieved, the mixtures are thermodynamically

instable [240]. Hence, macroemulsions can be defined as metastable liquid in liquid dispersions. The drop size in such systems usually ranges between 10 nm to 100 μm in contrast to the thermodynamically stable dispersion-type – the microemulsions. These emulsions, consisting of very small droplets in the micellar order of magnitude or of bicontinuous structures, commonly are achieved by a comparatively large amount of surfactant in combination with a cosurfactant. Since macroemulsions are instable, they are susceptible to a couple of physical phenomena (compare Figure II-16) [2, 234]:

- Coalescence – two drops merge into one.

- Ostwald ripening – diffusion of droplet molecules through the medium causes small drops to decrease and disappear while large drops grow.

- Coagulation – drops are in contact and stay together even during Brownian motion.

- Flocculation – drops merge together temporarily and detach during Brownian motion.

- Creaming – differences in density between drop and the medium result in a drop concentration either at the top or at the bottom of the container.

An emulsion can be called stable if "it does not change its appearance in three years or so and it is unstable if it has completely separated after a few minutes" [241]; Or more commonly: If no changes of the macroscopic, microscopic and useful properties appear during a defined period of time. Nowadays, industrial applications in cosmetics and pharmacy refer to 90 days average life at uncontrolled room temperature or it must be specified otherwise. To realize such highly stable dispersions, sophisticated concepts are required.

II.2.5.2 Stabilisation

Generally emulsions are stabilized by so-called emulsifiers which are surface active substances (surfactants). Due to their specific solubility properties they preferentially adsorb at the interface between oil and water, which entails a decrease in the interfacial tension. Emulsifiers improve the emulsions´ stability by decreasing the rate of aggregation and/or coalescence.

In 1949 the "HLB-scale" to characterize the amphiphilic properties of surfactants was introduced by Griffin, with HLB meaning **H**ydrophilic **L**ipophilic **B**alance. The HLB values reflect the ratio of hydrophilic- and lipophilic parts in a surfactant molecule and thus are a good orientation guide for their applications. It has been arbitrarily assessed that the HLB values present one fifth of the percentage of the molecular mass of the polar parts of a molecule. Therefore, the values range between 0 to 20 [242-243]. At the time of their introduction, the HLB values were merely valid for non-ionic surfactants. Later, Davies enhanced the concept by suggesting a simple group contribution method to evaluate the HLB of different surfactants – even charged ones – by their molecular structure [244-245]. The crucial physico-chemical properties salinity, pH-value and temperature are taken into account in a further development of the HLB concept: Shinoda´s phase inversion temperature (PIT) concept [246]. This method bases on the fact that especially non-ionic emulsifiers are highly temperature dependent and turn more lipophilic with increasing temperature due to the dehydration of the EO units. Upon heating of a w/o emulsion, prepared by using a non-ionic surfactant, a critical temperature (PIT) is reached at which the emulsion inverts to a w/o type. At this PIT the droplet size as well as the interfacial tension reaches a minimum. Yet, the rate constant for attaining steady droplet sizes increases rapidly close to the PIT. Thus, the small droplets are unstable and coalesce very rapidly. Upon rapid recooling of an emulsion, which was prepared at a temperature near the PIT, very stable, small emulsion droplets can be achieved [234].

As mentioned in the previous section, stabilisation can be achieved by means of surfactants. Yet also polymers or small particles are frequently used for this purpose.

Emulsions stabilized by particles are so-called Pickering emulsions. In 1907 Pickering generalized the initial observations of Perrin and Ramsden that fine solid particles wetted by water rather than oil acted as emulsifiers for o/w emulsions if they resided at the interface [16]. The process of stabilizing emulsions by particles is a virtually irreversible adsorption leading to outstanding stabilities of certain emulsions. This contrasts the behaviour of surfactant molecules, which are in rapid (< 1 ms) dynamic equilibrium between the oil and water interface and the bulk phase. The effectiveness of the solid particle stabilized emulsions depends on the particle size, particle shape, particle concentration, particle wettability and on the interaction between particles, among other things. At least three mechanisms are proposed for colloidal particles stabilizing emulsions. Firstly, the particles have to adsorb at the oil-water-interface and must remain there - forming a dense film – monolayer or multilayer – around the dispersed drops to impede coalescence. Secondly, additional stabilisation can be obtained by the development of a three–dimensional network in the continuous phase around the drops due to inter-particle interaction [247]. A third mechanism suggested by Friberg, bases on the formation of a liquid crystal at the oil-water interface [248]. For instance, Melzer [249] describes the realisation of a stable Pickering-emulsion with ethyl cellulose building a rigid shell at the oil/water interface. Further, May-Alert and List [250] published the stabilization of cosmetical and dermatological Pickering-emulsions by means of mixtures of emulsifiers composed of both, anionic and cationic surfactants - better known as catanionics or in this case complex-emulsifier. Upon mixing of anionic and cationic surfactants in equimolar amounts, commonly immiscible electroneutral aggregates are precipitated (compare chapter II.2.3). By controlled precipitation of such amphiphilic mixtures particle stabilized, additionally to surfactant stabilized, oil/water interfaces can be obtained. On the basis of Lange and Schwuger´s work [251], who described the behaviour of non-stoichiometric surfactant mixtures and the influence of the amphiphilic

alkyl chainlength, May-Alert deduced the impact of preparation conditions on the stability of emulsions. She could show that the combination of anionic and cationic surfactant, the order of adding the single components, the concentration of emulsifier, the precipitation rate, the temperature, the kind of oil and the sort of dispersing directly affect the quality of the obtained emulsion. Due to their wettability (hydrophilicity), short-chain catanionics tend to form o/w emulsions, whereas long-chain surfactant mixtures preferentially support w/o emulsions. The order of adding the components was found to directly influence the size of the precipitating crystals. The most stable emulsions were obtained by dispersing both surfactants in the oil-phase with subsequently adding the water. Among other things, the precipitation rate of catanionics, which is directly linked to the temperature, was found to restrict the preparation time of such emulsions and hence could influence the stability. Despite of this reports, only Pickering-emulsions stabilized with any kind of small solid particles [252-256], but no emulsions stabilized by precipitation of both anionic and cationic surfactants at the oil-water interface have been mentioned in literature for several years. Recently, N. Schelero *et al.* confirmed the findings of May-Alert and reported on stability evaluation techniques of catanionic emulsions of the cetyltrimethylammonium myristic acid system [17], which was established in the 1990 by Zemb *et al.* [159-160].

III. Experimental

This thesis was realized by means of a variety of methods, which are common standard for the investigation of Ionic Liquid- and surfactant properties, such as: Microscopy (light and electron), rheological investigations, differential scanning calorimetry, thermo-gravimetrical analysis, conductivity measurements, surface tension measurements, scattering techniques (light and X-rays), UV-absorption and fluorescence emission for cmc detection. The fundamentals of these techniques are elucidated in detail in a multitude of books and reports. For that reason only the basics of polarization microscopy – being by far the most frequently used technique within this work – will briefly be described in the following section

III.1 Microscopy

A huge variety of methods exists to determine structures of colloidal systems. Amongst the most popular are scattering techniques like light- and X-ray scattering. Those methods base on the principle of fitting the achieved data according to the properties of an artificial model system. Although these techniques can be very meaningful and can give very valuable hints towards the structure of the investigated system, they are still predicated on a couple of assumptions, which can have more or less impact on the final assertions to the structure [2]. Operations which circumvent that model construction of interactions are directly imaging microscopy techniques. However, also the conclusions drawn from these methods have to be handled with care due to mechanical restrictions in *e.g.* resolution [257].

III.1.1 Polarization Microscopy

Among the several physical techniques, like X-ray diffraction, nuclear magnetic resonance, calorimetry, and vapour pressure measurements, used to identify or locate mesomorphic phases [1-2, 4], the most widely used is the polarizing microscope. The structural differences between phases are evident in the microscope as very typical patterns or "textures" which constitute a convenient and dependable method for identification [1, 4, 258-268].

III.1.1.1   Polarization and Birefringence

Light is an electromagnetic wave. The electric and magnetic field are mutually perpendicular and transverse to the direction of propagation of the wave. The velocity of light, C, in a vacuum is 2.99793 x 10^{10} cm s^{-1}. Light cannot travel faster than this, but if it travels through a transparent non-absorbing medium, its velocity decreases. The refractive index η, of a material is defined as the ratio of the speed of light in a vacuum, C, to the speed of light in a material through which it passes, C_m.

$$\eta = \frac{C}{C_m}$$

III-1

The value of refractive index is always greater than 1.0, since C_m can never adopt a value higher than C. In general, C_m depends on the density of the material, with C_m decreasing with increasing density. Thus, higher density materials have higher refractive indices.The refractive index of any material depends on the wavelength of light, since different wavelengths are influenced to different extents by the atoms that make up the material.

Light can interact in a couple of additional ways with matter. Besides its refraction and reflection it also can undergo absorption or diffuse scattering [269].

Materials generally are classified as being either isotropic or anisotropic depending on their optical behaviour and whether or not their crystallographic axes are equivalent. Light entering an isotropic crystal is refracted at a constant angle and passes through the crystal at a single velocity without being polarized by interaction with the electronic components of the crystalline lattice. Isotropic materials have a single, constant refractive index for each wavelength [270]. Materials whose refractive index does depend on the direction of the incident light are called anisotropic materials [268, 270]. Such anisotropic crystals have crystallographically distinct axes. The optical axis of a crystal is that direction in which a ray of light does not suffer any birefringence (double refraction). Due to the internal structure of the anisotropic crystal (the arrangement of the crystal lattice, the form of molecules of which it is composed of *etc.*), light travels along the optical axis differently than in other directions. If the light beam was not parallel to the optical axis, then the beam is split into two rays (the ordinary and extraordinary) when passing through the crystal. These rays are mutually perpendicularly polarized and travel at different velocities. One of the rays travels with the same velocity in every direction through the crystal and is termed the ordinary ray. The other ray travels with a velocity that is dependent upon the propagation direction within the crystal. This light ray is termed the extraordinary ray.

The two independent refractive indices of anisotropic crystals can be quantified in terms of their birefringence (*B*). *B* is a measure of the difference in refractive index. Thus, the birefringence of a crystal is defined as:

$$B = \left| \eta_{high} - \eta_{low} \right| \hspace{4cm} \textbf{III-2}$$

where $\boldsymbol{n_{high}}$ is the larger refractive index and $\boldsymbol{n_{low}}$ is the smaller. This expression is valid for any part or fragment of an anisotropic crystal with the exception of light waves propagated along the optical axis of the crystal.

For a given propagation direction, there are generally two perpendicular polarizations for which the medium behaves as if it had a single effective refractive index. In a uniaxial material, rays with these polarizations are

called the extraordinary and the ordinary ray (*e* and *o* rays), corresponding to the extraordinary and ordinary refractive indices. Light propagating along the optical axis of a uniaxial crystal (*e.g.* calcite, quartz), provides no unusual results. In this case it travels along that axis with a speed independent of its polarization.
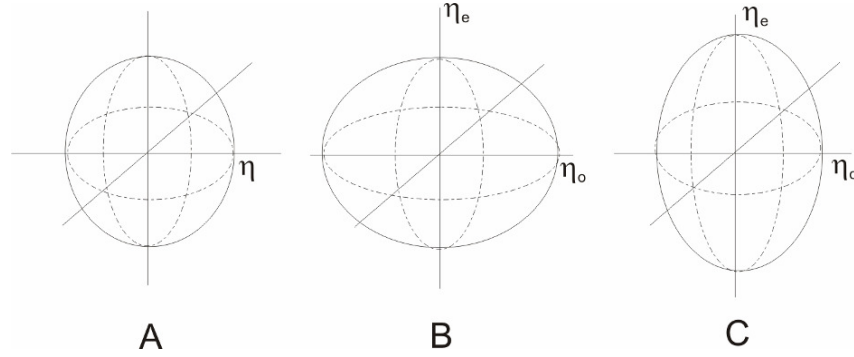
Figure III-1: Schematic presentation of Indicatrices: A) isotrop ($\Delta\eta = 0$); B) anisotrop ($\Delta\eta < 0$; $v_e > v_o$); C) anisotrop ($\Delta\eta > 0$; $v_e < v_o$).

In detail: for a uniaxial material the *z* axis usually is defined to be the optical axis. Hence, for rays propagating in the *xz* plane, the effective refractive index of the *e* polarization varies continuously between n_o and n_e, depending on the angle with the *z* axis. The effective refractive index can be constructed from the so-called Indicatrix, which depicts the orientation and relative magnitude of refractive indices in a crystal (Figure III-1). Uniaxial birefringent materials are classified as positively (or negatively) birefringent when, for light directed perpendicularly to the optic axis, the refractive index of light polarized parallel to the optic axis is greater (or smaller, respectively,) than light polarized perpendicularly to the optic axis.[6] In other words, the polarization of the slow (or fast) wave is parallel to the optical axis when the birefringence of the crystal is positive (or negative, respectively) [271].

The general behaviour of an anisotropic crystal between crossed polarizers is illustrated in Figure III-2. A birefringent crystal is placed between two polarizers (nicols) whose vibration directions are perpendicular to each other

(their orientation is indicated by the arrows next to the polarizer and analyzer labels in Figure III-2).

Birefringent Crystals Between Crossed Polarizers
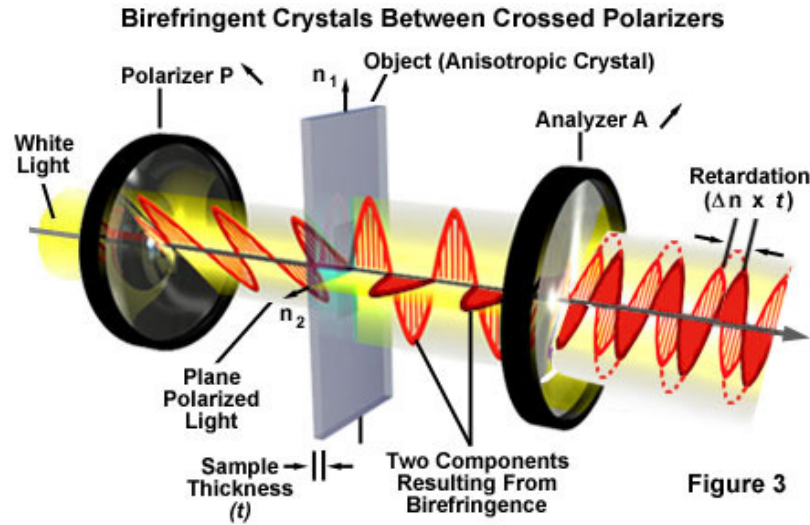
Figure III-2: Polarized light (P) passing through a birefringent crystal and a analyzer (A) [272]**.**

White light enters the polarizer (P) on the left. Its direction of polarization orientation is indicated by the arrow (next to the label). On its sequel path, the light is represented by a sinusoidal light wave. Adjacently, the polarized light enters the anisotropic crystal. Birefringent materials split light rays into separate o- and e-ray components whose electric field (E) vectors vibrate in mutually perpendicular planes. The o and e waves further become mutually shifted in phase due to differences in refractive index experienced by each wave during transit through the specimen. In the following the circumstance of the optic axis of the material being perpendicular to the incident beam, which is the usual case for most specimens that are mounted on a microscope slide and examined in the object plane of the microscope will be considered. In this case the o and e rays follow the same trajectory as the incident ray, while one ray lags behind the other and exhibits a phase difference according to the amount of birefringence. As the o and e waves vibrate in perpendicular planes, they cannot interfere to produce a resultant wave with an altered

amplitude. The mutually perpendicular orientation of the two electric field vectors and phase difference between the two rays result in a three-dimensional waveform of the superimposed wave pair, which is called elliptically polarized light.
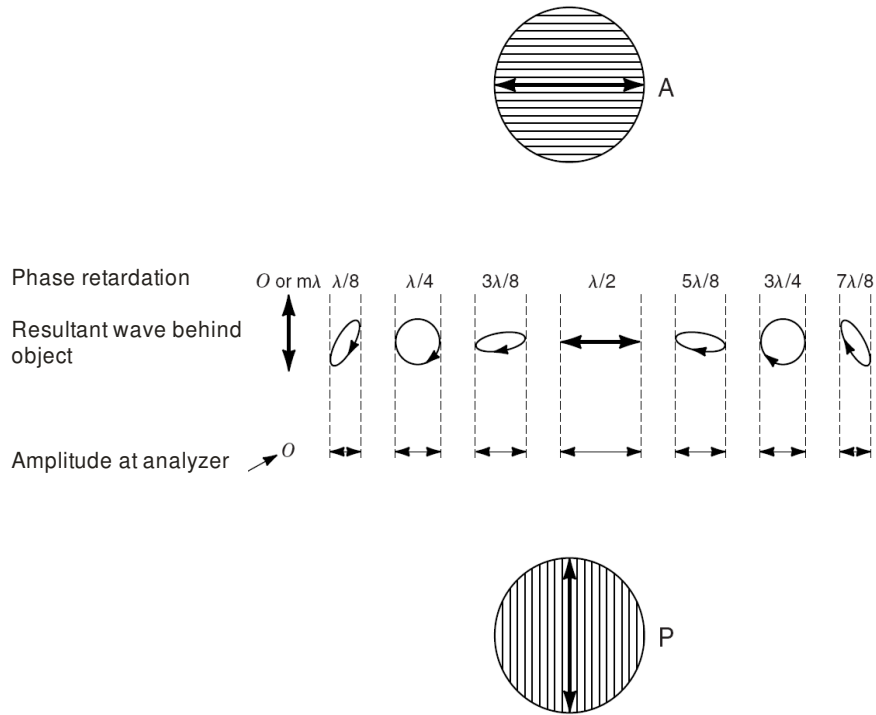
Figure III-3: Effect of relative phase shift between o and e rays on the waveform of polarized light. The orientations of the transmission axes of the polarizer and analyzer are indicated. The amplitudes of the components of vibration passing the analyzer are also shown [273].

The E vector of the recombined wave does not vibrate in a plane over the course of its trajectory, but progressively rotates about its propagation axis. For o and e waves of equal amplitude, the amount of ellipticity depends on the amount of phase shift or/ retardation (Figure III-3). The retardation of one ray with respect to another is indicated in Figure III-2 by $\Delta n \times t$. The

component of elliptically polarized light which can pass through an analyzer varies depending on the amount of phase shift and is shown in Figure III-3. Interference between two intersecting waves of light can only occur when their E vectors vibrate in the same plane at their point of intersection. An object can only be perceived due to differences in intensity and contrast when interference causes a change in the amplitude in the resultant wave. The observed intensity from the o and e waves vibrating in mutually perpendicular planes emergent from a birefringent object is simply the sum of their individual intensities; no variations in intensity are observed because interference cannot occur and the object remains invisible [273].

If polarizer and analyzer were oriented parallel and perpendicular, respectively, to the optical axis of an anisotropic crystal, the position of extinction is reached. No contribution from light passing through the analyzer (because of the single direction of light vibration parallel to the polarizer) can be detected. If the optical axis of the crystal was positioned at a certain angle with respect to the polarizer, a portion of light received through the polarizer is passed on to the analyzer. The maximum brightness for a birefringent material is achieved when the optical axis of the crystal is oriented at a 45 ° angle to both the polarizer and analyzer.

Like explained above, the ordinary and extraordinary rays passing through a birefringent crystal have different velocities. The retardation of one ray with respect to the other can be quantified using the following Equation:

$$\Gamma = t \cdot B \qquad\qquad \textbf{III-3}$$

Where Γ is the quantitative retardation of the material, t is the thickness of the anisotropic material and B is the birefringence (difference in refractive indices) as defined above. Obviously, the greater the difference in either refractive indices or thickness is, the greater is the degree of retardation [274]. The net result is that some birefringent samples acquire a spectrum of colour when observed in white light through crossed polarizers.

Quantisation of the colours seen in birefringent samples is commonly provided by means of the Michel-Levy chart (Figure III-4). This graph

summarizes the impact of the actual retardation, thickness, and birefringence of the sample on the polarization colours seen in the microscope with crossed nicols. The colour produced by the sample, when it is rotated to maximum brightness, can be traced down on the retardation axis to find the wavelength difference between the ordinary and extraordinary ray of the sample. Alternatively, by measuring the refractive indices of the sample and calculating the birefringence (B), the colour of the sample can be found in advance. By extrapolating the angled lines back to the ordinate, you can also calculate the thickness of the sample [259-268, 270-272, 274].
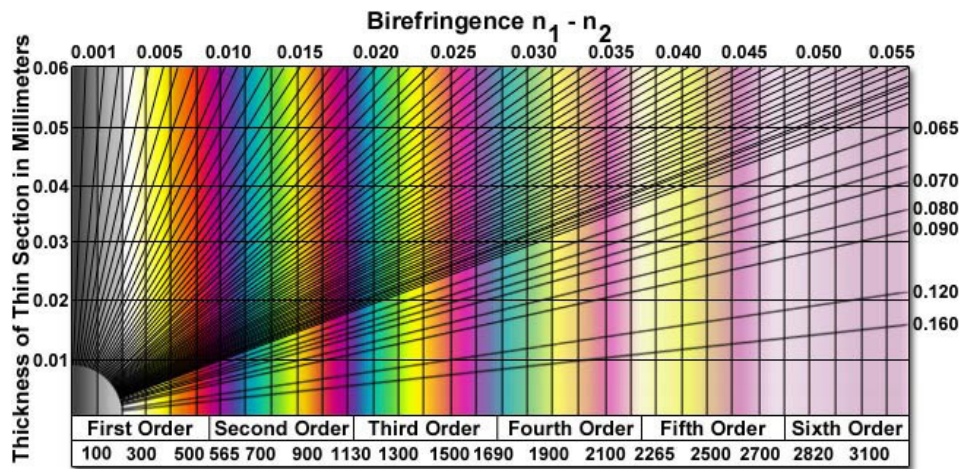
Figure III-4: Michel-Levy Chart, relating birefringence, thickness and the resulting observed colour. The bottom section of the Michel-Levy chart marks the orders of retardation in multiples of approximately 550 nanometers [272].

The polarized light microscope (Figure III-5) is designed to observe and photograph specimens that are visible primarily due to their optically anisotropic character. In order to accomplish this task, the microscope must be equipped with both a polarizer, positioned in the light path somewhere before the specimen, and an analyzer (a second polarizer), and placed in the optical pathway between the objective rear aperture and the observation tubes or camera port. Light from a light source located below the tube and stage of

the microscope is initially unpolarized. This light first passes through the lower polarizer, where it becomes polarized usually such that the light is vibrating from the users' right to left. These directions are referred to as East (right) and West (left). The light then passes through a hole in the rotatable stage of the microscope and enters the objective lens. Mounted within the microscope tube is the second polarizer, called the analyzer, which can be adjusted in the light plane or not. The analyzer has a polarization direction exactly perpendicular to that of the lower polarizer. These directions are usually referred to as North - South. If the analyzer is in, then the plane polarized light coming from the lower polarizer will be blocked, and no light will be transmitted though the ocular lens above. If the analyzer is out, so that it is not in the light path, then the polarized light will be transmitted through the ocular lens [274].
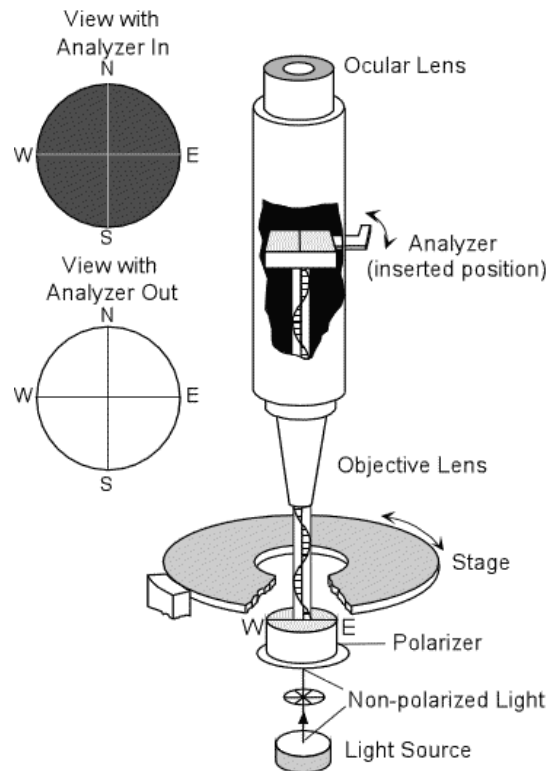
Figure III-5: Layout of a polarized light microscope.

III.2 Liquid Crystal Textures

The identification of liquid crystalline structures via interpretation and assignment of the textures that can be observed in polarized light is a highly efficient and hence frequent method. An understanding of textures in liquid crystalline phases is crucial as it offers the opportunity of the characterization and classification of mesophases type.
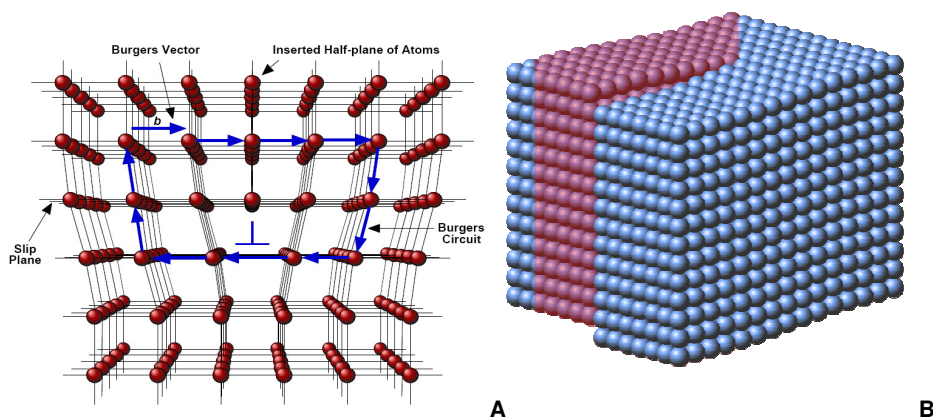
Figure III-6: A) Edge dislocation with Burgers circuit and vector (mathematical constructions to determine the direction of dislocation)[275]. B) Right handed screw dislocation[276].

The experimental analysis of liquid crystalline textures is strongly correlated to the phenomenon of topological defect formation. Mathematically, the structure of a perfect crystal is usually thought of as a rigid network of ions or molecules, where each has a fixed position in the lattice. The pattern repeats infinitely within the crystal in three dimensions. Yet, most of the real

crystals tend to posses defects or imperfections [277]. Such defects can either exist as localized faults and small misorientations in the structure, or in some cases extensive structural discontinuities. Due to the intermediate symmetry of liquid crystals between liquid and solid state, they possess a variety of defects and discontinuities. Additionally, arising from their fluid-like features, they can show strong changes in the orientational order, which results in the formation of disclinations. Disclinations are originated by the translational or rotational shift of material. In liquid crystals solely rotational dislocations lead to defect structures. In a three dimensional network edge and screw dislocations (Figure III-6) are as common as point singularities (Figure III-11).

A   **B**
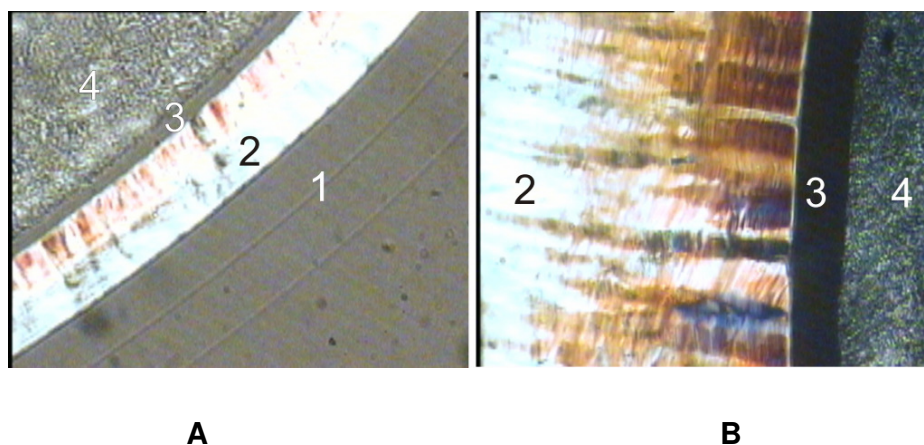
Figure III-7: Penetration-scan of C12EO4COO TEA (chapter IV.2) (A) and C12EO2COO TEA (chapter IV.2) (B). Showing I_1 phases (1), H_1 phases (2), V_1 phases (3) and mosaic structured lamellar phases (4).

The characterization of defects helps to identify and classify liquid crystalline structures. In complete perpendicular orientation of the optical axes of the molecules to the glass slide light extinction is observed. However, maximal brightness can be expected for parallel orientation. In the vicinity of defects, molecules or substructures are highly oriented in very typical patterns.

Depending on the general structure of the liquid crystal only a limited number of defects can occur, which results in very characteristic textures for the different mesophases [259, 261-268, 270, 277-278].
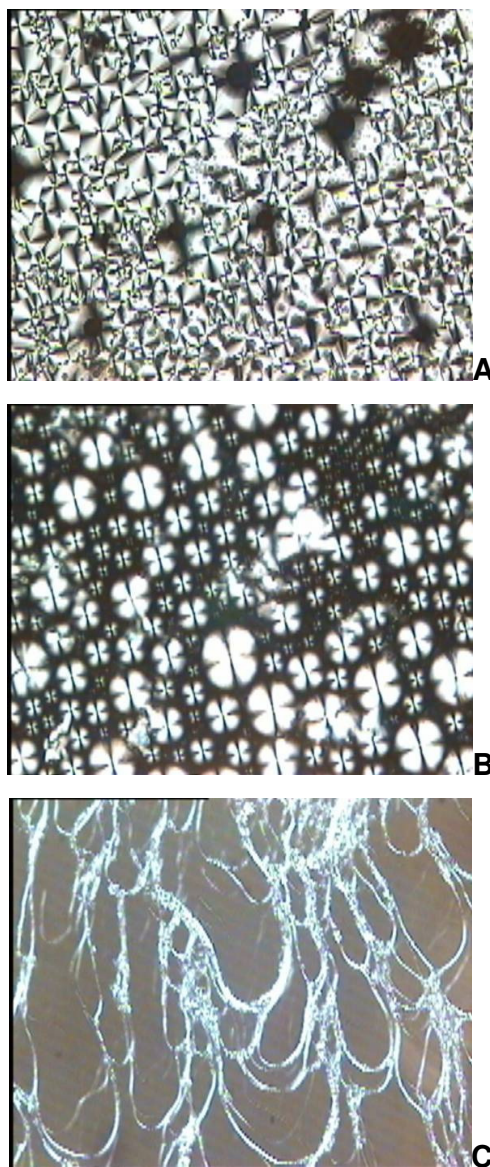
Figure III-8: Lamellar phase with A,B) coarse mosaic texture (maltese crosses) showing "positive" (narrow centres) and "negative" (broad centres) extinction corsses (A) and C) Oily streaks; Irregualr black areas are neat phase in planar orientation.

A differentiation of several mesomorphic phases is illustrated in Figure III-7. The pictures were obtained by allowing a drop of water to diffuse into a neat surfactant placed under a cover glass on the microscope slide. This procedure is called penetration scan. A lamellar phase (4), viscous isotropic phases (1, 3), and a hexagonal phase (2) can be seen.
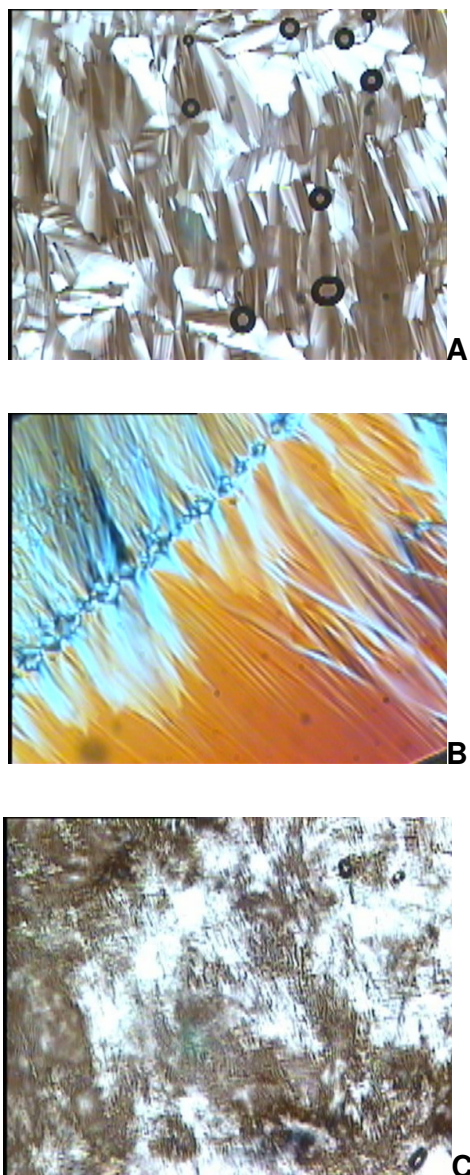
Figure III-9: Hexagonal phases with angular (A), fan-like (B) and non-geometric, striated, cloudy texture (C).

Figures III-8 and 9 are representatives of characteristic polarized-light textures of individual phases. Figure III-8 shows the common textures of lamellar phases. Although it is all lamellar, Figure III-8 C gives the impression of two phases. The irregular black areas arise from the fact that the smectic bilayers are parallel to the surface of the slide and the light is travelling along the optic axis of the structure (non-birefringent direction). The bright bands in the same Figure are so-called "oily streaks" in which the molecular layers are not planar but arranged in the complex "focal conic" (Figure III-11) pattern, a characteristic defect configuration of the lamellar structure. Another characteristic focal conic appearance is the complex network of extinction crosses (maltese crosses) illustrated in Figures III-8 A and B.
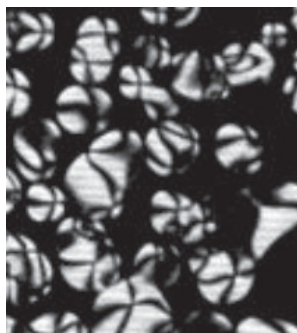
Figure III-10: Nematic structure with extrinction crosses [258].

Upon rotation of the microscope stage, the broad-centred crosses progress to the pinwheel-shaped crosses, making a lamellar phase unambiguously identifiable. Yet, in most cases, such a network of crosses is very fine (Figure III-8) giving the characteristic and common appearance on which the term "mosaic" texture is based.

Like explained in chapter II.2.2.2 the hexagonal phase expresses neither planar nor focal conic arrangements, which is an important distinction from the lamellar phase. However, this phase can assume non-geometric textures,

(Figure III-9 C), which commonly are described as cloudy. The lamellar phase however is never less geometric than a fine mosaic. The closely related angular and fanlike (Figures III- 9 A and B) textures of the H-phase are based on arrangements of the cylindrical molecular aggregates.
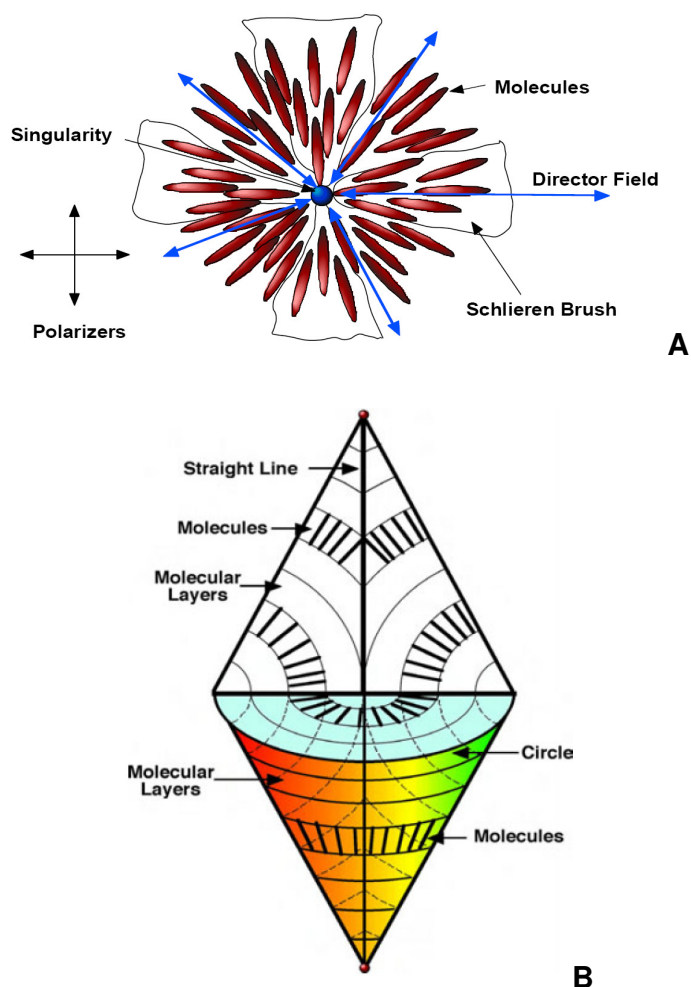
Figure III-11: A) Singularity defect originating Nematic brushes; B) Focal-conic defect (lamellar phases) [275].

In some surfactant systems nematic structures can appear. The nematic material is soft and often stringy in consistency. It is optically birefringent and exhibits characteristic microscopic textures under crossed polarizers,

such as in Figure III-10. These patterns, generally described as "schlieren", make it distinguishes it from lamellar, hexagonal, and the isotropic. The schlieren texture shows dark brushes, which correspond to the extinction orientation of the liquid crystal. Accordingly, the director of the molecules lies either parallel or perpendicular to the polarizer or analyzer axes [258-259, 261-268, 274-275]. Yet, nematic phases may undergo a high degree of disorder with only weak translational order. In these cases, the characteristic textures only can be identified while the sample is subjected to shear strain in a defined direction.

IV. Results and Discussion

IV.1 Lidocaine Carboxylates – A New Class of Pharmaceutically Active, Surfactant-Like Ionic Liquids

IV.1.1   Introduction

In many pharmaceutical formulations local anaesthetics are fundamental ingredients. Their structure allows the regionally very limited suppression of pain with scant influence on the central nerve system. Their effectiveness, in general, bases on the inhibition of signal-transfer by chemical reactions or physical interventions. The mode of action can be described with the help of three general theories [279-280]:

- Disturbance of the fluidity of the cell-membrane, the surface potential and the calcium-ion exchange of the cells

- Conformational change of proteins forming ion-channels [12]

The molecular structure of local anaesthetics is amphiphilic. They contain hydrophilic and hydrophobic parts which commonly are separated by amide or ester-bonds, respectively [281]. Local anaesthetics usually are classified by the two most frequent systematics, which distinguish the structure of the hydrophobic moiety or the type of bond that separates the hydrophilic and the hydrophobic part [280].

Lidocaine is a local anaesthetic of the amide type (Figure IV-1) [281]. Amide type anaesthetics are secondary or ternary amines with pK_a values around 7.7 - 9.9, which form stable water-soluble salts in presence of acids. At a pH

value of 7.4, which predominates in human tissue, they usually are existent in ionized form [282]. However, for accumulation at their destination the unprotonated equivalent of amide-type anaesthetics plays a major role as they only can pass the cell membrane in their uncharged modification [283-284]. At their location of action (inner wall of the cell membrane) the anaesthetics are bound to the Na^+/K^+-ATPase leading to an extension of the time of recreation by a factor of 10 - 1000 and in consequence to a reduction of the number of transmitted impulses [285]. Lidocaine is applied as surface-, conducting- and infiltration - anaesthetic [286].
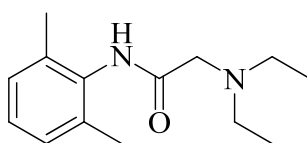
Figure IV-1: Chemical structure of Lidocaine

For surface applications, like in creams and sprays, the transdermal permeability plays a major role [287]. Several attempts have been made to improve this property. Amongst others, the dissolution of drug compounds, in neutral form, or chloride salts in oily media, or the formation of close ion-pairs where tested [288-290]. Furthermore, the encapsulation of Lidocaine in vesicular structures, *e.g.* of the phospholipids type, played a role in several research attempts in enhancing the trans-membrane uptake of the respective drug [291-292]. However, in almost all these attempts one has to deal with a couple of problems. Either the chemical stability of the drug in the mixture, the volatility of the used solvent, or its intrinsic toxicity, as well as the complexity or the physical stability of chosen formulations restricted their applicability. A study to overcome this status quo and to provide a solvent composition which stably dissolves drugs and improves the transdermal absorption is based on the use of water-free carbon acid based ionic liquids as solvents. The improved properties are explained by the formation of cluster ion compositions [293].

An even more elegant method is the neutralisation of the basic drug with a fatty acid. Considering the amphiphilic nature of the resulting salt, a better cell-membrane and hence, an enhanced transdermal permeability can be expected. In case of a pK_a difference of acid and base of approximately four units a complete proton-transfer can be assumed. However, for Lidocaine, with a pK_a of 7.9 [282] this presumption is not valid, as the pK_a values of short chain fatty acids are in the range of 4.5 - 4.9 [294] and for long-chain even higher [295-297]. Therefore, the species are assumed to be only partially charged and membrane uptake might be close to optimum.

n	Abbreviation
10	Lid C12
12	Lid C14
14	Lid C16
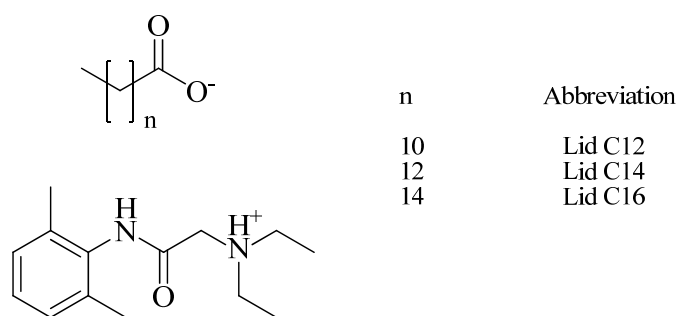
Figure IV-2: Chemical structure and abbreviation of the investigated Lidocaine carboxylates.

Although the outstanding property of this composition of being liquid at room temperature has already been assumed in an earlier work [293], its basic physico-chemical features have to our knowledge not yet been examined. Furthermore, Lidocaine carboxylates are prone to be used as surfactants due to their amphiphilic features. Just like other long-chain ammonium carboxylates their solubility is expected to be drastically improved compared to common alkali based soaps.

The above mentioned properties on the one hand give hint towards strongly facilitated applications in concentrated liquid formulations. Furthermore, Lidocaine carboxylates might become highly interesting for pharmaceutical formulations bearing local anaesthetics, like Propofol emulsions. Hence, we herewith present physical and chemical characteristics of Lidocaine fatty

carboxylates (Figure IV-2) in pure form, in mixtures with water, and in ternary systems.

IV.1.2 Chemicals and Methods

Lidocaine and the fatty acids (Lauric-, myristic- and palmitic acid) were provided by Sigma-Aldrich in purities of 99 % and higher and were used without further purification. To form the surfactants a small portion of Lidocaine was dissolved in chloroform. An equimolar amount of carboxylic acid, also dissolved in chloroform was added drop-wise. The solution was stirred for 15 minutes at ambient temperature followed by the removal of the solvent under reduced pressure. The resulting liquids or respectively pastes, clear to pale yellow, were dried several days, at least 24 hours, under high vacuum ($<10^{-5}$ mbar) and 40 °C. The water content was determined by coulombmetric Karl-Fischer titration to assure values below 500 ppm.

Melting points of the pure substances were determined by DSC measurements with a micro- DSC III+ (SETARAM, France), a Tian-Calvet microcalorimeter. The instrument was connected to a cooling thermostat working at 15 °C. To avoid steam condensation in the calorimetric wall, especially at low temperatures, a constant purge of dry nitrogen was circulated through the sample holders during the measurements. A standard batch vessel, made of Hastelloy C276 steel, was used throughout the present experiments. The samples were held at 20 °C below their melting point for 30 minutes and subsequently heated with 1 °C per minute. The onset of the resulting peaks in the detected heatflow was taken as the melting point.

Viscosity measurements were carried out on a Bohlin rheometer (type CVO 120 High Resolution) under argon atmosphere at controlled temperature. The temperature calibration was performed with a standard viscosity oil and a platinum resistance thermometer within a temperature range between (10 - 80 °C). The accuracy in temperature was estimated to be better than ± 0.2°C. The Lidocaine carboxylates were measured in the range of (10 to

80 °C), working with a CP40/4 ° cone. Samples were studied at shear rates ranging from (0.5 to 500 s^{-1}).

Thermal stability was studied using a thermogravimetric analyser from Perkin-Elmer TGA 7. Samples were measured at a heating rate of 10 °Cmin^{-1}, applying a continuous nitrogen flow. Decomposition temperatures were determined using onset points of massloss, being defined as the intersection of the baseline before decomposition and the tangent to the massloss versus temperature.

For the determination of phase diagrams, an Orthoplan polarizing optical microscope (Germany), a Linkam hot stage with a Linkam TMS90 temperature control and a Linkam CS196 cooling system (UK) were used to carry out the microscopy experiments. The sequence of mesophases was determined by the use of the optical microscopy penetration technique across a surfactant/water concentration gradient at various temperatures. This technique was already described by Lawrence and will not be detailed here [278]. Specific concentrations in 5 wt% steps between 10 and 90 wt% of surfactant in water were chosen to obtain the phase transitions as a function of temperature (0 to 90 °C) using the known textures for the various mesophases [258, 278]. The accuracy of the transition temperatures was ± 2 °C. The heating and cooling rates for all measurements were 10 °Cmin^{-1}. The same transition temperatures occur within ± 2 °C between the different heating and cooling scans.

Surface tension measurements were performed at 25 °C using a K100 tensiometer (Kruess GmbH, Germany). The instrument was equipped with a du Nouy Pt-Ir ring. The different concentrations of the system were achieved by automatic titration of Millipore water by the tensiometer by a double dosing system (Methrom Liquino 711). For this, the surfactant solution was reduced by 10 mL, while 10 mL of water was added. The solution was diluted 90 times, while each concentration was measured ten times to obtain a valid result. Each concentration was stirred for 300 s before the next measurements.

The solubility temperature T_s was determined by direct visual observation, spotting the temperature at which a surfactant solution turned completely clear and isotropic or turbid, respectively while heating. For this purpose, samples of different concentrations were prepared. In order to investigate different molar ratios, Lidocaine or respectively the corresponding carbon acid were added to a 1 wt% Lidocaine carboxylate stock solution in calculated amounts. After stirring for 2 h at 50 °C in order to homogenize, the samples were cooled down to 0°C and kept at that temperature for 2 h. Adjacent, the samples were slowly reheated with 5 °C/h and dissolution or cloud temperatures were recorded.

Micellar shapes were observed by cryo-TEM experiments at the University of Bayreuth at the Institute of Macromolecular Chemistry. The samples were observed with a Zeiss EM922 EFTEM (Zeiss NTS GmbH, Germany). .All examinations were carried out at about 90K. The used acceleration voltage of TEM was 200 kV. All images were registered digitally by a bottom mounted CCD camera system (Ultrascan 1000, Gatan, München, Germany) combined and processed with a digital imaging processing system (Digital Micrograph 3.9 for GMS 1.4, Germany).

Emulsion stabilities were determined by direct visual observation. 1 wt% stock solutions of LidC12 were prepared and mixed according to desired weight ratios with dodecane. Respectively, Lidocaine or sodium chloride were added to the 1 wt% Lidocaine carboxylate stock solution in calculated amounts prior to mixing with dodecane. The samples were homogenized with an Ultra Turrax at 36000 revolutions per minute for 3 min at room temperature. The resulting phase volume fractions were determined after 30 minutes and after 90 days of preparation time. Meanwhile the samples were kept at constant ambient conditions of 23 °C and under exclusion of light.

IV.1.2.1   Pure Compounds

The determination of the physical-chemical behaviour of Ionic Liquids (ILs) is crucial considering any potential application. Additionally to the electro-chemical properties, like conductivity and electro-chemical stability, mainly the liquidus range and the rheological features have to be discussed. The determined temperatures restricting the fluid state of the investigated compounds (Figure IV-2) are summarized in Table IV-1.

Table IV-1: Physical properties of investigated Lidocaine carboxylates.

Substance	T_m [°C]	H_m [kJ/mol]	S_m [kJ/molK]	T_d [°C]	H_2O [ppm]
Lid C12	2.2	22.7	0.08	243.5	364
Lid C14	19.6	35.6	0.12	254.6	340
Lid C16	33.8	49	0.16	246.8	278

T_m: Melting point; H_m: Melting heat; T_d: Decomposition temperature; S_m: Melting Entropy; H_2O: water content.

IV.1.2.1.1   Thermal Stability

The thermal stability of ILs is very sensitive to the type of cation and anion. Generally, it is found at temperatures of 300 °C or even above. The determined decomposition temperatures of the investigated Lidocaine carboxylates are significantly lower. The constricting points of the IL stability are their tendency to form H-bonds and the covalent hetero-atom carbon bonds, respectively. However, in this context it was shown that the decomposition temperature of protic ILs is much lower than that of simple salts as they are prone to form their neutral forms at elevated temperatures [39, 50-51].

Angell and co-workers [49] showed that the thermodynamic driving force for protic IL formation can be correlated to the difference in pK_as of anion and cation ΔpK_a [ΔpK_a(protonated base(HB)) - pK_a(acid (HA))], where HA and B signify the acid and base precursors, respectively. Thus, qualitatively, protic ILs made of stronger acid/base couples can be expected to yield lower equilibrium concentrations of acid and base, resulting in lower vapour pressures. Therefore, considering evaporation, protic salts generally exhibit comparatively only low thermal stabilities [52].

The values of Lidocaine carboxylates (Table IV-1) range in the upper half of thermal stability of protic ILs whose decomposition temperatures may be found far below 200 °C [52]. Lidocaine and fatty acids are a weak base and weak acids, respectively (compare chapter IV.1.1). Thus, the elevated thermal stability cannot be attributed to the pK_a difference, which in case of Lidocaine carboxylates should even enhance evaporation. More likely, the thermal resistence is due to the relatively strong H-bonds in the Lidocaine carboxylates and the partially aromatic character of the cation. Lidocaine bears two amine functionalities, which are prone to interact with the carboxylate oxygen atoms. The comparison with ethylammonium nitrate (EAN), which comprises a single ammonium functionality and expresses a decomposition/evaporation temperature of 210 °C may underline this estimation. Furthermore, Lidocaine bears a xylene functionality. Investigations have shown, that thermal carbon-carbon cleavages inside an aromatic nucleus are not very probable compared to the ones possible on an aliphatic chain. Likewise, tearing a hydrogen atom away from an aromatic moiety requires considerably greater energy than tearing away an aliphatic hydrogen atom. Apart from the high energy carbonyl group, all other bonds of Lidocaine require similar cleavage effort like those of EAN.

IV.1.2.1.2   *Melting Points*

The melting points, just like the fusion enthalpies of Lidocaine carboxylates rise significantly with increasing chainlength. In question of crystalline

packing, the generally weak van der Waals interactions perceptibly influence the structure and in consequence the melting point. Additionally, the overall molecular geometry varies with the number of carbons in the hydrophobic tail and the crystalline packing can undergo dramatic changes [2]. Compared to known surfactant-like ILs, *e.g.* long-chain imidazolium derivatives [39], the melting points are still distinctly low. This circumstance becomes clear as Lidocaine carboxylates can be assigned to the protic IL type. In this case, a significant fraction of uncharged species is present, which disturbs the crystal lattice and leads to an overall reduced impact of Coulombic forces [298].
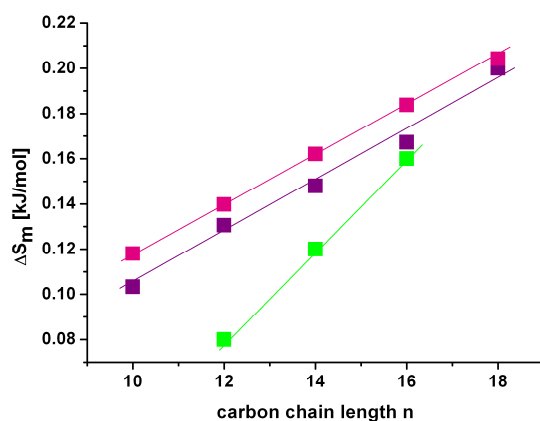
Figure IV-3: Chainlength *n* dependent melting entropies *ΔS$_m$*
of Lidocaine carboxylates ■ compared with
long-chain alkanes ■ and alcohols ■ [299].

Figure IV-3 shows the melting entropies of Lidocaine carboxylates in comparison to alkanes and alcohols of comparable chainlength. In all cases, the entropy rises nearly linearly with the length of the carbon tail. The melting entropy *ΔS$_m$* – the difference between entropy in liquid and in solid state – is a measure for the reduction of order during the phase transition solid → liquid [269]. At constant pressure it is defined as:

$$\Delta S_m = \frac{\Delta H_m}{T_m} \qquad\qquad\text{IV-1}$$

The linear relation in case of alkanes and alcohols can be interpreted as the result of the additivity of dispersion forces in the systems. Generally, the gain in entropy in case of alcohols is lower and shifted by a constant value compared to alkanes. As hydrogen bonds still exist in the melt of alcohols, the amount of order cannot be diminished by the same extent as for alkanes. The parallelism of the alkane and alcohol curve gives rise to the assumption that the number of hydrogen bonds does not change significantly during the fusion process [299]. This seems not true for the Lidocaine carboxylates. Although additionally to the hydrogen bonds, Coulombic forces can be expected for these compounds, one can still draw the conclusion that the total amount of interactions strongly changes with the number of carbons. While with shorter chains the ΔS_m values differ distinctly, the Lidocaine results approach those of the alcohol with a longer hydrophobic tail. Obviously, the electrostatic part of the interactions is diminished, whereas the hydrogen bonds and the dispersion interactions stay unaltered. This goes in line with a reduced acidity of the carbon acid with increasing chainlength and hence more neutrally charged compounds in the mixture. These are still capable to develop H-bonds, while Coulomb interactions vanish. A shift in pK_a of long-chain carbon acids has already been reported several times [295-297]. While an interpretation in such a measure is difficult in solvent free media, a tendency in readiness of proton uptake or cession can unambiguously be asserted and coincides with findings for carbon acids in binary mixtures with water.

IV.1.2.1.3   Rheology

The viscosity measurements of Lidocaine carboxylates were carried out under an argon atmosphere between 10 to 80 °C, revealing Newtonian behaviour over the whole temperature range (Figure IV-4 A). While Newtonian rheology is quite prevalent for common ILs, it is rather inconvenient for the surfactant like type. These ILs tend to form thermotropic liquid crystals, which usually strongly influence the observable rheological properties to that effect that pseudo-plastic shear rate dependence is quite frequent [20, 43]. However, likewise due to the protonation equilibrium of

Lidocaine carboxylates, the expression of mesophases is hindered. The strong Coulombic headgroup interactions are disturbed by the uncharged molecular species, which rather induce the formation of loose three dimensional networks than defined segregation. The over all "low"-energy interaction also serve as explanation for the outstandingly low viscosities [9, 41, 53].
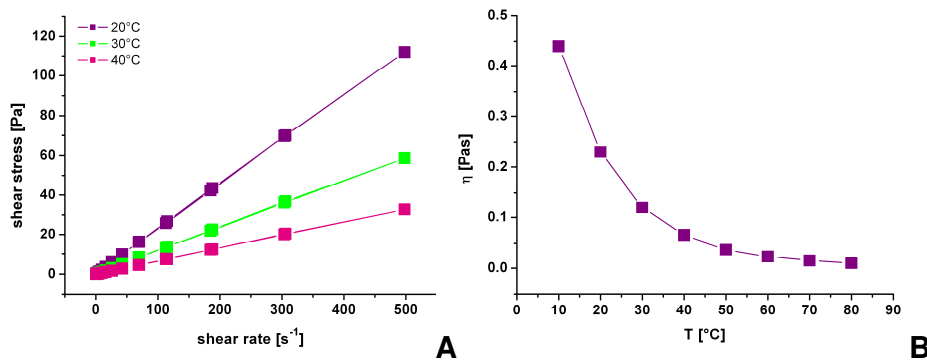
Figure IV-4: Shear stress versus shear rate of Lid C12, demonstrating the Newtonian behaviour (A), the straight lines represent linear fits. Exemplary viscosity η temperature relation of Lid C12 with VFT fit (B).

In consequence, the relative displacement of molecules in the mixture is facilitated. As expected, a characteristic exponential decrease in viscosity was detected with elevated temperature. The viscosity η data were found to be well described by the empirical Vogel-Fulcher-Tammann Equation (VFT) of the following form (Figure IV-4 B):

$$\eta = \eta_o \, \exp\left(\frac{B}{T - T_o}\right) \qquad\qquad \textbf{IV-2}$$

with the absolute temperature T and the fit parameter B, the so-called VFT temperature T_o and η_o, respectively [54].

IV.1.2.2 Binary Mixtures with Water

IV.1.2.2.1 Solubility Behaviour

Soaps, with their outstanding amphiphilic properties, up to date have been utilized for hundreds of years. The oldest and still most widely used surfactants are sodium and potassium carboxylates due to their easy preparation [4]. Nonetheless, these surfactants are restricted in their applicability by their limited solubility in water. Hence, considering any application of a new amphiphilic compound, its solubility behaviour is the most important feature. The most important criterion for a surfactant's solubility is its Krafft point T_{Krafft}. It is the temperature at which the solubility of a surfactant equals the critical micellisation concentration (cmc) and subsequently rises sharply [300].

Additionally, some surfactants show a lower demixing temperature, the so-called cloud point which is mainly observed in the case of uncharged amphiphiles [2]. However, a few investigations also reported on a liquid/liquid phase separation in mixtures of charged amphiphiles and water[301-302].
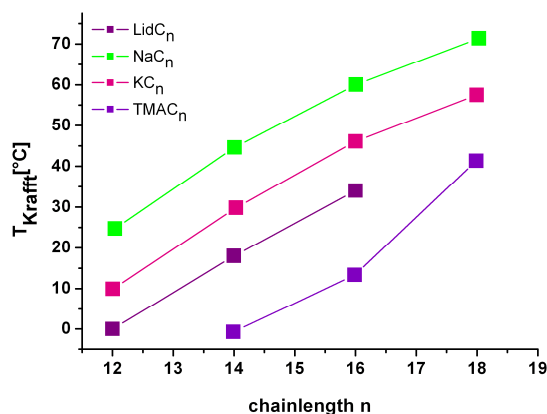

Figure IV-5: Comparison of T_{Krafft} of various carboxylate surfactants with increasing number of carbon atoms n [303].

Lidocaine carboxylates show interesting solubility behaviour between those of ionic and non-ionic surfactants. Figure IV-5 summarizes the experimentally determined data of the observed Krafft and cloud points for the investigated surfactants and compares them with published results for alkali soaps and tetramethyl ammonium (TMA) derivatives. While the Krafft point is still about 25 °C in the case of sodium laurate (NaC12), it is already about 45 °C for sodium myristate (NaC14) or even about 60 °C for sodium palmitate (NaC16) [304-306]. The type of the counterion markedly affects the Krafft point of a surfactant [307]. Obviously, substitution of the alkali ions in soaps by quaternary ammonium ions results in a significantly increased solubility. The Krafft point of NaC14 and KC14 can be dropped from 45 °C and 30 °C, respectively, to 0 - 1 °C with TMA as counterion [303, 308]. The substitution of alkali ions by Lidocaine equivalently helps to diminish the solubility temperature. However, the values distinctly stay above those of the quarternary ammonium ion (TMA).

The Krafft point of a surfactant is the result of the interplay between two competing thermodynamic forces. One is the free energy of the solid crystalline state and the other is the free energy of the micellar solution. A strong headgroup interaction and a good packing in a crystal lattice contribute to the crystal's stability, which is associated with a low free energy. Consequently, the Krafft point is elevated. In turn, a low free energy of the micellar solution, promoted by *e.g.* the hydrophilicity of a compound, favours the solubilised state. However, the energetic state of the micellar solution varies only slightly when changing the counterion, whereas the free energy of the crystalline state may change considerably from system to system. Hence, the latter contribution may be considered as the main driving force in determining the solubilisation temperature [4].

Table IV-2: Comparison of the cmc values of various laureates at 25 °C.

Substance	NaC12	KC12	TMAC12	LidC12
cmc [mM]	24.4	25.5	25	2.4

Obviously, the Krafft points of carboxylate surfactants decrease with increasing size of the counterion. This fact has already been reported for the homologous series of the alkali ions and can be continued by the implementation of TMA ions [309]. It has been shown that the micellar state of the $TMAC_n$ surfactants does not differ a lot from the NaC_n and KC_n soaps. Thus, the reason for the pronounced T_{Krafft} reduction of ammonium carboxylates with respect to the alkali soaps must be a high free energy of their crystalline state [303].

While comparing Lidocaine with the other counterions a further factor has to be kept in mind: Just like the carbon acid, Lidocaine can hydrate and dehydrate depending on the ambient conditions. The moderate pK_a values of acid and base likewise support the formation of uncharged species [282, 294]. The effect of these neutral compounds has already been discussed above. On the one hand, micelle formation is enhanced, which is reflected by the reduced cmc values (Table IV-2) compared to alkali and TMA soaps. On the other hand, the crystal state is energetically destabilized just like it is for ammonium compounds.

In total, the hydrophobicity of the Lidocaine carboxylates is higher than of soaps with ammonium ions with constant charge. Thus, the dissolved state is less promoted which consequently explains the intermediate solubility situation.

In contrast to common alkali soaps and ammonium carboxylates, the investigated Lidocaine compounds show a clouding phenomenon with elevated temperature. This observed turbidity generally appears below 50 °C and seems to be dependent of the chainlength (Figure IV-7). While for LidC12 the clouding can be detected at around 39 °C, it is shifted to 46 °C for the palmitate. Varying the mixing ratio r (Equation IV-3 with n being the number of moles) of Lidocaine and the corresponding acid this point is affected likewise. Although it slightly decreases with excess amount of Lidocaine, it rapidly converges to insolubility up to 100 °C with surplus carbon acid. Apparently, only a small region of total solubility can be

achieved, which is located at equimolarity of both components and expands towards slight excess of amine (Figure IV-6).

$$r = \frac{n_{Acid}}{n_{Acid} + n_{Lidocaine}}$$ **IV-3**

The temperature of clouding is drastically shifted to higher values while salt (sodium chloride) is added to the solution. This effect is less pronounced, if Lidocaine was in excess.

Just like the lower solubility border, the Krafft temperature, the clouding phenomenon has to be interpreted in terms of energetic equilibrium. The cohesion forces of the pure substrate antagonize the dissolved state which is driven by hydrophobic interactions. The temperature dependence of the dissociation constants generally follows the van t'Hoff law [269]:

$$\ln K = -\frac{\Delta H^0}{RT} + \frac{\Delta S^0}{R}$$ **IV-4**

with ΔH^0 and ΔS^0 being the standard dissociation enthalpy and entropy and R being the gas constant.
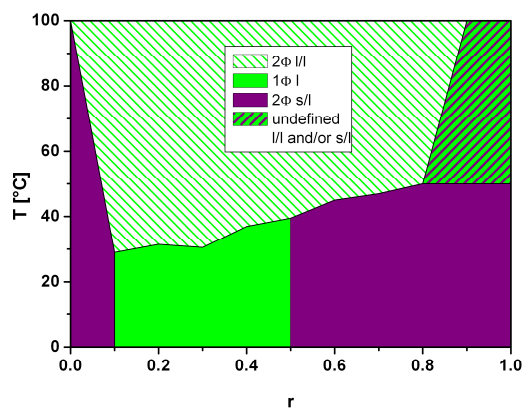

Figure IV-6: Phase behaviour of a 1 wt% solution of LidC12 depending on the molar ratio r of potentially anionic component in the mixture (Equation IV-3).

With negative dissociation energy the equilibrium is shifted towards the deprotonated species. It has been shown that with elevated temperature the pK_b of Lidocaine, [282] as well as the pK_a of carbon acids, is increased. Hence, their disposition to attract, or respectively repel, protons is reduced. Additionally to the hydration of the charged headgroups, the molecules are further stabilized by the formation of hydrogen bonds between their protic parts and water. The strength of these H-bonds is strongly temperature dependent and decreases with supply of thermal energy. Consequently, in addition to the reduced number of charged headgroups and hence possible hydration sites, the enhanced hydrophobic character leads to phase separation [2].

This clouding phenomenon was tracked by cryo-TEM measurements with an 1 wt% LidC12 sample below, close to (35 °C), and slightly above the temperature of phase transition (42 °C). At room temperature, the micelles had a worm like shape with almost infinite length interspersed with a few small vesicles. The portion of vesicles clearly rose while the temperature was elevated.
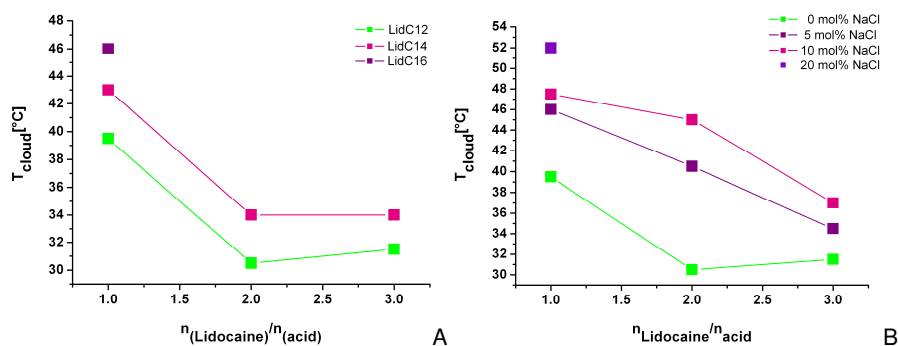

Figure IV-7: A) Cloud temperature of the investigated Lidocaine carboxylates in dependence of the molar excess of amine. B) Cloud temperature of LidC12 with varying sodium chloride content in dependence of the molar excess of amine.

At 42 °C, right above the macroscopic cloud temperature, dark spots with a diameter of several microns, probably composed of "knotted worms",

appeared on the cryo grid. Additionally, the long cylindrical aggregates, having a very high affinity to each other, were unambiguously pushed to the rim of the grid-cavities (FigureIV-8 E) and micro-phase separation was elucidated. These observations are in agreement with the reduced electrostatic repulsion of the micelles due to temperature dependent shift of protonation equilibrium. With the addition of extra hydrophobic compound the aggregation and hence the cohesion of amphiphilic molecules is enforced *inter alia* due to reduced electrostatic repulsion and the hydrophobic effect [90]. As soon as excess Lidocaine is present in the mixture, these agglomeration mechanisms are launched, resulting in diminished phase separation points. Nevertheless, the addition of base, even though it is weak, enhances the deprotonation slightly and thus the hydration of the carbon acid. This might be the reason for the extended solubility range towards amine excess. Rising amount of carbon acid on the other hand would not affect the protonation of Lidocaine due to its inappropriately high pK_a. The strong van der Waals interactions between the hydrophobic chains promote the crystalline state and consequently increase the Krafft boundary. The formation of mixed crystal systems can be expected entailing a lower surfactant concentration in solution. Subsequently, a higher cloud point follows.

The addition of sodium chloride introduces an elevation of the cloud temperature. Although sodium is known to form close ion pairs with carboxylate ions [101, 310], which is expressed by high Krafft temperatures, the solubility of alkali soaps with rising temperature is high as the ions are completely dissociated. Furthermore, the emerging Lidocaine chloride appears to have a salting-in effect. This is supported by the fact that the Krafft point of LidC12 is only marginally affected by the addition of sodium chloride (<0 °C for the pure LidC12 and <5 °C for 20 mol% of NaCl).

While excess Lidocaine is present, the electrostatic headgroup repulsions are weakened, as this hydrophobic compound still bears a certain polarity and hence can be expected to be mainly located between negatively charged carboxylate heads. Consequently, the cloud point again decreases and the

effect of increased solubility by sodium chloride becomes less pronounced (Figure IV-7).

IV.1.2.2.2   *Phase Diagrams*

The optically determined phase diagrams of all investigated Lidocaine carboxylates revealed lamellar phases as sole detectable liquid crystals, independently of the chainlength (Figure IV-9). Although, mainly wormlike micelles were observed in a 1 wt% LidC12 samples (Figure IV-8) no hexagonal phase formed with rising amphiphile concentration, which might have been expected. Hence, the micelles must undergo a shape transition towards double layer morphology. While the surfactant concentration increases, the neighbouring charged colloidal sub-moieties and consequently the surfactant headgroups approach due to simple geometrical considerations. Energetically unfavourable electrostatic repulsions and compression of the counterion cloud force the system according to the principle of least constraint towards a less charged state. The negatively charged carboxylates are reprotonated by H-transfer from the Lidocaine counterions, which is the basis of the so-called charge regulation effect [131, 311]. The micellar shape transformation now can be explained by the shift of the molecular geometry from truncated cones to cylinders and thus, a packing parameter from approximately ½ to 1 [2]. The cylindrical shape, evoked by diminished headgroup repulsion, sustains double layer formation and thus, disc-like micelles. The temperature dependent charge readsorption has already been discussed in detail in chapter IV.1.2.2.1. The pK_a dependent neutralization of the charged compounds elucidates varying packing parameters and explains the observed temperature regulated phase sequence with increasing concentration: micellar, lamellar, phase separation. The morphology shift of predominately worm like micelles to an equilibrium of these with small vesicles at low concentrations (Figure IV-8) underlines this assumption. While the temperature dependent phase equilibria are marginally affected by chainlength, the concentration constrained transitions are significantly shifted to higher amphiphile contents.
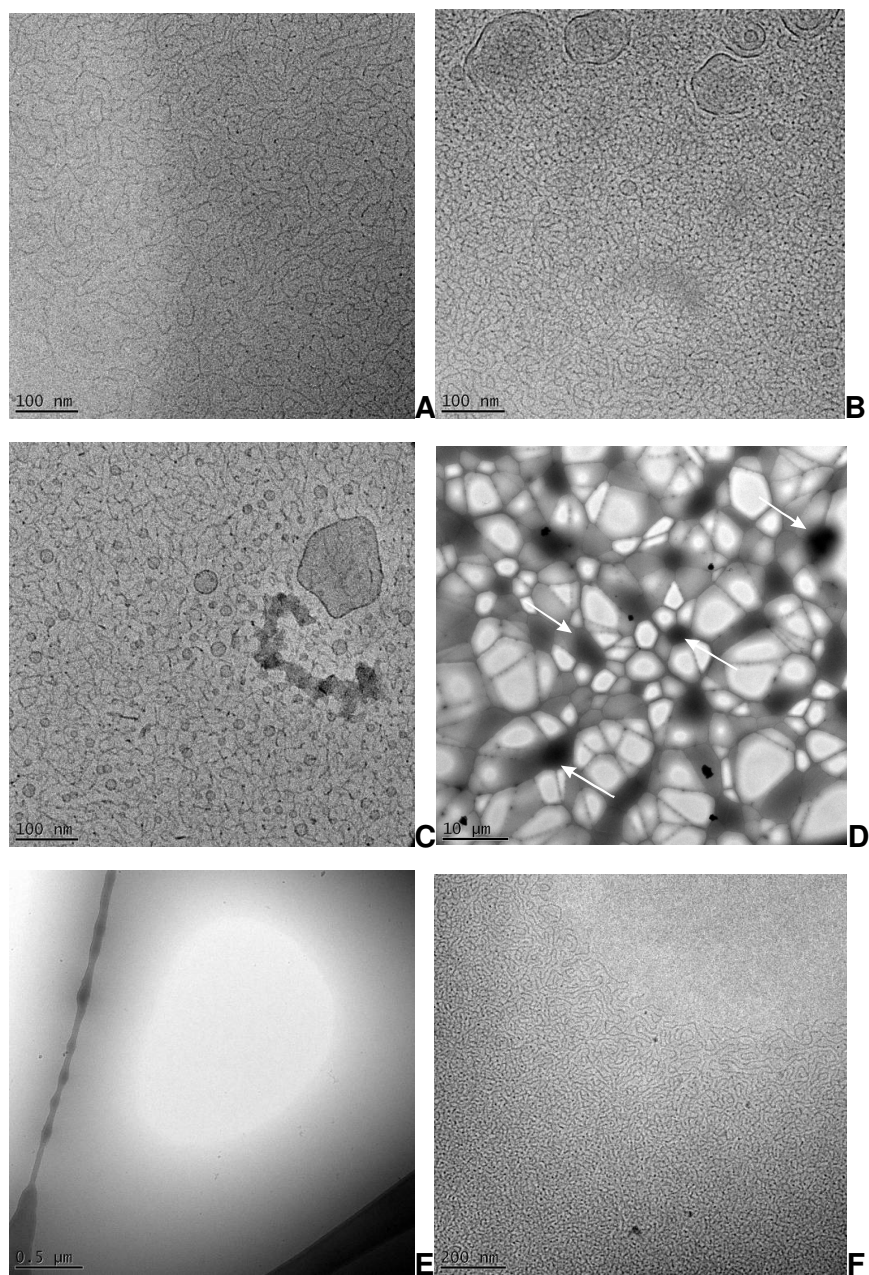
Figure IV-8: Cryo TEM pictures of LidC12 (1 wt%) at 23 °C (A, B), 35 °C (C) and 42 °C (D, E, F). White arrows point to examples of agglomerates. E and F exemplify micro phase separation.
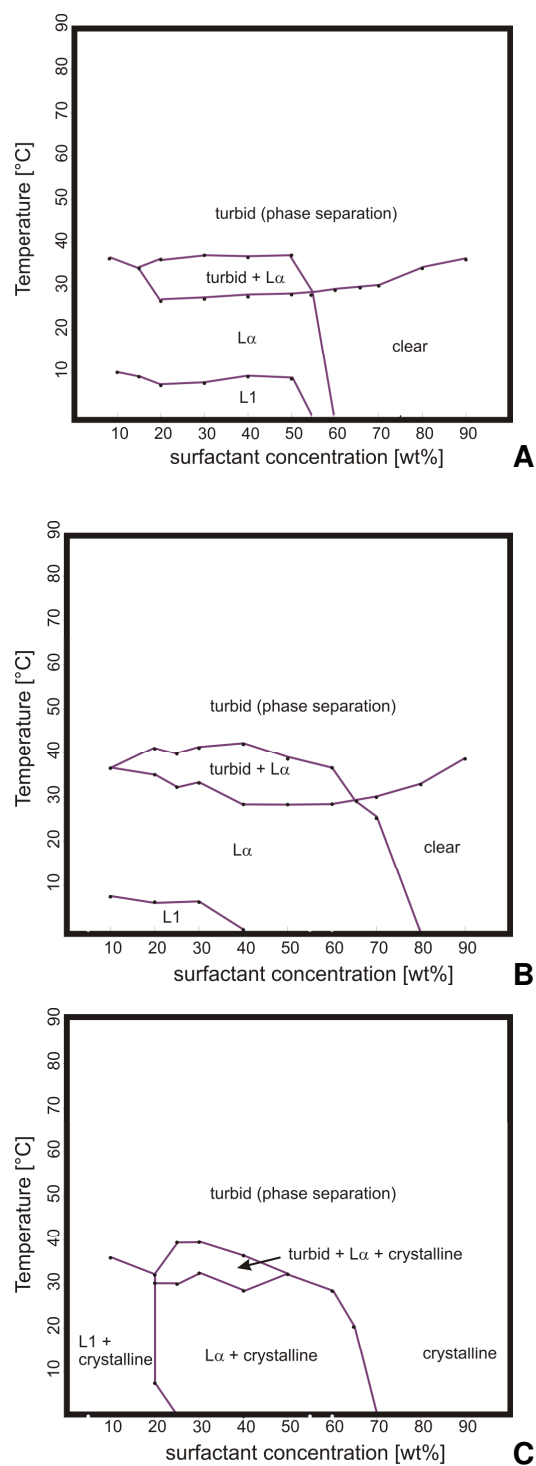
Figure IV-9: Temperature dependent binary phase diagrams of LidC12 (A), LidC14 (B) and LidC16 (C) in water. The lines are to guide the eye. The filled dots represent observed phase transitions.

Through higher pK_a values [295-297] the surfactant geometry of the myristate and palmitate derivatives can already be expected to approximate cylindrical conformation at lower concentrations. The deviating behaviour of Lidocaine palmitate may firstly be explained by its low solubility and secondly by the coarse choice of data points.

IV.1.2.3   Ternary Mixtures

In frequent clinical praxis Propofol oil in water emulsions are applied for injection narcosis. However, probands complain of acute injection pain which was tested to be overcome by the implementation of various appropriate measures [312-313]. Local anaesthetics have been proved to be the best alternative and thus, generally are administered separately or are mixed with the emulsion right before application [314-315]. If applied this way, emulsion stability was proved to be sustainably influenced, [316] which gave raise to enforced investigations on this topic. For example, the efficiency of compartmentalization of local anaesthetic and Propofol by its encapsulation in phospholipids vesicles has been tested [291]. In this context the direct stabilisation of such emulsions by surfactants, which are composed of local anaesthetics and non-toxic amphiphilic counterion, opens an elegant way to solve the stated problems.

On this account the basic emulsifying properties of Lidocaine laurate, being the most soluble amongst the tested amphiphiles, were investigated by means of the model system: water, dodecane, surfactant. Emulsions were prepared according to the method described in chapter IV.1.2. The results are summarized in Figure IV-10.

Obviously, LidC12 is better soluble in oil than in water as it shows an intensified affinity towards the stabilisation of water in oil emulsions (Figure IV-10 A) which is endorsed by the large concentration dependent extension range of inverse micelles (Figure IV-9 A).
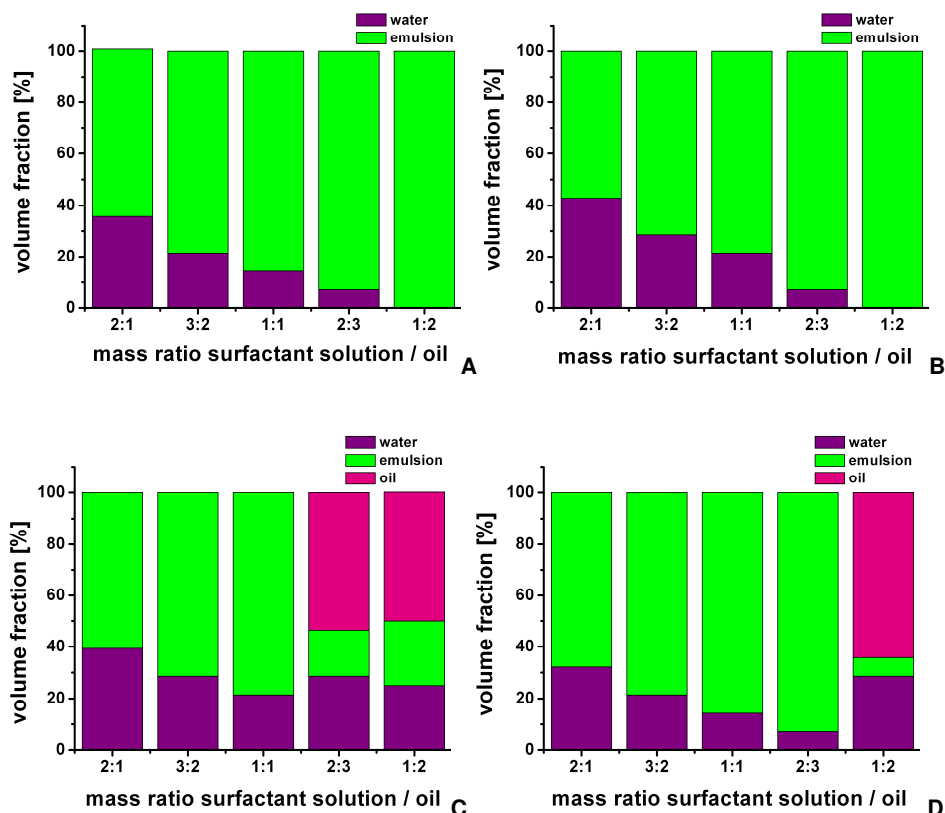
Figure IV-10: Volume fractions of the observed phases of 1 wt% LidC12 solution in the aqueous phase in dependence of the mass ratio surfactant solution / dodecane (oil) after 30 minutes (A) and 90 days (B) after preparation Figure (C) depicts the status with excess Lidocaine (nLidocaine/nlaurate = 2:1) and (D) with additional sodium chloride (5 mol%) 30 minutes after preparation.

The volume fraction of water, which can be incorporated by a micellar phase is restricted to a finite value depending on the micelle aggregation form. As no chain state polymorphism of LidC12 samples in pure form or in 1 wt% dilution in water were detectable via micro DSC-measurements, and as the tests were carried out well below the lamellar phase region, the simple mechanism of film stabilisation with a monolayer of surfactant molecules with high inter-chain flexibility can be presumed. Consequently, LidC12

samples cannot stabilize mass ratios of more than 33 wt% of water even though the surfactant concentration is likewise elevated (Figure IV-10 A). However, the stability of the produced emulsions is noteworthy as no change in volume fraction of the observed phases occurs within 90 days (Figure IV-10 B).

With additional Lidocaine in the mixture (Figure IV-10 C) the charge adsorption affects the emulsion stability. A smaller water fraction can be stabilised in oil compared to the pure LidC12. As the surface charge density of these micelles is lower than that of pure LidC12 micelles, their hydrophilicity is even more reduced. The modified surfactant geometry shifts the micellar shape, which in turn determines the volume fraction of the inner phase. On the other hand, excess oil forces the headgroups of the surfactant molecules in a reverse emulsion system to approach even further. The system reacts to this constraint by reducing its electrostatic repulsion and enhances the formation of neutral species. This finally results in an almost total loss of amphiphilicity of the surfactants and thus nearly complete phase separation of oil and water.

NaCl (Figure IV-10 D) on the other hand augments the systems´ hydrophilicity while it additionally affects it by a simple charge screening. Charge screening reduces the electrostatic repulsion and facilitates the coalescence of the separated droplets. These counter balancing effects are expressed accordingly in no variations of emulsion stabilised water fraction while nearly complete phase separation was observed at high oil fractions in contrast to the untreated LidC12 system where such an effect could not be detected.

IV.1.3   Conclusion

The physico-chemical properties of Lidocaine carboxylates were examined with particular regard to the potential applications of these compounds. The features of the pure substances, especially their low viscosity, make them prone for concentrated applications at ambient temperature. In binary mixtures with water their solubility and phase behaviour with regards to temperature, concentration, excess component and sodium chloride was determined. The low Krafft temperature and the formation of only sparsely viscous lamellar phases as lyotropic liquid crystals recommends applications in a wide concentration range and allows the production of concentrated formulations which stay easily pourable while diluted.

Highly stable water in oil emulsions are favoured which might undergo a drastic stability reduction while heated, as clouding phenomena were observed in binary mixtures with water. These lower demixing points are in the range of body temperature and hence, favour easy drug access in its lipophilic form by injection after being efficiently stabilized at ambient temperature. The system even allows fine-tuning of its critical temperatures by adjusting mixing ratios or adding salt. While the low melting points of the pure Lidocaine carboxylates unambiguously bear tremendous advantages with respect to their handling, they did not seem to affect the stability of the formed emulsions.

The observed phenomena are interpretable with a charge regulation as well as charge adsorption effects and different cation-anion affinities in combination with varying association behaviour. This makes the Lidocaine carboxylates highly valuable and predictable compounds for pharmaceutical formulations.

IV.2 *Physico-Chemical Characterisation of Alkylether-Carboxylate-Based Ionic Liquids in Pure Form and Binary Mixtures*

IV.2.1   Introduction

In the last years, the environmental impact of chemical substances has become an important aspect for the correct development of an industrial process. Currently, there are several new environmentally benign chemicals, which can replace those that are harmful to the environment. Ionic Liquids, which are composed of anions and cations of hydrophobic or hydrophilic nature, are a good example of such chemicals. Ionic Liquids have outstanding properties, like low volatility, non-flammability, high thermal stability, and high solvation capacity. These allow them to be tailored as clean solvents in several catalytic processes, electrolytes for batteries, photochemistry, electro-synthesis, among others [39, 78-81]. Also, their liquid range can be as large as 300°C, allowing for large reaction kinetic control and easy separation of organic molecules by distillation without loss of the ionic liquid. Up to date, many Ionic Liquids have been based on the imidazolium ring and, in a lesser amount, on alkyl pyridinium and trialkylamines [317]. Further, Ionic Liquids can generally be classified in two types, aprotic Ionic Liquids (AILs) and protic ionic liquids (PILs). In addition to the classic properties tailored by changing the anion or cation with different alkylchains, protic Ionic Liquids

are interesting because they have a highly mobile proton [52]. PILs are produced through proton transfer from a Brønsted acid to a Brønsted base. For example, Bicak [318] synthesised an Ionic Liquid formed from the neutralization of monoethanolamine with formic acid. Greaves *et al.* [52] showed different PILs from primary amines and organic and inorganic acids. Iglesias and co-workers proposed a family of such PILs achieved by modifying the aliphatic chain of the organic acid and/or the use of secondary and tertiary hydroxyamines [319-320]. These authors underlined the low cost, the simplicity of the synthesis and a variety of different applications of this new Ionic Liquid family. Moreover, the low toxicity of this kind of Ionic Liquids was verified. Thus, the knowledge of physico-chemical properties of this class either pure or in mixtures can be of technological and/or theoretical interest.

The investigation of long-chain Ionic Liquids attracted rather recent scientific interest. Long-chain ILs are composed of a charged hydrophilic headgroup and one or more hydrophobic tails. Due to their structure and their amphiphilic nature, they can self-assemble. In some ways, long-chain ILs are similar to conventional surfactants and can form aggregates [28]. The knowledge of the aggregation behaviour of such ILs is important to understand how ILs participate in a mixed solvent system. ILs containing the 1-alkyl-3-methylimidazolium ion, [CnMIM]$^+$, have been extensively studied in the field of colloid and interface science. Micellar aggregates formed by three different long-chain ILs based on [CnMIM]$^+$ have been presented previously [29]. Micellisation of a series of *N*-alkyl- *N*-methylpyrrolidinium bromides in aqueous solution has been studied by Baker and co-workers [30]. The aggregation behaviour of long-chain [CnMIM]$^+$ in a variety of other Ionic Liquids was studied by Li *et al.* [321]. It becomes obvious that despite aroused interest in long-chain ILs most of the investigations base on the classical, environmentally questionable imidazolium or pyridinium headgroups. Even less concepts deal with the possibility of melting point reduction by the combination of long-chain anions with smaller cations. Pereira *et al.* recently published a report on a class of biocompatible and biodegradable cholinium-based Ionic Liquids, the cholinium alkanoates with

medium chainlength. These molecules show a highly efficient and specific dissolution of the suberin domains from cork biopolymers [34]. Iglesias and co-workers reported on the synthesis and determination of thermophysical properties of new protic long-chain Ionic Liquids with oleate as anion- and ethanol or diethanolamine as cation [320]. However, apart from this implementation of a double bond in the long-chain anion, other concepts to impair crystal packing are insufficiently investigated.

Recently, Kunz, Buchner and co-workers as well as BASF presented polyethyleneoxyde based short chain carboxylates as efficient counterions to form Ionic Liquids with alkali cations [321-322]. They concluded that compared to common protic ionic liquids or imidazolium and pyridinium based Ils the polarity of these is largely reduced. They suggested a pronounced non-ionic character of the IL resulting from strong interactions between the cation and the carboxy-group of the anion. In addition to the ion pair formation with the carboxy-heads, which leads to a cross-linking within the system, the high viscosities of the investigated Ionic Liquids are explained by the interaction of the alkali cation with the ether moieties (EO). The pronounced flexibility of the EO groups serves as explanation for the low melting points.

These results initiated the transfer of the concept to long-chain alkylethercarboxylates. Although known for a long time, these surfactants turned interesting for industrial applications only in the 1980s [323], when environmental features of surfactants became important along with other properties of ethercarboxylates such as anticorrosiveness, electrolyte stability or alkaline stability, foam-enahncing ability, dispersibilty of *e.g.* silicone oils [324-326]. At the same time, in cosmetics more and more emphasis was made on mildness. Thus, the use of ether carboxylates in such products as shampoos, foam baths, and shower baths [327] began to develop. According to pK_a studies reported by Aalbers, an internal neutralization of the ether carboxylate micelles can result in a less anionic character than that of alkylsulfates [328]. Ethercarboxylate surfactants are weakly dissociated acids with a pronounced non-ionic behaviour at low pH (neutral acid form) and with anionic properties in neutralized or alkaline solutions (ionized form). As

a consequence, the combination with cationic surfactants, even in equimolar mixtures, does not necessarily lead to precipitation [153]. Anyhow, scientific investigations on alkylethercarboxylates mainly focused on binary mixtures with water, while their properties in pure form were ignored to the greatest possible extent [153, 329]. With small alkali ions the thermotropic examinations are rare [328], while they seem to miss completely for organic counterions and especially catanionic mixtures.

Only a few studies report on this subject – thermotropic phase behaviour of catanionics – in the absence of solvent. For example, the number of alkylchains in the catanionics has been varied [330] and the asymmetry in chainlength has been systematically changed [165]. Upon heating, solid–solid phase transitions were observed, just like the formation of a number of intermediate liquid crystalline phases, which mainly are of the smectic type. With respect to chainlength, the asymmetric catanionics have been pointed out to express a more complex thermal behaviour than the symmetric ones [164-165]. Basically, this was explained by a larger number of possible packing arrangements for the chains combined with the differences in the cationic and the anionic chainlength. Although, the thermotropic phases of catanionic surfactants have been subject to some research studies, they have been investigated to a much smaller extent than their lyotropic behaviour. For example, the nature of the thermotropic gel-to-liquid crystal phase transition in catanionic vesicles and bilayers in aqueous systems has been examined. Amongst others, Marques, Zemb, Tanaka and co-workers determined the influence of pH and ionic strength on the chain melting transition in catanionic vesicles and lamellar phases [331-333]. Hoffmann and his group reported on the reversible phase transition from vesicles to lamellar network structures triggered by chain melting [334], while Li *et al.* examined phase transitions in salt-free catanionic surfactant mixtures induced by temperature [335].

The entirety of the above stated facts entailed our investigations of alkyl ether carbon acids with small and long-chain organic counterions in pure form, as well as their examination in binary mixtures with water. In cooperation with

Kao chemicals, a huge producer of alkyl ether carboxylates and their acids, the influence of technically relevant impurities was determined. The main focal point thereby was on sodium chloride, synthetically provoked hydrophobic compounds and the distribution in chainlength as well as in the degree of ethoxylation as factors influencing the physico-chemical properties of the constituted salts. The investigated ion-combinations with corresponding abbreviations are given in Table IV-3.

IV.2.2 Methods

Technical grad alkylether carbon acids and corresponding non-ionic surfactants, diethyleneglycol monohexylether acetic acid (C6EO2COOH) and dodecyldimethylamine (DDMA) were provided by Kao Chemicals. Choline hydroxide was received from Sigma Aldrich as a 45 wt% solution of methanol. Dodecanol (> 98.5 %), tetra- (> 99 %), di- (> 98 %), pentaethylene glycol (> 97 %), sodium chloroacetate (> 98 %) and 1-bromo alkanes (> 99 %) were likewise delivered by Sigma Aldrich. Triethanolamine (> 99 %), sodium hydroxide (*p.a.*) and elementary sodium in paraffinic oil were provided by Merck.

The water content of all investigated Ionic Liquids was determined by coulombmetric Karl-Fischer titration to assure values below 500 ppm before any further investigation.

Melting points of the pure substances were determined by DSC measurements The data were recorded operating a Mettler DSC 30 in a nitrogen atmosphere using Al crucibles. The samples were investigated within a temperature range of (-100 – 50 °C). The heating rate was in all cases 10 °C min^{-1}. Phase transition temperatures were generally obtained from heating curves; melting points were determined by onset analysis. Glass transition points were likewise derived from the thermograms using onset temperature of the transition.

Viscosity measurements were carried out on a Bohlin rheometer (type CVO 120 High Resolution) under argon atmosphere at controlled temperature according to the method described in chapter IV.1.

Thermal stability was studied using a thermogravimetric analyser from Perkin-Elmer TGA 7 Exact description of the method compare chapter IV.1).

Hygroscopicity was obtained by observing the mass gain of a sample during 2 days while keeping it at room atmosphere and constant temperature of 20 °C. The gravimetric analysis was accomplished with a resolution of 1 µg.
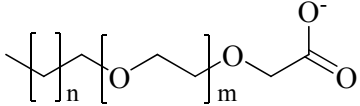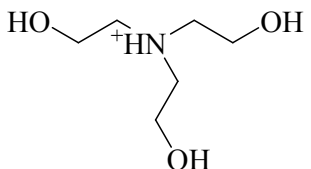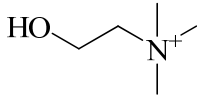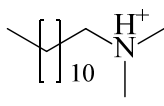
The specific heat capacities of the Ionic Liquids were measured using a Setaram Micro DSC III heat-flux calorimeter. In this type of calorimeter the output signal recorded is proportional to the total heatflow rate. The proportionality coefficient between signal and heatflow is taken as given by the manufacturer's original calibration polynomial. In order to minimize the vapour space, the level of the liquid in the cell is always filled to a maximum extent. Due to the very low amount of gas phase inside the cell, corrections for the vapour-phase heat capacity can be neglected. All samples were prepared gravimetrically [uncertainty ~1µg]. A scanning rate of 0.3 K min^{-1} has been selected in all the experiments. Heatflow signals for blank and reference (water, dodecane, and acetone) were used as average of three independent experimental runs within the period of heat capacity measurements.

For the determination of phase diagrams, an Orthoplan polarizing optical microscope (Germany), a Linkam hot stage with a Linkam TMS90 temperature control and a Linkam CS196 cooling system (Waterfield, UK) were used to carry out the microscopy experiments. The exact description of the method is given in chapter IV.1.

Surface tension measurements were performed at 25 °C using a K100 tensiometer (Kruess GmbH, Germany). The instrument was equipped with a du Nouy Pt-Ir ring. The different concentrations of the system were achieved by automatic titration of Millipore water by the tensiometer by a double dosing system (Methrom Liquino 711). (For details compare chapter IV.1)

The solubility temperature T_s was determined by direct visual observation, spotting the temperature at which a surfactant solution turned completely clear and isotropic or turbid, respectively while heating. For this purpose, samples of different concentrations were weighed in. In order to homogenize the samples, they were stirred at least 20 min at 50 °C. After cooling down to 0 °C and keeping at that temperature for 2 h, the samples were slowly reheated with 5 °C/h and dissolution and clouding temperatures were recorded.

Table IV-3: Investigated cations and anions with corresponding abbreviations.

Cations		*Anions*	
		n = 8; m = 5	C5EO8COO
	TEA	n = 6; m = 2	C6EO2COO
	Ch	n = 12; m = 2	C12EO2COO
		n = 12; m = 4	C12EO4COO
	DDMA	n = 8; m = 5.3	LF1
		n = 12-14; m = 2.5	RLM25
		n = 12-14; m = 4.5	RLM45

Dynamic light scattering (DLS) experiments were carried out with a CGS-II goniometer from ALV (Germany). All measurements were performed at a

scattering angle of 90 °. The measurement temperature was adjusted with a Lauda RS 6 thermostat. For each measurement standard glass cuvettes, cleaned with a cuvette cleaning apparatus in order to avoid any impurities or dust in the sample, were used. Furthermore, the samples were filtered directly into the cuvettes with cellulose acetate syringe filters (0.2 µm pore diameter) to avoid the presence of dust. For each measurement 10 runs each of 45 s duration were performed, the mean value of the ten runs was taken for the data analysis either by cumulant or single exponential fit.

IV.2.3 Synthesis

To unambiguously differentiate the impacts of various impurities, it was necessary to gain access to high purity grade alkyl ether carboxylates. For this purpose "single cut" acids, *i.e.* without any distribution in alkylchain or degree of ethoxylation, were synthesised. Subsequently, the desired impurities were added and the properties of the resulting Ionic Liquids were compared.

IV.2.3.1 Synthesis of Pure Alkyletheralcohols

The adequate ethyleneglycol (di-, tetra- or penta-) was dissolved in 50wt% NaOH (0.2 eq) and heated while stirring to 100 °C. 0.2 eq 1-bromoalcane (dodecane or octane) were added drop-wise within 20 min. After stirring over night the reaction mixture was cooled down to room temperature and extracted 3 times with hexane. The organic phase was washed subsequently with a saturated sodium chloride solution and dried over sodium sulfate for 2 hours. Hexane was removed by rotational evaporation. The raw product was adjacently distilled under high vacuum ($< 10^{-7}$ mbar) for purification (yield ~ 70 %) (Figure IV-11).

IV.2.3.2   Synthesis of Alkylether Carbon acid

Pure

Pure alkyl ether alcohol was dissolved in dry xylene and heated to 90 °C. Metallic sodium (1 eq) was added in small portions within 30 min under nitrogen atmosphere. The mixture was stirred at 90 °C until sodium was completely dissolved (~ 4 h). Dry, finely powdered sodium chloroacetate (1 eq) was added portion-wise under nitrogen atmosphere. The reaction mixture was stirred under reflux over night at ~ 110 °C. After cooling down to room temperature, 100 mL of water and 100 mL of diethylether were added.
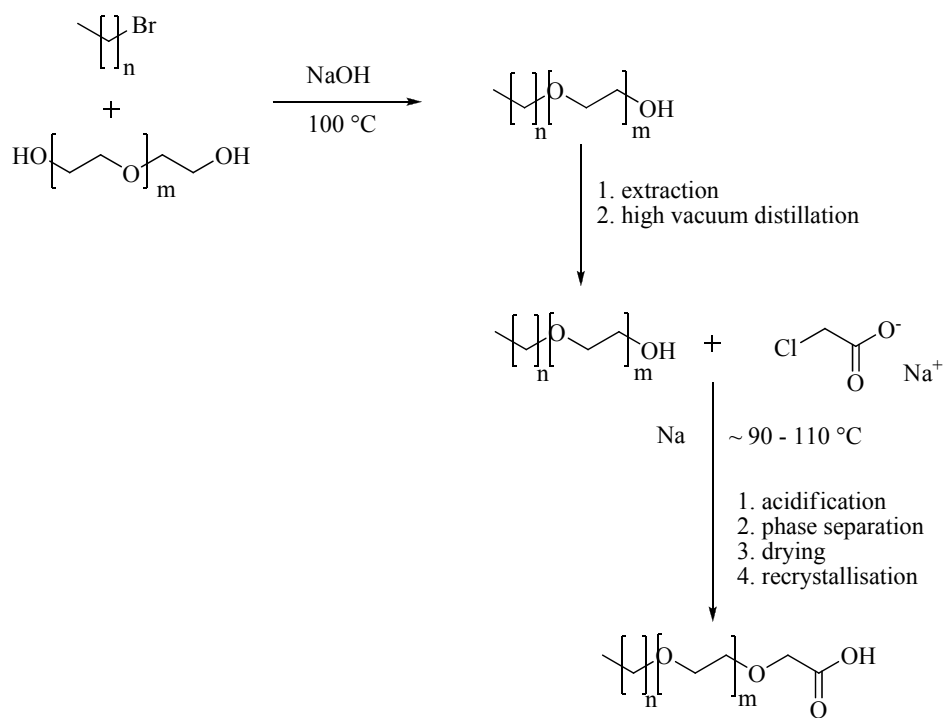

Figure IV-11: Scheme of the synthesis of pure alkylether alcohol and ~acid, respectively.

The mixture was acidified by drop-wise addition of concentrated HC1 to a pH < 2. Phases were separated and the solvents (xylene and diethylether)

were evaporated from the organic phase. The residue was dissolved in 100 mL of n-hexane and adjacently, the product was crystallized in a refrigerator (at about 4 °C). Furthermore, recrystallization from n-hexane was repeated a few times (~ 5 times). Before the last crystallization, the organic phase was dried over sodium sulfate and subsequently, n-hexane was evaporated in vacuo. Octyl-pentaethylene carboxylic acid was not recrystallized, but purified via chromatography with dimethylformamide as solvent (Figure IV-11).

### *Reduced Fatty Alcohol Content*

Fatty alcohols were removed from the provided non-ionic surfactants (Kao Chemicals) via high vacuum distillation ($<10^{-7}$ mbar). Subsequent to the analysis by NMR, those non-ionics were etherfied by Kao to the corresponding acids. These acids were recrystallized several times with n-hexane or dimethylformamide (LF1), respectively. The purity was analyzed via NMR. Acid values were determined by titration with NaOH.

IV.2.3.3   Synthesis of Ionic Liquids

Equimolar amounts of alkyl ether carbon acid and ammonium base (TEA and DDMA) were dissolved in a small amount of chloroform (or respectively ethanol in case of commercial products) and stirred at room temperature for 30 min. In case of choline hydroxide, the base was added to the acid drop-wise as a commercially available solution in methanol without further addition of solvent (Figure IV-12). Afterwards, the solvent was evaporated under reduced pressure. The resulting Ionic Liquids were dried under high vacuum at 40 °C for at least 24 h. The accordant ion combinations are summarized in Table IV-3.

To artificially control the pollution of the Ionic Liquids with a defined amount of ester, which presents the main impurity of commercial grad acids, 19.8 mol% of corresponding fatty alcohol were added to the pure acid. The mixture was homogenized and heated to 50 °C for 60 min. Subsequently, the

residual acid was neutralized with the ammonium base according to the above mentioned way.
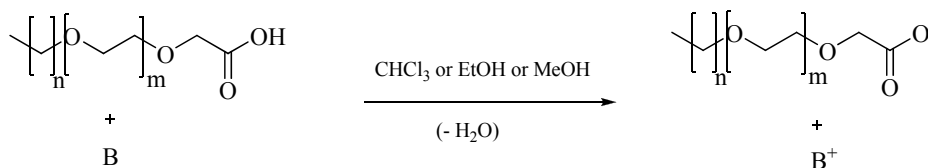
B: basic for of the corresponding amine
B$^+$: acidic form of the corresponding amine

Figure IV-12: Scheme of the synthesis of the Ionic Liquids.

The impurity sodium chloride (NaCl) was added after the synthesis of the Ionic Liquids. Thus, approximately 0.5 wt% of NaCl were added to the pure Ionic Liquid. The mixture was stirred at 50 °C and re-dried under reduced pressure for several hours. After re-cooling, the residual sodium chloride was separated via centrifugation and the supernatant liquid was used for further examinations.

The technical grade- and/or reduced fatty alcohol-acids were transformed according to their acid values transferred by Kao.

If not explicitly mentioned otherwise, all Ionic Liquids (pure and impure) were featured by water contents below 500 ppm prior to physico-chemical investigation.

IV.2.4   Results and Discussion

IV.2.4.1   Pure ILs

In a first part some of the most important physical and chemical properties of the neat, *i.e.* undiluted Ionic Liquids in pure and commercial grade, will be presented. Amongst others the thermal stability, the rheological properties, and the range of liquid state will be discussed.

IV.2.4.1.1   *TGA Measurements*

The thermal stability is an important feature of Ionic Liquids. ILs are discussed to replace organic solvents as reaction media [39]. Commonly used organic solvents are characterized by either a high vapour pressure or a low boiling point or both. Since Ionic Liquids do not have an appreciable vapour pressure, they can be applied in liquid state up to the temperature of thermal destruction [39].

All of the tested compounds showed decomposition only above or at least close to 200 °C (Table IV-4). Decomposition temperatures of common Ionic Liquids can be found in the same range [336]. In case of the pure substances the highest stability was proved for the TEA ILs followed by Ch and DDMA. No significant difference in thermal destruction occurred for Ch or TEA species with either two or four ethoxy-units in the anionic part. In contrast to that, the catanionic ILs with four EOs had a lower onset but a less steep decomposition curve than those with two ethoxy units (Figure IV-13 A). *Id est* the compounds started to decompose earlier but slower than the derivatives with less oxygen. A mixture of both ethoxy-species leads to a reduction of thermal stability (Figure IV-13 B). However, a chain shortening in the anion while the degree of ethoxylation stood constant clearly

destabilized the compound and made it more fragile towards thermal destruction.

As soon as the samples are artificially polluted with the ester of fatty alcohol and acid (~ 20 %) or NaCl (saturated) the samples start to degrade at lower temperatures. With a temperature-reduction of 10 – 50 °C the ester had a much higher impact than the salt with only 5 – 10 °C (Figure IV-13 C and D). Furthermore, the impurities induced a second step of degradation.
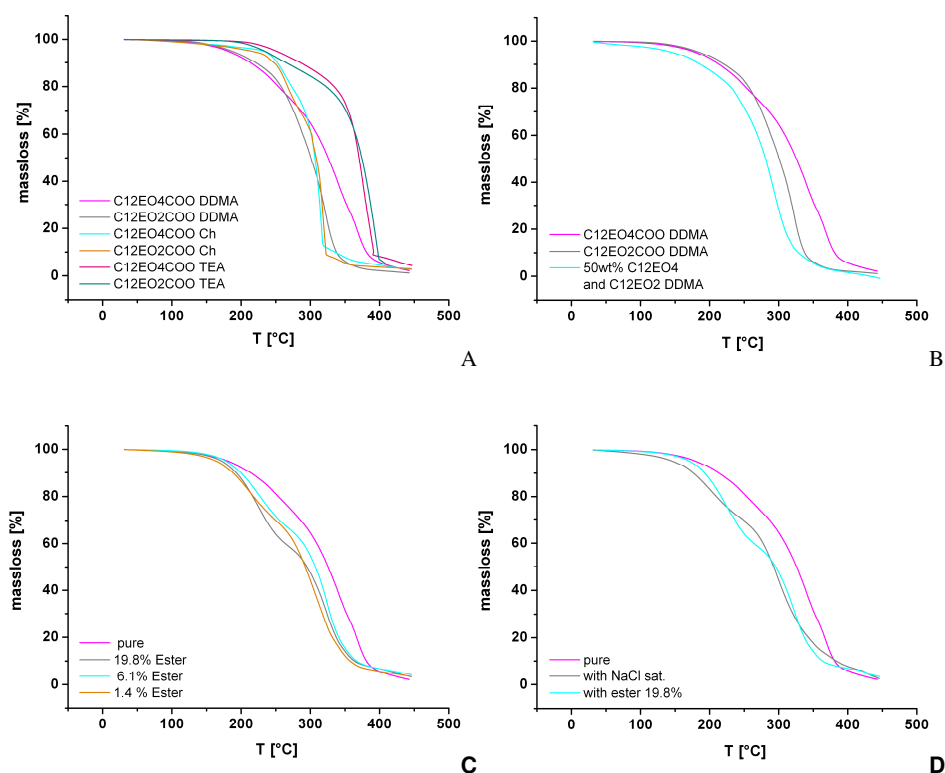

Figure IV-13: Temperature dependent massloss curves. A) comparison of different counterions and degree of ethoxylation. B) Influence of EO mixture. C) Effect of increasing amount of non-polar ester impurity on C12EO4COO DDMA. D) Comparison of sodium chloride and ester impurity on C12EO4COO DDMA.

All technical grade Ionic Liquids showed two decomposition steps. The first onset point was constant within the series of one type of counterion.

Comparing the different counterions with each other, the highest onset can be found for choline followed by TEA and DDMA with a decrease of approximately 20 °C each time. However, the second onset increases differently within one type of counterion, 20 °C for TEA and DDMA and 40 °C for Ch, moving from 2.5 to 4.5 EOs.

In the majority of cases, the pure forms showed higher stability than their technical grade equivalents. However, this conclusion is difficult since the method of evaluation can lead to uncertainties of up to 10 °C. In the case of the pure Ionic Liquids a clear trend of more or less stable species can be assessed. While TEA leads to the most resistant derivatives, the point of decomposition decreases by 40 °C for choline species and further 10 to 20 °C for DDMA. However, the diversity of impurities in the commercial grade ILs is too high, to fix certain tendencies.

The thermal stability of ILs is very sensitive to the type of cation and anion. Generally, it is higher than 300 °C on average [51-52]. The determined decomposition temperatures of the investigated alkyl ether carboxylates are significantly lower. This effect can likely be ascribed to the well-known poor thermal stability of alkylammonium ions [337]. It has to be noted, that in case of protic ILs the thermal lability is composed of two factors: Namely the real thermo-chemical destruction of the compounds and their physical evaporation. These compounds are prone to form their corresponding neutral species at elevated temperatures [39, 50-51]. Their polarity drops entailing less energetic attractions accompanied by facilitated evaporation whose rate is enhanced with rising temperature. Therefore, protic salts exhibit comparatively only low thermal stabilities [52]. Furthermore, the constricting points of the IL stability are the tendency to form H-bonds and the covalent hetero-atom carbon bonds, respectively. As the configurations in the investigated molecules are very similar, the driving force must be the hydrogen bonds. This is underlined by the result of highest thermal resistance of the TEA species followed by Ch. Due to its three additional hydroxyl groups the hydrogen bond formation potential is significantly elevated for TEA compared to Ch which comprises only one OH. This elucidates why the

DDMA compounds are most easily evaporated at higher temperatures as it completely lacks hydroxyl functionalities.

The impact of the degree of ethoxylation is only marginally pronounced. The covalent bonds just like the hydrogen bond formation potential are in the same order of magnitude, independent of the number of oxygens present. This becomes evident, *e.g.* in comparison of the decomposition temperatures of the C8EO5COO compound with the longer carbon-, but shorter EO chain derivatives. Values within the same order of magnitude were detected within the uncertainty of the measurement.

 The introduction of a second decomposition/evaporation step with artificial impurification might be attributed to the following effect: Simply, another species is present with deviating thermal properties. Namely ester – if this was the impurity – and sodium carboxylate – if NaCl was the impurity – which is formed by ion exchange due to the stronger attraction of sodium by the headgroup than an ammonium ion [310]. Attractive forces, mainly H-bonds, are partially modified and a further step in the thermogram can be detected. This assumption is supported by the finding of similar onset temperatures with increasing amount of ester, which due to the lack of charge forms weaker H-bonds, while the perceptual massloss is shifted. These explanations may also hold for the interpretation of the behaviour of technical grade compounds. A diversity of species is present: mainly IL with varying EO degree and chainlength of the anion as well as ester impurity. Likewise, two steps were observed in polluted pure and technical grade case. Furthermore, the catanionic long-chain ILs clearly expressed lower stability than those with OH functionalities. However, further interpretation is critical as the transition temperatures are in close vicinity and the uncertainty of the method can be assumed with approximately 10 °C in this case.

Table IV-4: Decomposition temperatures T$_{dec}$ and glass transitions T$_g$ of the investigated substance.

Substance		T_{dec} [°C]	T_g [°C]	Substance	T_{dec} [°C]	T_g [°C]
C12EO2COO TEA	pure	345	-39	C8EO5COO TEA	351	-57
	+ 20% fatty alcohol ester	300	-43	C8EO5COO Ch	280	-60
	NaCl sat.	295	-40	C8EO5COO DDMA	180	-57
C12EO2COO Ch	pure	307	-44	RLM25 TEA	205	-42
	+ 20% fatty alcohol ester	265	-48		337	
	NaCl sat.	255	-44	RLM25 Ch	224	-47.5
C12EO2COO DDMA	pure	230	-37.5		310	
	+ 20% fatty alcohol ester	200	-43	RLM25 DDMA	179	-43
	NaCl sat.	190	-37		321	
C12EO4COO TEA	pure	345	-42	RLM45 TEA	209	-47
	+ 20% fatty alcohol ester	290	-45		328	
	NaCl sat.	285	-41	RLM45 Ch	226	-54
C12EO4COO Ch	pure	309	-49.5		315	
	+ 20% fatty alcohol ester	270	-50	RLM45 DDMA	183	-47
	NaCl sat.	265	-50		352	
C12EO4COO DDMA	pure	250	-41.8	LF1 TEA	213	-63
	+ 20% fatty alcohol ester	210	-48		358	
	NaCl sat.	195	-41	LF1 Ch	223	-66
C6EO2COO TEA	pure	251	-60.6		309	
C6EO2COO Ch	pure	260	-73.6	LF1 DDMA	179	-62
C6EO2COO DDMA	pure	184	-66 poorly defined		331	

IV.2.4.1.2 *DSC Measurements*

Ionic Liquids are prone to be applied at high temperature due to their high stability and low vapour pressure. Just like the decomposition temperature the point determining the lower limit of the range of liquid state is of high interest. In case of room-temperature ILs, melting points or glass transitions occur at quite low temperatures, likewise enabling applications below 0 °C or lower [39].

It is evident from Table IV-4 that all investigated carboxylate ILs are liquid at room temperature and exhibit a glass transition at around -40 °C or even below. This transition is lowest for the choline derivatives (with approximately -65 °C) whereas it is very similar for TEA and DDMA (with approximately -50°C). In the ranking of variation of the anion the lowest transitions occur for the LF1 species followed by RLM45 with 20 °C higher glass-points and RLM25 with only about 5 °C difference to RLM45. In all cases, one or more endothermic transitions appear at approximately 5 °C (Figure IV-14).

In case of the pure derivatives, all-transitions rise by circa 5 °C compared to the technical grade equivalents. The order of counterions leading to higher or lower transition stays the same.

Artificial pollution (Figure IV-14) with the ester of dodecylpolyethoxy carbon acid and dodecanol leads to a decrease in transition temperatures of approximately 5 °C. Furthermore, an increase in endothermic transitions above 0 °C occurs for the DDMA species, whereas no impact on the number of phases can be found for choline and TEA. The saturation of the ILs with NaCl has almost no impact on the transition temperatures. Solely with DDMA an increase in the number of phases is detected.

Conclusion can be made that pollutions, artificially added or due to technical grade, show only a small impact on phase transitions. Generally, this effect is due to the thermodynamic phenomenon of melting point reduction which describes the shift of the chemical potential of a liquid with solute to lower

values compared to the pure substance [269]. Transitions above 0 °C must be due to thermotropic behaviour since they also appear in the pure species. Further, transition temperatures obviously correlate with the degree of ethoxylation and only secondarily with the chainlength.
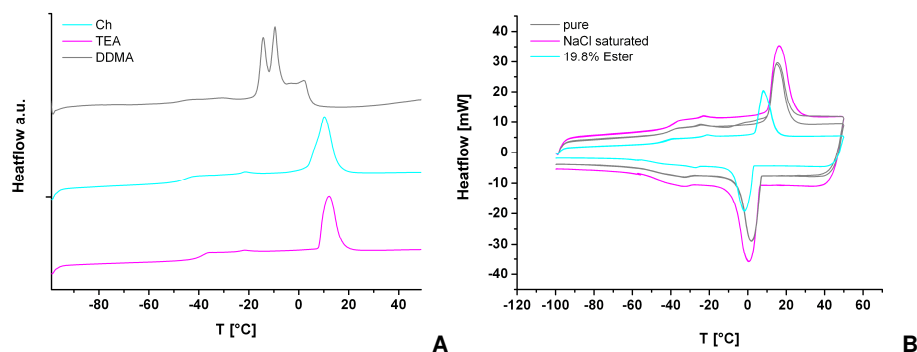

Figure IV-14: A) Counterion dependent thermograms of the C12EO4COO species. B) Impurity dependent thermograms of C12EO2COO Ch.

The melting point of a substance is determined by the energetic difference between its molten and crystalline form. Thus, low melting points are, amongst other impacts, a consequence of disturbed crystalline packing. Generally, the larger, the less symmetric and the easier polarizable the ions are, the lower fusion temperatures can be expected. Comparing these results for different counterions suggests that the liquid range of the ILs towards low temperatures is only marginally affected when changing the cations. Nevertheless, in almost all investigated cases Ch leads to the ILs with lowest transitions. Clearly, TEA is the bulkiest of the investigated ions and hence should induce the lowest glass transitions. However, the lowest values were found for Ch. Although flexibility and sterical hindrance are more pronounced for TEA, its ability to efficiently form hydrogen bonds is superior to that of Ch with only one hydroxyl group. Thus, structuring is enforced by TEA and higher transition temperatures are the consequence. The findings go in line with the behaviour of common RTILs and previous observations by Xu *et al*. A minimum in the relationship between T_g values

(which are representative for the cohesion energy) and molar volumes V_m (which characterize the inter ionic spacing) was identified for a variety of quaternary ammonium RTILs with distinct halogenated anions [338]. However, although the molecular volume is much higher than that of TEA and Ch (V_m(TEA) = 126.47 cm^{-3} mol^{-1}, V_m (Ch) = 103.32 cm^{-3} mol^{-1}, V_m (DDMA) = 221.1 cm^{-3} mol^{-1}) DDMA can be easier packed due to its linear shape. Thus, the alkyl ether carboxylate anion is apparently the driving force for the large liquid range of the examined ILs. Earlier studies on quaternary ammonium RTILs reported an increase of T_g when alkyl ether groups were inserted into the alkyl side chain of the cation, while others observed a decrease [337, 339]. These diverging results may base on two opposite effects of the alkyl ether groups. On the one hand, the introduction of ether functionalities increases the polarity of the system relative to simple alkylchains. On the other hand, it also enhances the chain flexibility, which causes lower T_g values. In the present case, the pronounced chain flexibility seems to outbalance the higher polarity. This becomes further manifest while comparing the transition temperatures of choline dodecanoate with C6EO2COO Ch. Choline dodecanoate forms thermotropic liquid crystals at 68 °C and melts into an isotropic liquid phase at about 120 – 150 °C [340]. Thus, substitution of two CH$_2$ groups by two oxygens in the alkylchain provokes a melting to glass point reduction of more than 190 °C.

IV.2.4.1.3   Viscosity

For any utilization, like dissolution or lubrication, which are classical applications of Ionic Liquids, the viscosity of the substances is a crucial factor. Many ILs with outstanding properties have restricted applicability due to their unfavourable fluidity. The range of viscosity of common Ionic Liquids varies from almost water to honey-like [317].

The rheological features of the investigated compounds strongly depended on the chosen combination of ions. The results revealed TEA and Ch to be the cations, which induce highest viscosities. For EO2 and EO4 these viscosities

were even above 80000 mPas (20 °C). In contrast to that, the fluidity of DDMA species never exceeded 150 mPas (20°C). All Ionic Liquids showed pseudo-plastic behaviour for C12EO2COO as counterion, which indeed shifted to Newtonian for DDMA at 30 °C (Figure IV-15). In all the other combinations merely Newtonian behaviour was observed for this long-chain cation over the whole temperature range from 10 to 80 °C.
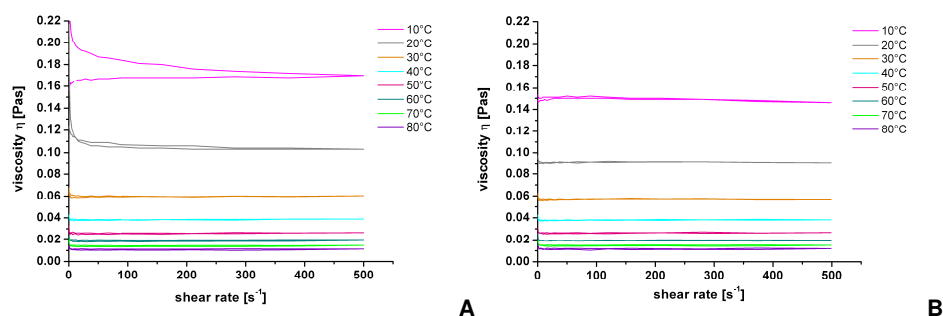

Figure IV-15: Shear rate dependent viscosities of C12EO2COO DDMA (A) and C12EO4COO DDMA (B) at various temperatures.

In all investigated cases LF1 entailed ILs with shear rate independent, comparatively low viscosities (700 mPas TEA, 300 mPas Ch, 120 mPas DDMA (20 °C)) (Figure IV-16). With additional ethoxy units in the anion, while carbon chainlength was kept constant, a drop of rheological transition temperature of pseudo-plastic to Newtonian was observed. After polluting the samples with ester, the viscosity was drastically reduced to half of the value of the untreated substance. Likewise, the transition temperatures (pseudo-plastic to Newtonian) were found at lower values.

For technical grade compounds, less than a half of the viscosity values of the corresponding unpolluted substances were measured. Also for substances with commercial purity, the transition temperatures were much lower.

In general, the number of EO units and the chainlength of the cation define the viscosity and the rheological behaviour. Two trends can be fixed: The longer the chain of the cation or the more EOs the less viscous.
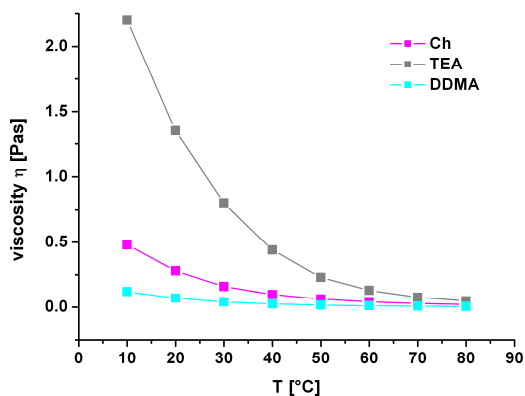
Figure IV-16: Viscosity versus temperature of the investigated Newtonian LF1 ILs.

The viscosity increase with rising ion size diameter has been discussed frequently in literature. This behaviour is a common phenomenon and usually is explained by enforced van der Waals interactions, which provoke higher viscosity values [338-339]. It has been recently pointed out that small quaternary ammonium ions are suitable for the design of low viscous RTILs. For example, Jiang *et al.* reported that the combination of small tetraalkylammonium ions with certain amino acids yields RTILs with viscosities as low as 81 mPas (tetraethylammonium and α-alanine) [341]. The results can be interpreted in terms of a balance between attractive and repulsive forces: the inter-ionic coulomb energy decreases with growing cation size, while the van der Waals energy increases. Yet, simply explaining these results with increasing cation radius is misleading, because lowest viscosities were found for the long-chain DDMA ion, which in return bears the highest molecular volume. Insertion of functional groups such as -OH in the ammonium ions further promotes larger viscosity values. Generally, the additional hydroxyl groups of TEA and Ch enhance intermolecular interactions due to H-bond formation. Hence, the cohesive energy of the system is raised implicating higher viscosities. Furthermore, TEA and DDMA are protic bases which can be protonated or deprotonated as reaction upon environmental constraints. In this case, a significant fraction of uncharged species is present, which disturbs the crystal lattice and leads to an overall reduced impact of Coulombic interactions. TEA and DDMA

146

potentially could act similarly in their nature of organic bases; significant discrepancies appear in their physical features. All three types of cations are expected to undergo similar attractions to the carboxylic site as well as the ether functionalities of the anion. It has been shown recently that three dimensional networking in sodium alkylethercarboxylates originates very high viscosities [342]. While the comparatively small TEA and Ch ions may still fit in the meshes of this construct, the long hydrophobic chains of DDMA and especially their flexibility are prone to destroy H-bond- and electrostatically based networks. In consequence, the relative displacement of molecules in the mixture is facilitated. The strong Coulombic headgroup interactions are disturbed. The high entropy of this system also serves as explanation for the outstandingly low viscosities and the frequently observed Newtonian behaviour at low temperatures. While Newtonian rheology is quite prevalent for common ILs, it is rather inconvenient for the surfactant like type. These ILs tend to form thermotropic liquid crystals, which strongly influence the observable rheological properties to that effect that pseudo-plastic shear rate dependence is quite frequent. Pseudo-plasticity is the dominating rheological behaviour of the investigated substances in this work [20, 43].

The influence of the ether groups on the viscosity has been shown to be highly dependent on the place of insertion of the functionality and hence, the configuration of the ions [339]. Contradicting results have been reported in several investigations discussing the impact of CH_2 substitution by ether moieties on melting- and rheological behaviour of Ionic Liquids [337, 339]. Although the exact reasons for the effect of the alkyl ether group on the viscosity of these salts are not yet well understood, it is believed to be associated with the competing influences of ion–ion and van der Waals interactions and degrees of freedom of the ions in these salts. Considering the fact that the polarity is higher for an alkyl ether group than for an alkyl group, it could be expected that viscosities increase due to enhanced intermolecular interactions. On the other hand, ether functionalities introduce high chain flexibilities, which counterbalance the raised polarity. In this case, lowest viscosities just like glass transitions were observed for the ILs with higher

degrees of ethoxylation. Consequently, flexibility dominates over the polarity of the ether groups and leads to systems with overall weaker intermolecular interactions. This becomes further manifest in the reduced pseudo-plastic – Newtonian transition temperature with increasing number of ethoxy units. As the pronounced chain mobility anticipates efficient liquid crystal formation, the expressed thermotropic phases are prone to thermal disorganization.

IV.2.4.1.4 *Heat Capacity*

Additionally to temperature of decomposition and range of liquid state, the heat capacity C_p is an important thermodynamical property of substances applied *e.g.* as lubricants. The knowledge of the specific heats is crucial for the evaluation of ILs for thermal storage and heat transfer applications. They are likewise important in classifying Ionic Liquids as solvents in any application, where heat has to be added or removed.

The chosen method allowed only the investigation of low viscous samples. For that reason, merely DDMA compounds were examined. The heat capacities of exemplary ILs were measured between 10 °C and 30 °C. The values for 25 °C are summarized in Table IV-5.

Common heat capacities for short chain Ionic Liquids are in the range of 0.6 kJmol^{-1}K^{-1}. Longer-chain derivatives range between 1 and 1.5 kJmol^{-1}K^{-1} [343]. Compared with traditional organic solvents, the heat capacities of Ionic Liquids are generally higher; for example, the heat capacities of water, ethanol, nitromethane, and benzene are between 75 and 292 Jmol^{-1}K^{-1} , at 298 K [344].

The values determined in this investigation range between 1.27 and 1.50 kJmol^{-1}K^{-1}. The highest heat capacity was detected for RLM45 DDMA with 1.50 kJmol^{-1}K^{-1} followed by its pure equivalent C12EO4COO DDMA with only 0.03 kJmol^{-1}K^{-1} less. The heat capacities of the C12EO2COO derivatives are significantly lower. However technical grade ILs show conspicuously raised values compared to their equivalents without any

distributions. The values of the specific heat of the artificially polluted species range between technical and pure compounds.
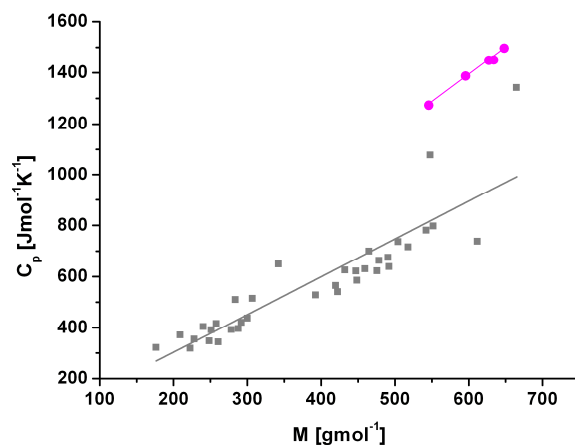

Figure IV-17: Heat capacity data in dependence of the molar mass determined within this work (●) and taken from literature (■) [344]**.**

The heat capacity of a compound is defined as the amount of energy per molecule that the compound can store before the temperature of the compound increases. Generally, the energy can be stored in translational, vibrational, and rotational modes [269]. Therefore, one would expect that a molecule containing more atoms would have more energy storage modes and thus a higher heat capacity. Rooney and co-workers have demonstrated the impact of increasing chainlength upon heat capacity [345]. They postulated that with each additional -CH_2- group the heat capacity rises by approximately 35 $Jmol^{-1}K^{-1}$ at 298 K. Thus the use of a group contribution method might be a reliable way to model the heat capacities of Ionic Liquids, since each additional group seems to have a unit-wise effect on the overall value. Significant changes in the heat capacity as a function of the anion are likewise observed, which demonstrates that the heat capacity increases with the size of the anion. As found for other properties, such as density or viscosity, the anion generally has a greater impact on the heat capacity than the cation [346-347]. The influence of impurities on the heat capacity is difficult to quantify precisely since only a small number of heat capacity data points

have been reported to date. However, few studies present lowered heat capacities with increasing water or chloride content compared to the dried and/or halide free samples [345].

Table IV-5: Investigated alkylether Ionic Liquids and corresponding heat capacity values.

Substance	$Cp \ [Jmol^{-1}K^{-1}]$
C12EO4COO DDMA	1450
C12EO2COO DDMA	1273
C12EO2COO DDMA 19.8% Ester	1292
LF1 DDMA	1449
RLM25 DDMA	1387
RLM45 DDMA	1497

The most enlightening interpretation of C_p data is a plot of the heat capacity at a particular temperature as a function of the molar mass of the IL. This is shown in Figure IV-17 for the compounds measured in this work, as well as a couple of data presented in a report of Crosthwaite *et al.* who collected data for 43 different ILs [344]. Clearly, the heat capacities presented in literature increases approximately linearly with rising molar mass of standard ILs. As this property is correlated to energy storage modes, elevated C_p values with higher molar mass is self-evident. As a combination of two long-chain molecules, one even with EO units, has been investigated in this work, high heat capacity might be explicable. Obviously, the molar heat is correlated to the number of ethoxy units and increases linearly with the molar mass of the compounds. However, the values are outstandingly high compared to commonly known ionic liquids. A shift of more than $550 \ Jmol^{-1}K^{-1}$ was

observed compared to ILs with simple aliphatic chains. This fact is probably due to the high mobility of the investigated anions. Their ether functionalities express a significantly more pronounced flexibility compared to linear alkylchains. Thus, the number of degrees of freedom of the system is higher, more molecular conformations are available and likewise more energy storage modes. Although a debased heat capacity of ILs was reported for water and halogenides as impurities, as mentioned above, the pollution with long-chain uncharged ester molecules with similar chain flexibility support specific heat as well as a distribution in chainlength or degree of ethoxylation. These inhomogenities still render similar interaction sites. Like the other charged molecules, they facilitate the loosening of the three dimensional network which mainly bases on electrostatic and H-bond interactions allowing the system a higher flexibility with less input of energy.

IV.2.4.1.5 *Hygroscopicity*

The water content of a substance is a limiting factor for many applications. Several fields of use, like electrochemistry, are completely inaccessible if the water content was too high or the water uptake can not be controlled without complex methods. In addition it is well-known that water is almost inevitable in Ionic Liquids (ILs). Even those ILs classified as hydrophobic ones can be saturate with about 1.4 wt% of water, which is a significant molar amount. For more hydrophilic ILs, water uptake from air is even more pronounced. This means that all commercial products contain a certain amount of water, which depends on the production conditions and the logistics, since the ILs can reasonably be expected to come into contact with traces of water. Depending on the application, this water content can cause enormous problems. The presence of water generally has significant influence on the physicochemical properties of ILs. It has been demonstrated that a simple 0.1 molar fraction of water content (which means about 1 wt% of water in the sample) decreases viscosity by about 20 % [348] and it increases the electrical conductivity even by about a 30% [349]. As mentioned above, the content of water within an IL is of main interest from the practical point of few. To

design any proposed application the different physical magnitude values are of high importance.

By excessive drying of the samples, it was ensured that their water content was well below 0.1 % before starting the measurement (Table IV-6). Maximum water contents after the investigated period of time between approximately 2 and 7 wt% were observed. The Water content of the technical grade compound was lower compared to the pure equivalent. The EO4 sample attracted less water than the investigated EO2 species. While the DDMA and Choline samples seem to have reached saturation after the investigated period of time the water content of the TEA compound appeared to increase further (Figure IV-18).
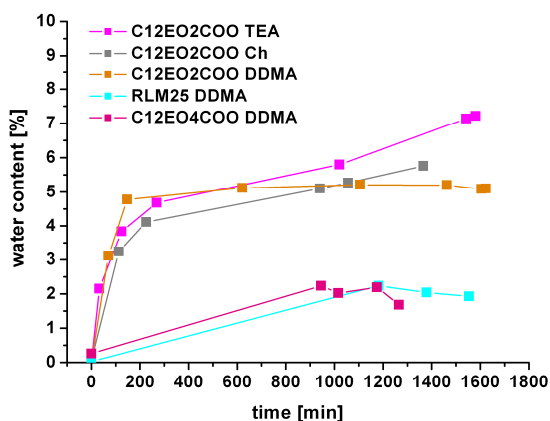
Figure IV-18: Experimentally determined water contents of exemplary Ionic Liquids as a function of the time, while being left open to the atmosphere.

Cuadrado-Prado *et al.* have measured the quantity of mass adsorbed by six Ionic Liquids according to the humidity grade of the atmosphere [350]. Their results showed that the water adsorbs to the surface of the IL, generating a film on it. The quantity of adsorbed water strongly depended on the chemical nature of the Ionic Liquid. However, for the same family of compounds the increase in alkylchainlength decreased the adsorbed quantity of water. It was

concluded that if the alkyl chainlength was diminished, the number of anchorage sites for water molecules to be adsorbed was increased. These results revealed that the reduction of the carbon chain by two atoms increases the number of water adsorption sites by more than 85 %.

Thus, in the present case it can be concluded that due to the increased number of oxygen in the TEA sample and the long-chain of the DDMA cation, the catanionic sample is more hydrophobic. Hence, a smaller amount of water can be adsorbed. Furthermore, the technical grade sample contains lots of ester - comparatively less hydrophilic than the charged equivalent - impurities which lead to percental less water uptake compared to the pure substances.

Table IV-6: Experimentally determined water contents (Karl Fischer) right before the beginning of the hygroscopicity test.

Substance	Water content [%]
C12EO2COO TEA	0.038
C12EO2COO Ch	0.074
C12EO2COO DDMA	0.021
RLM25 DDMA	0.014
C12EO4COO DDMA	0.0117

However, these results need to be handled with caution because the quantity of adsorbed water also depends on the area of open surface to the atmosphere. The detectable amount of water will rise with the surface of the Ionic Liquid; however, not proportionally. Albeit, all measurements were carried out in equal sample holders and similar masses of the Ionic Liquids were investigated no distinct care was taken on surface smoothing. Particularly in the case of the high viscous sample, this might have had a not negligible impact. Furthermore, relative humidity profoundly influences the total water content. The data presented here were collected within four

weeks. However, the samples were open to room atmosphere during the measurement and thus, results were influenced by meteorological conditions, which have not been recorded.

IV.2.4.2   Binary Mixtures with Water

All of the investigated Ionic Liquids also have surfactant properties due to the amphiphilic nature of their anionic and/or their cationic part, respectively. Hence, their properties in binary mixtures with water will be discussed in this second part.

IV.2.4.2.1   *Surface Tension*

Detergent properties strongly correlate with the reduction of the surface tension γ of water by a surfactant. The lower the surface tension the better the "cleaning" powers of the investigated amphiphile. Furthermore the cmc (critical micellar concentration) gives a hint to the amount of detergent necessary for optimal applications [4].

Table IV-7 summarizes the cmc as well as the corresponding surface tension values γ of the investigated compounds. Since in the technical grade products a diversity of substances with varying surface active properties was present, a defined concentration dependant investigation of these surfactants was not possible unambiguously. Hydrophobic impurities, expected to dominate the surface properties in these technical grade samples, are known to reduce surface tension [2]. Consequently, γ of the surfactant made out of the provided alkylethercarboxylate ILs are in the same order of magnitude, or even below, the values of the pure compounds. No significant difference in cmc or surface tension between desalted technical grade products and samples with reduced fatty alcohol was determined.

The surface tension values of all investigated surfactants ranged between 25 and 30 mN/m. As soon as the pure samples were artificially polluted with ester, the values were even reduced by 5 mN/m, circa.

Table IV-7: Cmc and surface tension (γ) values above the cmc (concentration-independent constant region) of the investigated substances.

Substance		*γ* [mN/m]	*cmc* [mol/L]	*Substance*	*γ* [mN/m]	*cmc* [mol/L]
C12EO2COO TEA	pure	29 +/- 1	0.0002	RLM25 TEA	26.1 +/- 0.1	n. d.
	19.8% Ester	27 +/- 1	0.00005	RLM25 Ch	30 +/- 4	0.0002 +/- 0.0001
C12EO2COO Ch	pure	27 +/- 1	0.0002	RLM25 DDMA	26.1 +/- 0.1	0.00001 +/- 0.000005
	19.8% Ester	26 +/- 1	0.00003	RLM45 TEA	30 +/- 2	0.00017 +/- 0.00005
C12EO2COO DDMA	pure	26.6 +/- 0.05	0.00007	RLM45 Ch	32 +/- 2	0.00014 +/- 0.00005
	19.8% Ester	25.6 +/- 0.2	0.00003	RLM45 DDMA	25.5 +/- 0.1	0.000028 +/- 0.0000005
C12EO4COO TEA	pure	30 +/- 1	0.0002	C6EO2COO TEA	30 +/- 2 ?	~0.27
	19.8% Ester	26 +/- 1	0.00005	C6EO2COO Ch	30 +/- 2 ?	~0.28
C12EO4COO Ch	pure	28 +/- 1	0.0002	C6EO2COO DDMA	25.3 +/- 0.2	0.001
	19.8% Ester	26 +/- 1	0.00004	C6EO2COO DDMA NaCl sat.	25.2 +/- 0.2	0.0008
C12EO4COO DDMA	pure	29.2 +/- 0.2	0.00009	C12 Na	n. d.	0.031 (*)
	19.8% Ester	26.2 +/- 0.3	0.00006	C12EO2COO Na	n. d.	0.0063 (*)
				C12EO2COOH	n. d.	0.00007 (*)

n. d. = not determined γ = surface tension

(*) = taken from [328]   cmc = critical micelle concentration

Cmcs ranged between $4 \cdot 10^{-5}$ and $2 \cdot 10^{-4}$. Values were highest for Ch and TEA (very similar) and lowest for DDMA. With reducing the number of EO units from four to two, the cmc value was lowered. Addition of ester resulted in a decrease in cmc.

The C6EO2 salts displayed an intermediate role between surfactant and hydrotrope. The choline and TEA derivatives clearly no longer could be described as surfactants, because their cmc or in this case more probable "cac" (critical aggregation concentration) were comparably high (close to 0.3 M). On the other hand, the DDMA salt showed a cmc in the range of 0.001 M, which is still below that of DDMA Cl$^-$ with 0.014 M [351]. The explanation is given by the less hydrophobic counterion Cl$^-$ and hence less attraction between anion and cation. By adding NaCl to the solution, again a significant "salting-out" effect was detected, as the cmc as well as the surface tension was reduced compared to the pure compound.
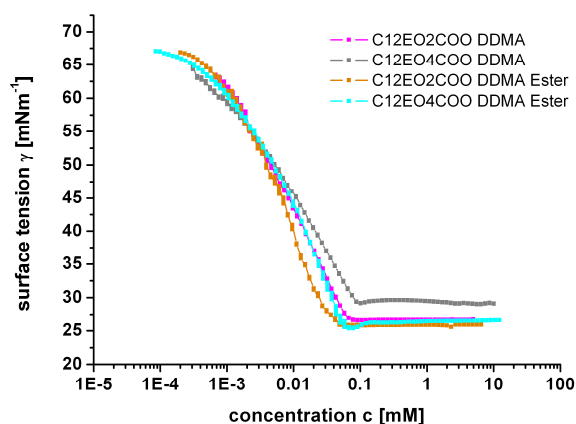
Figure IV-19: Surface tension versus concentration of different catanionic ILs with and without 19.8 mol% ester impurity.

The unambiguous and expected, conclusion can be drawn that the more hydrophobic the investigated substance the lower the cmc as well as the surface tension. All surface tensions values are low compared to classical

anionic surfactants, like SDS with 40 mN/m [2]. Klein *et al.* discussed the micellisation of long-chain carboxylates with choline as counterion [352]. No difference between sodium, potassium or Ch with the same chainlength was found. As described before it was concluded that for the sodium compound, no association between the organic counterion and the carboxylate can be expected in the dilute system which entailed similar cmc values. However, in this investigated case the determined critical micellar concentrations of all organic counterions are significantly shifted to lower values compared to the sodium alkylethercarboxylate (Table VI-7). Obviously, the size of TEA and Ch in addition to their ability to form H-bonds, alongside with the Coulombic headgroup interactions and the high flexibility of the ether units of the anion support facilitated three dimensional networking and hence, enforce micelle formation.

Table IV-8: Area per surfactant. All values belong to the surface tension tangent between ln(c) = -3 to -5.

Substance	*Area per surfactant a_s [$Å^2$]*
C12EO2COO DDMA	94
C12EO2COO DDMA Ester	88
C12EO4COO DDMA	105
C12EO4COO DDMA Ester	77

Due to the lack of extra hydroxyl groups of the DDMA compounds, another effect must originate the extremely low cmc values. The dissolved state of the long hydro carbon chain of the cation is energetically highly unfavourable; hence, the van der Waals interactions between the long tails of anion and cation alongside with their strong electrostatic interactions trigger aggregation. This is a well-known phenomenon of catanionic surfactant systems [125]. These systems exhibit a drastically lower value of the cmc, relative to the pure components. The so-called "interaction parameter", which is a measure of the synergistic interactions between the two surfactants, has a large negative value in this case. This fact commonly is interpreted in terms

of strong electrostatic interactions between the charged headgroups. Electrostatic attraction however, is strongly correlated to the separating distance of the charges. Thus, the increasing cmc with rising number of EO units in the catanionic mixture (Figure IV-19) is originated by two main contributions: On the one hand, polarity of the anion will rise, entailing higher hydrophilicity and water solubility. On the other hand, a bigger volume is required proportional to the number of ether groups due to the increased number of degrees of freedom of the chain. The evaluation of the occupied area per surfactant molecule a_s via Gibbs isotherm [2] (Equation IV-5) supports this assumption.

$$a_s = -\frac{2RT}{N_A}\frac{d\ln(c)}{d\gamma} \qquad\qquad \textbf{IV-5}$$

Where R is the gas constant, T is the absolute temperature, N_A is the Avogadro constant, c is the molar concentration and γ is the surface tension. Values were determined by constructing tangents to the surface tension concentration graph while approximating the cmc (Figure IV-20).
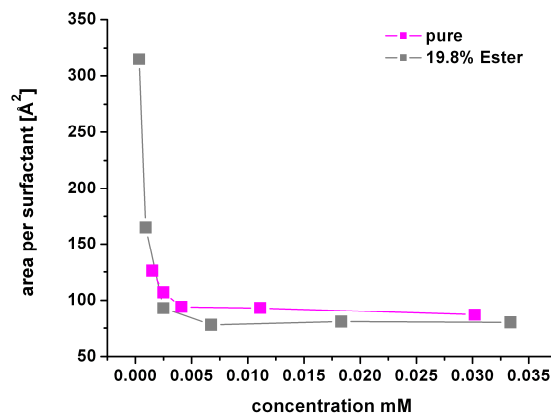
Figure IV-20: Concentration dependent area per C12EO2COO DDMA with and without ester impurity.

The IL with less EOs requires a smaller area than the one with four ethoxy units. Hence, the cationic and anionic charges are further separated and

packing turns less optimal. This becomes evident as soon as the values are compared to classical catanionics like hexylammonium dodecylsulfate with an area per surfactant of only 62Å^2 [353]. However, the catanionic attraction-factor still shows a high impact, as the occupied area per chain in our case is between 47 and 52, whereas values for sodium laurate and sodium dodecyl sulfate are even 67 [297] and 62 [2], respectively. Uncharged impurities like the ester reduce electrostatic repulsion of even charges and thus entail a further reduction of area per molecule.

IV.2.4.2.2   *Krafft - / Cloud-Temperatures*

Hydrophilicity or ~phobicity is closely correlated to the water solubility of a substance. As most surfactants are used in hydrous mixtures their miscibility with water is a criterion with immense importance. The Krafft-point, being the interception of the temperature dependant cmc (critical micellar concentration) and the solubility curve, is an adequate measure to differentiate the solubility of different surfactants. Conventionally the solubility temperature of 1 wt% solutions, which usually leads to surfactant solutions well above the cmc, is defined as Krafft-temperature [2]. The temperature at which a phase separation occurs with rising temperature is commonly called cloud point and is a prevalent phenomenon of non-ionic surfactants [2].

Besides the freshly prepared mixtures of DDMA with C12EO2COO and RLM25, respectively, all 1 wt% samples of the investigated ion combinations were clear and hence dissolved at room temperature.

In the first heating cycle the DDMA C12EO2COO samples appeared turbid up to 95°C. All these samples were completely soluble below approximately 10°C and gave a viscous isotropic solution. During reheating a slow bluish re-clouding of the samples appeared. The formerly white samples (at room temperature freshly mixed) stood clear and bluish for at least 6 weeks over the whole investigated temperature range from 0°C to 95°C. These observations gave hint towards the assumption of the appearance of a

vesicular phase. Due to the fact that this bluish state does not appear spontaneously upon mixing, it cannot be assumed as thermodynamically stable, like described for some catanionic mixtures [161]. A NaCl content of more than 10 wt% leads to a quick phase separation of the pure compounds. Whereas the technical grade purity samples stood bluish to slightly turbid. However, the solubility of the investigated samples without NaCl even seemed to rise with increasing surfactant concentration ending in clear, dissolved samples at room temperature at 53 wt% (Figure IV-22 C).
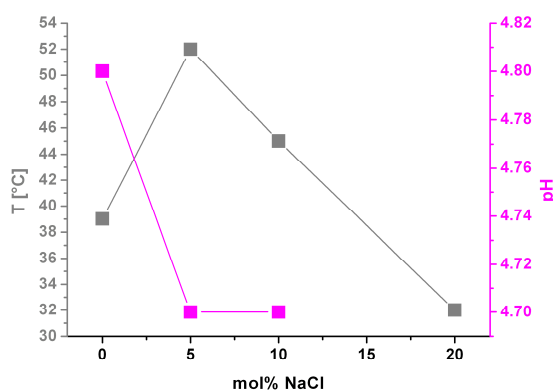
Figure IV-21: Cloud temperature and pH of a 1 wt% solution of RLM45 DDMA in dependence of the sodium chloride content.

In case of the EO4COO DDMA samples a clouding phenomenon was observed. The samples turned bluish and finally white at approximately 39 °C (Figure IV-21). The addition of sodium chloride (< 5 mol%) first lead to an increase of the clouding temperature. This effect was inversed by rising amount of salt leading to solutions becoming turbid at temperatures below that of the unpolluted samples (salt content > 20 wt%).

Equimolar catanionic mixtures often tend to precipitate [137, 140], which is negotiated in the C12EO4 DDMA samples by the high fraction of oxygen, and hence polarity and flexibility of the molecules. Surprisingly, no lower demixing temperature (Krafft point), but a cloud point appears for EO4,

which is typical for non-ionic surfactants with EO-units. The ethoxy units in combination with the pseudo zwitter-ionic character grant a high solubility, due to the flexibility and the enhanced polarity, even at low temperatures. Anyhow, the overall hydrophobicity in combination with the temperature-dependent dehydration of the EO-groups leads to a phase separation and a clouding phenomenon. Furthermore, due to a rise in temperature, more neutrally charged species can be expected in the mixture, which supports the phase separation and thus, the clouding of the EO4 species. This effect is more pronounced, since the pK_a of the carbon acid rises with temperature and hence, less hydrophilic compounds are present

Though, a liquid/liquid phase separation phenomenon is rarely observed in ionic surfactant solutions, mainly because of the repulsive electrostatic effect between aggregates. Nevertheless, a few reports dealing with turbidity and clouding in ionic systems can be found in literature.[354-355] For example, an ionic surfactant system with a large hydrophobic headgroup (*e.g.*, surfactants or added salts with a tributyl headgroup) was observed to display the cloud point phenomenon [354].

On this basis, several catanionic surfactant mixtures were designed that expressed liquid/liquid phase separations. Depending on the differences in the structure of the expressed aggregates, the clouding of catanionic surfactant systems can be usually divided into several classes. The entanglement of rod-like micelles [140], the birefringent L_α phase [147], or densely packed vesicles[301] could induce demixture. A similar phenomenon was described by Zemb and co-workers for catanionic vesicles consisting of a mixture of myristic acid and hexadecyltrimethylammonium hydroxide [161]. Although, the Krafft point of the system was detected above 55°C, highly stable vesicles in "crystalline" modification were even observed at room temperature, while no precipitation occurred within years. The packing parameter of a vesicular phase is close to one. In this case, one can expect a molecular conformation with closest ethoxy interactions, without interdigitating water, while the polar headgroups can still be kept hydrated. Hence, vesicles might not only be found below the Krafft point, but also

above the cloud temperature. Wang *et al.* supposed a possible temperature driven liquid/liquid phase separation mechanism in catanionic surfactant mixtures with huge flexible cationic headgroups [301]. The group stated that in the vesicle region of catanionic mixed surfactant systems, the aggregates can attract each other at a certain concentration and mixed ratio upon heating when hydrophobic interactions and catanionic interactions come up to a certain degree. At the critical temperature more and more vesicles aggregate, if the surface charge was low enough. These super-structured vesicles form a type of three-dimensional network, which contains much water. The network structure separates from the original phase. Thus, this mechanism might exactly be the basis of our observations. Enforced by temperature dependent hydrophobisation of the system, as more non charged compounds are present and the EOs get dehydrated, aggregates start to attract. However, the C12EO4COO DDMA probably is not composed of vesicles but rods, as the first liquid crystal with rising concentration is a hexagonal phase.

NaCl in lower concentrations is "salting-in" the surfactants, *i.e.* the cloud point is shifted to higher temperatures. Probably, sodium partially replaces the ammonium counterion which goes in line with the concept of "matching water affinities" implemented by Collins [99]. This conception describes ion affinities and the formation of close pairs on the basis of polarizability and size of the ions. As sodium hydroxide is a stronger base compared to DDMA an increased dehydration of the acid can be expected and hence, a better solubility due to the higher polarity. At high salt contents a "salting-out" of the surfactant occurs as it enhances the phase separation process by a charge screening phenomenon. The electrostatic repulsion and thus the Debye screening length is reduced leading to an approximation of the charged aggregates. Due to the charge regulation effect [131, 311] a rehydration of the acid can be assumed. These assumptions are supported by the initially decreasing pH-value followed by a re-increase with rising NaCl content (Figure IV-21). Sodium chloride also disturbs the water structure around the ethoxy units and thus leads to a further hydrophobization of the molecules.

Generally, for non-ionic surfactants the cloud temperature strongly depends on the polyoxyethylene chainlength. For example the cloud point of a 1 wt% solution of C12EO8 is around 80°C, while it is ca. 50°C and 10°C for C12EO6 and C12EO4, respectively [10] Thus, interestingly, the system with less EO units behaves completely against expectations because a two phase region at low temperatures was observed. After homogenization of the systems with less EO units at low temperatures the formation of stable, small aggregates (probably vesicles or discs) is observed, while thermally driven phase separation does not occur anymore. In all probability, a classical phase separation of lamellar phase and water was obtained. Due to van der Waals interactions (amongst others) between the layers, a lamellar phase generally is restricted in its repeating distance which separates from water. However, it has to be kept in mind that a protic system was examined. In general the pK_a values of an acid and a base are diminished with reduced temperature. Hence, more charged species can be expected. Though, not equal amounts of cationic and anionic species will appear. Consequently, a slight curvature is introduced and vesicles or discs are formed. It has been shown recently that not all liquid-liquid phase separations occur at a defined temperature. The clouding in various catanionic systems is strongly time dependent. Complete vesicular based phase separation was observed for a special cationic anionic mixture within 2 hours. Yet, it takes about 10 days and more than 1 month, if small modifications in molecular structure were conducted [301]. Hence, the observed aggregates of C12EO2COO and DDMA most likely are only kinetically stable. Sodium chloride drastically reduces Debye screening length inducing an accelerated phase separation. With increasing concentration, the formation of aggregates in the low micron scale at reduced temperature was not observed. In this case molecules and aggregates approximate closer and will react on the entailed electrostatic repulsion by the formation of more uncharged species. This mechanism counterbalances the pK_a dependent charge increase at lower temperatures. Consequently, no curvature is introduced. However, the upper dissolution line shifts to lower temperatures with rising amount of amphiphile (Figure IV-22 C). This observation is difficult to explain. It might be due to the fact that with increased surfactant content the aggregates must not be separated thus far to

"incorporate" all the excess water. Hence, although the molecules might on total be less charged and less hydrophilic, less energy is necessary to take up water.

However, a detailed interpretation of the observed phenomena in this context and a verification of the above stated assumptions afford further experimental evaluation of the structural properties of the investigated system. In this context scattering methods in combination with electron microscopy and *e.g.* zeta-potential measurements might be adequate.

IV.2.4.2.3 *Phase Diagrams in Water*

For any application of surfactants in water, the knowledge of the concentration dependant phase diagram is crucial. The information of the highest concentration of water in the surfactant or *vice versa* before meeting a high viscous liquid crystal is of particular interest. In most cases the range of high viscous liquid crystals, like the hexagonal and the cubic phase, is aspired to be avoided. In other cases, like liquid hand soaps, the viscous but still capable of flowing lamellar phase should be adjusted. In the subsequent section the nomenclature of the various phases follows mainly the system given in reference [4].

IV.2.4.2.3.1 Results

a) Pure Ils in Water

C12-chains:

i) <u>Choline and TEA</u>

Ch and TEA both show a discontinuous, and a bicontinuous cubic phase as well as a broad hexagonal and a lamellar phase independent of the degree of ethoxylation of the counterion (Figure IV-22 A, B). The cubic phases start to form between 25 to 30 wt% of surfactant. In the case of TEA at high concentrations, an inverse micellar phase L_2 can be observed, whereas the Ch

samples seem to merge into a smectic liquid crystal. All liquid crystals persist at least up to 90°C.

The sequence of phases for EO4 equals the one for EO2. Though, with four EOs, the discontinuous cubic phases expand, whereas the hexagonal phase shrinks to the benefit of the biscontinuous cubic phase (Figure IV-22 F).

 After the addition of 19.8 mol% of dodecanol-alkylether carbon acid ester, the phases are shifted to lower concentrations (Figure IV-22 G) and the cubic ones even vanish at temperatures below 90 °C for TEA.

ii) <u>DDMA</u>

The C12EO4COO DDMA sample (Figure IV-22 H) shows a hexagonal and a biscontinuous cubic phase (which disappear at 40°C), a lamellar as well as an L_2 phase. With addition of the ester, the high viscous liquid crystals vanish completely and a nematic phase at low concentrations and high temperatures as well as at high concentrations and low temperatures emerges instead (Figure IV-22 I).

Whether polluted or not, in the case of two EO groups solely this phase sequence of double-layered aggregates exists (Figure IV-22 C). However, the lamellar phase starts at lower concentrations and the nematic phases (existence uncertain in case of pollution) expand over a wider range of temperature.

C6:

Although an aggregation occurs only at very high concentrations, liquid crystalline phases can still be observed for all the investigated counterions. However, the concentrations of the first appearance, range around 55 wt% or even higher. While in case of TEA only a hexagonal phase appears, choline leads to an additional cubic and lamellar phase (Figure IV-22 D).

In case of DDMA solely a lamellar phase was detected (Figure IV-22 E).
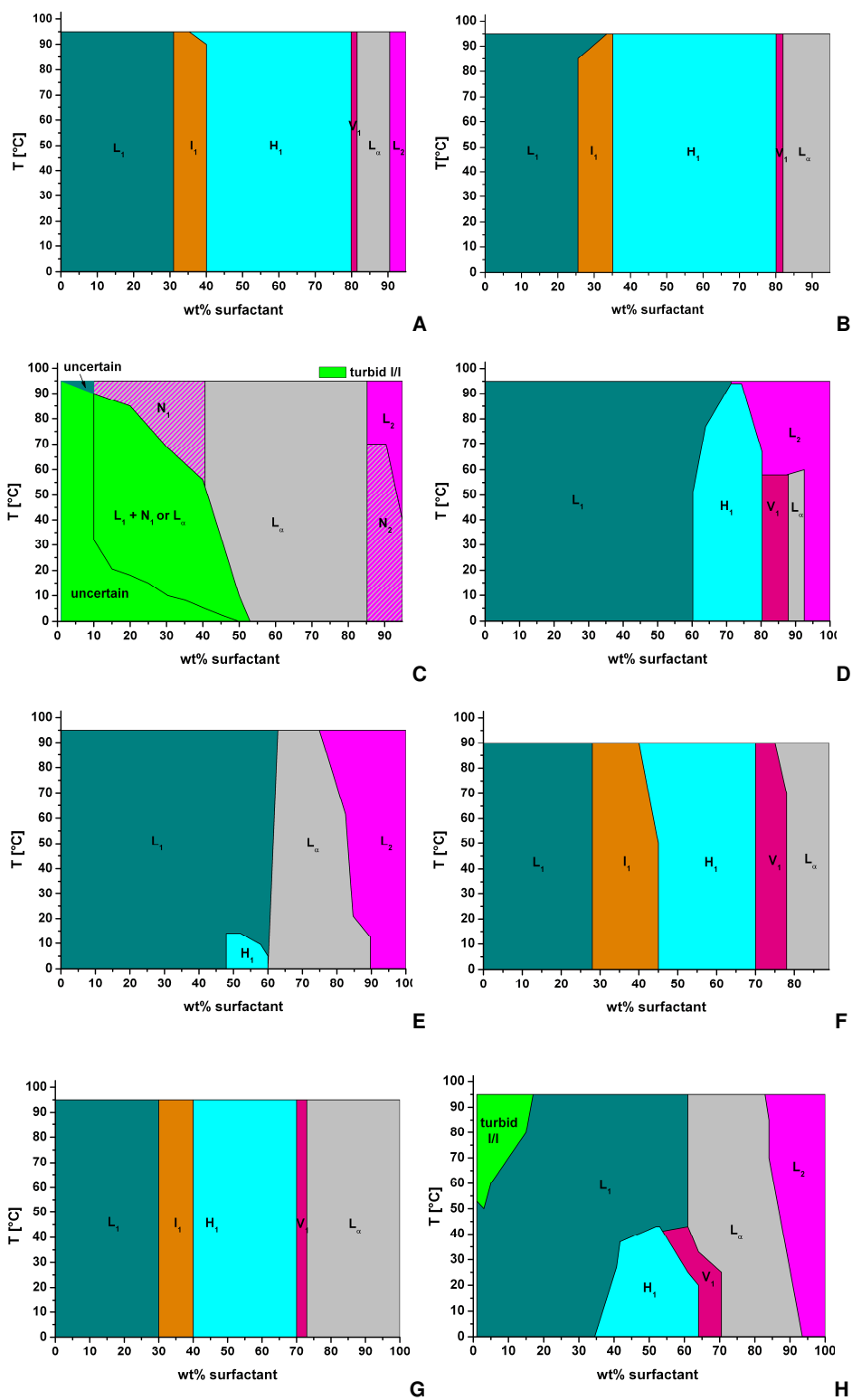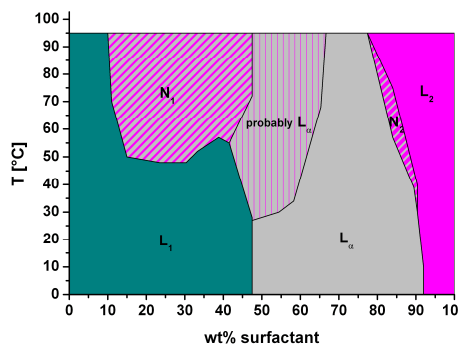
Figure IV-22: Selected phase diagrams of the pure investigated ILs in water. A) C12EO2COO TEA; B) C12EO2COO Ch; C) C12EO2COO DDMA, clouding not shown; D) C6EO2COO Ch; E) C6EO2COO DDMA; F) C12EO4COO Ch; G) C12EO4COO Ch 19.8% ester; H) C12EO4COO DDMA; I) C12EO4COO DDMA 19.8% ester.

The saturation of the Ionic Liquids with NaCl had no major influence on the phase diagrams. The order and type of phases persisted. Merely small changes in the concentration dependence were detected.

b) Technical-Grade ILs in Water

None of the investigated systems showed a biscontinuous cubic phase (Figure IV-23). Only TEA RLM45 expresses a discontinuous I_1, which melts at 70 °C. 5 – 10 wt% shifts to higher concentrations were detected for RLM25 with Ch and TEA in comparison to RLM45.

DDMA RLM25 and 45 samples exhibit merely lamellar phases and micellar solutions. No nematic phases were observed. (Figure IV-23 A).

For all species the LF1 ILs generate a hexagonal and a lamellar phase with their widest expansion in concentration for DDMA (40 – 90 %) and their

highest temperature stability for Ch and TEA (80 °C and 70 °C) (Figure IV-23 D, E, F).
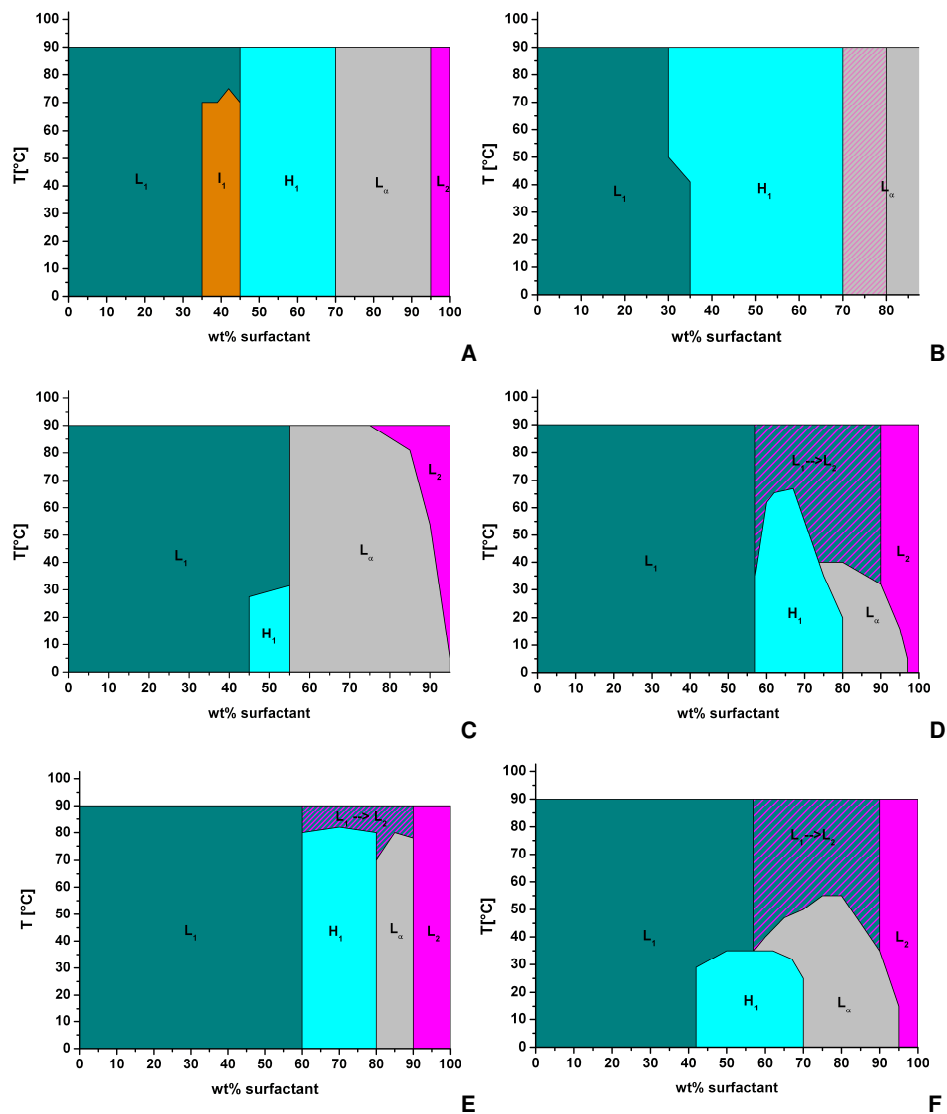
Figure IV-23: Selected phase diagrams of technical grade ILs in water; unaccounted for solubility borders: A) RLM45 TEA; B) RLM45 Ch; C) RLM45 DDMA; D) LF1 TEA; E) LF1 Ch; F) LF1 DDMA.

IV.2.4.2.3.2   Discussion

a) General Considerations

The forces responsible for micelle-shape and mesophase structure can be divided into intra- and inter-micellar contributions [4, 10]. The former determine the shape right above the cmc, while the latter take account of inter-micellar interactions at higher concentrations. At the cmc, micelle shape is determined by the surface area per molecule a_s at the alkyl-chain/water interface, and the curvature of the interface. Interactions between hydrated headgroups (electrostatic, solvation, steric) commonly result in a repulsive force. The minimisation of hydrocarbon-chain/water interactions gives an attractive force. These are dominant contributions. Yet, depending on the value of a_s, there is also a repulsive force within the alkyl-chain region. This force arises from the unfavourable entropy change caused by restrictions on the conformations of the chains with small a_s values. To summarise, the balance of forces determines the aggregate shape within packing constraints. There are two major effects of inter-micellar forces. First, considering the micelles to be hard-core particles at the cmc, an order/disorder transitions is observed upon increasing volume fraction of surfactant. Spherical micelles pack closely into a regular cubic array. Long rod-like micelles commonly form a hexagonal array, while a lamellar phase is built of bilayers. Theoretically, a lamellar phase can occur without any water being present. Two large lamellae in any volume are aligned to some extent, because they cannot pass through each other. Hence, the lowest theoretical volume fraction for a lamellar phase is just above the cmc. Of course, in reality the repulsions between micelles are not of the hard-sphere type. Occuring so-called soft core repulsions can be thought of as arising from interactions between hydrogen-bonded water network structures on adjacent micelle surfaces. Theoretical considerations suggest an exponential fall-off of these forces with increasing distance from the surface. For polyoxyethylene surfactants it is

expected that this force is accompanied by another repulsive force due to restrictions on the conformation of EO groups. This arises from steric hindrance as soon as micelles are close together. At the L_1 boundary the repulsion is just strong enough to cause ordering. Yet, the micelle separation has to be reduced further, before the inter-micellar repulsions are sufficiently large to offset unfavourable inter-micellar curvature. The effects of curvature and the magnitude of a_s are expected to increase with the number of EO units, as it is observed in practice for classical non-ionic surfactants [4, 10].

Thus, the observed mesophase sequences can mostly be explained on the basis of the above mentioned mechanisms.

b) TEA and Ch

Equal Chainlength, Equal Degree of Ethoxylation

Like already described, the liquid crystalline order of TEA equals that of choline. Nevertheless, minor differences were observed. The phase transition of the micellar L_1 to cubic I_1 phases can be described by an order/disorder mechanism. Hence, those micelles with large repulsive forces will not arrange on a three dimensional lattice that easily. TEA bears a pronounced potential of sterical hindrance. This is *e.g.* expressed in its low pK_a value (Table IV-9). However, just like in the process of micelle formation (cmc) the basicity itself reveals only a minor impact on the formation of an ordered phase. Yet, with approaching aggregates due to increasing concentration, the counterions are likewise approximating. The strongly hydrated TEA tends to deplete other cations from its vicinity. In case of a close cation-cation approximation, on the one hand the water structure around the hydroxy groups is influenced and on the other hand the number of degrees of freedom of the three alkylchain is restricted. Thus, a shift of the first appearance of the I_1 phase to higher concentrations can be observed for TEA compared to Ch.

The transition of L_α to L_2 generally is assigned to interplay of headgroup hydration and its occupied area and the entropy of the aliphatic chains [10]. At these high concentrations the counterions are much closer associated. In this case a distinct influence of the basicity of the cations can be expected. Choline is a much stronger base than TEA. Hence, the carbon acid will be deprotonated to a much higher extent than in the case of the bulky amine. Consequently, the headgroups are subjected to stronger electrostatic repulsion. The accessible volume for the alkylchains is larger and thus, more conformational modifications can be achieved. The entropic pressure responsible for a phase transition is low, which is opposed to the TEA case.

Table IV-9: pKa values of the investigated amine-bases.

Substance	pKa
TEA	7.8 [356]
Ch	13.9 [357]
DDMA	9.97 [358]

Equal Chainlength, Different Degree of Ethoxylation

Figures IV-22 B and F illustrate that additionally to the exchange of bulky counterion, the degree of ethoxylation influences the mesophase sequence. With rising EO number hydrophilicity just like the flexibility of the system increases. The mobility of the ether chain entails sterical intra-molecular repulsions within one and between separated aggregates. Thus, the L_1/I_1 transition can only be achieved at higher concentrations of surfactant. The alteration of spherical to rod-like micellar shape is likewise triggered by the same mechanism. Hence, it can also be observed only at elevated concentrations. Such shape transitions generally occur because unfavourable curvature is balanced by inter-micellar repulsion. The mechanism further involves constraints on the value of the headgroup area due to finite alkylchainlength and micelle-surface-area/volume ratio [10]. The most

remarkable observation in the C12EO4COO Ch and TEA phase diagrams is the fact that compared to the EO2 equivalents the hexagonal phase disappears at lower concentrations to the benefit of the biscontinuous cubic liquid crystal. This contradicts observations of non-ionic surfactants, where mesophases boundaries are shifted to higher concentrations with rising number of EO units. This is due to their stronger hydration and higher flexibility [10]. However, for geometrical reasons the counterions approximate at higher concentrations. Intermolecular attraction might be enforced with increasing degree of ethoxylation, because the H-bond formation potential rises proportionally. Cations with more or less hydroxyl-groups prone to interact with ether functionalities were investigated. The enhanced counterion association results in a reduced electrostatically driven repulsion and thus, in a smaller effective area per molecule. Consequently, the H_1/V_1 shape originated mesophases transition is shifted to lower concentrations.

Different Chainlength, Equal Degree of Ethoxylation

Drastic reduction of carbon chainlength with constant EO number induces a pronounced shift of liquid crystals to higher concentrations. The relation of surface per molecule to its total length has to give lower values. The observed sequence of phases with increasing surfactant concentration is in agreement with the basis of intra-micellar curvature being opposed by inter-micellar repulsions. More interestingly, no I_1 phase can be detected for the investigated C6EO2COO ILs, although the packing parameter is reduced in this case. Spherical shaped micelles, whose appearance is already highly probable in case of the longer-chain derivatives, can be expected. A micelle shape transition of the type sphere → rod → bilayer can occur if the unfavourable curvature energy was balanced by a contribution from micelle interactions. This type of transition is accelerated when a_s approaches the packing limits of spheres or rods. If the repulsions between the new shapes are sufficiently large, then an ordered phase can form immediately. Thus, the observation of the sequences: spherical micelles → hexagonal phase → lamellar phase is possible[10].

c) DDMA

Generally, no such pre-liquid-crystalline shape transition is observed if the small bulky counterions were exchanged by the long-chain DDMA.

Different Chainlengths, Equal Degree of Ethoxylation

Like expected with decreased number of carbons in the tail of the amphiphile, the first mesophases to appear is no longer a lamellar, but a hexagonal phase. This observation perfectly correlates with a reduction in molecular volume and thus, the packing parameter. If the overall shape of a surfactant is similar to a cylinder [125], which is common for catanionics with pseudo double chain nature, the first arising liquid crystal will be a lamellar, or a nematic phase respectively (which is quite rare in lyotropics).

Thus, with the elongation of the acid carbon chain the molecular geometry approximates cylindrical shape and a bilayer structure is favoured. As mentioned above, a lamellar phase could occur directly above the cmc as long as no vesicles or disc-like micelles are formed. However, a nematic phase was detected at low and high concentrations via polarizing microscopy. The structural foundations of nematic liquid crystals are rod or disc-like aggregates with a pronounced priority long range order at least in one dimension [4, 258]. Based on this fact and the exposed observations a concentration dependent vesicle and or disc-micelle formation followed by a lamellar phase is assumed for the C12EO2COO DDMA salt.

Equal Chainlengths, Different Degree of Ethoxylation

In return, the insertion of further EO units promotes the shift of molecular geometry towards cone-like shape, due to the increased required space of the headgroup. In consequence, rod-micelles are formed and the first appearing mesophases is a hexagonal one. Just like the flexibility of the EOs, the degree of protonation of acid and base affects the concentration dependent phase transitions. The mesophases sequence of C12EO4COO DDMA was tailed by pH measurements (Figure IV-24). Obviously, with increasing concentration

and consequently lower area per molecule the pH rises. This leads to the assumption that due to charge regulation [311] the electrostatic constraints are overcome by reprotonation of the carbon acid. pH and the number of uncharged molecules escalates right before a phase transition. This adumbrates that the system tries to delay the inevitable energetically induced phase transition in a last effort.
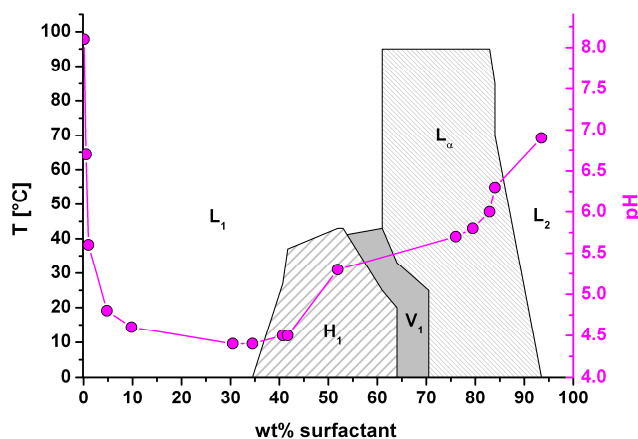
Figure IV-24: Correlation between pH (at 25 °C) and lyotropic mesophases of C12EO4COO DDMA.

There are at least two factors that are responsible for temperature dependent phase transitions. The first one is a decrease in the area per molecule and the second a decrease in inter-micellar repulsions [4, 10]. In the present case both possibilities are probable. On the one hand, mesophase transitions are observed at lower surfactant concentrations as temperature increases. This indicates that the intra-micellar interactions (particularly curvature) are dominating. On the other hand, temperature dependent clouding (chapter VI.2.4.2.2) is obtained, which is due to reduced inter aggregate interactions. The temperature induced phase transition arises from a decrease in the hydration of EO groups with increasing temperature. Furthermore, electrostatic repulsion is reduced since more neutral species are present due to the pK_a dependence of both, acid and base. The maximum temperature for the existence of mesophases represents the point at which the surface area reaches the shape transition packing limit. These contributions explain the

observed phase sequence of H_1, V_1 and L_α for C12EO4COO DDMA with rising temperature at approximately 60 wt%.

d) Impurities

The addition of amphiphilic uncharged substances (dodecyl alkylether carbon acid ester) lead to less repulsion of the packed molecules. Since such molecules insert into the micelles between the surfactant molecules a shift in relation of surfactant headgroup area and chain volume is the result. The curvature of the corresponding aggregates is reduced. Hence, in the case of C12EO4COO DDMA the micelles do not bear a rod-like shape anymore, but disc-like. Accordingly, no hexagonal and cubic phases are observed any more. The effects on the TEA and Ch samples are less evident, but can be explained in the same way. Although the phase sequences persist, their critical transition concentrations are shifted to lower amounts of surfactant. Light scattering and surface tension experiments gave first hints towards bigger micelle sizes accompanied by smaller areas per molecule by polluting the samples with ester. Thus, the intermolecular-, the inter-aggregate-repulsion and the aggregate-curvature are lower in this case. The critical values of the phase-transition-inducing parameters are reached at lower surfactant concentrations.

e) Technical Grade Surfactants

Comparison Pure Ils/Technical Grade ILs

In the case of the technical grade substances, the distribution of ethoxy units just like the uncharged impurities lead to a reduction or even complete disappearance of cubic or nematic phases. The first appearance of a liquid crystalline phase is shifted to higher concentrations in the phase diagrams basing on commercial-acid-ILs. Additionally, equivalent phases, like for example the hexagonal phase can already be detected at higher water contents compared to the pure substances. Although, the diversity of present species is

not negligible in the technical products, the above stated mechanisms still seem to be valid. Obviously, the pollutants lead to an efficient reduction of the area per molecule, which is even more pronounced than in the case of ester polluted pure surfactant. Thus, either more uncharged amphiphiles reducing electrostatic headgroup repulsion, or more long-chain derivatives determining the minimal area per headgroup until phase transition occurs, are present. Analysis data of the corresponding technical grade acids supported both assumptions.

LF1

All of the LF1 species show a similar mesophases sequence. However, DDMA expresses a hexagonal phase at lower concentrations than TEA and Ch. This observation correlates with less pronounced inter-micellar repulsions due to efficient counterion binding. Though, the comparatively lower H_1/L_α transition concentration can be attributed to the larger volume occupied by the chains compared to the headgroup area. Likewise, this fact serves as explanation for the temperature dependent phase transitions already below 60°C.

The LF1 TEA liquid crystals are more fragile towards thermal constraints than its choline equivalents, though they appear at similar concentrations. With elevated temperature the ethoxy units of the anions become dehydrated. However, TEA seems to offer the opportunity of binding water molecules more efficiently than choline by its three hydroxy groups. Thus, micelles already form at lower temperatures.

IV.2.5   Conclusion

The physico-chemical properties of various alkyl ether carboxylates with different ammonium based counterions were examined with particular regard to the potential applications of these compounds. It was demonstrated that the unusual chemical structure of the investigated type of carboxylates leads to peculiar physicochemical properties of the Ionic Liquid formed by these compounds. Their features, in pure and diluted form, were correlated to chainlength, degree of ethoxylation and technical grade purity of the acids. In addition, the influence of the type of counterion and of synthetically relevant impurities, namely sodium chloride and the ester of acid and fatty alcohol was determined.

In binary mixtures with water, the investigated systems seem to represent an intermediate state between ionic and non-ionic surfactants. The properties are strongly dependent on the number of ethoxy units. Choline and TEA as counterions lead to compounds with the characteristics of mainly anionic surfactants, which only marginally differ from each other. The DDMA salts basically show properties of true catanionics. Like in the water-free case, the flexibility and hydrophilicity of the ether groups prevents these long-chain surfactant mixtures from precipitation. On the other hand, a liquid/liquid phase separation occurs at rising temperatures. For certain ion combinations this lower demixing point is in the range of body temperature. Hence, applications in human or health care, which acquire stable formulations outside and easily accessible drugs inside the body, are favoured. In case of two ether groups an optimum for pseudo-double chain behaviour is reached and kinetically stabilized aggregates were observed above the cloud temperature. In the concentration dependant phase diagram solely low viscous double-layer lamellar phases appear.

The features, especially of the catanionic species, like their low viscosity and outstanding heat capacity, make these substances prone for concentrated applications at ambient temperature. The low Krafft temperature and the

formation of sparsely viscous lamellar phases as lyotropic liquid crystals recommends applications in a wide concentration range and allows the production of concentrated formulations which stay easily pourable while diluted.

All the observed phenomena are interpretable with charge regulation, charge adsorption effects and different cation-anion affinities in combination with varying association behaviour due to modified hydration. Merging the knowledge about carboxylate and EO-based non-ionic surfactants makes the properties of those new compounds predictable. By variation of the ion combination their features in water-free as well as in diluted systems are easily tuneable. Due to this fact, and the low toxic impact of the chosen ions, those new alkylethercarboxylate Ionic Liquids are very valuable compounds for any application of surfactant-like Ionic Liquids.

IV.3 New, Cationic Surfactant-Like Ionic Liquids with Oligoether Carboxylate Counterions – Physico-Chemical Properties in Pure Form and in Binary Mixtures with Water

IV.3.1   Introduction

As already mentioned in previous chapters, Ionic liquids (ILs) are a class of organic molten electrolytes at/or near ambient temperature [39]. Their physical and chemical properties can be tailored by careful selection of cation and anion. Due to their outstanding properties and the task-specific tuneability, ILs have attracted much attention as electrolytes [78-79] and solvent media for reactions and extractions [39, 55]. Obviously, the standard compounds seem to be ILs composed of 1-alkyl-3-methylimidazolium cation C_nMIM. Their properties have been extensively studied in the field of colloid and interface science.

The investigation of long-chain Ionic Liquids attracted rather recent scientific interest. Such ILs resemble conventional surfactants and thus are prone to form aggregates [28]. This property has been elucidated in several research attempts. For example, Law and Watson measured the surface tension of a series of C_nMIM X [65-66]. Further, long-chain ILs have been found to form thermotropic liquid crystal [359]. At the same time, the aggregation behaviours

of ILs in aqueous solution have also been studied due to the close resemblance of long-chain ILs to the structure of conventional cationic surfactants. For example the behaviour of C_{10}MIM Br in aqueous solution has been studied[360]. Butts and co-workers explored the surface, and aggregation behaviours of aqueous mixtures of 1-alkyl-3-methylimidazolium halides with a variety of methods [361]. Baker's group examined the micellisation of a homologous series of *N*-alkyl-*N*-methylpyrrolidinium bromides in aqueous solution [30]. Aggregation behaviour of different ILs in aqueous solutions has been investigated using for example ^{1}H NMR, steady-state fluorescence spectroscopy, and refractrometry by Singh *et al.* [362].

Despite aroused interest in long-chain ILs, most of the investigations base on the classical, environmentally questionable imidazolium or pyridinium headgroups. Several reports underlined disadvantageous toxicological impact of these cations [71, 363-365]. For that reason, some investigations in the short chain branch of Ionic Liquids dealt with the replacement of such classical cations with compounds of natural origin, like choline [34]. However, the improvement of long-chain IL properties in this area is only scarcely developed [320].

Recently, Kunz, Buchner and co-workers have presented oligoether based short chain carboxylates (TOTO) as efficient counterions to form Ionic Liquids with alkali and quarternary ammonium cations [321-322]. A comparatively low toxicity of some derivatives of these ion combinations has been shown. The workgroup concluded that the polarity of these ILs can easily be tuned by the choice of the cation. They suggested a pronounced non-ionic character of the alkali ILs, which entailed very high viscosities. On the other hand, upon the utilization of quaternary ammonium ions (TAA) [366], the viscosities of the resulting Ionic Liquids were presented to be more than 600 times lower, while conductivities increase by a factor of up to 1000 compared to the alkali counterparts. Solvent polarities further revealed that these TAA ILs are more polar than those obtained with sodium. The pronounced flexibility of the ether groups served as explanation for the low melting points.

Based on this work, the combination of various long-chain primary ammonium species with the TOTO anion (Figure IV-25) are going to be discussed in the following section. Their properties as pure Ionic Liquids, as well as their surfactant features in binary mixtures with water will be presented.

n	Abbreviation
7	C8 TOTO
9	C10 TOTO
11	C12 TOTO
13	C14 TOTO
15	C16 TOTO
17	C18 TOTO
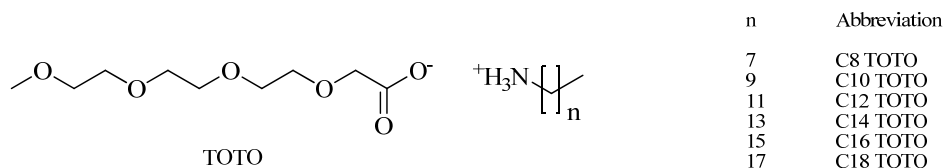
Figure IV-25: Structure of the investigated long-chain primary ammonium TOTO ILs.

IV.3.2   Chemicals and Methods

2,5,8,11-Tetraoxatridecan-13-oic acid (TOTOA) was synthesised according to a procedure described previously [342]. The purity of TOTOA (99.4 - 99.7%) was verified by GC-analysis. Ionic Liquids were obtained by direct neutralization of the free TOTO acid and the respective primary amine. The following amines were used: Octylamine (99 %, Aldrich), decylamine (98 % Aldrich), dodecylamine (> 99 %, Aldrich), tetradecylamine (> 98.5 %, Fluka), hexadecylamine (> 98 %, Aldrich) and octadecylamine (> 99 %, Aldrich). For further purification purposes, octylamine and decylamine were distilled prior to using, while tetradecylamine and hexadecylamine were recrystallized. Dodecylamine and octadecylamine were used without further purification. To avoid too high neutralization heats, the acid and the base were each dissolved in ethanol prior to mixing. After stirring the neutralized mixtures for about 2 h, the solvent was removed either by a rotary evaporator. Subsequently, the salts were dried for about 3 days at 40 °C in high vacuum ($p < 10^{-8}$ bar), yielding colourless or slightly yellow liquids or

solids, respectively. The purity was confirmed by means of ^{1}H-NMR, ^{13}C-NMR as well as mass spectroscopy and elemental analysis.

The water content of all investigated Ionic Liquids was determined by coulombmetric Karl-Fischer titration to assure values below 500 ppm before any further investigation.

Viscosities, thermal transition features and decomposition temperatures were determined according to the methods described in chapter IV.1.

Densities, ρ, required for the calculation of molar volumes, and molar conductivities, were measured at room temperature (25 °C) and over a temperature range of 283-333 K in steps of 10 K, utilizing a vibrating tube densimeter (Anton Paar DMA 60). Calibration of the instrument was achieved by measuring purified dry nitrogen and degassed water. The uncertainty of ρ values is estimated to be less than 0.1 kg m^{-3}.

Conductivities of the pure substances were determined at ambient temperature (25 °C) as well as in steps of 10 °C between 0 and 100 °C. Measurements were carried out with an custom-designed apparatus built in-house [367]. It consists of a precision thermostat, a symmetrical Wheatstone bridge with Wagner earth, a sine generator and a resistance decade. Temperature accuracy is estimated to ± 0.01 K (NIST traceable platinum sensor, ASL). Three capillary cells, each containing a three-electrode setup, with cell constants ranging from 224 to 1161 m^{-1} were utilized. Cell constants were derived by measuring aqueous KCl solutions according to a procedure described by Barthel et al. [368] Resistance measurements were performed at frequencies between 480 Hz and 10 kHz. R values at infinite frequency were obtained by linear extrapolation. The relative uncertainty of the obtained electrical conductivities is judged to be less than 0.5 %. The reported temperature dependence of cell constants [367] was not taken into account since the changes in the conductivities when correcting for this effect were marginal and within the given limits of error.

The critical micellisation concentrations (cmcs) in water were determined by conductivity measurements. Cmcs can be obtained from the breakpoint in the

plot of the conductivity versus the concentration. Experiments were conducted at 25 °C using an autobalance conductivity bridge (Konduktometer 702, Knick, Germany) equipped with a Consort SK41T electrode cell. In order to obtain specific conductivities, the cell constant was determined by measuring known conductivities of $0.01\,m$, $0.1\,m$ and $1\,m$ potassium chloride (KCl) solutions at 25 °C.

Equivalent conductivities at infinite dilution, as well as association constants were estimated by means of conductivity measurements of sample concentrations (in water) well below the cmc. The experimental setup was equal to that of the conductivity measurements of the pure substances. Cells with cell constants of 11.62, 212.75 and 396.61 m^{-1} were utilized.

Binary phase diagrams in water were determined by optical polarizing microscopy following the procedure described in chapter IV.1. Samples were examined in 5 wt% steps; close to mesophases boarders in 2.5 wt% steps. Furthermore, phases were confirmed by small angle X-ray scattering (SAXS) at the laboratoire LIONS/CEA in Saclay (France). X-ray radiation with wavelength $\lambda = 1.54$ Å is provided by a copper rotating anode operating at 3 kW equipped with a multilayer Xenocs mirror as monochromator and a three slit collimation system. The scattered X-rays were detected by a two dimensional automatic image plate (Mar300, Marresearch). Calibrations were performed by measuring standards such as Lupolen. With a sample to detector distance of 122 cm the accessible q-range was 0.3-6.3 nm^{-1}. Samples were enclosed between Kapton sheets with sample thicknesses of 1.5 mm. Acquisition times varied between 900-3600 s. Radial averaging was performed with ImageJ Software. Data are going to be presented in means of intensity as a function of q. The scattering vector q is defined as *$4\pi/\lambda \cdot sin(\theta/2)$* (scattering angle θ)

Cytotoxicity tests were performed with the HeLa (cervix carcinoma, ATCC CCL17) cell line using the MTT assay procedure according to Mosmann [369] and modified by Vlachy *et al.* [370]. The IC$_{50}$ value (in mol/L), which represents the concentration of test substance that lowers MTT reduction by 50 % compared with the untreated control, was calculated for each substance

from the concentration-response curve. Experiments were repeated four times. Maximal observed (absolute) standard deviation was about 10 %.

Biodegradability was studied according to the OCDE 301F standard at the institute of Agro Industrie Recherches et Developpements (Route de Bazancourt, 51110 Pomacle, France). Biodegradation of a substance is calculated from the ratio of real biological (BOC) and theoretical oxygen consumption, which reflects the amount of oxygen demanded for complete oxidation of a compound calculated from its molecular structure. The BOC was determined by means of an IBUK respirometer, which allows the detection of oxygen consumption during the degradation process. Experiments were performed at 20 °C for 28 days in a medium containing bacteria collected from the local wastewater treatment plant. Several parameters served as criteria for the validity of the experiments:

- The degradation of sodium acetate (chosen as standard) had to reach a level higher than 60 % after 14 days.

- The mineral medium has to exhibit an oxygen consumption below 60 mgL^{-1} after 28 days and if possible comprise between 20 and 30 mgL^{-1}.

- After 28 days the pH has to be between 6 and 8.5.

IV.3.3 Results and Discussion

IV.3.3.1 Properties of Pure ILs

IV.3.3.1.1 *Decomposition Temperatures T_d*

As explained in previous chapters (II.1.2.1; IV.1.2.1.1, IV.2.4.1.1), the thermal stability of ILs is sensitive to the type of cation and anion. For common simple salt ILs it is found at temperatures of 300 °C or even above.
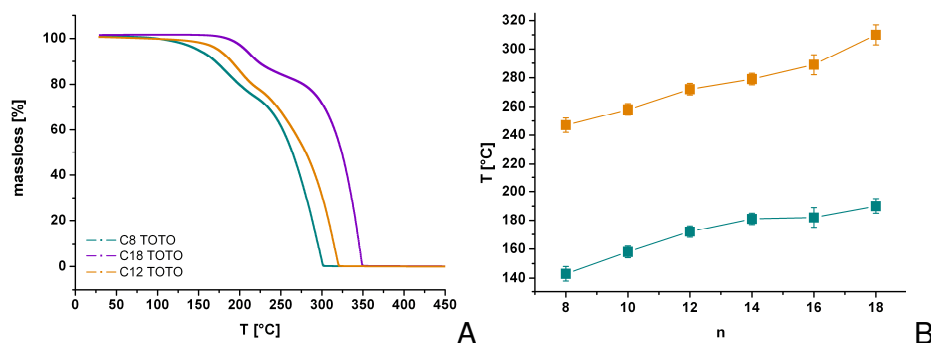
Figure IV-26: Exemplary massloss/temperature curves of some investigated compounds (A). Onset temperatures of the first ■ and the second ■ step of the massloss curves in dependence of the carbon chainlength *n* of the ammonium ion (B).

However, the decomposition temperature T_d of protic ILs is much lower [39, 50-51]. Yet, the term decomposition has to be handled with care. Generally, for protic ILs the decomposition temperature is a combination of real destructive decomposition of the molecules and a physically driven evaporation. The ratio between both mechanisms is determined by the pK_a difference of the protonated forms of the cation and the anion. The combination of weak acids and bases generally yields ILs with a high amount of uncharged species and

thus, a comparatively high vapour pressure, which results in low evaporation ("decomposition") temperatures [49].

The results of thermal evaporation/decomposition behaviour determined by thermogravimetrical analysis (TGA) of the investigated TOTO compounds are summarized in Figure IV-26. In all cases, the massloss curves expressed two steps, whose onset temperatures were shifted to higher values upon increased number of carbons n in the ammonium chainlength.

This behaviour can easily be understood upon consideration of the fact that TOTOA as well as the long-chain amines are weak acid and weak bases, respectively. The pK_a of TOTOA is approximately 4.72 (data not shown), whereas the pK_a values are reported to range between 10.60 and 10.70 [371]. Hence, a not negligible amount of uncharged species can be expected in the mixture, which is even supposed to increase with rising temperature. Protonation equilibria of most organic acids and bases are known to be shifted to the neutral forms with elevated temperature [9]. Thus, the first step in the massloss curve can probably be assigned to the evaporation of the amine. The evaporation temperature of TOTOA ranges between 145 and 150 °C at pressures below 10^{-5} mbar. Furthermore, the onset temperature of the first step in the TGA curves rises with the chainlength of the amine. Thus, the evaporation of TOTOA at these temperatures is unlikely. Consequently, the second step must be due to the final chemical decomposition and/or evaporation of the residual compounds.

IV.3.3.1.2 *Thermally Induced Phase Transitions in the Pure Compounds at Medium Temperatures*

In the DSC scans solely one endothermic transition (ranging from -20 °C to 90 °C) was detected for all investigated TOTO Ionic Liquids (Figure IV-27). C10 and C12 TOTO showed a single, but comparatively broad peak, with a width of nearly 20 and 15 °C, respectively. Upon increasing chainlength, the peaks became sharper and more symmetric.
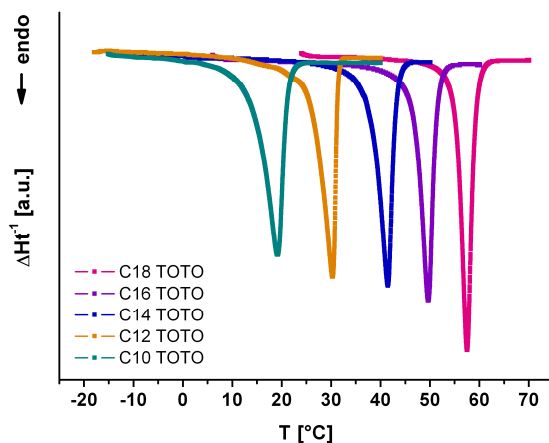
Figure IV-27: Heatflow versus temperature curve in dependence of the ammonium chainlength of the TOTO ILs.

Polarizing microscopic observation revealed the endothermic peaks to be related to the transition from the crystalline to the isotropic liquid state. No further transitions were observed until decomposition. There was no significant indication for liquid crystalline (LC) behaviour observed during the melting process of any of the samples. Nevertheless, an LC existence cannot be excluded unambiguously. With decreasing chainlength kinetically hindered crystallization was observed; *i.e.* crystalline and liquid isotropic areas coexisted over a wide temperature range (nearly 20 °C for C10 TOTO with a heating rate of 10 °C). Samples crystallized from the melt exhibited the "zig-zag" blade and focal conic texture (typical for a smectic order), which is exemplarily depicted for C12 and C16 TOTO in Figure IV-28.

In Table IV-10, melting transition parameters for C12 TOTO are compared to several other dodecylammonium compounds. Smaller halides exhibit relatively small enthalply changes in comparison to perfluoropropionate (C12 PFP) and picrate (C12 Pic) [372]. C12 TOTO seems to constitute an intermediate case, indicating the importance of the nature and the structural arrangements of ionic layers in the crystalline state.

Like most compounds, which contain long hydrocarbon chains, surfactant crystals exhibit numerous quantitative variants of the bilayer structures with

alternating head-to-head or tail-to-tail arrangement [165, 373-375]. Upon heating, the crystalline surfactant phase undergoes the solid-phase transitions as a response to specific thermal molecular motions. The number and kinds of phase transitions of single-chain surfactant molecules can vary from a simple phase transition, the solid crystalline–isotropic liquid [372], to a complex polymorphism.
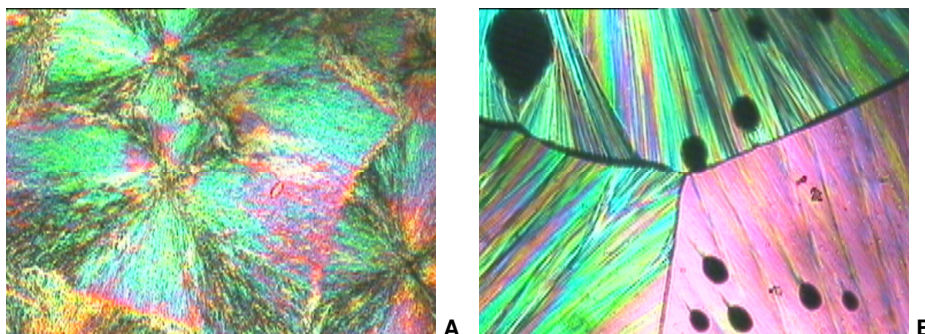
Figure IV-28: Textures of C12 TOTO at 15 °C (A) and C16 TOTO at 25 °C (B) crystallized from the melt (crossed nicols).

Generally, alkylammonium compounds behave like most amphiphilic compounds with hydrocarbon chains. They may take up a variety of conformations as a function of temperature; *i.e.*, they exhibited polymorphism and mesomorphism [374-375].

Ammonium cations and halide or complex metal anions extend bidimensionally to form an ionic layer, which is sandwiched between the hydrocarbon chain layers. The Coulomb interactions within the ionic layer are strong compared to the van der Waals forces in the hydrocarbon layer. The conformational and/or positional disorders of the alkylchains at lower temperature lead to the polymorphic transition(s), while the ionic layers remain virtually unchanged.

Table IV-10: Transition temperatures T_t and ~ enthalpies ΔH_t of the melting of
dodecylammonium with different counterions: TOTO (C12 TOTO),
picrate (C12 Pic), chloride (C12 Cl), bromide (C12 Br) and
perfluoropropionate (C12 PFP) [372].

Substance	*T_t [K]*	*ΔH_t [kJmol^{-1}]*
C12 TOTO	293	15.3
C12 Pic	385	39.2
C12 Cl	458	1.8
C12 Br	465	1.7
C12 PFP	312	29.5

At higher temperature, the bidimensional disorder of the ionic layers leads to the transition from the solid crystalline to the liquid crystalline organization, and finally to the isotropic liquid disorder. This polymorphism and mesomorphism is particularly pronounced in the case of the small halide dodecylammonium compounds [374-375]. Thus, merely a small input of energy suffices to finally transform the liquid crystal into the isotropic, liquid state in these cases. This assumption explains the comparatively low ΔH_t values of the bromide and chloride derivatives. Generally, van der Waals interactions and long-range Coulomb forces govern the inter-layer interactions in most bilayer compounds, which contain the alkylammonium cation. Additional hydrogen bonds between the NH$_3$ groups and picrate anions in C12 Pic [372], enhance these interactions. These additional forces served as explanation for the higher transition enthalpies compared to halide counterions. In the picrate case, the disordering of the alkylchains and the ionic layers occurred simultaneously during melting to the isotropic phase, while crystallization from the molten samples was kinetically controlled [372]. These observations are very similar to those made in the present case of TOTO ILs.

The failure of mesomorphic transitions might be interpreted in means of interplay of additional H-bonds and the bulky counterion. In contrast to picrate, TOTO bears a high degree of conformational flexibility due to its ether units. This property drastically influences the melting transition

temperature. While C12 Pic melts at approximately 112 °C (Table IV-10), the transition temperature drops to 20 °C for C12 TOTO.
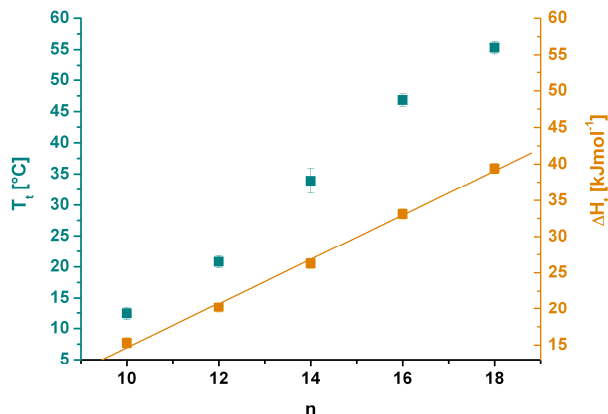
Figure IV-29: Onset temperatures T_t and enthalpies ΔH_t of the melting transition of the TOTO ILs in dependence of the ammonium chainlength n. The full line presents a linear fit.

The impact of the bulky, flexible TOTO anion, which destabilizes the crystalline state, further becomes manifest in the comparatively low melting enthalpies. The value of C12 TOTO is less than half of that of C12 Pic. From the plot of the transition heat versus the chainlength of the ammonium (Figure IV-29) an increment of 3.05 kJmol^{-1} per CH$_2$ unit can be deduced. This value is significantly lower than that of common alkanes with 4.45 kJmol^{-1} [331]. The effective cohesive energy in the C12 TOTO crystal is comparatively low. Consequently, both, the melting enthalpy as well as the transition temperature are shifted to lower values. Hence, C12 TOTO is a real room temperature long-chain Ionic Liquid.

IV.3.3.1.3 *Viscosities and Conductivities of the Pure ILs*

Figure IV-31 shows the viscosities and conductivities of the different investigated C$_n$ TOTO ILs as a function of temperature. The experimental

data can in both cases be well described by the Vogel-Fulcher-Tamman (VFT) equation (Equation IV-6 and IV-7). This Equation generally was fitted to the features of compounds revealing glass transitions. Nevertheless, reasonable values can be obtained in the present case. In addition to the temperature T and the gas constant R, it contains three adjustable parameters, namely the factor η_0 or κ_0, the pseudo-activation energy E, and the so-called VFT temperature T_0 [376].

$$\eta = \eta_0 \exp(\frac{E}{R(T - T_0)})$$ IV-6

$$\kappa = \kappa_0 \exp(-\frac{E}{R(T - T_0)})$$ IV-7

The results of corresponding fits are summarized in Tables IV-11 and IV-12.

As evident from Figure IV-30 (A), the viscosities of the investigated TOTO ILs increase with the chainlength of the ammonium cation, while an inverse trend is observed for their conductivities (Figure IV-30 (B)). This behaviour is a common phenomenon and can be explained by enhanced van der Waals interactions. These provoke higher viscosities, and a lower charge density per unit volume, which accounts for the decrease of the specific conductivity [338-339, 377].

At 30 °C, the viscosities of the investigated ammonium ILs vary with increasing chainlength between 201 mPa s and 357 mPas, and the conductivities between 0.003 mS cm^{-1} and 0.002 mS cm^{-1}. The magnitude of η is comparable with those of common long-chain Ionic Liquids with anions such as PF$_6^-$ or TFSI [377]. The comparison of the conductivities to literature data is difficult, since values are rare for long-chain derivatives. Hexyl- and octyltrimethylammonium Ionic Liquids with TFSI counterions have been reported to express conductivities of 0.043 to 0.035 Sm^{-1} [377]. In this context, the values of the investigated TOTO ILs seem outstandingly low. This fact can easily be understood by the protic nature and the small pK$_a$ difference of base and acid (compare previous sections IV.3.3.1.1 - 2) of C$_n$ TOTOs.

Hence, a considerable amount of neutral species is existent in the mixture, which consequently originates such low κ values.
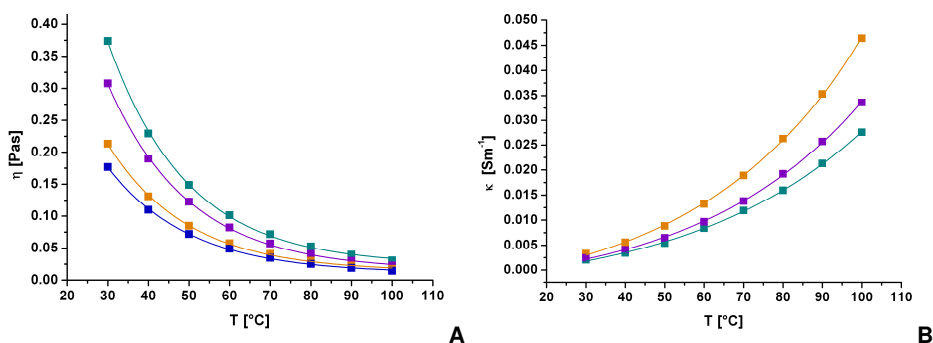
Figure IV-30: Viscosities η (A) and specific conductivities κ (B) of the C12 ■, C10 ■, C8 ■ and C6 ■ TOTO as a function of temperature. Full lines represent fits according to the empirical Vogel-Fulcher-Tamman Equation. Corresponding fit parameters are given in Tables IV-11 and IV-12.

Most interestingly, the TOTO anion enables the formation of RTILs with different simple and commercially available cations, which cover a wide range of accessible viscosity and conductivity values. Essentially, by exchanging Na (η (Na TOTO) ~ 95000 mPas at 30 °C) [342] for long-chain primary ammonium compounds, the viscosity at 30 °C of the resulting TOTO IL is reduced by a factor of beyond 400. Replacing sodium by ammonium ions, the three dimensional cross-linked structure characterizing Na-TOTO seems to be broken up, since interactions between the cation and the carboxylate group are weakened. Further, the long-chains of the ammonium compounds prevent additional interactions of the cationic moiety with the ether functionalities of the TOTO ion like described in the sodium case [322]. Consequently, the viscosity is drastically reduced. Yet, the conductivity stays in the same order of magnitude. Low conductivities in the sodium case were attributed to the strong three dimensional networking and thus, the enhanced molecular character of the compounds. In the present case, as described above, the presence of really uncharged species is likely to cause this

phenomenon. These assumptions are corroborated by the Walden plot (see below).

Table IV-11: VFT parameters obtained from fits of temperature-dependent viscosity data according to Equation IV-6 for C8, C10 and C12 TOTO Ionic Liquids.

Substance	η_0 [Pas]	E [kJmol^{-1}]	T_0 [K]
C8 TOTO	0.000063	10.58	-127
C10 TOTO	0.000013	16.58	-169
C12 TOTO	0.000132	10.09	-123

Table IV-12: VFT parameters obtained from fits of temperature-dependent specific conductivity data according to Equation IV-7 for C8, C10 and C12 TOTO Ionic Liquids.

Substance	κ_0 [Sm^{-1}]	E [kJmol^{-1}]	T_0 [K]
C8 TOTO	17.1	11.20	145
C10 TOTO	9.4	10.34	152
C12 TOTO	3.3	7.91	174

The association of cations with anions can be quantified by the use of a Walden plot as suggested by Angell and co-workers [59, 338]. The Walden rule relates the ionic mobility (represented by the molar conductivity Λ_m) to the fluidity $(1 / \eta)$ of the medium. If the ions could move independently from their next neighbours, i.e. the salt is fully dissociated, the plot gives a line of unit slope such as for dilute aqueous KCl solutions. In turn, if ion pairs are formed, the movement of the distinct ions will be correlated. Consequently, a negative deviation of the ideal line should be detected. Angell and co-workers classified ILs as "good" and "poor", according to a small or large vertical deviation (ΔW) of the ideal KCl line, respectively. ILs with $\Delta W < 1$

(close to the KCl line), combine high fluidities with high conductivities and are therefore referred to as "good" Ionic Liquids. Such ILs are additionally featured by low vapour pressures [59, 338].
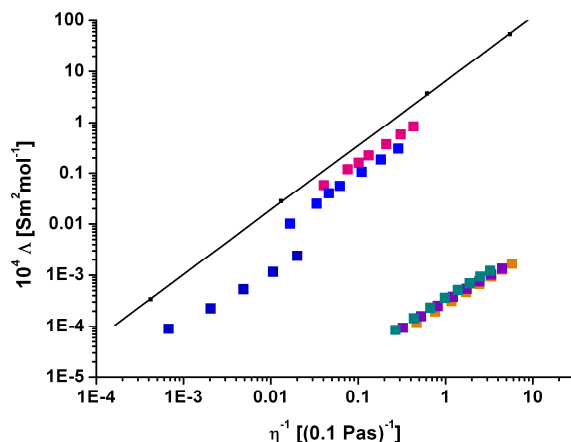
Figure IV-31: Walden plot of C8 ■, C10 ■ and C12 ■ TOTO Ionic Liquids for temperatures ranging from 30 to 100 °C; comparison to the ideal KCl line (full line), Na ■, tetraethylammonium (TEA) ■ and tetrapropylammonium (TPA) ■ TOTO (values taken from ref [366].

As evidenced by the Walden plot (Figure IV-31) and the ΔW values (Table IV-13), the C_n TOTO ILs are located far from the ideal line ($\Delta W > 1$) and thus, belong to the class of "poor" Ionic Liquids, according to Angell. An equal conclusion has been drawn for the Na TOTO IL [342]. This classification of C_n TOTOs bases on the outstandingly low conductivity of the ammonium TOTO salts while for the sodium salt the enormous viscosity seems to be the main reason. In line with the trend indicated by the viscosity and conductivity data, ΔW increases with rising the number of carbons in the aliphatic chain of the ammonium from three (TPA) to eight and higher (C8, C10, C12). Additionally, the deviation from the ideal KCl line becomes more pronounced at elevated temperature. This indicates a correlated movement of adjacent ions, i.e. the salt is incompletely dissociated, like already stated above.

Interestingly, TOTO salts of small tetraalkylammonium (TAA) ions have recently been proved to belong to the class of "good" Ionic Liquids [366]. In view of the proposed cross-linked structure of Na-TOTO, the differing positions of TAA- ILs in the Walden plot was ascribed to a more "loose" three-dimensional organization, simply due to the larger cation sizes. In addition, the higher ionicity of TAA- ILs was explained by weakened ionic interactions between cations and anions as compared to alkali-TOTO ILs.

Table IV-13: Deviation ΔW of C8, C10 and C12-TOTO Ionic Liquids of the ideal KCl line in the Walden plot at different temperatures.

T [°C]	30	40	50	60	70	80	90	100
C8 TOTO	4.3	4.4	4.4	4.4	4.4	4.5	4.5	4.5
C10 TOTO	4.2	4.2	4.3	4.3	4.4	4.4	4.5	4.5
C12 TOTO	4.2	4.2	4.2	4.2	4.3	4.3	4.4	4.4

IV.3.3.2 Structures in Binary Mixtures with Water

IV.3.3.2.1 Critical Micellar Concentration (cmc) in Water

Critical micellar concentrations were derived from the breakpoint in conductivity versus concentration curves (Figure IV-32 A). Figure IV-32 B proves the linear dependence of the cmc of the chainlength n of the ammonium ion. A linear decrease by a factor of four per addition of two CH_2 groups, being common for ionic surfactants, could be deduced. The Klevens equation (Equation IV-8) summarizes this typical feature of ionic surfactants [94]. The logarithm of the cmc is a linear function of the alkyl chainlength:

$$\log cmc = An + B \qquad\qquad \text{IV-8}$$

For mono-ionic surfactants, the constant A typically adopts the value 0.3 [87], which is in good agreement with that found for the investigated surfactants (0.29). The parameter B is a constant for a particular ionic head at a given temperature. A value of 1.54 could be derived for C_n TOTO salts. For alkylammonium chlorides (C_n Cl) a value of 1.7 could be deduced, with the help of literature data (Table IV-14). Hence, a consistency can be stated.
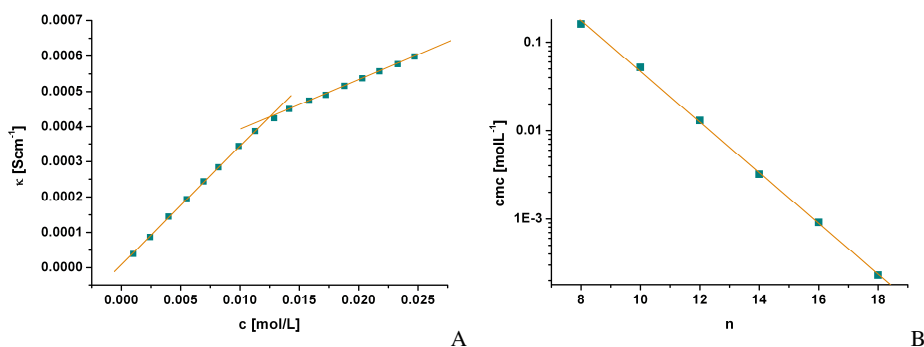
Figure IV-32: Concentration dependent plot of the specific conductivity κ of C12 TOTO at 25 °C (A). Cmcs in dependence of the chainlength n of the ammonium ions (B). The straight lines are linear fits.

In Table IV-14, the values of the cmcs for the investigated TOTO salts are compared with those of the related alkylammonium ions with different counterions. Apparently, the cmcs of C_n TOTO are in the same order of magnitude as those of the alkylammonium halogenides. Moreover, the cmc of C12 TOTO coincides nearly exactly with that of C12 Cl, indicating that the exchange of the halogenides does not noticeably influence micelle formation.

Micellisation of ionic surfactants in aqueous solutions is opposed by headgroup electrostatic interactions, which however are balanced to a large extent by counterions bound at the micelle/solution interface. The replacement of an inorganic by an organic anion in dodecylammonium salts *e.g.* alkanesulfonates, lead to significant reductions in cmc values

(Table IV-14). This was ascribed to the effect of the hydrophobic interaction of organic counterion with exposed hydrocarbon groups at the micelle/solution interface [378].

Table IV-14: Comparison of cmc and degree of counterion association β in dependence of the counterion (Cl = chloride, Br = bromide, PSulf = propylsulfonate) of decyl and dodecylammonium ions.

Substance	cmc [mM]	β	T [°C]
C10 TOTO	52.1 +/- 0.3	-	25
C12 TOTO	13.0 +/-0.4	0.77 +/- 0.03	25
C10 Cl [379]	64	-	25
C10 Br [379]	52	-	25
C12 Cl [380]	13.1	0.83	25
C12 PSulf [378]	~ 10	0.63	20

Yet, in the present case no difference between the cmc values of halogenides and TOTO salts could be detected. For further confirmation of the same mode of action for both types of counterions, the degree of counterion binding to the micelles β was compared. For that purpose the molar equivalent conductivity at 25 °C was plotted against the root of concentration of C12 TOTO (Figure IV-33). This method allowed the derivation of molar equivalent conductivity at infinite dilution (Λ^0). Taking into account the single ion conductivity of dodecylammonium (λ^+), which is 18.65 Scm^2mol^{-1} according to Sugihara *et. al.* [378], the single ion conductivity of TOTO (λ^-) could be deduced by means of the following Equation:

$$\Lambda^0 = \lambda^+ + \lambda^- \qquad \textbf{IV-9}$$

The values of the micelle ionization degree α at the cmc were calculated from the obtained conductivity, using Equation IV-10 derived by Evans [381].

$$S_2 = N^{2/3} \alpha^2 (S_1 - \lambda^-) + \alpha\lambda^- \qquad \textbf{IV-10}$$

Hence, the degree of counterion binding is given by:

$$\beta = 1 - \alpha \qquad\qquad\qquad \textbf{IV-11}$$

In Equation IV-10, S_1 and S_2 denote the slopes of the plot of the specific conductivity as a function of the concentration below and above the cmc (Figure IV-33). N terms the aggregation number at the cmc and was estimated to equal that of C12 Cl ($N = 56$) [380]. However, the value of β derived from Equation IV-11 is not very sensitive to the value of N. The uncertainty given in Table IV-14 defines the limits of β, upon consideration of 15 % deviation of N.
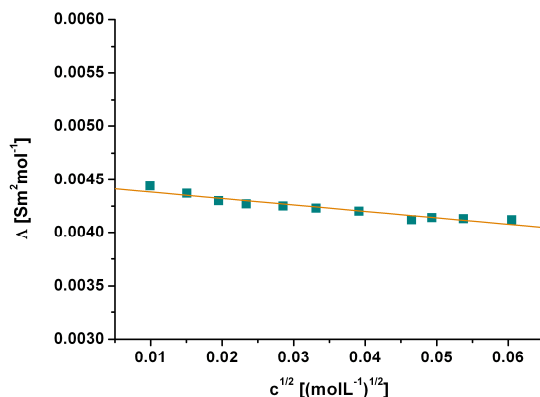
Figure IV-33: Dependence of the equivalent conductivity Λ of C12 TOTO in dependence of the concentration c.

At low concentrations, a similar mode of action of TOTO and chloride combined with long-chain alkylammonium ions can be deduced upon consideration of the corresponding cmc- and β values. This effect probably is due to the fact that the ether functionalities of the TOTO ion tend to preferentially being hydrated, rather than being adsorbed to or intercalated into the micellar headgroup "sub"-phase. Both alternatives would influence the degrees of freedom of the ether units as well as the surrounding water-structure in an energetically unfavourable way.

IV.3.3.2.2   *Phase Diagrams in Water*

As a first step towards the determination of phase diagrams of the long-chain ammonium TOTO salts, the penetration scan technique. This is a fast method to obtain information on the mesophases sequence of a surfactant in water. Exemplary photographs of the penetration scans of C14 TOTO and C16 TOTO at 10 and 25 °C are shown in Figure IV-34.

In all investigated cases (C12, C14 and C16 TOTO) a sequence along rising surfactant concentration of micellar (L_1), discontinuous cubic (I_1), hexagonal (H_1), reverse micellar (L_2) and solid (S) could be identified at low temperatures. The exact phase boundaries were determined by examining samples of different concentrations between crossed polarizers as a function of temperature. Moreover, the Krafft boundary – the boundary between the crystalline and the "molten" aliphatic chains – was visually spotted by detecting the temperature where the samples turned transparent. Accordingly, Figure IV-35 shows the aqueous binary phase diagrams between 0 and 90 °C of C12, C14 and C16 TOTO.
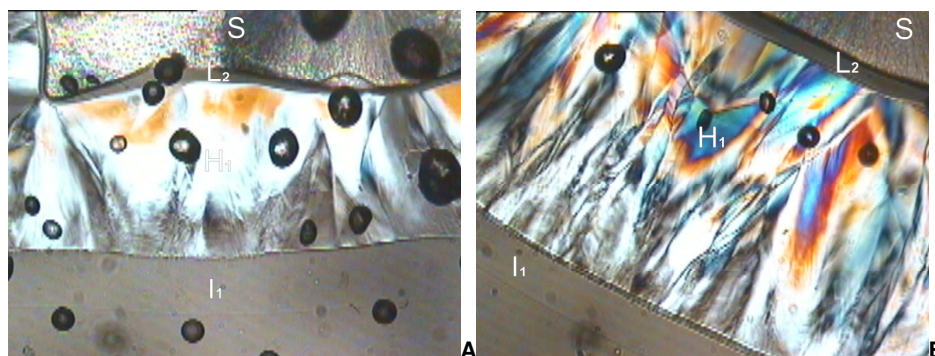
Figure IV-34: Penetration scans of C14 TOTO (A) and C16 TOTO (B) at 10 and 25 °C, respectively with a magnification of 100x and semi-crossed nicols.

The phases were confirmed by small angle X-ray scattering (SAXS). Selected diffractograms of C14 TOTO expressing typical patterns for the different phases are depicted in Figure IV-36.
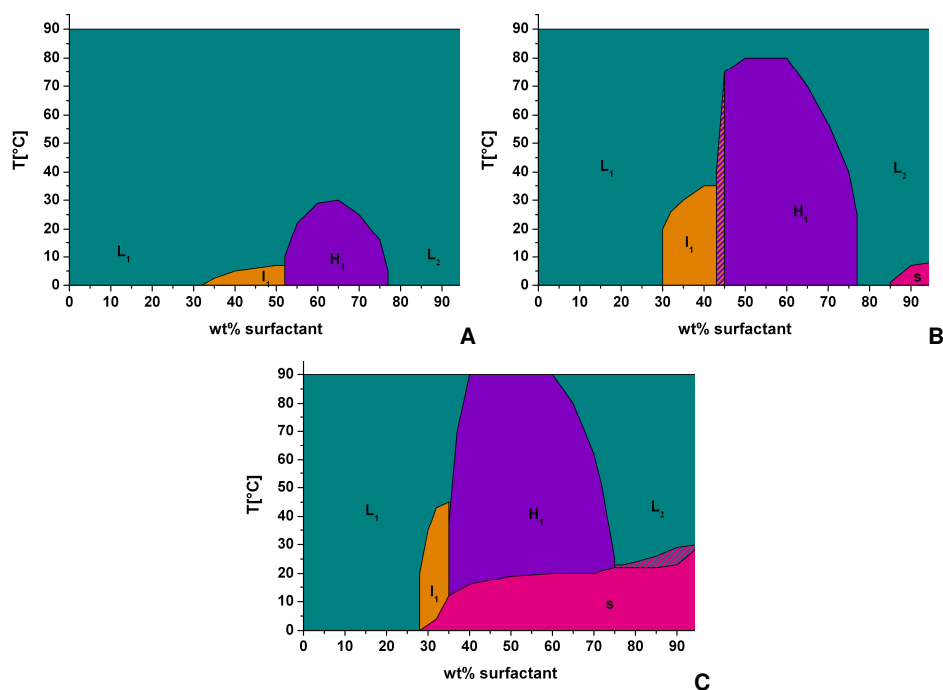
Figure IV-35: Binary phase diagrams of C12 (A), C14 (B) and C16 (C) TOTO in water between 0 and 90 °C. The hatched domains represent two phase regions, which were optically birefringent.

Figure IV-36 A reflects the X-ray pattern situation at the cubic hexagonal phase boarder in all investigated samples. The diffraction pattern shows double peaks in every Bragg reflection. The most common cause for such a pattern is inhomogeneity in the sample, i.e., two domains in different hydration states. In that case, one set of the peaks normally would disappear when the sample came to equilibrium. The cubic space groups could not be identified unambiguously due to the restricted number of peaks. The hexagonal phase was confirmed over the whole concentration range (Figure IV-36 B, C) assumed for its existence by optical microscopy. At high sample concentrations, a broad peak was detected which could be assigned to the reverse micellar phase (Figure IV-36 D). 99 wt% samples exhibited a lamellar peak periodicity superimposed by a broad peak (Figure IV-36 E). Thus, the sample either was not completely monophasic and the coexistence of a smectic crystals and an L_2 phase was detected, or the bilayers were

interspersed with periodically arranged holes/defects, expressing a so-called mesh-phase [4].
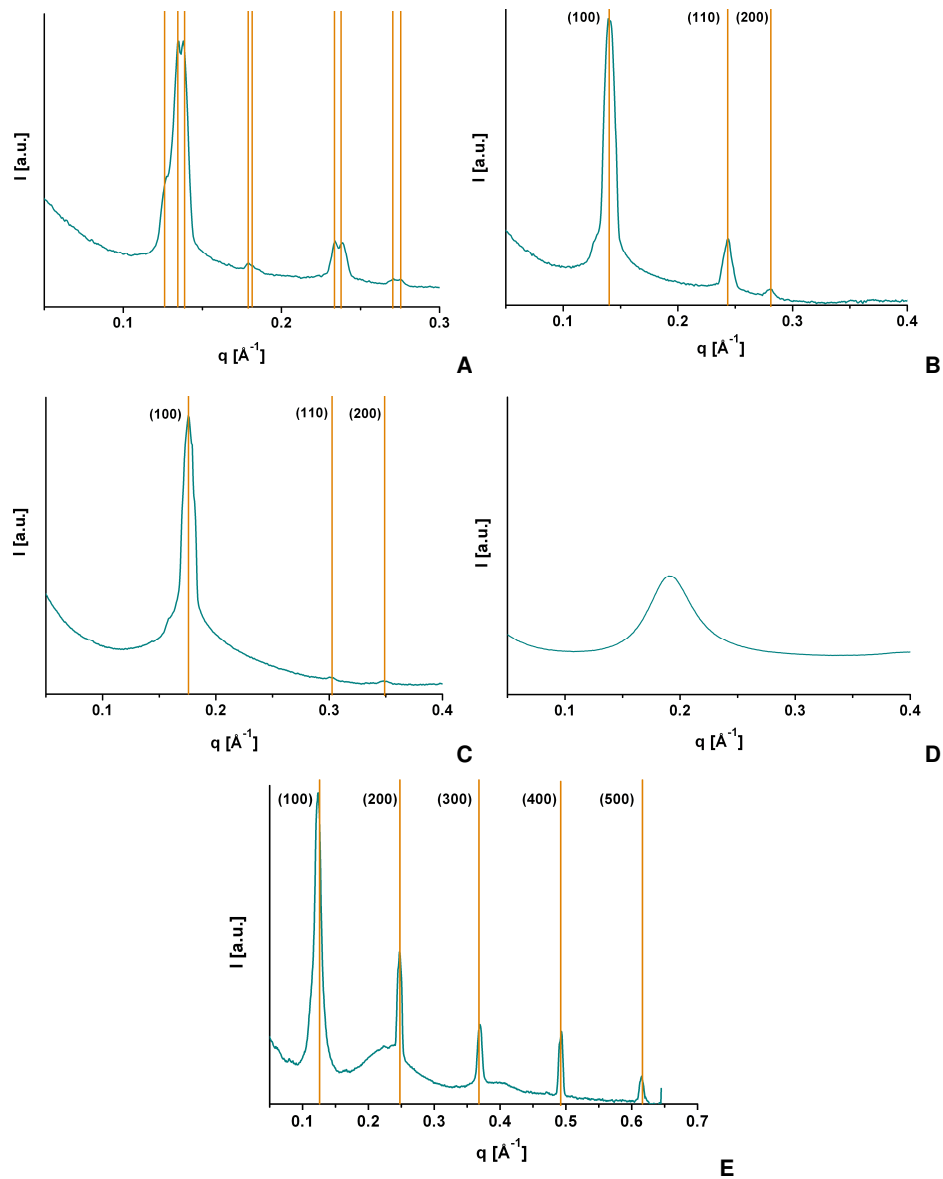
Figure IV-36: Exemplary radial averaged SAXS spectra of C14 TOTO at 25 °C: 45 wt% (A), 55 wt% (B), 75 wt% (C), 85 wt% (D) and 99 wt% (E). Peak positions with corresponding Miller indices are indicated by the vertical lines.

Following the phase shifts in the phase diagrams with growing alkylchainlength, there are mainly three points to be considered: the progression of the Krafft boundary, the extent of each phase in dependency of the surfactant volume fraction and its thermal stability.

While C16 TOTO starts to become insoluble above 0 °C at approximately 28 wt%, C14 TOTO expresses only a small area of undissolved state at very high concentrations. C12 TOTO is even soluble over the whole investigated temperature and concentration range. The Krafft and the melting temperatures are known to correlate. The melting point difference of C14 and C16 TOTO is approximately 17 °C (Table IV-10), which nearly exactly equals the difference in solubility temperature at 95 wt% of surfactant.

Obviously, the hydrophobic effect is only marginally pronounced in the case of TOTO salts, in contrast to some other surfactants. For example, classical sodium soaps show thermotropic phase transitions which chainlength-dependently vary by scarcely 10 °C [382], while their Krafft points can differ by nearly 50 °C (T_{Kr} (NaC12) ≈ 20°C and T_{Kr} (NaC18) ≈ 70°C) [304].

The concentration of surfactant at which a cubic discontinuous phase can first be detected stays nearly constant, independent of the chainlength of the ammonium ion. Yet, the onset, with rising concentration, of the hexagonal phase shifts to lower amounts of amphiphile, while the offset remains unaltered in the row C12, C14, C16 TOTO.

The transition of a micellar to a discontinuous cubic phase is an order/disorder phenomenon and merely restricted by the volume fraction of surfactants and their aggregates (upon consideration of micelles as hard spheres). A hexagonal phase occurs at volume fractions above the close-packing limit of spherical micelles. This phase change is due to an alteration of micellar shape. It generally involves constraints on the value of the surface per molecule due to finite alkylchainlengths and thus, restricted surface-area/volume ratios within a certain type of aggregate. Hence, increasing chainlength of a surfactant, considering an equal headgroup and counterion situation, shifts the onset point of the I_1/H_1 transition to lower volume

fractions. The H_1/L_2 concentration dependent boundary is independent of the alkylchainlength. Generally such a boundary is not very common for ionic surfactant water systems at room temperature [10]. Hence, it must be attributed to the special features of the TOTO counterion. In non-ionic systems, H_1/L_2 boundaries are frequently observed at lower temperatures. This transition has been attributed to a sudden formation of structured water around the ether moieties (EO) at a certain water content, starting from the pure surfactant entailing a drastic reduction in area per alkylchain [10]. The repulsions across the EO-medium increase within a very small region of concentration, which enables mesophases formation. The free energy of this water structure formation is high at low temperatures and decreases with rising temperature. This means that the water structure does only form upon sufficiently higher water contents. On the other hand it fails to appear at high temperatures. The reason for this is that EO-EO interactions become more favourable than EO-water interactions, which gives the ether units more conformational freedom. Further, the hydrophobic effect (the repulsion of alkylchains and water) is reduced. Consequently, the area per molecule increases again. However, the complete melting of a mesophases occurs at higher temperatures with increasing chainlength. Thus, the negative curvature due to alkyl-chain conformational degrees of freedom causes small micelles to change to mesophases at larger values of a as the alkyl-chainlength is increased [10].

Table IV-15: Density ρ_{Surf} and volume V_S of one C_n TOTO molecule at 25°C. The volume of the lipophilic part V_L and the length of the fully extended alkylchains r_{max} were calculated according to Tanford

Substance	$\rho_{Surf} [gL^{-1}]$	$V_S [Å^3]$	$V_L [Å^3]$	$r_{max} [Å]$
C16 TOTO	945.5	814	457.8	21.75
C14 TOTO	962.7	751	404	19.21
C12 TOTO	980.8	690	350.2	16.68

Although in the present case of long-chain ammonium cation and TOTO anion there is no covalent connection between the ether groups and the alkylchain, the above stated explanations for common non-ionic surfactants seem to be perfectly adaptable. These assumptions are further supported by the evaluation of small angle X-ray data within the hexagonal phases.

In order to estimate the radius of the lipophilic part r_L and the effective area a_L of the alkylchain at the water/alkylchain interface, the volume fraction of the surfactant ϕ_S and of the lipophilic part ϕ_L are essential. ϕ_S is given by Equation IV-12, wherein c denotes the weight fraction of surfactant. Further, ρ_{Surf} and ρ_W are the densities of surfactant and water ($\rho_W = 997.1$ gL^{-1}), respectively. Values of ρ_{Surf} were obtained by extrapolating density data at elevated temperatures to 25 °C or by estimation according to the CH$_2$-increment derived from shorter chain derivatives.

$$\phi_S = (1 + \frac{\rho_{Surf}(1-c)}{\rho_W c})^{-1} \qquad\qquad \textbf{IV-12}$$

Consequently, ϕ_L can be calculated according to Equation IV-13, where V_S and V_L designate the volume of surfactant and of the lipophilic part, respectively.

$$\phi_L = \frac{V_L}{V_S}\phi_S \qquad\qquad \textbf{IV-13}$$

From the density measurements the molar volume of surfactant and therewith the volume of one surfactant molecule V_S (Table IV-15) was derived. The volume of the aliphatic chains V_L was estimated by the expression of Tanford (Equation IV-14) [104].

$$V_L = 27.4 + 26.9n_C \qquad\qquad \textbf{IV-14}$$

With n_C being the number of carbon atoms in the hydrophobic tail. For further comparison the maximum (all-trans conformation) lengths r_{max} of the respective alkylchains, which can also be calculated by the expression of Tanford (Equation IV-15) are likewise given in Table IV-15.

$$r_{max} = 1.5 + 1.265 n_C \qquad\qquad \textbf{IV-15}$$

With the inter-layer spacing d, given by the position of the first scattering peak ($d= 2\pi/q$), the radius of the lipophilic part r_L and the cross-sectional area a_L at the alkylchain/water interface in the hexagonal phase are given by Equations IV-16 and IV-17, respectively [383]:

$$r_L = d(\frac{2}{\sqrt{3}\pi}\phi_L)^{1/2} \qquad\qquad \textbf{IV-16}$$

$$a_L = \frac{2V_L}{r_L} \qquad\qquad \textbf{IV-17}$$

The results for the cross-section area at the alkylchain/water interface a_L and the radius of the lipophilic part r_L in the hexagonal phase of C16 TOTO are shown in Figure IV-37 as a function of the surfactant volume fraction ϕ_S. In the region of lower volume fractions, r_L increases approximately linearly with rising amount of surfactant. After a short, nearly constant region, the value of the radius of the lipophilic part drops drastically at volume fractions close to the boarder to the L_2 phase. The area per alkylchain at the polar/non-polar interface behaves exactly oppositional.
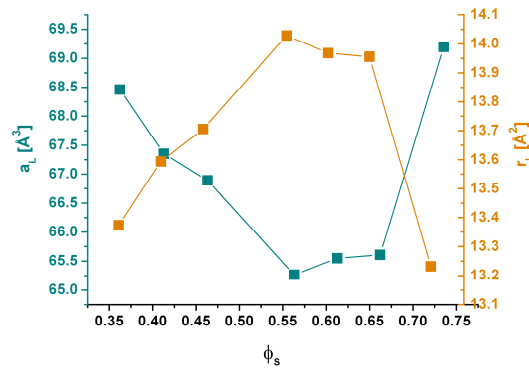
Figure IV-37: Radius of the lipophilic part r_L and the area at the polar-nonpolar interface a_L in the hexagonal phase of C16 TOTO as a function of the surfactant volume fraction ϕ_S.

Based on the theory of non-ionic surfactants, these data perfectly reflect the assumption made in a previous section for the phase transition at the H_1/L_2 boarder. The cross-sectional area drastically decreases with increasing water content close to the concentrated mesophases boarder, probably due to the formation of structured water. The further sequel of the area in dependence of the concentration equals that of common surfactants: Upon rising water content, the area per hydrocarbon chain increases steadily.

Compared to the length of the alkylchain r_{max} in the all-trans conformation (Table IV-15), r_L is approximately 35 to 39 % shorter. Generally, most surfactants merely undergo a chainlength compression of 10 to 20 % [110]. The results presented here are due to the large TOTO anion. On the one hand it is questionable to what extent this ion should be considered in the calculation of the surfactant volume, which in turn significantly influences the further calculations. On the other hand, a close adsorption of the TOTO ion to the headgroups in the concentrated domain of the phase diagram seems not implausible. A not negligible repulsive force due to its conformational flexibility supplies extra space for the alkylchains in the interior of the aggregates. The aliphatic moieties exploit the gained conformational freedom, which is expressed by shorter average chainlengths and relatively large cross-sectional areas at the polar/non-polar interface, compared to common ammonium surfactants with values around 50 Å^2.

IV.3.3.3 Biodegradability and Cytotoxicity of TOTO ILs

IV.3.3.3.1 *Biodegradability*

Biodegradation studies are a powerful method to asses the fade in the environment of organic contaminants of anthropogenic origin. According to appropriate legislation of novel compounds, the environmental risk assessment and required. The OCDE standard defines organic molecules as biodegradable if 60 % of the substance has been degraded within 10 days

after the 10 % level had been reached, and if globally at least 60 % have been consumed after 28 days. However, for surfactants the criterion is less strict. Following the European standard CE2004/648 [384], a surfactant is to be classified as biodegradable if 60 % degradation is achieved after 28 days.

Figure IV-38 shows the biodegradation profiles of C12 TOTO as a function of time. For comparability reasons, the evolution of the biodegradation of the standard compound sodium acetate (NaOAc) as well as of the common long-chain Ionic Liquid 1-hexadecyl-3-methylimidazolium chloride (C16MIM Cl) is likewise depicted. It is obvious that C12 TOTO meets the 60 % criterion. Yet, in contrast to NaOAc, biodegradation only starts after a short retardation period. Such behaviour generally can give hint towards cytotoxic effects of the investigated compounds. On the other hand, C16MIM Cl is not degraded at all. The percental biodegradation after 28 days even tends to values lower than the starting point of observation. This observation might become evident upon consideration of the crucially influencing factors of biodegradation.
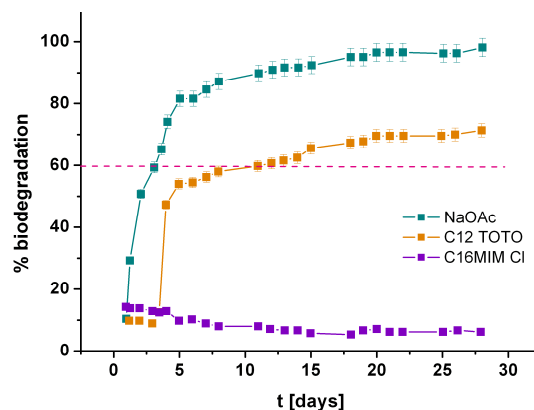
Figure IV-38: Biodegradation as a function of time of C12 TOTO ■ and C16MIM Cl ■ with NaOAc ■ as standard. The dashed line marks the 60 %-criterion for readily biodegradable surfactants.

First of all, the number of micro organisms capable of metabolizing the organic compound restricts the degradation rate. The inhibition effect spotted

for the TOTO compound at the beginning of the measurement as well as the decreasing biodegradation with time of C16MIM Cl both indicates cytotoxic effects. Generally, cationic surfactants are known to bear toxic potential due to their charge which entails fast adsorption to cells. However, the toxic potential of the imidazolium compound evidently is much more pronounced

Further, the bioavailability of the organic substance has to be considered upon interpretation of their biodegradation profiles. This criterion mainly depends on the chemical fate and the mass transfer (*e.g.* from adsorbed to the aqueous phase, or dissolution rate) of an organic compound. Yet, both investigated compounds are soluble at room temperature. Fast chemical degradation due to *e.g.* hydrolysis can be excluded for both amphiphiles. However, the adsorption of the investigated cationic surfactants to the walls of the measurement cell is not unlikely, as most surfaces in nature are negatively charged [87]. This fact further promotes an incomplete degradation within the investigated period of time.

IV.3.3.3.2 *Cytotoxicity*

The cytotoxicities of the synthesised long-chain TOTO surfactants on the HeLa cell line, expressed in IC_{50} values, are summarized in Figure IV-39. The results are compared to the common cationic alkyltrimethylammonium bromide (C_nTAB) and dodecylammonium chloride (C12 Cl) surfactants as well as the classical long-chain 1-alkyl-3-methylimidazolium chloride Ionic Liquids (C_nMIM Cl).

Under the chosen conditions the TOTO based surfactants express comparatively low cytotoxicities. The IC_{50} value of C12 TOTO approximately equals that of C12 Cl, revealing a minor impact of the TOTO anion. Evidently, the toxicity decreases with shorter alkylchains, which becomes specifically pronounced upon carbon numbers in the aliphatic tail below twelve. Furthermore, a distinct influence of the cationic headgroup was detected. This becomes particularly clear upon comparison of C12 Cl and C12MIM Cl whose IC_{50} values differ by nearly one order of magnitude.

Considering the mechanism of toxic action of a surfactant, it generally has to adsorb to a cell-membrane in a first step. This action must be electrostatically driven in the case of cationic amphiphiles [210, 385]. However, the pronounced differences in IC_{50} values between various headgroups suggest an additional factor of influence. According to recent SAR (structure activity relationship) studies applied to Ionic Liquids, the cytotoxicity is expected to increase linearly with rising hydrophobicity of the investigated compound [363-365, 386]. This trend is confirmed by the analysis of the chainlength dependence of the present data. Furthermore, the trimethylammonium as well as the methylimidazolium headgroup can be considered to be more hydrophobic than a primary ammonium moiety, which in consequence explains the increased toxic impact. Though, conclusions must be carefully drawn, since cytotoxicity does not increase linearly with the hydrophobic character of a compound. Recent investigations of odd and even numbered fatty acid soaps suggested a more specific mechanism, supplementary to the simple hydrophobicity [15].
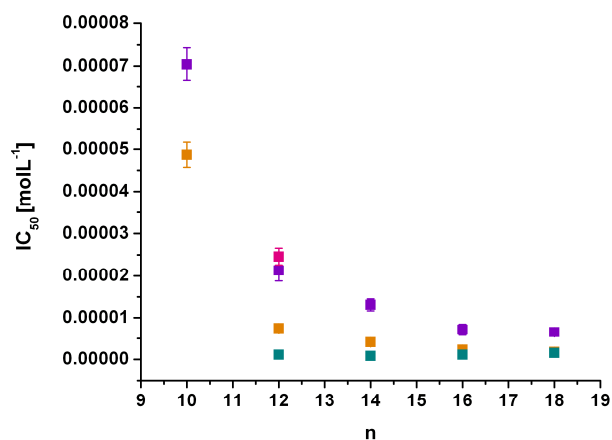
Figure IV-39: The mitochondrial reduction of MTT (expressed in IC_{50} values) after 72 h of incubation with different cationic surfactants: C_n TOTO ■, CnTAB ■, C_nMIM Cl ■ and C12 Cl ■.

IV.3.4   Conclusion

Long-chain primary ammonium salts of the 2,5,8,11-tetraoxatridecan-13-oic acid (TOTOA) were proven to form room temperature Ionic Liquids up to a chainlength of twelve carbon atoms. The outstanding flexibility of the anion just like the fact that both, a weak acid and a weak base were combined, probably account for the detected properties. Low viscosities, low conductivities and low thermal stabilities must be ascribed to the pronounced non-ionic character of the investigated ILs due to charge readsorption. According to the Walden plot concept, introduced by Angell *et al*., for the classification of Ionic Liquid properties, C_n TOTO salts range in the order of "poor" ILs. However, this finding is not outstandingly disadvantageous since scarcely any long-chain Ionic Liquid can be classified as "good" due to their low charge densities. Yet, The TOTO anion is obviously capable for forming RTILs with a variety of cations. The viscosity, conductivity and solvent polarities of TOTO ILs can be effectively tuned over a large range by varying the cation. Thus, truly task-specific design is permitted.

Surfactant properties in binary mixtures with water can even be considered to be significantly improved. The formation of highly viscous liquid crystals, like the hexagonal and cubic phase, can be efficiently shifted to lower temperatures upon exchanging the common halogenid counterions by TOTO. This fact, in combination with the unaltered toxicity upon the introduction of the huge ethercarboxylate, the ready biodegradability, as well as the liquid state in pure form, renders the presented cationic TOTO salts interesting alternatives to common cationic surfactants in a variety of applications.

IV.4 Physico-Chemical and Toxicological Properties of Novel Choline- and Ectoine-Based Cationic Surfactants and Spontaneously Formed Low-Toxic Catanionic Vesicles Thereof

IV.4.1   Introduction

In the context of drug- [387-388], gene delivery [389-390] and drug antimicrobial activity [391], micelles and vesicles are colloidal aggregates of great biomedical interest [6]. Such carrier-vesicles have been classically achieved by polar lipids or their mixtures (liposomes) or by mimicking non-natural double-tailed surfactants, such as dialkyldimethylammonium halides [388]. Yet, classical liposomes often present drawbacks for applications, mainly due to the easy chemical degradation of the lipids and their relatively complex preparation procedures [392]. This problem was approached in several studies of cross-interaction of lipids and surfactants [392]. In this context, mixtures of oppositely charged surfactants (catanionics) have emerged in the last 10 - 15 years as a promising alternative, which expresses highly stable vesicles [135, 182, 393]. The most outstanding advantages of catanionic systems compared to conventional liposomal vesicles are:

- They generally form spontaneously upon mixing,

- they bear long-term stability and in many cases exist as equilibrium structures,

- they often present chain melting transitions well below room temperature and

- they offer the possibility of charge adjustment, due to variation of the surfactant mixing ratio.

The vast majority of investigations dealing with catanionic systems reported on the structural/equilibrium state of the aggregates. Typically, the vesicles are composed of conventional ionic surfactants. These systems have been shown to possess good encapsulation properties both for probe molecules and some currently used therapeutic drugs. In addition such systems have been employed in the context of non-viral vectors for gene delivery [6, 394-395]. Despite their relevance for potential biomedical uses, the assessment of the biological properties of catanionic vesicles has been less explored. A few recent reports have addressed the mechanisms behind the toxicity of such vesicles [370, 396-398]. Parallel to the investigation of the biological impact of catanionic systems the trend to design novel amphiphiles that, in addition to the desired performance, have enhanced biocompatibility and biodegradability was accelerated [398]. Particularly, the common cationic surfactants were spotted to bear most undesirable biological impact. By replacing common headgroups by others based on natural raw products, less toxic molecules are expected to be generated [398]. For that purpose, amino acid-based surfactants, which are composed of an amino acid moiety as the polar headgroup being attached to one or more alkylchains have attracted great interest. They have been reported to be more biocompatible and environment-friendly than surfactants with conventional hydrophilic moieties [398]. Especially cationic amino acid surfactants have been shown to posses this property in addition to lower persistence in the environment than the widely used quaternary ammonium surfactants [181, 390, 398-399]. Adjacent to the amino acid approach, sugar based headgroups were tested with regard to their biological impact. Within this context, I. Rico-Lattes and co-workers published on sugar-derived bi- and tricatenar catanionic surfactants capable

of effectively encapsulating hydrophilic drugs [6]. Furthermore, Benvegnu and his group described the synthesis, properties and potential applications of cationic surfactants based on natural glycine betaine and vegetable oils as renewable raw materials [400]. Additionally, Holmberg and co-workers reported on the hydrolysis and biodegradation of cationic ester containing surfactants with betaine and choline headgroups [401-402].

Prior to these studies, the investigation of further ammonium based headgroups with biological origin has been only scarcely developed. Apart from glycine betaine, amino acids and a few reports on choline (see above), the area of biologically originated osmolytes has been totally ignored. On this account, we selected choline (Ch) and ectoine (Ecto) (Figure IV-40) as adequate cationic headgroups of amphiphiles with scarce toxicological and biological potential of harm. Ectoine, as small organic, amphoteric and water-binding molecule, occurs widely in aerobic, chemoheterotrophic, and halophilic organisms that enable them to survive under extreme conditions [14]. It generally is compatible with the cellular metabolism without adversely affecting the biopolymers or physiologic processes. Thus, it is a so-called compatible solute. The protective function of the compatible solutes in a low water environment might be explained by the "preferential exclusion model" [403]: The solutes are excluded from the immediate hydration shell of, for example a protein, because of an unfavourable interaction with the surface of the protein. Consequently, the protein is preferentially hydrated, which promotes its native conformation. Since compatible solutes do not interact directly with the protein surface, its catalytic activity remains unaffected. Supplementary, the protective properties of ectoine have been transferred to human skin, which lead to its wide application in *e.g.* anti-aging and sun-screen products [404]. Choline on the other hand, as an ion of biological origin, was recently proved to be a bio-compatible alternative to the simple tetraalkylammonium ions in soaps [352]. Choline, formerly known as vitamin B_4, has several key functions in the body [13]. Its molecular structure is shown in Figure IV-40. For instance, it serves as a precursor for phospholipids and acetylcholine [13]. Generally, choline hydroxide (ChOH) as a strong base provides a technologically interesting alternative to alkali or

alkaline-earth metal hydroxides, particularly in the field of wafer cleaning in semi-conductor industry [405].

On that account, herewith basic micellisation and toxicological properties of newly synthesised choline and ectoine surfactants with iodide and methylsulfonate, respectively as counterions are reported. In addition, results will be presented for novel catanionic vesicles prepared from mixtures of the ecologically sustainable cationic surfactants with choline carboxylate soaps, whose low biological impact has recently been proved [15].

A   **B**
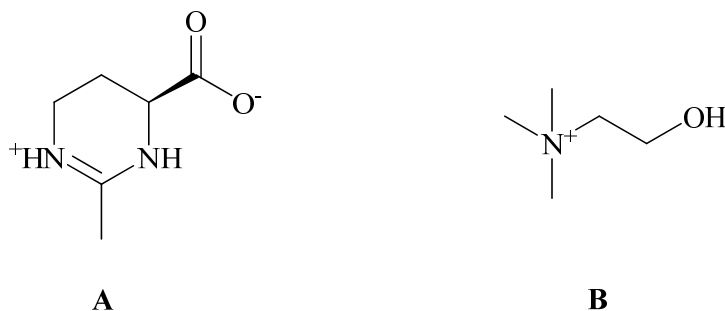
**Figure IV-40: Chemical structure of ectoine (Ecto) (A) and
choline (Ch) (B).**

IV.4.2   Chemicals and Methods

Methylsulfonic acid (> 99 %), ectoine (> 97 %) and myristoylchloride were received from Sigma. Sodium hydride (> 95 %), lauroylchloride (98 %), palmitoylchloride (> 98 %), methyliodide (99 %), choline iodide (98 %) and tetradecanol were provided by Aldrich. Decanol (> 98 %), dodecanol (> 98 %) and 2-chloro-N, N-dimethylethylamine hydrochloride (> 98 %) were received from Fluka. Sodium hydroxide (*p.a.*) and the anion exchange resin III were delivered by Merck whereas choline chloride (> 98 %) was received from Alfa Aesar. All solvents were used in *p.a.* quality. If not mentioned otherwise in the synthesis section, all chemicals were used without further purification

The critical micellisation concentrations (cmcs) were determined by conductivity measurements as described in chapter IV.3.

Solubility temperatures were determined by turbidity measurements using an automated home-built apparatus. Sample holders were placed in a computer-controlled thermostated bath. Light emitted by a LED crosses the samples and the transmitted light is detected by a light-dependent resistor (LDR). Samples were cooled if necessary until precipitation occurred and adjacently reheated at a rate of 1 °C/h.

Measurements of the surface pressure were accomplished with a Langmuir Blodgett trough. Surface pressure/area isotherms of the surfactants were obtained using a computer controlled NIMA Langmuir trough (NIMA Technology, UK) with a total area of 560 cm^2. Different surfactant concentrations (2.5, 5, 10, 40 mg mL^{-1}) in chloroform were prepared and spread onto a water sub-phase at room-temperature. A minimum period of 20 min was allowed for the evaporation of the solvent before compression. The isotherms were measured using the Wilhelmy plate method with a compression speed of 200 cm^{2}min^{-1} and a continuous readout. Solubility of the surfactant in water was checked on several compression-decompression steps with waiting times of several minutes. The stability of the monolayer was checked on compression until a certain pressure and left for a certain period of time.

For the determination of phase diagrams, an Orthoplan polarizing optical microscope (Germany), a Linkam hot stage with a Linkam TMS90 temperature control and a Linkam CS196 cooling system (Waterfield, UK) were used to carry out the microscopy experiments. The exact method is described in detail in chapter IV.1.

Vesicles were prepared by two different methods: The pure surfactants were weighed in according to the desired molar ratio r:

$$r = \frac{n_{Anionic}}{n_{Anionic} + n_{Cationic}} \qquad \text{IV-18}$$

where *n* is the amount in mol of anionic or cationic surfactant, respectively. Adjacently, the samples were diluted with Millipore water to achieve the pre-calculated total molar amphiphile concentration *c*.

$$c = \frac{n_{Anionic} + n_{Cationic}}{V_{Solution}} \qquad \text{IV-19}$$

The second method based on the mixture of micellar stock solutions of the single surfactants corresponding to the desired end-ratio *r* and total concentration *c*. Independently of the use of pure or diluted surfactant, the solutions were stirred at least 24 h to equilibrate. Aggregate shapes were obtained by cryo-TEM experiments. The samples were observed with a Zeiss EM922 EFTEM (Zeiss NTS GmbH, Germany). All examinations were carried out at 90K.

The cytotoxicity tests were performed with the HeLa (cervix carcinoma, ATCC CCL17) cell line using the MTT assay procedure according to Mosmann [369] and modified by Vlachy *et al.* [370] as described in detail in chapter IV.3. The IC$_{50}$ value (in mol/L) represents the concentration of test substance that lowers MTT reduction by 50 % compared with the untreated control.

Biodegradabilities of selected cationic surfactants were studied according to the OCDE 301F standard at the institute of Agro Industrie Recherches et Developpements (Route de Bazancourt, 51110 Pomacle, France). (For method and evaluation criteria see chapter IV.3).

IV.4.3 Synthesis

IV.4.3.1 Choline Ester Surfactants

The choline ester surfactants treated within the framework of this work, were established following three different methods. The first approach leaned towards the solvent-free synthesis proposed by U. Storzer [406]. The ester functionality in this method is achieved by a simple one step procedure with an intermediating deep eutectic solvent.

At room temperature, 1 eq of methylsulfonic acid was added drop-wise to 1 eq of choline chloride. After a few minutes a clear solution formed (Figure IV-41 (1)). Adjacently, the mixture was heated to 120 °C and the corresponding acidchloride (*e.g.* lauroylchloride 1 eq) was added drop-wise within 60 min while the released hydrochloric acid gas was conducted via a bubble counter (Figure IV-41 (1.1)). To ensure the completion of the reaction the solution was stirred for further 60 min with subsequent pressure reduction to $< 10^{-1}$ mbar accompanied by step-wise temperature increase to 150 °C within 120 min. The reaction yielded a white solid (~ 100 %) with approximately 95.1 % purity.

However, this simple and economic method faced the problem of nearly 5 % impurity, which was to be removed only by a great effort (*inter alia* several recrystallization steps). These impurities were mainly due to decomposition of the thermally labile choline, as trimethylamine, presenting a known degradation product of choline, was detected. Thus, the synthesis was modified to permit working at lower temperatures. The first step of the procedure described above, leading to the deep eutectic choline methylsulfonate mixture with residual HCl, was maintained (Figure IV-41 (1)). However, this salt-blend now was dissolved in dichloromethane while the acid chloride was added drop-wise. Adjacently, the temperature was raised to 50 °C and the mixture was stirred under reflux for further 3 h

(Figure IV-41 (1.2)). Subsequently, the solvent was removed under reduced pressure and the product was recrystallized from ethanol/diethylether yielding a white solid with more than 99 % purity.
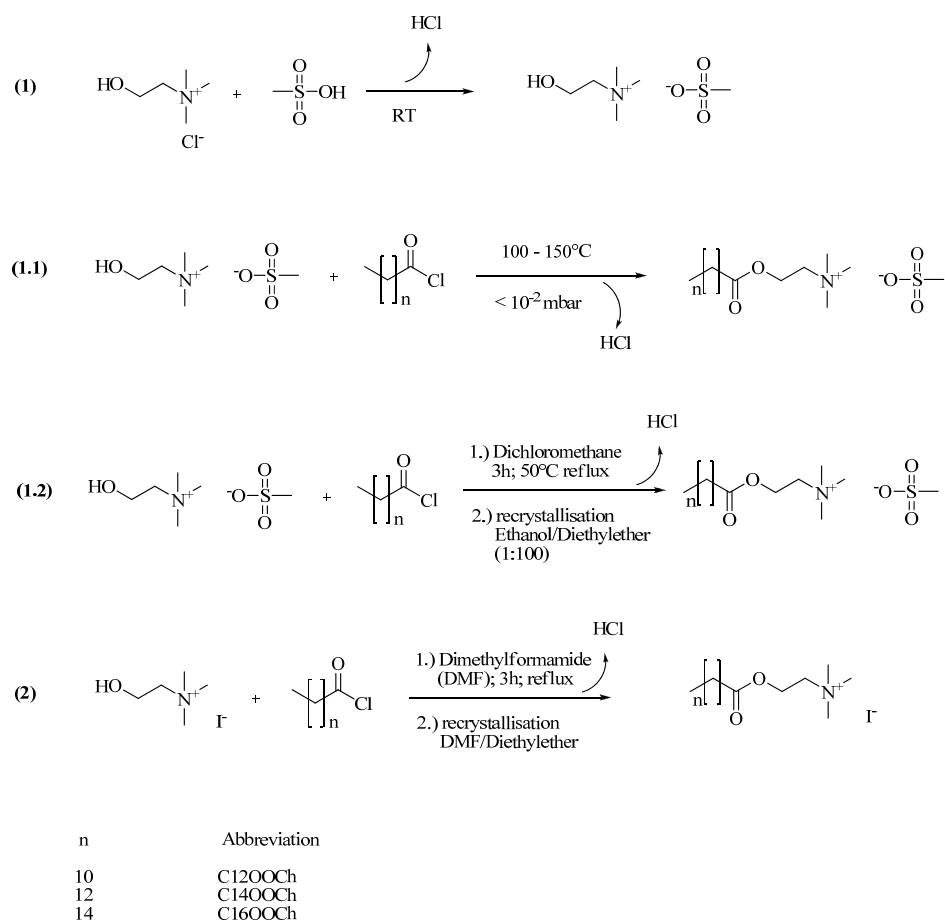
Figure IV-41: Schemata of the syntheses of choline based ester surfactants (CnOOCh) with methylsulfonate (MeSulf) as counterion with (1.2) and without (1.1) solvent, and iodide (I) as counterion (2).

As the counterion of a surfactant is known to exert a dominating influence on its physico-chemical properties, a further synthesis was conducted yielding iodide choline esters. For that purpose, choline iodide (1 eq) was reacted with lauroylchloride (1 eq) while dissolved and refluxed in dimethylformamide

(DMF) for 3 h (Figure IV-41 (2)). The generated HCl-gas, and the solvent were adjacently removed under reduced pressure. The product was recrystallized several times from DMF/diethylether and subsequently dried under vacuum while light was excluded. Although, a yield of only 56 % could be achieved, a purity of more than 98 % was realized.

IV.4.3.2   Choline Ether Surfactants

The introduction of the single oxygen ether functionality was furnished in a one-step procedure in which the alcohol was reacted with 2-chloro-*N,N*-dimethylethylamine in the presence of a base (Figure IV-42). This reaction was studied for dodecanol and proceeds presumably through the formation of the reactive *N,N*-dimethylaziridinium ion intermediate.

At room temperature and inert atmosphere (nitrogen), a solution of dodecanol (1 eq) in dry DMF was added to sodium hydride (7 eq) suspended in dry DMF over a 30 min-period. 2-Chloro-*N,N*-dimethylethylamine hydrochloride (3 eq), dried by azeotropic distillation with toluene and stored over phosphorus pentoxide, was then added portion-wise over 60 min. The reaction mixture was heated at 50 °C for 3 h. The solvent was removed under reduced pressure and the crude product then dissolved in water. The aqueous phase (its pH was approximately 12) was extracted in five attempts with diethyl ether. The ether phase was then extracted four times with 6 M hydrochloric acid. The pH of the water phase was adjusted to 12-13 by adding 5 M aqueous NaOH. This aqueous phase was finally extracted with ether (4 x) and the ether phase then was washed with brine and dried over anhydrous magnesium sulfate. The solvent was removed under reduced pressure to give the intermediate product. After extraction, the product was obtained with a purity of 97 % or higher.

To obtain the quarternary ammonium derivative, *N,N*-dimethyl-3-oxa-1-dodecylamine was added to methyliodide (5 eq). The mixture was stirred at room temperature for 24 h. A pale yellow solid was formed. The product was washed with several portions of diethyl ether, recrystallized from

ethanol/diethyl ether and then dried in vacuum. The purity of the salts generally was > 95 %, as judged from their NMR spectra.
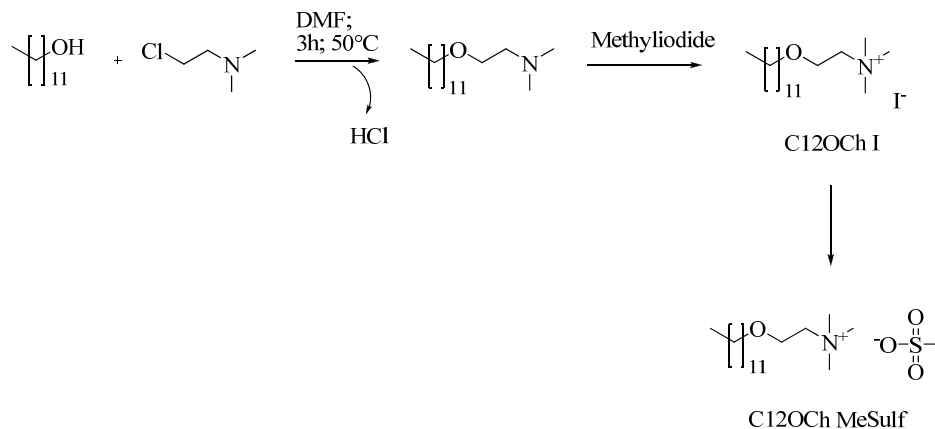
Figure IV-42: Scheme of the synthesis of the choline-based ether surfactants.

To ensure comparability, methylsulfonate derivatives of the surfactants were accomplished. For that purpose, a strongly basic anion exchange resin was loaded with methylsulfonate. Subsequently, the surfactant was eluted with water, which adjacently was removed under reduced pressure and under exclusion of light. The product was recrystallized several times from ethanol/diethyl ether yielding white to pale yellow solids with a purity of nearly 98 %.

IV.4.3.3 Ectoine Ester Surfactants

The formation of the ester functionality between the ectoine zwitter-ion and a long carbon chain was conducted by a classical acid-catalysed esterification (Figure IV-43).

Ectoine (1 eq) was suspended in the corresponding fatty alcohol (~ 20 eq) in a two-necked flask with attached Dean-Stark apparatus with reflux

condenser. While the mixture was stirred, the temperature was raised to 120 °C and hydrochloric acid gas was conveyed through it. After two hours, a clear solution was formed. However, for completion of the reaction the procedure was continued for further 10 to 15 h. Subsequently, the residual fatty alcohol was removed under high vacuum ($< 10^{-4}$ mbar). The product was dissolved in chloroform and washed several times with water. Adjacently, it was recrystallized repeatedly from acetonitrile (yield ~ 50 %; purity ~ 98 %).

n	Abbreviation
9	EctoC10
11	EctoC12
13	EctoC14
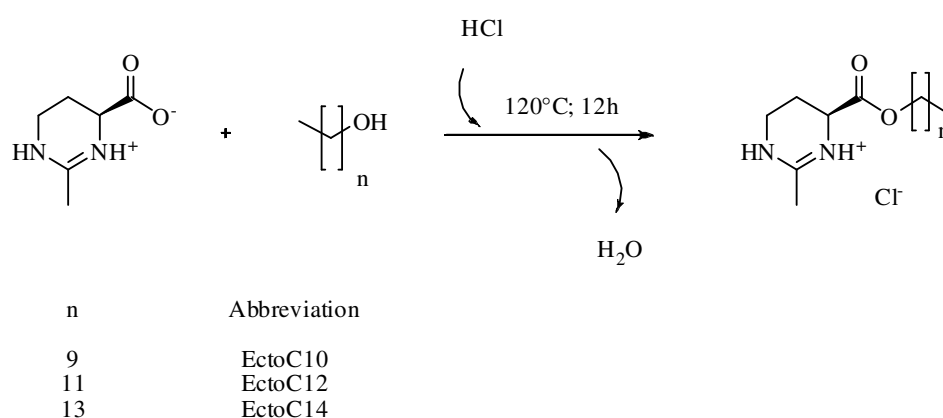
Figure IV-43: Scheme of the synthesis of ectoine-based ester surfactants.

The synthesis of the dodecyl-ectoine-ester with methylsulfonate (EctoC12 MeSulf) as counterion was accomplished with a long chain alcohol according to the method described in chapter IV.4.3.1. (Figure IV-41 (1.2)). The solvent was acetonitrile. Methylsulfonic acid was added in 10 mol% excess. The product was dissolved in water and extracted with chloroform. The solvent was removed under reduced pressure and the crude product was recrystallized from acetonitrile (yield ~ 49%; purity > 98%)

IV.4.4   Results and Discussion

IV.4.4.1   Aggregation and Solubility

IV.4.4.1.1   *Cmc*

The values of the cmcs of the investigated surfactants are compared with structurally related cationic amphiphiles in Table IV-16. Apparently, the cmc of CnOOCh MeSulf decreases linearly by a factor of four per addition of two CH_2 groups. This feature, typical for ionic amphiphiles, can be illustrated by Equation IV-20, where the logarithm of the cmc is a linear function of the alkylchainlength n [94].

$$\log cmc = A - Bn \qquad\qquad\qquad \textbf{IV-20}$$

In this Equation, A depends on the surfactant headgroup, temperature, and the addition of inert electrolytes and B represents the contribution of each methylene group in the lowering of the cmc by the tail. Figure IV-44 shows the cmc values represented according to Klevens Equation compared to those presented in literature for alkyltrimethylammonium bromides (C_nTAB). The B values are in very good agreement with data in the literature [87]. The B value is strongly correlated to the charge per headgroup q and can be calculated using the following linear Equation [407]:

$$B = (0.499 \pm 0.007) - (0.234 \pm 0.011)q^2 \qquad\qquad \textbf{IV-21}$$

Data obtained in this work gave $q^2 = 0.85$ for the investigated alkyltrimethylammonium surfactants. This value is in good agreement with the charge distribution estimated using semi-empirical quantum chemical methods [407]. Expectedly, the B value of CnOOCh MeSulf equals that of C_nTAB within an uncertainty of 0.001. However, a significant difference in

the value of *A* was detected, giving rise to the assumption, that the intermolecular headgroup interactions were modified with the replacement of the counterion and the insertion of an ester-functionality.
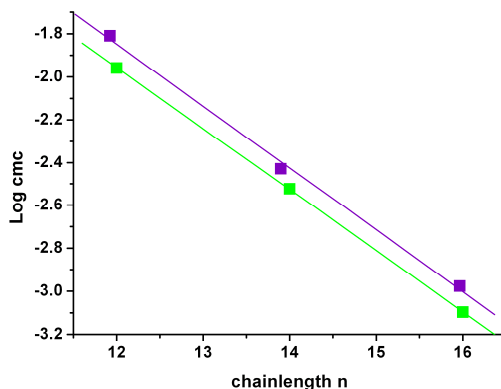
Figure IV-44: Dependence of the cmc in water of the investigated choline ester surfactants ▪ on the alkylchainlength *n* in comparison to common alkyltrimethylammonium bromides (CnTAB) ▪. The straight lines are linear fits.

It is a known fact that aggregation behaviour of amphiphilic molecules varies with their counterions. Several research approaches dealt with the investigation of the impact of the counterion on certain specific parameters, like the cmc, the aggregation number N_{Agg}, the area per molecule a_s, or the degree of micelle ionisation α. For instance, Berr *et al.* tried to elucidate the role of the anion in C_nTA systems [408]. They concluded that additionally to the bare size of the ion, the ability to delocalize the charge influence counterion-micelle binding. Furthermore, they assumed the interaction of the ion with water to play an important role in the counterion-micelle interplay. These findings underline the concept of "matching water affinities" [100], which evaluates ion association in terms of size, polarity and hydration. Collins concludes in this theory, that "like likes like". Thus, big, polarizable and similarly hydrated ions preferentially associate with ions of equal characteristics and the other way round. Yet, the combination of differently featured ions leads to an enhanced dissociation.

Table IV-16: Comparison of critical micellar concentration (cmc) of the investigated surfactants with structurally related compounds at a certain temperature T, including further aggregation parameter: Degree of micelle ionisation α, area per molecule a_s and aggregation number N_{agg}.

Substance	cmc [mM]	α	a_s [Å²]	N_{agg}	T [°C]
C12OOCh MeSulf	0.0111	-	-	-	25
C14OOCh MeSulf	0.003	-	-	-	25
C16OOCh MeSulf	0.0008	-	-	-	45
C12OOCh I	0.0052	-	-	-	50
C12OCh I	0.0034	-	-	-	45
C12OCh MeSulf	0.0065	-	-	-	25
EctoC12 MeSulf	0.0051	-	-	-	25
C12OCh Cl [409]	0.007	0.23	-	-	25
C12OOCh Br [402]	0.0072	0.28	-	-	25
Dodecyltrimethylammonium chloride (DTACl)	0.017 [410]	0.26 [408]	-	37 [408]	25
Dodecyltrimethylammonium bromide (DTAB)	0.015 [411]	0.29 [408]	-	51 [408]	25
Dodecyltrimethylammonium methylsulfonate (DTAMeSulf) [408]	-	0.29	-	47	25
Tetradecyltrimethylammonium bromide (TTAB) [411]	0.0035	0.24	-	81	20
Dodecylpyridinium chloride [411]	0.017	0.37	52.5	44	20
Dodecylpyridinium bromide [411]	0.012	0.26	51.8	58	20
Dodecylpyridinium iodide [411]	0.0052	0.21	51.6	77	20

For that reason, although the ion diameter is significantly larger, similar or even slightly reduced interactions with trimethylammonium headgroups were found for methylsulfonate compared to bromide [408] (Table IV-16). Though, iodide, which in fact is bigger and more polarizable than bromide, leads to strong cation/anion association. This becomes evident, when the aggregation

numbers, the cmc and the counterion dissociation values of iodide and bromide surfactants are compared [411] (Table IV-16). While the first parameter increases, the latter two decrease with the exchange of bromide by the more polarizable halide. The enhanced ion association reduces intermolecular headgroup repulsion and thus, entails facilitated aggregation. These considerations elucidate the fact of reduced cmc upon replacement of MeSulf by iodide in the C12OOCh surfactants. The bromide derivative, produced by Holmberg and co-workers obviously express intermediate values [402].

The introduction of an ester or an ether functionality between the alkylchain and the charged headgroup in both cases lead to lower cmc values. Mandru pointed out that with the presence of an -OCH$_2$CH$_2$- moiety the number of methylene groups removed from the aqueous environment increases [409]. Thus, one can conclude that oxyethylene (EO) groups occurring between an alkylchain and an ionic group increase the number of the methylenes of the alkylchain involved in the formation of hydrophobic bonds. However, this assumption is only valid for the first EO group which does not give rise to the flexibility of the carbon chain. The ester functionality does not lead to a cmc reduction by the same extent as the ether group. Its polarity is higher, thus it can be expected to be stronger hydrated and the packing in an aggregate becomes less efficient.

The exchange of the trimethylammonium (TMA) group by ectoine has a major impact on the aggregation behaviour. Although, the apparent length of the hydrocarbon chain is reduced, the cmc is drastically lower in case of the ectoine ester. This observation may be attributed to two major factors: Firstly, ectoine is a protic headgroup which can counterbalance the increased electrostatic repulsion during aggregation by charge regulated deprotonation. Secondly, pure ectoine is known to intra-molecularly stabilize its zwitter ionic form via very efficient hydrogen bond formation [412]. Such H-bonds can also be expected to form between adjacent surfactant molecules with ectoine headgroups. Thus, aggregation is energetically favored.

IV.4.4.1.2   *Solubility*

The solubility temperature of a surfactant is determined by its Krafft temperature T_{Kr}. Just above this point, solubility increases rapidly and a homogenous solution is formed. The Krafft temperature of a surfactant is determined by the balance of the free energy of the hydrated crystalline state and the free energy of the micellar solution. Although the energetic impact of dissolved aggregates can vary, the main driving force generally is the efficiency of crystalline packing of the molecules. Amongst other things, a strong headgroup interaction, distinct counterion binding, or the degree of saturation contribute to the crystals stability. Particularly, the intensified van der Waals interactions with increasing aliphatic chainlength lead to elevated Krafft temperatures (Table IV-17).

Naturally, it can be derived from the present data that the solubility temperature increases proportionally to the alkylchainlength due to enhanced van der Waals interactions.

Further, the introduction of a functional group between the charged head and the aliphatic tail seems to have a major impact on the solubility. At first glance, one may speculate that ester bonds will restrict efficient packing in the crystalline lattice as the Krafft temperature of the C16 choline ester is distinctly higher than that of *e.g.* CTAB. However, like described above, the ester functionality (with two accompanying CH_2 moieties) rather acts as an extension of the carbon chain. Thus, the C12 ester has to be compared with equivalent C14 surfactants, *etc.* Evidently, the additional functionality does not significantly influence the energetic state of the crystal, as the Krafft temperatures are almost equal for C14OOCh MeSulf and CTAB. Though, the micellar state might be energetically unprivileged as the conformational freedom of the surfactant tails and the packing into closed aggregates could be more difficult. This becomes evident in the comparatively high cmc in spite of the long carbon chain of C12OOCh MeSulf.

Table IV-17: Krafft temperatures T_{Kr} of the investigated compounds compared to structurally related surfactants.

Substance	$T_{Kr}[°C]$
C12OOCh MeSulf	< 0
C14OOCh MeSulf	24
C16OOCh MeSulf	50
C12OOCh I	41
C12OOCh Br	< 0
C12OCh I	46
C12OCh MeSulf	<10
Ecto C12 MeSulf	< 0
DTAB	< 0 [402]
Hexadecyltrimethylammonium bromide (CTAB)	26 [413]

Yet, the strength of counterion association should be clearly kept in mind. While the energetic state of the micellar solution varies only slightly when changing the counterion, the free energy of the crystalline state may change considerably from system to system. The general trends of ion size and polarizability can equally be applied for the interpretation of the Krafft-point and the cmc. For example, for alkali alkanoates the Krafft point increases as the atomic number of the counterion decreases, while the opposite trend is observed for alkali sulfates [101]. For cationics, the Krafft point is typically higher for bromide than for chloride, and even higher for iodide [4]. However, the concept of relating solubility to counterion size is too strongly facilitated for the explanation of our findings. Firstly, the interaction strength between water and an ion is primarily determined by the size of the ions. Interactions of water with small ions are more favourable because of the localization of

the charge. The second factor that determines water-ion interactions is the magnitude of charge located on the ions surface atoms that are directly coordinated with water. This charge in turn depends on the chemical structure of the ion. A strong internal polarization of the ion, which leads to larger partial charges on its surface atoms, results in more favourable interactions with water. Thus, although methylsulfonate is already a big ion – due to geometrical and bond length considerations – it still should be smaller than iodide. Furthermore, the charge is localised to a certain part of the ion, which should enhance its hydration in comparison to the bigger halide with no priority polarisation. Our findings reflect this circumstances as the solubility temperatures are elevated more than 35°C for the iodide derivatives in comparison to the methylsulfonate compounds.

IV.4.4.1.3   Hydrolysis

However, the confirmation of the assumptions in the previous sections by determination of the area per molecule a_s of the choline esters turned out to be kind of difficult. The chosen methods – evaluation of the concentration dependant surface tension and the surface pressure in a Langmuir-Blodgett-trough – based on the surface properties of the molecules. Yet, the analysis of the surface isotherms suggests the conclusion that no stable monolayers were achieved. A continuous reduction in surface pressure at constant conditions with time was observed (Figure IV-45). Hence, one conclusion would be that molecules vanish from the surface upon presser and dissolve or aggregate within the bulk phase. However, if this was true they should re-adsorb upon film-relaxation, which was not the case.

Figure IV-46 shows the surface pressure as a function of the area per molecule curves of C12OOCh I, which was surveyed in defined time interval. Although the film had time to relax at least several minutes, no re-adsorption was achieved. Obviously, the surface pressure was subjected to a constant shift to lower values. While a kinetically strongly hindered re-adsorption has to be considered, another explanation is more likely. As soon

as the headgroup repulsion becomes less pronounced, the molecules possibly pack closer and in consequence require a smaller volume. Upon hydrolysis of the ester bond the choline ion and the slightly polar, mainly undissociated fatty acid are formed. Choline is very soluble and thus, directly moves into the bulk while the acid can be expected to accumulate at the air water interface. Even though the number of carbon chains stays constant, the repulsion between the surfactant headgroups is screened by the uncharged acid functionality. Consequently, the required area per molecule shrinks, which entails a reduced surface pressure.
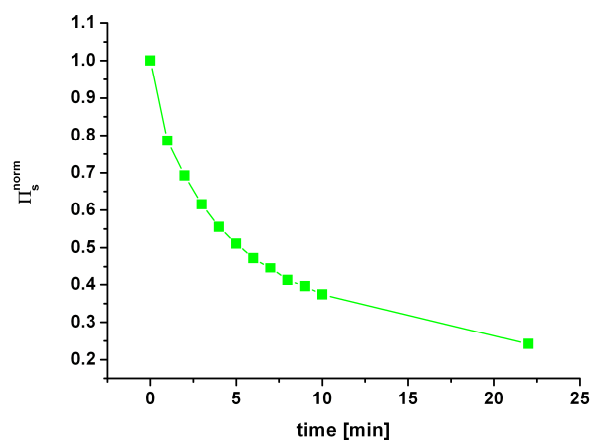
Figure IV-45: Development of normalized surface pressure Π_s^{norm} of C16OOCh MeSulf (normalized to the value right after 20 min equilibration time) with time.

Though, after several film-strain and relaxation cycles a_s reaches an unrealistically low value (Figure IV-46). With proceeding hydrolysis more and more acid is produced. It is a known phenomenon, that the cmc is diminished upon the addition of hydrophobic or marginally polar compounds – the fatty acid in the present case. With a reduction of the cmc at constant temperature, the Krafft point drops and the investigated amphiphile becomes more soluble. More molecules move from the interface into the bulk, which explains the small areas per molecule detected after a certain period of time.
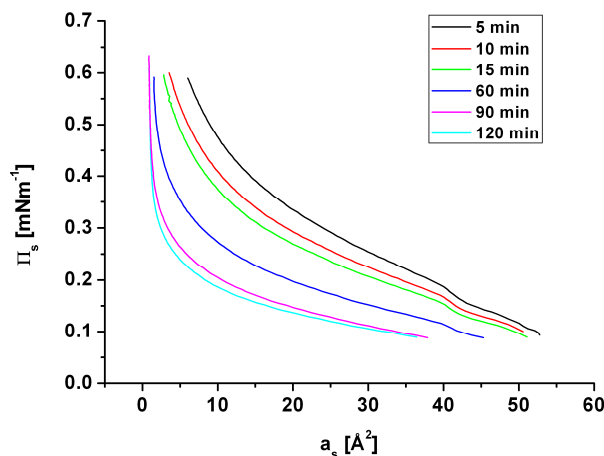
Figure IV-46: Surface pressure Π_s/ area per molecule curves of C12OOCh I in dependence elapsed time after 20 min of equilibration.

Holmberg and co-workers gave a rate constant of hydrolysis of C12OOCh Br of approximately 0.06 per day [402]. This means that after one hour 0.3 % and after 24 hours scarcely 6 % for the original amount of substance should have undergone hydrolysis. This finding does not correlate with ours. According to our data, we can assume a rate constant, which is a multiple of that derived by Holmberg. The explanation for that observation possibly is given by the larger pH in vicinity of the cationic headgroups compared to the bulk phase. This catalytic phenomenon has already been described for micelles [401]. It leads to an accelerated rate of hydrolysis compared to the monomers. Cationic micelles attract negative ions like hydroxide ions. This gives rise to a locally increased pH, which in turn facilitates ester hydrolysis. With increasing charges per area even more anions should be found in the vicinity of the cationic charges. Upon constraint on the monomer film, one can assume much closer packed headgroups than in simple micelles and consequently a strongly accelerated hydrolysis. This effect even overrules the impact of the preferential adsorption of iodide ions (due to their higher polarizability) to ammonium headgroups, compared to bromide in the Holmberg case. Hence, iodide should replace the smaller more hydrated

hydroxide in the vicinity of the cationic heads and thus, decelerate the rate of hydrolysis. However, this was not observed.

IV.4.4.1.4   Phase Diagrams

The temperature and concentration dependent phase diagrams of C12OOCh I and C12OOCh MeSulf are shown in Figure IV-47. Both diagrams resemble each other to a high extent. In each case merely a lamellar mesophase was observed at approximately 25 to 30 wt%. According to the Collins concept of "matching water affinities" [8, 99-100] iodide should be found in close vicinity of the cationic headgroups, since both show high polarizabilities. Methylsulfonate on the other hand already bears a dipolar structure and a hydrophobic moiety. This structure should enhance preferential adsorption at the interface of the micellar interior and the water. Both mechanisms lead to a reduced headgroup repulsion which entails packing parameters close to one. This in turn favours the formation of bilayer structures.

Both surfactants show a reduced solubility with increasing concentration. Though, the overall solubility of the iodide derivative is significantly lower than that with methylsulfonate as counterion, which has already been described in the previous section.

The sole significant difference of both diagrams is the appearance of two liquid/liquid phase separation domains at high concentrations and high temperatures for the methylsulfonate compound. The first two phase region, (2Φ turbid/iso) starting at approximately 50 wt% and 50 °C, consists of an isotropic phase, which is covered with a low viscous turbid (lamellar) layer. At approximately 70 wt% and constant temperature this upper phase turns clear and isotropic (2Φ iso/iso). Obviously, the first temperature driven phase separation at lower concentrations from lamellar to lamellar + water must be due to reduced inter-layer repulsion or even increased attraction of the lamellae as no shape transition of the aggregates is considered.
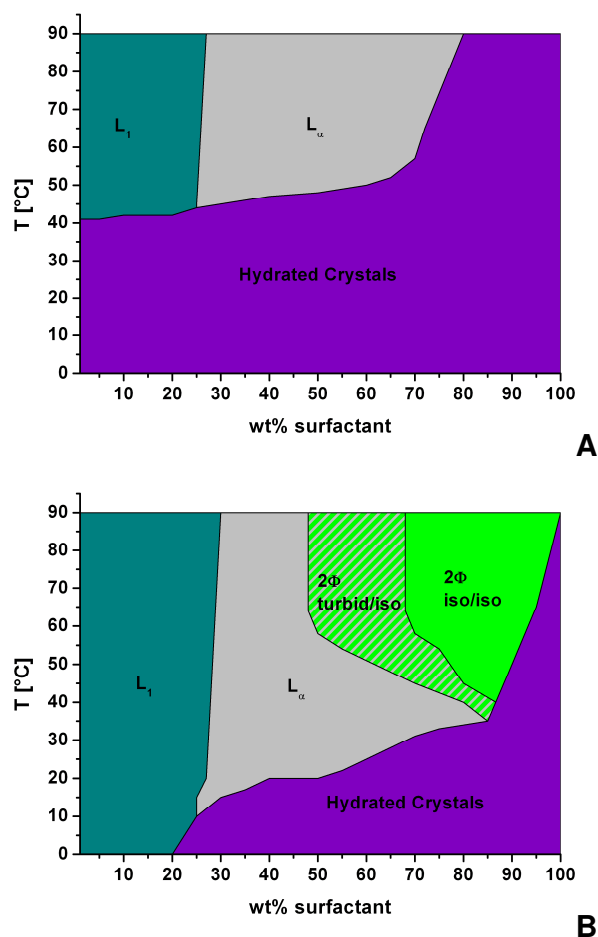
Figure IV-47: Phase diagrams of C12OOCh I (A) and C12OOCh MeSulf (B). In (B) two different liquid/liquid phase separations at elevated temperature were observed.

The dehydration of the hydrophilic parts with rising temperature cannot serve as explanation for the phase separation as in this case it would have to be observed for the iodide species as well. While phase separation with rising temperature is a common phenomenon with non-ionic surfactants, it is only scarcely reported with ionic surfactants. Workgroups investigating lower consolute behaviour in charged systems generally achieved phase separation by the addition of either salt [414], which drastically reduced Debye screening length between the single aggregates, or the use of amphiphiles (generally cationic) with large hydrophobic headgroups [301, 354], such as tributylammonium. The mechanism of the second strategy bases on

energetically unfavourable hydrophobic interactions of the aliphatic chains attached to the head combined with a low surface charge.
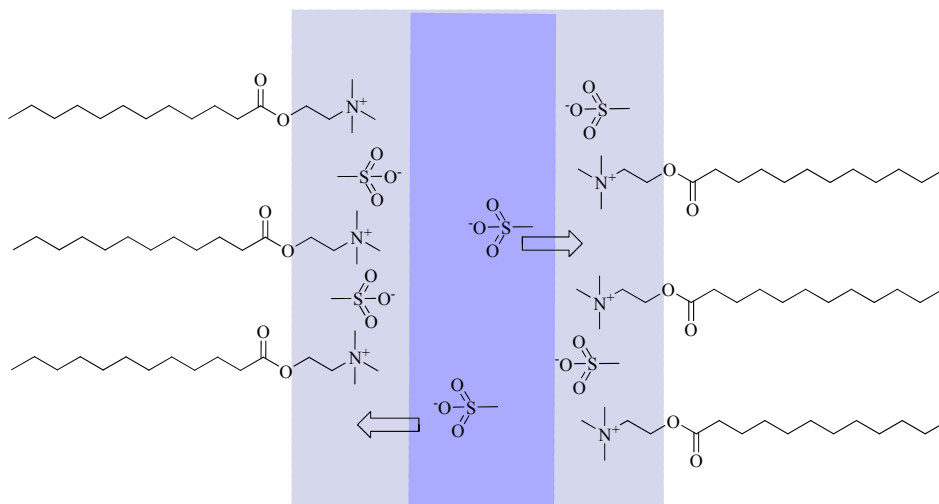
Figure IV-48: Adjacent lamellae of C12OOCh MeSulf, which are separated by a water layer (blue). With increasing temperature, the anions are pushed into the headgroup layer.

A similar mechanism can be expected for C12OOCh MeSulf if an arrangement of the heads and the anions like shown in Figure IV-48 was assumed. From the viewpoint of energy, it is disadvantageous for the hydrocarbon chains to directly contact water due to the hydrophobic effect, which becomes even more pronounced with rising temperature. Thus, the dipolar methylsulfonate ions will be pushed even further into the headgroup layer, where the interaction of the methyl functionality with water is reduced to the greatest possible extent. This action entails a drastic loss of surface charge of the aggregates and hence, electrostatic repulsion between adjacent lamellae is minimized. Van der Waals interactions gain importance and water is expelled.

The second phase separation (2Φ iso/iso) clearly is an entropically driven phenomenon. Like mentioned in the previous section, the area per molecule generally is reduced with increasing temperature. If the concentration is raised, this effect will be even more pronounced. On comparing reversed and lamellar phase the reversed phase is favoured at higher temperatures and concentrations. As the area per molecule approaches the limit of the all-trans cross-sectional area within the lamellar phase, the reversed phases offer more conformational degrees of freedom available to the chains. In practice the alkyl-chain curvature effect is likely to transform bilayers into reversed structures. Thus, the phase separation between water and a L_2 phase becomes clear when these considerations are combined with the above mentioned low inter-aggregate electrostatic repulsion at elevated temperatures.

IV.4.4.2   Catanionic Vesicles

In order to detect the formation of vesicles, several pairs of the above mentioned cationic molecules were tested in combination with choline carboxylates with varying chainlength (ChC_n) in different mixing ratios.

Almost all investigated mixtures showed the ability to spontaneously from vesicular aggregates (Figure IV-49-50). Nearly none of the solutions expressed a pure vesicular phase. However, in most cases, a mixture of several aggregate shapes (mainly vesicles and sheets). The shape of the aggregates strongly depended on the type and the ratio of the blended surfactants. In all cases, the vesicle population was relatively polydisperse. Precipitation occurred in every sample with a mixing ratio of anionic and cationic surfactant around equimolarity. Nevertheless, certain careful tendencies can be fixed:

- With increasing amount of cationic surfactant in the mixture of C16OOCh MeSulf and ChC12 the average size of vesicles rose while their membranes contemporaneously became more rigid, as more facetted aggregates were observed (Figure IV-49 A – C). Close to

equimolarity the polydispersity in size and in shape was highest. If the C16 cationic ester was exchanged by its shorter chain equivalent C12OOCh MeSulf, this effect became less evident (Figure IV-50 D and E). Hence, the chainlength of the surfactants has a major impact on the shape of the equilibrium aggregate.

- The exchange of the ester functionality by an ether group (investigated system: C12OCh MeSulf ChC16) favoured the formation of discs rather than vesicles in equilibrium with huge sheets (Figure IV-50 A, B). Such discs could be detected in the excess charge parts of the cationic/anionic ratio.

- In EctoC14 Cl ChC14 samples, the dominating aggregates likewise were vesicles and membranes. However, with excess cationic surfactant, rather small and relatively monodisperse vesicles were observed (Figure IV-50 C). On the other hand, the average size of the aggregates rose drastically with increasing content of anionic surfactant. In the $r > 0.5$ region membrane rigidity was enhanced, which became clear as many big vesicles with defects, or pores, could be observed in equilibrium with edged sheets (Figure IV-50 D). Upon dilution of such a sample, the size of the sheets shrunk and facetted vesicles in equilibrium with discs were detected (Figure IV-50 E).

The starting point for the description of bilayer organization in solution is the examination of the bending free energy. It considers the principle radii of curvature of the structures, the spontaneous radius of curvature, the mean and Gaussian curvature elastic constants, respectively, and the surface of the bilayer membrane [2]. The differences of the bending free energy, of different catanionic aggregate geometries can often be in the order of k_BT, leading to the possibility of multiple structures in equilibrium [415]. The two elastic constants determine the shape and the number of coexisting aggregates.
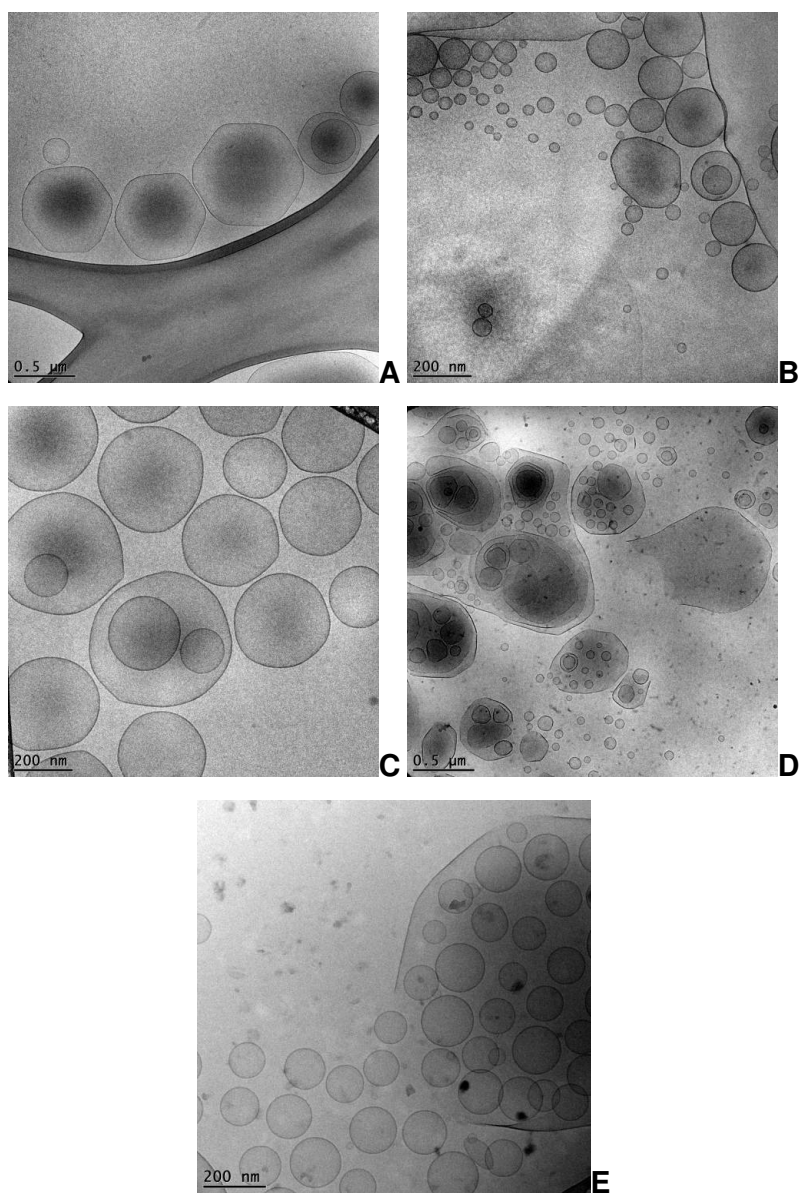
Figure IV-49: Cryo-TEM pictures of C16OOCh (A, B, C) and C12OOCh (D, E) MeSulf mixed with ChC12. The samples had a total surfactant concentration of 0.01 M. The molar ratios of anionic to cationic surfactant varied: r = 0.3 (A), r = 0.56 (B), r = 0.7 (C), r = 0.56 (D) and r = 0.7 (E).

The magnitude of the mean elastic constant reflects the energy needed to bend the bilayer away from its spontaneous radius of curvature. If this

modulus was in the order of $k_B T$, thermal fluctuations give rise to significant curvature fluctuations, which lead to a net repulsive interaction between bilayers at short distances. This sterical repulsion *e.g.* can stabilize unilamellar vesicles over multilamellar ones [416]. However, a variety of coexisting structures is only possible for systems with a spontaneous curvature (interior and exterior membrane have different compositions) and a positive Gaussian curvature modulus, which defines the topology of the structures formed [157, 416]. Many examples were presented in literature with a variety of coexisting aggregation forms [415]. The factors of influence were determined to be, the surfactant and counterion chemistry, the concentration and of course the temperature. However, the molecular origins of the spontaneous radius of curvature and the elastic moduli are not yet fully understood in detail.

In a series of articles during the last years, Zemb and co-workers discussed the shape control of giant catanionic aggregates without counterions [132, 157, 159-162, 417]. Below the chain melting temperature of the amphiphiles [331, 333], they found icosahedra like vesicles with pores at the vertices and micron-sized discs, depending on the mixing ratio of cationic and anionic surfactant. They explained their findings by a co-crystallization/charge-segregation mechanism. Upon cooling of vesicles with homogenously distributed molecules in the liquid state, crystal growth within the bilayer takes place in a defined molar ratio of anionic and cationic surfactant. Excess component is expelled from these crystallites and accumulates at their edges, where they induce high spontaneous curvature. Thus, either rims of discs or punctures in membranes and vesicles are observed. Consequently, all three aggregation forms are coexistent.

These explanations can be adapted to our findings. The longer the chain of a surfactant molecule the higher the chain melting temperature in bilayer aggregation [418]. On the other hand, a huge misfit in chainlengths of the mixed molecules can lead to a reduced chain melting temperature [331]. This gives explanation for facetted vesicles preferentially being observed in the cation rich part of the phase diagram of the C16OOCh MeSulf/ChC12

mixture. With rising amount of ChC12 the chain melting temperature probably fell below room temperature and the chains were in their molten conformation. Thus, the molecules were randomly distributed and no segregation was detected.
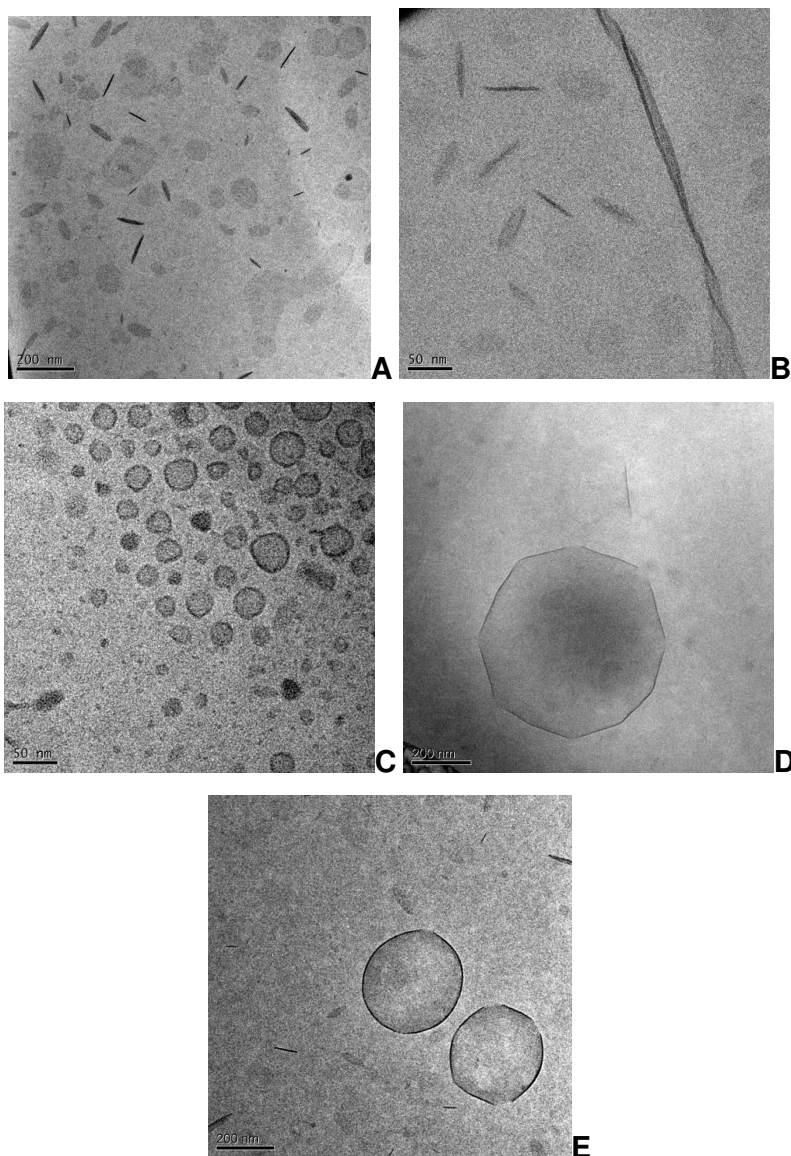
Figure IV-50: Cryo-TEM pictures of ChC16 + C12OCh (A, B) and ChC14 + EctoC14 Cl (C, D, E). The samples had a total surfactant concentration of 0.01 M (A – D) and 0.005 M (E). The molar ratios of anionic to cationic surfactant varied: r = 0.22 (A), r = 0.7 (B), r = 0.24 (C) and r = 0.75 (D, E).

Yet, Zemb and his workgroup reported exactly the converse phenomenon on salt-free catanionic mixtures composed of CTAOH and myristic acid [331]. They observed an increasing chain melting temperature with excess acid, while an excess of cationic surfactant did not seem to have a major impact. However, further investigations revealed that upon the addition of huge amounts of HCl the transition temperature was shifted to lower values [333]. Here, the screening of the electrostatic repulsion between ammonium groups (which should increase the melting point) was assumed to be overcome by a screening of the electrostatic attraction between carboxylate and ammonium heads. Thus, the combination of misfit in chainlength and screening of headgroups might explain the microscopic observations. However, further investigations are necessary to prove this assumption.

The point of fusion of the C12OOCh MeSulf/ChC12 mixture can already be expected below room temperature and hence, no significant impact of mixing ratio was observed. Yet, the ether based catanionic mixtures again suggested molecular segregation. Although no significant difference occurred between the discs with excess cationic and excess anionic surfactant, the system traversed a region with big vesicles and sheets close to equimolarity (not shown). This observation might be explained by a more homogenous distribution of counter charged molecules around equimolarity.

Similar results were found for the ectoine based surfactant mixtures. Aggregate size grew as soon as the molar ratio approached equimolarity, while it was reduced with rising amount of excess surfactant. At a ratio r of 0.24 – excess cationic surfactant – very small vesicles were observed (Figure IV-51 C), while at r = 0.8 the vesicles even totally vanished to be replaced by long cylindrical aggregates (not shown). Upon dilution the observed sheets in the EctoC14 Cl/ChC14 system significantly shrank, which might be due to the fact that in this case counterions are expected to be less bound to the surfactant headgroup. Hence, bending energy is decreased leading to a membrane being stronger curved, which finally results in smaller aggregates.

To verify the mechanism suggested above, which generally was discussed for true catanionics in earlier reports [331, 333], the role of the counterions and

particularly their association should be elucidated in further experiments. The exact determination of chain melting temperatures and measurements of the surface charge and thus approximation of the counterion distribution are indispensable in this context.

IV.4.4.3 Biodegradability and Cytotoxicity

IV.4.4.3.1 *Biodegradability of Selected Cationic Surfactants*

The evaluation of biodegradability of anthropogenic organic substances is an essential parameter for environmental risk assessment and required according to appropriate legislation. Correspondingly, the biodegradability of choline and ectoine esters with sodium acetate as standard was investigated.
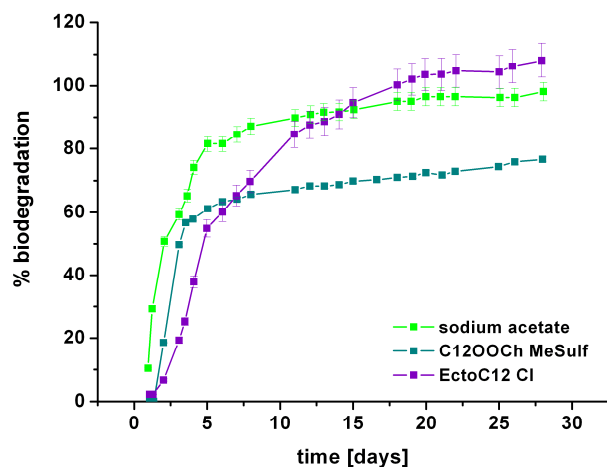
Figure IV-51: Biodegradation of selected new cationic surfactants as a function of time (sodium acetate as standard). The lines are to guide the eye.

Generally, with regard to the OCDE standard, organic molecules can be considered as biodegradable if 60 % of the substance is degraded within 10

days after the 10 % level had been reached, and if globally at least 60 % have been consumed after 28 days. Following the European standard CE2004/648 [384], surfactants can already be classified as biodegradable if 60 % degradation is achieved after 28 days.

Figure IV-51 shows the biodegradation profiles of C12OOCh MeSulf and EctoC12 Cl as a function of time. It is obvious that the two investigated compounds meet the latter criterion already before 10 days. Nevertheless, a significant difference in total degradation after 28 days was detected. While the ectoine ester has completely faded after the investigated period of time, the choline ester reached a biodegradability level of only 76 %.

Biodegradation generally is influenced by several factors. First of all, the number of micro organisms capable of metabolizing the organic compound restricts the degradation rate. In the present case, biodegradation was initiated immediately for the choline ester, indicating that no inhibition effect occurred in the biological medium due to potential toxicity of the tested surfactants, which would influence the number of bacteria available. On the other hand, the ectoine ester showed a slight retardation in the biodegradation profile, which might indicate a higher cytotoxic impact. Another restricting factor is the bioavailability of the organic substance. This feature of an organic substrate mainly depends on its chemical fate, its dissolution rate and the mass transfer (*e.g.* from adsorbed to the aqueous phase). However, both examined cationic esters were soluble down to 0 °C. Thus, neither the charge, which would be the main criterion for adsorption to surfaces, nor the chainlength, which could restrict solubility, can serve as explanation for the observed differences. Moreover, the choline and ectoine headgroups themselves should not have any aberrant harmful impact on the environment, since both are compatible solutes which are known not to interact with the cell metabolism. The only outstanding difference is the lability of the ester functionalities of the two surfactants. Holmberg and co-workers investigated the rate of hydrolysis of choline and betaine esters [401-402]. They concluded that the betaine derivatives showed strong pH-dependence. They revealed to be more stable at higher and less stable at lower pH than the choline

compounds. In ectoine, the carbonyl group is in closer vicinity to an electron acceptor than in choline, with its larger distance of ester and ammonium moiety. This fact enforces the partial positive charge at the carbonyl C-atom in ectoine and thus, entails facilitated OH^--driven hydrolysis. Yet, this circumstance reduces the proton induced ester cleavage of ectoine. However, the positive charge in ectoine is delocalized, which suggests that upon proton attack, it is mainly located at the nitrogen atom with a higher distance from the ester functionality.

In summary, both investigated ester-based surfactants can be considered as readily biodegradable as they pass the 10 day window criterion. Their degradation is similar to the nowadays widely used cationic ester-quat amphiphiles, which likewise are regarded as biodegradable [419].

IV.4.4.3.2 *Cytotoxicity of the Investigated Cationic Surfactants and their Catanionic Mixtures with Choline Carboxylates*

Cationic Surfactants

The cytotoxicities of the synthesised cationic surfactants on the HeLa cell line, expressed in IC_{50} values, are summarized in Table IV-18. The results are compared to the cationic surfactants dodecyl- (DTACl), tetra- (TTACl), hexadecyltrimethylammonium chloride (CTACl) and the ester quat dioleoylethylhydroxyethylmonium methylsulfonate (Tetranyl CO 40), which are widespreadly used in commercial applications.

Under the chosen conditions all ester based surfactants express relatively low cytotoxicities. The IC_{50} values are in the same order of magnitude like that of the commercial ester quat. However, the choline derivatives seem to be slightly less toxic than the compounds with equal chainlength and an ectoine headgroup. This finding is supported by the retarded biodegradation of the ectoine compound (see previous section). As the first interaction step of a surfactant with a cell-membrane is its adsorption, which generally is electrostatically driven in the case of cationic amphiphiles [210, 385], one might

easily interpret these differing toxicities with sterical hindrance of choline. In fact, the positive charge of choline is "hidden" behind three methyl groups, whereas it is more or less freely accessible in ectoine. Thus, ectoine based surfactants will adsorb faster and generally a higher toxicity is generated within the same period of time.

Table IV-18: IC$_{50}$ values of selected synthesised cationic ester and ether surfactants with the corresponding standard deviations *SD* in comparison to classical DTACl, TTACl, CTACl and Tetranyl CO 40.

Substance	*IC$_{50}$ [mol/L]*	*SD [mol/L]*
C12OCh I	$3.0 \cdot 10^{-6}$	$4 \cdot 10^{-7}$
C12OCh MeSulf	$2.6 \cdot 10^{-6}$	$4 \cdot 10^{-7}$
C12OOCh MeSulf	$3.1 \cdot 10^{-4}$	$2 \cdot 10^{-5}$
C14OOCh MeSulf	$2.5 \cdot 10^{-4}$	$7 \cdot 10^{-6}$
EctoC10 Cl	$1.1 \cdot 10^{-4}$	$1 \cdot 10^{-5}$
EctoC12 Cl	$7.3 \cdot 10^{-5}$	$6 \cdot 10^{-6}$
EctoC14 Cl	$5.0 \cdot 10^{-5}$	$4 \cdot 10^{-6}$
DTACl	$7.7 \cdot 10^{-6}$	$7 \cdot 10^{-7}$
TTACl	$3.3 \cdot 10^{-6}$	$3 \cdot 10^{-7}$
CTACl	$2.3 \cdot 10^{-6}$	$1 \cdot 10^{-7}$
Tetranyl CO 40	$1.8 \cdot 10^{-5}$	$3 \cdot 10^{-6}$

According to SAR (structure activity relationship) concepts of recent studies, the cytotoxicity is expected to increase linearly with rising hydrophobicity of the investigated compound [363-365, 386]. This trend is confirmed by the analysis of the chainlength dependence of the present data. The IC$_{50}$ values of the C14

choline- and ectoine esters are significantly lower than those of the corresponding shorter chain equivalents. Though, interpretation has to be made with care as a recent analysis of the cytotoxicity on human cell lines of odd and even numbered anionic fatty acid soaps revealed non linear behaviour [15].

The replacement of the easily cleavable ester group by the more resistant ether functionality drastically increased cytotoxicity. This finding is the result of two facts: On the one hand, less surfactant molecules are present in the case of the ester compounds due to its hydrolysis. This leads to the loss of amphiphilic character. Hence, less surfactant molecules are incorporated in the cell membrane, whose curvature undergoes a smaller variation and resists disruption. On the other hand, the ester functionality is more hydrophilic than the ether group. This fact even accelerates the uptake of C12OCh into the membrane compared to the ester and thus, the membrane collapse is enhanced.

Obviously, neither the counterion nor the ether functionality has a significant impact on the cytotoxic effects of the surfactants. Considering the two extra CH_2 groups in the choline moiety, the IC_{50} values of C12OCh can be found well between that of TTACl and CTACl. Furthermore noteworthy is the fact that apparently the monomer concentration of C12OCh I was sufficient to induce cell death, as its Krafft temperature (see above) actually is well above the temperature of investigation with 36 °C. Hence, any cooperative, aggregate-related effects can be excluded.

Catanionic Mixtures

Catanionic systems are considered as simple and cheap drug carriers of particular interest on an industrial scale. However, the efficiency of these systems has rarely been questioned from a mechanistic point of view. Nevertheless, to optimize these systems for drug delivery, it is crucial to understand the process involved in the interaction between catanionic vesicles and cell membranes. As catanionic surfactants are comparable to

phospholipids due to their packing parameter and their charge, two pathways of interactions can be imagined between vesicles thereof and cells: endocytosis and/or fusion [396, 420]. Up to now, few works have described the interaction of catanionic vesicles on cells [6, 370, 396-397].
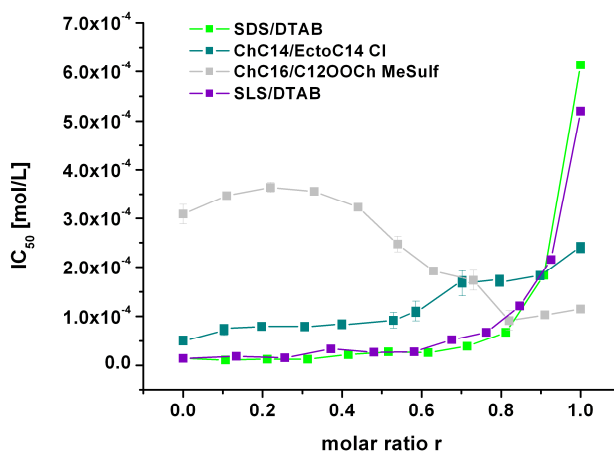
Figure IV-52: **The mitochondrial reduction of MTT (expressed in IC$_{50}$ values) after 72 h of incubation with different catanionics in dependence of their molar ratio *r*.Data for SDS/DTAB and SL/DTAB are taken from [370].**

The toxicity of catanionic surfactant mixtures composed of ChC14/EctoC14 Cl and ChC16/C12OOCh MeSulf were analyzed for different surfactant ratios *r* and compared to data recently published by Vlachy *et al.* [370], who discussed the systems of SDS/DTAB and SL/DTAB. The results are presented in Figure IV-52. The classical compositions of SL and SDS with DTAB showed very similar behaviour. Obviously, only small amounts of cationic surfactant were sufficient to increase the toxicity of the mixture significantly. Thus, the cationic surfactant could be deduced to be the dominant part in a catanionic mixture over a wide range of ratios. However, already at lower ratios, close to equimolarity, the IC$_{50}$ values of the mixture started to diverge to the value of the pure anionic surfactant in both investigated cases. In the mixture of ChC16/C12OOCh MeSulf the anionic surfactant bears the higher toxic potential. Again, at comparatively high *r*

values, the IC_{50} value of the blend started to approximate the value of the pure ester with rising amount cationic surfactant. This fact underlines the assumption of a preferentially cationic driven toxicity mechanism, which is not unlikely due to the commonly negative surface potential of cells [210, 385].
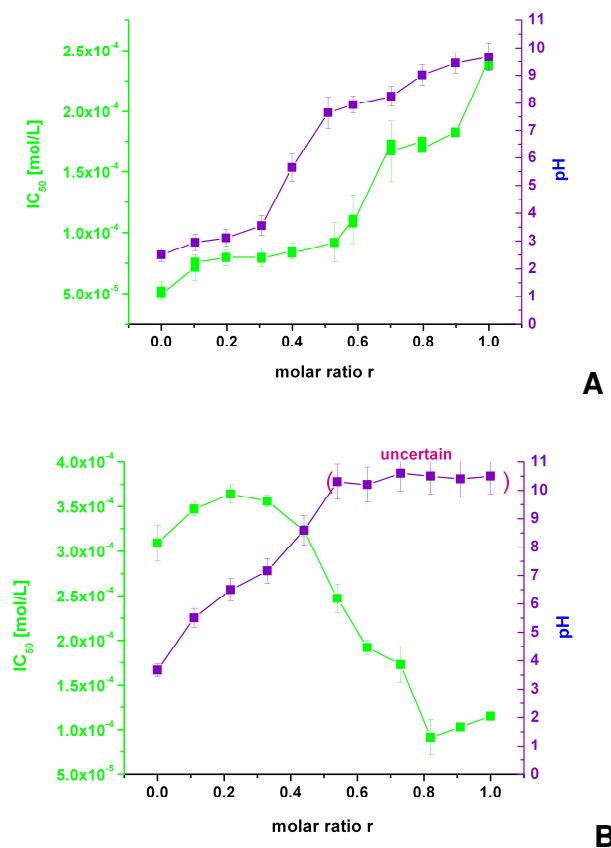
Figure IV-53: IC50 and pH values of ChC14/EctoC14 Cl (A) and ChC16/C12OOCh MeSulf (B) in dependence of their molar composition *r*.

Vlachy *et al.* considered the rising IC_{50} close to pure anionic surfactant to originate from nearly completely bound cationic surfactant to the catanionic aggregates. The reason why larger amounts of cationic surfactant are needed in the case of ester type compounds probably arises from the fact that their potential of hydrolysis (compare section biodegradability) increases with elevated pH. An OH⁻ catalyzed hydrolysis should be facilitated due to the

positive charge in the vicinity of the ester bond. Thus, the cytotoxicity should be closely correlated to the pH of the catanionic stock solutions. This assumption is proved by the data shown in Figure IV-53 B. With higher initial pH more cationic surfactant gets hydrolysed and the IC_{50} value is lifted proportionally. This speculation even explains the minimum of toxicity in the mixture of ChC16/C12OOCh MeSulf at around $r = 0.2$. A cation dominated mechanism still is assumed. The pH starts to rise upon the first addition of anionic surfactant; likewise the concentration of cationic surfactant is reduced. However, the toxicity does not directly converge to the value of the anionic surfactant but rises with decreased rate of cation-hydrolysis. With further increasing concentration of anionic surfactant, its toxicity starts to dominate the few cationic surfactant molecules left (note: the total surfactant concentration was kept constant).

In the case of the investigated ectoine system (Figure IV-53 A), the pH curve is not directly correlated with the toxicity. The pH reflects the faster hydrolysis of ectoine esters compared to choline (note: pH rises already at lower r values), which was discussed in a previous section. However, the kind of stronger and faster adsorption of the ectoine surfactant to the cell membrane, due to less steric repulsion, counterbalances this effect and the toxicity directly starts to rise with small amounts of cationic surfactant in the mixture. The apparent plateau in cytotoxicity cannot be fixed unambiguously within the error of the method and therefore is not object of the discussion.

IV.4.5   Conclusion

The synthesis, the aggregation behaviour and the biological properties of cationic surfactants basing on the compatible solutes choline and ectoine have been presented in this work. The micellisation studies showed that the compounds are very efficient surface active equivalents to common cationic amphiphiles. The ecological impact, in terms of biodegradability and cytotoxicity, was presented to be remarkably low of the ester surfactants. However, an ether bond does not influence these properties compared to common aliphatic compounds. Furthermore, it was shown that, depending on the chainlength and the mixing ratio of cationic surfactant with low toxic choline soaps, very stable vesicles of the spherical or facetted type could be produced. The cytotoxicity of these catanionics was determined to comparatively low in contrast to common cationic anionic surfactant mixtures. The cationic amphiphile was confirmed to be the restricting part in terms of cytotoxicity, independent of the toxicity of the anionic surfactant. Overall, these results show that catanionic vesicles based on osmolyte surfactants – either of anionic or cationic nature – could constitute viable agents for molecular delivery in medicinal, pharmaceutical or personal care applications.

IV.5 Evaluation of Novel, Low Toxic, True Catanionics as Emulsion Stabilizing Agents

IV.5.1 Introduction

Emulsions offer the opportunity to solubilise relatively large amounts of hydrophobic active. For that reason they accompany our lives in a multitude of circumstances [5]. Generally, several strategies exist to stabilize the interfacial film of oil and water. The most frequently used technique is the application of surfactants. Furthermore, it is now well established that solid particles of colloidal size provide a mechanical barrier against coalescence of emulsion droplets. So-called Pickering emulsions have been discussed in a multitude of publications [255, 421-423].

The process of stabilizing emulsions by particles is a virtually irreversible adsorption, which generally entails extreme stability. In contrast, surfactant molecules are in rapid (< 1ms) dynamic equilibrium between the interface and the immiscible bulk phases [2]. This usually leads to emulsions, which are more fragile against external constraints.

However, to exploit both strategies the stabilisation of emulsions by the simultaneous precipitation of anionic and cationic surfactants at the oil-water interface has only scarcely been subject of investigations. For example microemulsions basing on catanionic mixtures with and without salt have been extensively studied [142, 145, 424-425], while reports on thermodynamically

unstable macroemulsions are rare in literature. Though, it is empirically known since the early seventies that mixtures of both types of charged surfactants and lipids represent extremely efficient emulsifiers. Several formulations especially in pharmaceutical industry base on that knowledge [250-251].

Recently, Zemb and co-workers presented a concept to efficiently stabilize emulsions according to the Pickering mechanism via co-crystallisation of the true catanionic system hexadecyltrimethylammonium hydroxide (CTAOH) and myristic acid (C14) at the oil-water interface [17, 426]. They concluded that several layers of lamellar stacks of frozen catanionic bilayers around the oil droplet originate the outstandingly high stability. As this system bases on the stabilisation by the crystalline L_β phase it bears the potential to temperature-dependently switch between the particle and the classical surfactant stabilisation mechanism. This very interesting observation might offer a way to easily tune the stability of an emulsion. However, the highly toxic potential (chapter IV.4.4), especially of the long-chain cationic surfactant in this system, may restrict its potential applications.

Basing on the idea to stabilize emulsions by precipitated catanionics [250], a new low-toxic alternative will be presented in this chapter. According to the concept of Zemb, the long-chain trimethylammonium cation is replaced by a choline ester, while the anionic part remains a fatty acid. In a first brief section the synthesis is presented while in the further parts the applicability of this catanionics in "switchable" emulsions is evaluated. The main criterion to exploit the systems tuneability is the chain melting temperature of the various mixtures. Thus, this property is discussed with respect to the mixing ratio of anionic and cationic component as well as their chainlengths. In a last section the stability of emulsions with the novel catanionic mixtures is presented in dependence of the storage time and ~temperature.

IV.5.2   Materials and Methods

Myristoyl chloride (> 98 %) was received from Sigma. Lauroylchloride (98 %), lauric acid (> 98 %) and palmitoylchloride (> 98 %) were provided by Aldrich. Choline chloride (> 98 %) was received from Alfa Aesar. Myristic acid (> 98 %) was provided by Fluka, whereas palmitic acid (> 98 %) was received from Riedel-de Haen. 2-(2-(2-(dodecyloxy)ethoxy)ethoxy)acetic acid (C12EO2) and 3,6,9,12,15-pentaoxaheptacosan-1-oic acid (C12EO4) were synthesised according to the method described in chapter IV.2. All solvents were used in *p.a.* quality. If not mentioned otherwise in the synthesis section, the chemicals were utilized without further purification.

Samples for cryo TEM, differential scanning calorimetry (DSC) and infrared (IR) measurements were prepared by weighing the pure equimolar catanionics and diluting them with millipore water to achieve a total surfactant concentration of 0.25 M. For the investigation of the samples with varying molar surfactant ratio *r* (definition see section IV.4.1.2) pure catanionic (C12C12) (definition of abbreviation see next section) and lauric acid were mixed with millipore water. The total concentration was kept at 0.25 M. All samples were stirred at 50 °C at least for 24 h or until they turned homogeneous.

Cryo TEM investigations were performed at the University of Bayreuth according to the method described in chapter IV.1.

Chain melting temperatures were determined by means of differential scanning calorimetry (DSC) measurements using a micro- DSC III+ (SETARAM, France). Detailed information see chapter IV.1. The samples were equilibrated at approximately 10 °C below their expected chain melting temperature for 30 minutes and subsequently heated (generally 1 Kmin^{-1}) to ensure optimal peak separation. The onset of the resulting peaks in the detected heatflow curve upon heating was taken as the temperature of phase transition.

DSC measurements of the solvent-free equimolar catanionics were performed at a DSC 7 (Perkin Elmer, Germany). If not explicitly mentioned elsewhere, the heating rate generally was 10 °Cmin^{-1}. The water content of all investigated substances was determined by coulombmetric Karl-Fischer titration to assure values below 500 ppm before any further investigation.

The Fourier transformed infrared spectroscopic (FT-IR) investigations were performed on a FT-IR spectrometer 610 (JASCO Inc., USA). The lipid samples were placed in a thermostated cuvette with KRS-5 windows (Korth Kristalle GmbH, Germany) separated by a 12 µm Sn-spacer. Temperature was varied over 10-60°C with an external temperature controller. After 30 min thermostatisation time, 50 interferograms were accumulated, apodized with a Happ-Genzel function, Fourier-transformed and converted to absorbance spectra. Data points were collected every 2 – 5 °C. The positions of the peak maxima of the evaluated absorption bands were determined with a precision better than 0.4 cm^{-1}.

Emulsion stabilities were determined by direct visual observations. 1 mL of C12C12 stock solution with a total surfactant concentration of 0.25 M and 1.3 mL of dodecane were mixed in standard vials. The samples were homogenized with an Ultra Turrax at 36000 revolutions per minute for 3 min at room temperature. The resulting volumes of oil, water and emulsion phase, respectively, were determined in defined time intervals after preparation, by tracking the phase's heights. By this means, volume fractions of the total mixture as well as of the emulsion phase could be deviated. The total observation time was 6 months. Each sample was produced twice. One was kept in the fridge at 3 °C and the other in a thermostated room at 20 °C.

IV.5.3   Synthesis

The pure, true catanionics in equimolar ratio were prepared according to the slightly modified synthesis described in chapter IV.3. The scheme of synthesis is presented in Figure IV-54. At room temperature, 1 eq of fatty

acid and 1 eq of choline chloride were mixed in a round bottle flask. Whilst heating to 115°C the corresponding fatty acid chloride (same chainlength as the acid) was added drop-wise to the continuously stirred mixture. After a few minutes a clear solution emerged. Adjacently, the mixture was heated to 125 °C while the released hydrochloric acid gas was conducted via a bubble counter. To ensure the completion of the reaction the solution was stirred for further 60 min with subsequent pressure reduction to $< 10^{-1}$ mbar. The product was recrystallized several times for further purification and subsequently dried under vacuum.

n	Abbreviation
10	C12C12
12	C14C14
14	C16C16
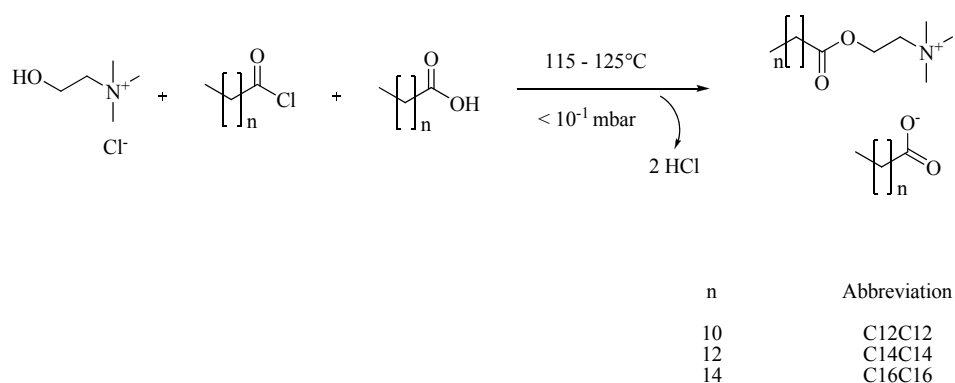
Figure IV-54: Scheme of the synthesis of pure choline ester carboxylates.

This method turned out to be inappropriate for the synthesis of catanionics of unequal chainlengths of cationic and anionic component. A transesterfication could be detected with an effectiveness of virtually 50 mol%. Thus, four components in equimolar ratio were present in these mixtures. Unfortunately it was not possible to develop an adequate synthesis evading this problem in the framework of this thesis.

IV.5.4   Results and Discussion

IV.5.4.1   Melting and Structure

Catanionics just like phospholipids are bilayer-forming amphiphiles. The alkylchains within these bilayers may either exist in the crystalline or in the fluid state. The different meso-structures between the completely frozen and the totally liquid state have been extensively studied for phospholipids. Rippled or interdigitated chain conformations have been described [418, 427-429]. The most frequently used techniques for that purpose are differential scanning calorimetry (DSC) and Fourier transformed infrared spectroscopy (FT-IR). Phase sequences similar to phospholipids can be expected for the pseudo double-chained catanionic amphiphiles. However, only few reports have highlighted this topic so far [164-165, 331, 333, 430].

IV.5.4.1.1   *Melting at Equimolar Conditions*

IV.5.4.1.1.1   Binary Mixtures with Water

Structural Pre-Investigations

In equimolar conditions, precipitation is often observed in catanionic mixtures [431]. Generally, the surfactant-rich phase either consists of a densely packed lamellar phase (L_β) or of a three-dimensional network (L_c), which can be redispersed to independent bilayers upon rising temperature [432].

At room temperature, the equimolar mixtures of C14C14 and C16C16 turned out to be turbid, comparatively low viscous solutions, whereas the C12C12 samples were more viscous and slightly bluish. This crude observation already gave a first hint to the structural state of the mixtures. Cryo TEM measurements revealed the C12C12 sample to be composed of membranes with regular circular holes (Figure IV-55).
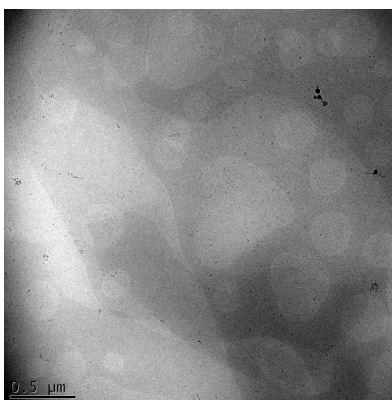
Figure IV-55: Cryo TEM picture of C12C12 (0.25 M).

The pK$_a$ of fatty acids is relatively high [295]. Thus, even at equimolar conditions, a noticeable amount of fatty acid is protonated leaving a net positive charge on the surface of the aggregates. The charged headgroups repel each other and hence introduce an unfavourable curvature in the system. This disadvantageous energetic contribution is overcome by segregation of the charges to rims or edges. Punctured membranes, huge discs or facetted vesicles with pores at the vertices are the result. Zemb and his workgroup described such structures for the system CTAC14 below its chain melting temperature [132, 157, 159-162, 417]. The size of the holes, observed in the C12C12 sample suggests pronounced electrostatic repulsions. As the pK$_a$ of carbon acids rises with temperature [9], more "neutralized" positive charges can be expected at lower temperatures resulting in smaller or less holes. Further investigations are necessary to prove this assumption. Furthermore, it should be noted that the picture in Figure IV-56 was taken above the chain melting temperature of C12C12 (see next section). Thus, the co-crystallization mechanism (compare chapter IV.4.4.2), which served as explanation for punctured structures in the work of Zemb, seems to be supporting but not necessary.

Chain Melting

As a first parameter the transition temperatures of the chain melting process of equimolar anionic/cationic mixtures in dependence of the alkylchainlength were investigated. The number of carbons in the aliphatic chain was varied from 12 to 16, both, in the anion and the cation, while the total surfactant concentration was kept constant. The determination of the symmetric CH_2 stretching vibrations as a function of the temperature is an appropriate method to determine chain melting processes.

The shift of the peak position with temperature (FigureIV-56 B), which can be taken as a measure for the changes in fluidity, is caused by an increase of the translational and rotational mobility of the acylchains by introducing more and more gauche conformers [429]. From the corresponding evaluation, given in Figure IV-56 B for the investigated amphiphiles, the following characteristics are apparent:

a) With increased temperature a shift of peak position of approximately 1.5 to 3 units was observed. The lower wavenumber (ν) range represents the crystalline, the upper the liquid state of the hydrocarbon chains. This shift comes about at higher temperatures when the aliphatic chains are longer. This observation goes in line with the increased cohesive energy due to enhanced van der Waals interactions between long carbon chains

b) The absolute values of the wavenumber shift are smallest for C16C16 and highest for C12C12.

c) The wavenumber values for the peak position in the crystalline phase are significantly higher for C16C16 compared to the shorter equivalents.

d) The slope of the peak position-temperature curve is most precipitous for the shorter chain catanionics.
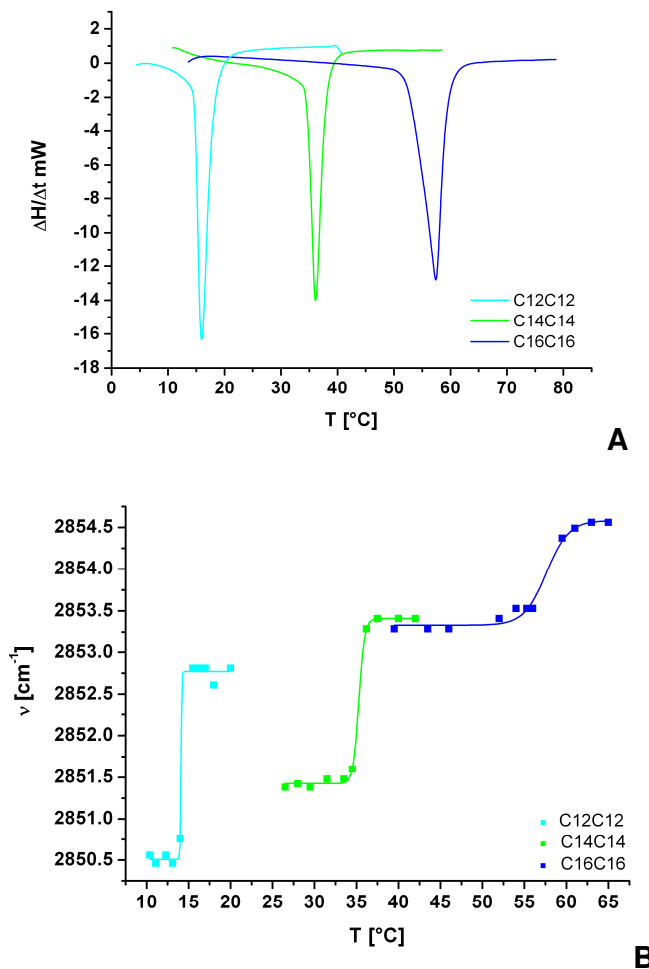
Figure IV-56: DSC curves of the solutions of C12C12, C14C14 and C16C16 (0.25 M, heating rate 1 Kmin^{-1}) (A). Maximum of the peak position of the symmetric stretching vibration ν (CH$_2$) versus temperature of 5 wt% solutions of the same substances (B). The full lines present sigmoidal fits.

The last three observations b), c) and d) can be explained by the pronounced flexibility of longer-chains. Those already bear a higher amount of gauche conformations in the crystalline state than the corresponding shorter catanionics. These conformations grant pronounced interactions with the molecules next but one neighbour, which in turn aggravates the transition from solid to fluid.

These considerations are further substantiated by the evaluation of the thermograms of the investigated compounds in aqueous solution (Figure IV-56 A). In all cases, a pronounced endothermic peak was observed in the DSC curves, which can be associated with the chain melting of the compounds in the bilayer. A flat and broad pre-melting transition was observed for the shorter chain compounds. The derived transition temperatures (main transition) fit well to those found by means of IR measurements.

The formation of intermediate structures with interdigitated or tilted molecules is likely for the shorter chain derivatives [418]. Such behaviour is often observed for the transition from lamellar gel-, to rippled or interdigitated phases in phospholipids, where the alkylchains become reorganised but remain in crystalline state [418, 427-429]. Yet, this reorganisation generally is more pronounced if packing frustrations in the lamellar bilayer are present. This in turn can be a result of a large mismatch in anionic and cationic chainlength or *e.g.* strong headgroup repulsions [331]. In the present case, the headgroup repulsions stay nearly unaltered with increasing chainlength. However, enhanced chain flexibility with rising number of carbons in the hydrophobic tail may compensate the packing frustration. Consequently, such a pre-melting phenomenon is only observed in the case of the shorter chain catanionics.

The peaks became more intense and are shifted to higher temperatures with increasing chainlength. In addition, the transitions extend over a wider temperature range. With rising number of carbons in the aliphatic chains the inter chain van der Waals attractions become more pronounced. Thus, more energy and higher temperatures are needed to induce melting of the surfactant chains. However, the broader peak of C16C16 supposes a gradual process. This might be explained by the more pronounced entropic factor. The degrees of freedom of a carbon chain rise with its length. This entropic consideration is the reason for carbon chains to take all-trans conformation with a lower preference upon elongation. Nevertheless, this net-repulsive contribution is

counterbalanced by an enhanced entanglement of the chains. Consequently the melting transition becomes more and more a gradual less defined process.

The transition enthalpies ΔH_t, just like the corresponding transition temperatures T_t determined by DSC measurements rise with increasing chainlength of the ions (Table IV-19). In general, transition temperature and transition enthalpy are proportional to the chainlength, which can be explained by the increase of the cohesive energy between the chains. However, the ΔH_t values of the substances investigated within the framework of this thesis are outstandingly low. Chain melting of C12C12 merely consumes 20 kJmol^{-1}. In contrast, significantly higher values for dodecyltrimethylammonium laurate (DTAC12), which bears the same headgroups and acylchainlengths, were reported (~ 26 kJmol^{-1}) [331].

Table IV-19: Transition temperatures T_t and ~ enthalpies ΔH_t of the investigated equimolar catanionics in comparison to literature data of similar compounds. Values were taken from the heating cycle. For ΔH_t the catanionic pair was considered as two molecules.

Substance	T_t [°C]	ΔH_t [kJmol^{-1}]
C12C12	14.6	20.0
C12C12 *	60 – 70 °	83.1 $^+$
C14C14	34.5	38.6
C16C16	53.0	39.3
C16C16 *	70 - 80 °	90.2 $^+$
DTAC12 [331]	~9.5	~26
TTAC12 [331]	20.6	34.0

*) undiluted systems
°) transition at highest temperature
$^+$) whole melting process

If one considered the additional two CH$_2$ units, which are accounted for the choline headgroup one even should compare C12C12 with the equimolar combination of tetradecyltrimethylammonium and lauric acid (TTAC12). Its chain fusion enthalpy appears to be nearly 75 % higher than that of C12C12,

making the difference even more conspicuous. Obviously, these observations cannot be a result of electrostatic headgroup influenced interactions since both types of true catanionics bear exactly the same charged moieties. Hence, the sole structural difference is the ester functionality in vicinity of the cationic ammonium head. Evidently, the presence of this functional group disrupts the effectiveness of the chain packing and thus renders the crystalline lamellar state less stable. From the slope of the ΔH_t versus chainlength curve one can deduce an increment of 2.40 kJmol^{-1} per CH_2 group for the choline ester system. Alkyltrimethylammonium laurate catanionics and n-alkanes on the other hand give values of 4.45 kJmol^{-1} or 4.05 kJmol^{-1}, respectively [331]. Thus, the effective cohesive energy between the chains is about half for the choline ester derivatives. Consequently both, the melting enthalpy as well as the transition temperature are shifted to lower values.
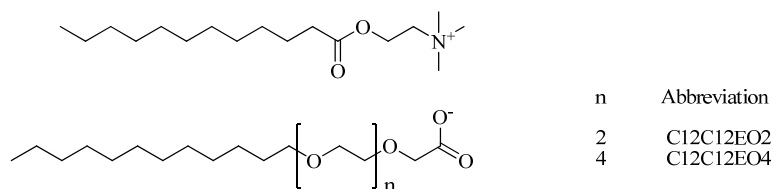
Figure IV-57: Structure of investigated true catanionics with ether functionalities.

At this point it should be mentioned that interestingly the excursion to C12 chain catanionics of similar composition like those discussed above – choline ester combined with long-chain carbon acid – but ether moieties (under investigation two and four units) introduced between the carboxy function and the aliphatic chain of the anionic surfactant (Figure IV-57) did not reveal any chain melting point between 5 – 90 °C. This observation might be attributed to the hydrophilicity and flexibility of the ether groups, which introduce a curvature in the amphiphilic membrane and thus the chain packing becomes less efficient. Consequently, the chains are in fluid state already at lower temperatures.

Solvent-free Conditions

In contrast to the diluted compounds, the pure, undiluted, catanionics expressed several thermotropic transitions, which suggests the existence of a variety of mesophases (Figure IV-58). The total melting enthalpy is much higher for the pure systems. Naturally, the comparison of dilute and pure samples is difficult since a variety of forces exists in the one case, which do not subsist – or just in much alleviated form – in the other case. Instancing, the electrostatic headgroup repulsion between adjacent layers can be considered. This force will undergo another pronunciation in the solvent-free case than in the diluted samples. On the other hand further solvent/headgroup interactions have to be considered in mixture with water, which miss in the pure form.
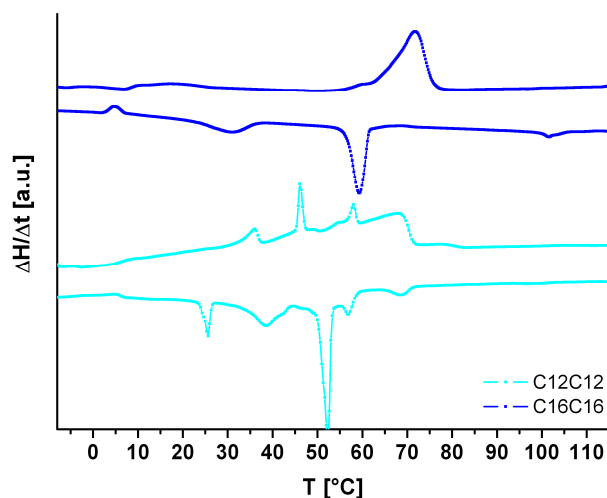
Figure IV-58: Thermograms of pure C12C12 (10 Kmin^{-1}) and C16C16 (20 Kmin^{-1}) indicating a variety of mesophases.

The total melting heat of C16C16 was found to be very similar to that of C12C12 (Table IV-19). This contradicting observation is probably due to the restricted temperature range of investigation. The highest investigated temperature of the pure samples was 120°C. Thus, the existence of transitions beyond that temperature cannot be excluded unambiguously. Nevertheless,

the observed melting enthalpies are in a reasonable order of magnitude compared to similar systems which base on the combination of alkylammonium cations with alkylsufate anions [164]. Furthermore, the single peaks in thermotropic investigations of pure substances should be considered differentially, since their impact, basing on the respective structure modification, can diversify explicitly upon chainlength variation [164].

The nature of the transitions was studied by polarizing microscopy. In all cases a transition of solid crystals (C) to a liquid crystalline phase (LC) was observed, which existed up to the maximal temperature of investigation (120°C). Crossed nicols revealed focal conic structures in the LC phase of C12C12 (Figure IV-59) and C14C14, which are typical for smectic structures (chapter III.1.1.2).
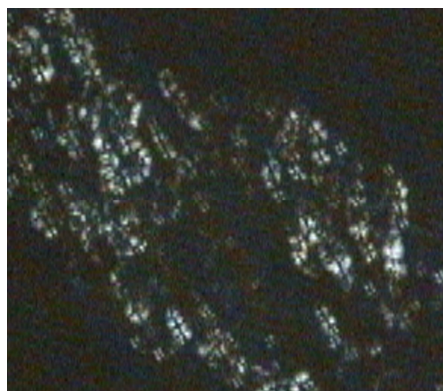
Figure IV-59: Micrograph of C12C12 at 83 °C depicting a homeotropic texture with some residual focal conics (crossed nicols, 20x).

The texture of liquid crystal of the C16C16 phase cannot be assigned unambiguously. The observed C/LC transitions clearly correspond to the DSC peaks at 60 – 70 °C for C12C12 and 70 – 80 °C for C16C16 (Figure IV-58). According to that, all peaks detected at lower temperatures must correspond to single peaks and could not be assigned to concrete structural modifications.

Polymorphism in the crystalline as well as in the liquid crystalline state is known for equimolar catanionic systems [164-166, 330]. The most frequently observed mesophase is the smectic one, as catanionics are prone to form double layer structures due to their cylindrical molecular shape. Generally, in the solid smectic state the double headgroup layer is separated by two aliphatic chain layers, composed of an equimolar mixture of cationic and anionic surfactants of the same hydrocarbon chainlength, which are packed parallel to each other. Intra-lamellar electrostatic interactions between cationic and anionic headgroups reduce the surface charge through the formation of tight ion pairs. Frequently, the chains are crystallized in all-trans conformation with a tilted angle towards the bilayer plane [164].
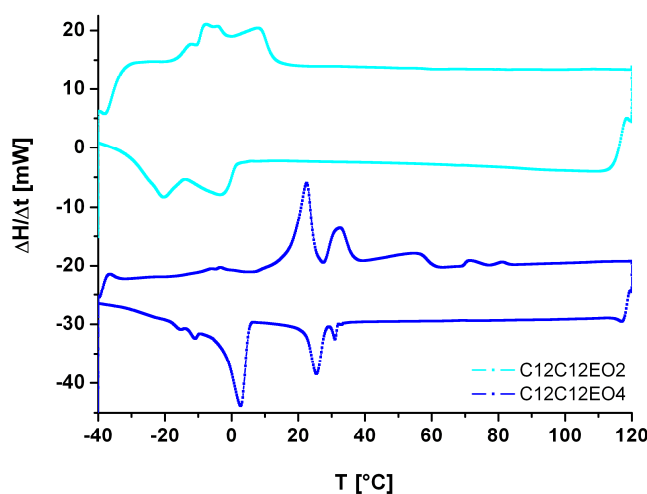
Figure IV-60: Thermograms of pure C12C12EO2 and C12C12EO4 (20 Kmin^{-1}) indicating a variety of mesophases transitions at low temperatures..

Again, a comparison to the C12 chain system with ether functionalities (EO) in the anionic amphiphile should be drawn. In the dilute system it has already been shown that no chain melting occurred within the investigated temperature range. In the pure state, likewise, a shift of transitions to lower temperatures was detected (Figure IV-60), which is even more pronounced in the case of two EO groups than in that of four. This finding should become clear upon consideration of the enhanced flexibility of the ether groups

compared to simple aliphatic chains, which makes the formation of ordered structures more unfavourable. Thus, lower temperatures suffice to shift the structure into the next higher energy level. However, if flexibility rises with the number of EO units even lower transition temperatures for four than for two inserted ether groups should be found. Yet, the antipodal observation was made. This results can be explained by considering that upon the insertion of ether functionalities the total number of carbons in the chain is increased and thus in turn the van der Waals interactions. Additionally, more ether-oxygen counterion interactions are present in the EO4 case. Consequently, more energy is required to shift the conformational order.

IV.5.4.1.2   Chain Melting of Solutions in Water with an Excess of Lauric Acid

In the previous part of this chapter solely equimolar conditions of the choline ester/fatty acid systems were studied. In the following section the chain melting behaviour in dependence of excess lauric acid will be discussed. Unfortunately, due to restrictions of the method of synthesis, the phase diagram with excess cationic surfactant could not be investigated.

For the following discussion the molar surfactant ratio r is defined according to:

$$r = \frac{n_{Anionic}}{n_{Anionic} + n_{Cationic}}$$
         IV-22

where n corresponds to the molar amount of anionic or cationic surfactant, respectively.

For a rising content of dodecanoic acid an increase in chain melting temperature was observed (Figure IV-61). Lauric acid is a weak acid and thus difficult to deprotonate. Consequently, an excess of it does not sustainably destabilise the lamellar structure. The chain melting temperature is a function of the headgroup interactions more than a function of the chain interactions:

The polar head of the lauric acid is smaller than the polar head of the choline ester, moreover there are strong hydrogen bonds between the carboxylic groups resulting in a transition temperature increase with *r*.
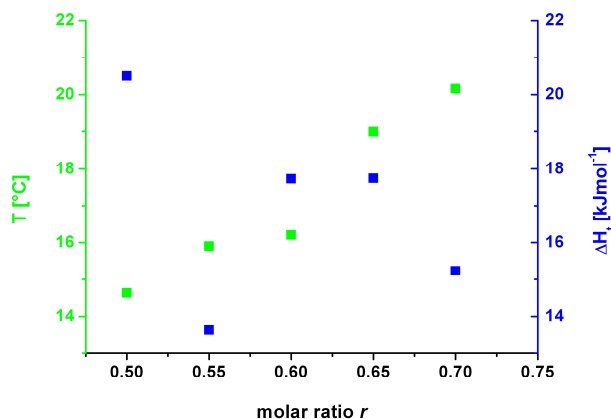
Figure IV-61: Melting temperatures ■ and transition enthalpies of the main transition ■ as a function of the molar ratio *r* of lauric acid and choline ester.

Peaks of varying anionic/cationic mixing ratios determined by DSC measurements are depicted in Figure IV-62. The sample with a ratio of 0.55 – close to equimolarity – shows a pronounced pre-melting followed by a sharp melting transition. Upon increasing the content of lauric acid, on the one hand the peaks become more symmetric; on the other hand their width increases significantly.

The first broad peak in case of r = 0.55 might be an indication of a structural reorganisation, like already explained for equimolar conditions in section IV.5.4.1.1.1. With increasing amount of acid the structural mismatch in the lamellar phase, which resulted from electrostatic repulsion of the ammonium groups, seems to be reduced. Strong H-bonds between the partially undissociated lauric acid stabilize the lamellar structure. Zemb and co-workers reported that the system CTAOH/myristic acid expresses interdigitated bilayers in case of excess cationic surfactant. A normal lamellar

phase was found for excess fatty acid [331]. Furthermore, measurements of the electrophoretic mobility revealed a zetapotential still being positive at an *r* value of 0.6 [333]. Hence, the transference of these facts to the present case of choline ester and lauric acid helps to elucidate the observations. While at r = 0.55 a pre-melting is still possible due to a frustration in the lamellar structure, at r = 0.65 any miss-fits have already been compensated by the excess of acid. The broad peak in this case supposes a gradual melting process. Fluid-like and crystalline chains coexist over a wide temperature range, due to the non-ideal mixture between the components. Such a miscibility gap between liquid and solid state of the carbon chains in amphiphilic systems has been described by several authors [333, 418, 431]. r = 0.6 seems to represent an intermediate case, which becomes obvious in the consideration of the peak morphology. While its overall shape is already relatively broad, a distinct hump on its lower temperature boarder indicates the existence of a second process – probably pre-melting.
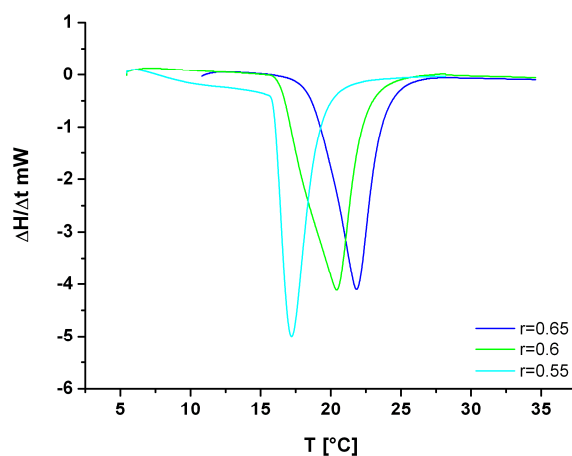
Figure IV-62: DSC curves of C12C12 with varying r values, a total surfactant concentration of 0.25 M and a scanning rate of 1 Kmin⁻¹.

IV.5.4.2 Emulsions

The aim of this work was to determine the effect of storage temperature upon an emulsion stabilized by true catanionic aggregates in their crystalline form

at low temperatures, which change to a molten state with rising temperature. To evaluate the stabilizing mechanism of the above described amphiphiles and its temperature dependence 1.3 mL of dodecane were mixed with 1 mL of C12C12 catanionic solution with a surfactant concentration of 0.25 M. The mixing procedure is described in detail in section IV.5.2. The development of r-value dependent phases – oil, water or emulsion – was checked in consecutive time intervals, to a maximum period of six months. In the following section the term "phase" will not be used in its strict thermodynamic definition, but for optically unambiguously distinguishable, liquid solutions with a distinct separation plane.

The results for mixtures observed 24 hours (C) and six months after preparation, are summarized in Figure IV-63. The samples were either stored in the fridge at 3 °C (A) or in a thermostated room at 20 °C (B) No alteration of the emulsion or the excess phases was detected within the first week, independent of the storage temperature. At lower r-values, *i.e.* comparatively more cationic surfactant, a two phase system composed of a water-in-oil emulsion (destroyed upon dilution with water) and excess water phase was observed. With increasing content of lauric acid (higher r-values) three phase systems developed with a pronounced reduction of the emulsion volume fraction. The emulsions, in the two as well as in the three phase cases, contained a significantly higher volume fraction of dodecane than of water (Figure IV-64).

During the storage period the two phase systems collapse to the benefit of an excess oil phase. Hence, now for all mixing ratios finally three phases emerged. Interestingly, not exclusively dodecane was ejected from the emulsion, but water was absorbed simultaneously by the emulsion in all cases (Figure IV-64). With proceeding time, the volume fractions of water and oil incorporated in the emulsion converged to similar values (Figure IV-64). This process was accelerated if the mixtures have been stored at higher temperatures (Figure IV-64). The total volume fraction of emulsion remained approximately constant – within the error of the measurements of approximately 5 % – for each r-value during the investigated period of time.

The sole exception exhibits r = 0.8 at 20 °C storage temperature with a significantly reduced amount of emulsion within six months.
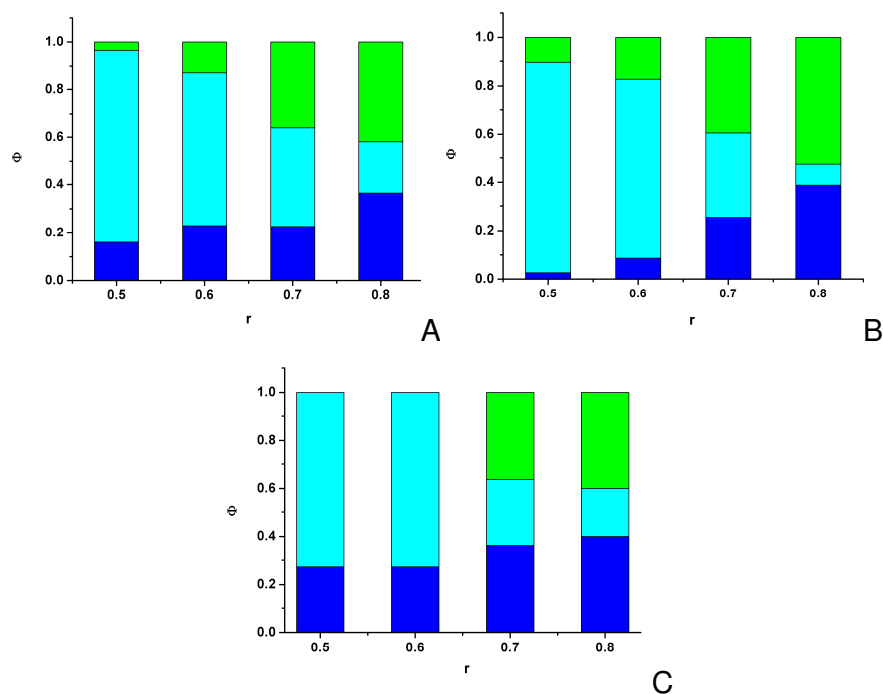
Figure IV-63: Volume fractions Φ of excess oil ■, excess water ■ and emulsion phase ■ in dependence of the molar ratio *r* of the catanionic mixture C12C12 after 6 months storage at 3 °C (A) or respectively 6 months at 20 °C (B) or 24 hours (C), respectively. None of the samples showed any temperature-dependence after 24 hours.

Generally, a surfactant helps to compartmentalize a mixture of two immiscible components on a sub-micron scale by the stabilisation of interfaces. This can be achieved either by the formation of small droplets or bicontinuous structures. In the droplet case, a surfactant prefers the solvent to form the outer, continuous phase, which provides its best solubility. This statement is known as the Bancroft rule [238-239] (compare chapter II.2.5) and is based on the combination of hydrophilicity and geometrical considerations of the surfactant molecule. This affects the curvature of the formed aggregates, which is reflected in the so-called packing parameter [2, 102].
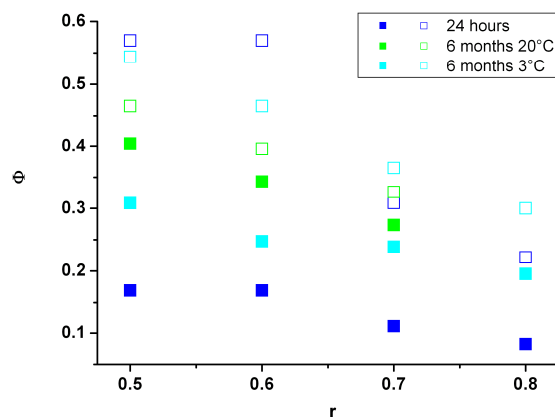
Figure IV-64: Composition of the emulsion expressed in volume fractions Φ of oil (open symbols) and water (filled symbols) in dependence of the molar ratio *r* of the catanionic mixture C12C12, the storage time and ~ temperature.

In the present case catanionic systems, which easily form bilayer structures were investigated. Thus, the packing parameter of the pseudo double chained ion pair is close to one. However, in section IV.5.4 it was suggested that even at equimolar conditions excess positive charge should be present due to the incomplete dissociation of the fatty acid. This charge actually is supposed to introduce a net curvature in the aggregates plane towards the water phase. Yet, right after preparation, a water-in-oil emulsion and excess water was observed. While evaluating the r = 0.5 case two facts have to be kept in mind:

- during preparation at room temperature the aliphatic chains of the surfactants were in the molten state and

- an additional increase of temperature in the samples due to the preparation method using an ultra turrax has to be expected

The solubility in the bulk phases of one of the two amphiphilic components can be expected to be higher than that of the other one. Such a mechanism was proposed by Marques, Silva and co-workers, who investigated equimolar mixtures of hexadecyltrimethylamminium and octylsulfate [425].

Microemulsion stability, solubility at room temperature and the coexistence of several lamellar phases were explained with the escape of one of the amphiphiles to the surrounding bulk. Especially at higher temperatures the exchange rate between aggregate and bulk is accelerated. The solution rate of the choline ester is considered to be higher than that of lauric acid. Thus, during preparation the curvature of the interfacial membrane is no longer influenced by the excess positive charge. The pronounced ion pair formation between positively and negatively charged headgroups in combination with excess undissociated fatty acid, which forms strong hydrogen bonds, even allows the assumption of a comparatively small area per molecule compared to the required volume of the hydrophobic tails (with additional ester functionality). Thus, a packing parameter > 1 is suggested. In consequence, the membrane bends towards the water. This explains the initial formation of water-in-oil emulsions at conditions of small amounts of excess fatty acid (r <0.7). A second scenario seems reasonable: The choline ester dissolves partially in the water phase during preparation. However, this has no impact on the membrane curvature, as in the oil-free water surfactant system excess charge seems to be segregated to form membrane defects (compare section IV.5.4.1). These holes might vanish with the dissolution of choline ester. Thus, the finally formed emulsion might have the structure of swollen bilayers, which cannot swell infinitely with water due to the relative hydrophobicity of the amphiphile and the van der Waals interactions between the hydrocarbon layers. Upon cooling and storage of the emulsions it becomes energetically more favourable for the choline ester to readsorb at the interface, which globally renders the membrane more hydrophilic and potentially less curved. Hence, water is taken up with time while oil is expelled from the emulsion due to the electrostatic repulsion of adjacent (now again positively charged) aggregates. This process of exchange of molecules with surrounding bulk phases obviously is accelerated if the aliphatic chains were molten during the storage period. More energy is afforded to break the attractive forces between the amphiphilic molecules if they were in crystalline state.

Furthermore, the solubility of lauric acid in dodecane has to be considered likewise. Especially at higher r-values the dissolution of lauric acid should be the driving force for the observed three phase systems. The choline ester in these cases is kept tightly bound in the amphiphilic membrane due to the strong electrostatic interactions. Thus, its dissolution can be neglected. Actually the amphiphilic system should be featured by an even more pronounced hydrophobicity. Hence, a bigger volume fraction of emulsion was expected. However, considering the dissolution of undissociated lauric acid, which by itself exhibits only feeble interfacial properties, in dodecane, a comparatively smaller amount of amphiphile is left to stabilize an emulsion phase. Thus, none of the immiscible phases can be completely consumed by the emulsion. Consequently, immediately after preparation, a three phase system emerges with a smaller volume fraction of emulsion with rising amount of lauric acid. This emulsion bears approximately thrice the volume of oil compared to water. The relative composition of the emulsion phase as a function of r is nearly constant. This suggests a similar composition of the interfacial film independent of the initial molar ratio of the catanionic mixture. With proceeding time, the emulsions converge to a composition of equal volume fractions of oil and water. There is no reasonable explanation for that phenomenon but perhaps the formation of a bicontinuous emulsion structure with zero overall curvature could occur. The question to be elucidated is, whether the systems eventually converge to a stable microemulsion state.

At this point it should be mentioned that all the explanations on the structural and molecular behaviour of the emulsions given above lack any experimental ratification. Although, the assumed mechanism seems to fit well the so far achieved results, further measurements are inevitable. To eventually clarify the real mechanism a detailed structural analysis by means of scattering methods and fluorescence microscopy is strongly recommended. Further, surface charge determinations would be particularly eligible.

IV.5.5   Conclusion

Additionally to the synthesis, the first physico-chemical characterisations of counterion free catanionics based on fatty acids and environmentally friendly choline esters (compare chapter IV.4) have been presented in this chapter. The focus was laid on the evaluation of these surfactant mixtures as adequate emulsion stabilizers according to the Pickering mechanism. For that purpose the chain melting temperature in dependence on the chainlength, as well as on the molar ratios of amphiphiles was determined by means of DSC and FT-IR measurements. The data could be interpreted in terms of intermolecular interactions, dissociation equilibriums and charge segregation. Emulsions prepared of water, dodecane and C12C12 were investigated in dependence of time, temperature and molar ratio of the catanionic. With rising content of lauric acid, a smaller volume fraction of emulsion was achieved. Neither the mixtures stored below, nor above the chain melting temperature of the catanionics were very stable with regard to its oil/water ratio. While freshly prepared emulsions showed a volume ratio of oil:water of 3:1, the composition shifted to nearly 1:1 after six months. Yet, the total volume fraction of emulsion stood approximately constant. A theoretical explanation for the emulsion stability was given. However, further measurements are inevitable to verify the proposed theory.

V. Conclusion

This thesis can be subdivided into two main parts:

In the first part the formation of surfactant-like Ionic Liquids by means of the combination of carboxylate and ammonium ions was studied. Several successful concepts were presented.

- It was shown that Lidocaine carboxylates are isotropic liquids up to an alkylchainlength of twelve C-atoms. Their physico-chemical properties, like their low viscosity, recommend them for concentrated applications at ambient temperature. In binary mixtures with water low Krafft temperatures of the shorter chain derivatives, a cloud point phenomenon at elevated temperatures and sparsely viscous lamellar phases were detected. Furthermore, the formation of highly stable water in oil emulsions was proved. All phenomena could be interpreted by means of ion affinities and pK_a value differences. The determined properties seem to make Lidocaine carboxylates are highly potential compounds for pharmaceutical formulations.

- In chapter IV.2 the formation of room temperature Ionic Liquids with anionic or respectively catanionic surfactant properties was demonstrated. The outstanding physico-chemical properties can mainly be attributed to the choice of long-chain ether carboxylates as counterions. Their features, in pure and diluted form could be correlated to chainlength, degree of ethoxylation and technical grade purity of the acids. In addition, the influence of the type of counterion and of industrially relevant impurities was determined. In binary mixtures with water, the investigated systems were shown to combine characteristics of ionic and non-ionic surfactants. The outstanding properties of the catanionic species, like their low viscosity and high heat capacity recommend their application in pure form *e.g.* as lubricating agents. Their high solubility and the formation of sparsely viscous lamellar phases allow the production of concentrated formulations, which stay easily pourable while diluted. By variation of the ion combination they are easily tuneable making those

compounds real task specifically designable surfactant-like Ionic Liquids.

- Furthermore, short chain oligoether carboxylates (TOTO) were proved to present adequate counterions for long-chain primary ammonium compounds to form room temperature ILs with cationic surfactant properties. Low viscosities, low conductivities and low thermal stabilities can be ascribed to the pronounced non-ionic character of the investigated ILs. Additionally to the internal charge readsorption, the flexibility of the anion leads to their classification as "poor" ILs according to the standard introduced by Angell *et.al*. Surfactant properties in binary mixtures with water were shown to resemble those of the corresponding ammonium halogenides. Yet, the formation of highly viscous liquid crystals, like the hexagonal and cubic phase, can be efficiently shifted to lower temperatures.

In the second part of the present thesis, the synthesis and the physico-chemical characterisation of biologically sustainable cationic and catanionic surfactants was demonstrated.

- The synthesis, the aggregation behaviour and the biological properties of choline and ectoine based surfactants have been exposed. Micellisation studies showed that these compounds might present efficient equivalents to common cationic amphiphiles. The biodegradability and cytotoxicity, was shown to be remarkably low of ester type surfactants. Additionally, low-toxic, stable catanionic vesicles were accomplished by the combination of the synthesised cationic surfactants with choline soaps. The cytotoxicity of these mixtures was compared to classical SDS/DTAB catanionics. The promising results suggest these catanionic vesicles as delivery media for active agents in cosmetic or pharmaceutical applications.

- In the last section, the first physico-chemical characterisations of counterion free catanionics based on fatty acids and long-chain choline esters have been presented. In order to evaluate these mixtures

as adequate emulsion stabilizers according to the Pickering mechanism chain melting temperatures in dependence on the chainlength, as well as on the molar ratios of amphiphiles were determined. Emulsions prepared of water, dodecane and C_{12}-chain catanionic were investigated in dependence of time, temperature and molar ratio of the catanionic. Stable emulsions were prepared. Yet, a significant impact of storage temperature could be deduced.

A successful concept for the efficient melting point reduction in ionic surfactants was presented. Furthermore, several new biocompatible cationic surfactants and their mixtures with low toxic soaps have been introduced. The basic physico-chemical features of all presented systems have been determined and interpreted. All compounds express promising properties, valuable for a multitude of applications. Thus, further investigations, determining profound characteristics of the systems, seem to be worth being accomplished.

VI. Literature

[1]   Holmberg, K.; Shah, D.O.; Schwuger, M.J. (2002) *Handbook of Applied Surface and Colloid Chemistry*; John Wiley & Sons

[2]   Evans, D.F.; Wennerström, H. (1999) *The Colloidal Domain: Where Physics, Chemistry, Biology, and Technology Meet*; Wiley-VCH

[3]   Holley, W. *Emulgieren, Homogenisieren, Grenzflächenvergrößerung, Technologie von Salben, Suspensionen und Emulsionen*; Asche: Stuttgart.

[4]   Holmberg, K. (2002) *Handbook of Applied Surface and Colloid Chemistry*; John Wiley & Sons

[5]   Mollet, H.; Grubenmann, A. (2000) *Formulation Technology: Emulsions, Suspensions, Solid Forms*; Wiley-VCH

[6]   Soussan, E.; Cassel, S.; Blanzat, M.; Rico-Lattes, I. (2009) *Angewandte Chemie Internationale Edition*, 48: 274.

[7]   In REACH, Nr. 1907/2006; EG, 2007.

[8]   Collins, K.D. (1997) *Biophysical journal*, 72: 65-76.

[9]   Lide, D.R. (2002) *CRC Handbook of Chemistry and Physics*; CRC Press

[10]   Mitchell, D.J.; Tiddy, G.J.T.; Waring, L.; Bostock, T.; McDonald, M.P. (1983) *J. Chem. Soc., Faraday Trans.*, 1: 975.

[11]   Elsässer, S. (2008) *Körperpflegekunde und Kosmetik*; Springer: Heidelberg.

[12]   Feinstein, M.B.; Volpi, M.; Perrie, S.; Makriyannis, A.; Sha´afi, R.I. (1977) *Mol. Pharmacol.*, 13: 840.

[13]   Blusztajn, J. (1998) *Science*, 281: 794.

[14]   Graf, R.; Anzali, S.; Buenger, J.; Pfluecker, F.; Driller, H. (2008) *Clinics in Dermatology*, 26: 326.

[15]   Klein, R.; Maurer, E.; Kraus, B.; Brunner, G.; Estrine, B.; Touraud, D.; Heilmann, J.; Kunz, W. (2010) *Green Chem*, submitted.

[16]   Pickering, S.U. (1907) *J. Chem. Soc.*, 91: 2001.

[17]   Schelero, N.; Lichtenfeld, H.; Zastrow, H.; Möhwald, H.; Dubois, M.; Zemb, T. (2009) *Colloids and Surfaces A: Physicochemical and Engineering Aspects*, 337: 146-153.

[18]   T. Welton. (1999) *Chem. Rev*, 99: 2071.

[19]   Holbrey, J.; Seddon, K.R. (1999) *Clean Prod. Proc.*, 1: 223.

[20]   Seddon, K.R. (1997) *J. Chem. Tech. Biotech*, 68: 351.

[21]   Walden, P. (1914) *Bull. Acad. Imper. Sci.*: 1800.

[22]   Wier, T.P.; Hurley, F.H.; . Electrodeposition of aluminum. 1948.

[23] Chum, H.L.; Koch, V.R.; Miller, L.L.; Osteryoung, R.A. (1975) *J. Am. Chem. Soc.*: 3264.

[24] Wilkes, J.S.; Levisky, J.A.; Wilson, R.A.; Hussey, C.L. (1982) *Inorg. Chem.*, 21: 1236.

[25] Hussey, C.L.; . (1988) *Pure and Applied Chemistry*, 60: 1763.

[26] Dent, A.J.; Seddon, K.R.; Welton;, T. (1990) *Chemical Communications* 4: 315.

[27] Wilkes, J.S.; Zaworotko, M.J. (1992) *Chemical Communications* 13: 965.

[28] Luczak, J.; Hupka, J.; Thöming, J.; Jungnickel, C. (2008) *Colloids Surf. A Physicochem. Eng. Aspects*, 329: 125.

[29] Bowers, J.; Butts, C.P.; Martin, P.J.; Vergara-Gutierrez, M.C. (2004) *Langmuir* 20: 2191.

[30] Baker, G.A.; Pandey, S.; Pandey, S.; Baker, S.N. (2004) *Analyst*: 890.

[31] Ruta, M.; Laurenczy, G.; Dyson, P.J.; Kiwi-Minsker, L. (2008) *Journal of Physical Chemistry C*, 112: 17814.

[32] Jiménez, A.E.; Bermúdez, M.D.; Carrión, F.J.; Martínez-Nicolás, G. (2006) *Wear*, 261: 347-359.

[33] Couling, D.J.; Bernot, R.J.; Docherty, K.M.; Dixona, J.K.; Maginn, E.J. (2006) *Green Chem*, 8: 82.

[34] Garcia, H.; Ferreira, R.; Petkovic, M.; Ferguson, J.L.; Leitão, M.C.; Gunaratne, H.Q.N.; Seddon, K.R.; Rebelo, L.P.N.; Pereira, C.S. (2010) *Green Chem*, 12: 367.

[35] Plechkova, N.V.; Seddon, K.R. (2007) *Chemical Society Reviews* 37: 123.

[36] Wasserscheid, P.; Keim, W. (2000) *Angewandte Chemie (Int. ed.)* 39: 3772.

[37] Wasserscheid, P. (2003) *Chemie in unserer Zeit* 37: 52.

[38] Hamnett, A.; Hamann, C.H.; Vielstich, W. (1997) *Electrochemistry*; Wiley-VCH

[39] Wasserscheid, P.; Welton, T. (2003) *Ionic Liquids in Synthesis*; Wiley-VCH

[40] Fannin, A.A.; Floreani, D.A.; King, L.A.; Landers, J.S.; Piersma, B.J.; Stech, D.J.; Vaughn, R.L.; Wilkes, J.S. (1984) *Journal of Physical Chemistry C*, 88: 2614.

[41] Bonhote, P.; Dias, A.-P.; Papageorgiou, N.; Kalyanasundaram, K.; Graetzel, M. (1996) *Inorganic Chemistry*, 35: 1168.

[42] Freemantle, M. (1998) *Chem. Eng. News*, 76: 32.

[43] Gordon, C.M.; Holbrey, J.D.; Kennedy, A.R.; Seddon, K.R. (1998) *Journal of Materials Chemistry*, 8: 2627.

[44]   Ngo, H.L.; LeCompte, K.; Hargens, L.; McEwen, A.B. (2000) *Thermochimica Acta* 357.

[45]   Hagiwara, R.; Ito, Y. (2000) *Journal of Fluorine Chemistry*, 105: 221.

[46]   Saha, S.; Hayashi, S.; Kobayashi, A.; Hamaguchi, H.O. (2003) *Chemistry Letters* 32: 740.

[47]   Holbrey, J.D.; Reichert, W.M.; Nieuwenhuyzen, M.; Johnson, S.; Seddon, K.R.; Rogers, R.D. (2003) *Chemical Communications*, 14: 1636.

[48]   Koelle, P.; Dronskowski, R. (2004) *Inorganic Chemistry*, 43: 2803.

[49]   Belieres, J.-P.; Angell, C.A.; (2007) *Journal of Physical Chemistry Biophysical Chemistry*, 111: 4926.

[50]   Susan, M.A.B.H.; Noda, A.; Mitsushima, S.; Watanabe, M. (2003) *Chemical Communications*, 8: 938.

[51]   Ohno, H.; Yoshizawa, M. (2002) *Solid State Ionics*, 154.155: 303.

[52]   Greaves, T.L.; Weerawardena, A.; Fong, C.; Krodkiewska, I.; Drummond;, C.J. (2006) *Journal of Physical Chemistry Biophysical Chemistry*, 110: 22479.

[53]   Cooper, E.; O´Sullivan, E. (2000) *The Electrochemical Society*, 92: 386.

[54]   Harris, K.R.; Kanakubo, M.; Woolf, L.A. (2007) *Journal of Chemical & Engineering Data*, 52: 1080.

[55]   Earle, M.J.; Seddon, K.R. (2000) *Pure Appl. Chem.*, 72: 1391.

[56]   Liao, Q.; Hussey, C.L. (1996) *Journal of Chemical and Engineering Data* 41: 1126.

[57]   Seddon, K.R.; Stark, A.; Torres, M.-J. (2000) *Pure and Applied Chemistry Letters*, 72: 2275.

[58]   Wasserscheid, P.; Keim, W. (2000) *Angewandte Chemie (Int. ed.)*, 112: 3926.

[59]   Yoshizawa, M.; Xu, W.U.; Angell, C.A. (2003) *Journal of the American Chemical Society*, 125: 15411.

[60]   Earle, M.J.; Esperanca, J.M.S.S.; Gilea, M.A.; Lopes, J.N.C.; Rebelo, L.P.N.; Magee, J.W.; Seddon, K.R.; Widegren, J.A. (2006) *Nature*, 439: 831.

[61]   Carmichael, A.J.; Seddon, K.R. (2000) *Journal of Physical Organic Chemistry* 13: 591.

[62]   Muldoon, M.J.; Gordon, C.M.; Dunkin, I.R. (2001) *Journal of the Chemical Society Perkin Transactions*, 24: 433.

[63]   Mara, G.F.; Fernandes, C.J.; Coutinho, J.A.P. (2007) *Journal of colloid and interface science*, 314: 621.

[64]   Ghatee, M.H.; Zolghadr, A.R. (2008) *Fluid Phase Equilibria*, 263: 168.

[65]   Law, G.; Watson, P.R. (2001) *Langmuir*, 17: 6138.

[66]   Law, G.; Watson, P.R. (2001) *Chemical Physics Letters*, 345: 1.

[67]   Dong, B.; N.Liao; Zheng, L.Q.; Yu, L.; Inoue, T. (2007) *Langmuir*, 23: 4178.

[68]   Ranke, J.; Stolte, S.; Stormann, R.; Arning, J.; Jastorff, B. (2007) *Chemical reviews*, 107: 2183.

[69]   Cho, C.; Pham, T.; Jeon, Y.; Vijayaraghavan, K.; Choe, W.; Yun, Y. (2007) *Chemosphere*, 69: 1003.

[70]   Kulacki, K.; Lamberti, G. (2008) *Green Chem*, 10: 104.

[71]   Stepnowski, P.; Skladanowski, A.; Ludwiczak, A.; Laczynska, E. (2004) *Human & Experimental Toxicology*, 23: 513.

[72]   Zhao, D.; Liao, Y.; Zhang, Z. (2007) *Clean: Soil, Air, Water*, 35: 42.

[73]   Garcia-Lorenzo, A.; Tojo, E.; Tojo, J.; Teijeira, M.; Rodriguez-Berrocal, F.J.; Gonzalez, M.P.; martinez-Zorzano, V.S. (2008) *Green Chem*, 10: 508.

[74]   Stolte, S.; Arning, J.; Bottin-Weber, U.; Matzke, M.; Stock, F.; Thiele, K.; Uerdingen, M.; Welz-Biermann, U.; Jastorff, B.; Ranke, J. (2006) *Green Chem*, 8.

[75]   Stolte, S.; Arning, J.; Bottin-Weber, U.; Müller, A.; Pitner, W.; Welz-Biermann, U.; Jastorff, B.; Ranke, J. (2007) *Green Chem*, 9.

[76]   Garcia, M.; Gathergood, N.; Scammells, P. (2005) *Green Chem*, 7: 9.

[77]   Gathergood, N.; Garcia, M.T.; Scammells, P.J. (2004) *Green Chem*, 6: 166.

[78]   Matsumoto, H.; Zhou, Z.B. Ionic liquid, its manufacture, and secondary lithium battery and double layer capacitor comprising the liquid. Technology, N.I.o.A.I.S.a., Ed.: Japan, 2005.

[79]   Endres, F. (2007) *Nachrichten aus der Chemie*, 55: 507.

[80]   Gorlov, M.; Kloo, L. (2008) *Dalton Transactions*, 20: 2655.

[81]   Swatloski, R.P.; Spear, S.K.; Holbrey, J.D.; Rogers, R.D. (2002) *Journal of the American Chemical Society*, 124: 4974.

[82]   Nagano, T.; Takahashi, T.; Sugai, H. Paint compositions containing polyolefins and an ionic liquid. Japan, 2006.

[83]   Buehler, G.; Zharkouskaya, A.; Feldmann, C. (2008) *Solid State Sciences*, 10: 461.

[84]   Doerr, N.; Kenesey, E.; Oetsch, C.; Ecker, A.; Pauschitz, A.; Franek, F. (2005) *Tribology and Interface Engineering Series*, 48: 123.

[85]   Evans, D.F. (1998) *The Colloidal Domain: Where Physics, Chemistry, Biology, and Technology Meet*; Wiley-VCH

[86]   Myers, D. (2005) *Surfactant Science and Technology*; John Wiley & Sons

[87]   Rosen, M.J. (2004) *Surfactants and Interfacial Phenomena*; Wiley & Sons

[88]   H. Mollet and A. Grubenmann; , s.E. (2000) *Formulation Technology: Emulsions, Suspensions, Solid Forms*; Wiley-VCH

[89]   Rosen, M.J. (1976) *Journal of Colloid and Interface Science*, 56: 320.

[90]   Tanford, C. (1980) *The Hydrophobic Effect: Formation of Micelles and Biological Membranes.*; Wiley

[91]   Evans, D.F. (1988) *Langmuir*, 4: 3.

[92]   Kronberg, B.; Costas, M.; Silveston, R.; . (1994) *Journal of Dispersion Science and Technology*, 15: 333.

[93]   Lindman, B.; Wennerstroem, H. (1980) *Topics in Current Chemistry*, 87: 1.

[94]   Klevens, H.B. (1953) *Journal of the American Oil Chemists' Society*, 30: 74.

[95]   Shinoda, K.; Nakagawa, T. (1963) *Colloidal Surfactants*: 129.

[96]   Shinoda, K.; Yamaguchi, N.; Carlsson, A. (1989) *The Journal of Physical Chemistry*, 93: 7216-7218.

[97]   Gu, T.; Sjöblom, J. (1992) *Colloids and Surfaces*, 64: 39-46.

[98]   Nilsson, F.; Soederman, O.; Johansson, I. (1997) *Langmuir* 13: 3349.

[99]   Collins, K.D. (2004) *Methods*, 34: 300-311.

[100]   Collins, K.D.; Neilson, G.W.; Enderby, J.E. (2007) *Biophysical Chemistry*, 128: 95-104.

[101]   Vlachy, N.; Jagoda-Cwiklik, B.; Vácha, R.; Touraud, D.; Jungwirth, P.; Kunz, W. (2009) *Advances in Colloid and Interface Science*, 146: 42-47.

[102]   Israelachvilli, J.N.; Mitchell, D.J.; Ninham, B.W. (1976) *Journal of the Chemical Society Faraday Transactions 2 Molecular and Chemical Physics*, 72: 1525.

[103]   Israelachvili, J.N. (1985) *Intermolecular and Surface Forces: With Applications to Colloidal and Biological Systems*; Academic Press

[104]   Tanford, C. (1972) *Journal of Physical Chemistry* 76: 3020.

[105]   Helfrich, W. (1973) *Z. Naturforschung*, 28c: 693.

[106]   Demus, B.; Goodbye, J.; Gray, G.W.; Spiess, H.W. (1998) *Handbook of liquid crystals*; Wiley-VCH: New York.

[107]   Klaus, A. Liquid crystals. Institute of Physical and Theoretical Chemistry, University of Regensburg, 2009.

[108]   Eicke, H.F. (1985) *Modern Trends of Colloidal Science in Chemistry and Biology.*; Birkhauser-Verlag

[109]   Holmes, M.C. (1988) *Current Opinion in Colloid & Interface Science*, 3: 485.

[110] Tiddy, G.J.T. (1980) *Phys. Rep.* , 57: 1.

[111] Winsor, P.A. (1968) *Chem. Rev.* , 68: 1.

[112] Seddon, J.M. (1990) *Biochim. Biophys. Acta*, 1: 1031.

[113] Clint, J.H. (1990) *Surfacactant Aggregation*; Blackie: Glasgow.

[114] Ramamoorthy, A. (2007) *Thermotropic Liquid Crystals - Recent Advances*; Springer

[115] Sakya, P.; Seddon, J.M.; Templer, R.H.; Mirkin, R.J.; Tiddy, G.J.T. (1997) *Langmuir*, 13: 3706.

[116] Gulik, A.; Delacroix, H.; Kischner, G.; Luzzati, V. (1995) *Journal de Physique II*, 5: 445.

[117] Seddon, J.M.; Bartle, E.A.; Mingins, J. (1990) *J. Phys: Condensed Matter*, 2: 285.

[118] Luzzati, V.; Spegt, P.A. (1967) *Nature*, 215: 701.

[119] Scriven, L.E. (1976) *Nature*, 263: 123.

[120] Baumgärtel, H.; Franck, E.U.; Grünbein, W. (1994) *Topics in Physical Chemistry - Liquid Crystals*; Springer: New York.

[121] Robinson, B.H. (2003) *Self assembly*; IOS Press: Amsterdam.

[122] Förster, G.; Meister, A.; Blume, A. (2001) *Current Opinion in Colloid & Interface Science*, 6: 294-302.

[123] Nelson, D.; Cox, M. (2001) *Lehninger Biochemie*; Springer

[124] Hargreaves, W.R.; Deamer, D.W. (1978) *Biochemistry*, 17: 3759.

[125] Schmölzer, S.; . Kinetik der Vesikelbildung in katanionischen Tensidsystemen. Universität Bayreuth: Bayreuth, 2003.

[126] Holmberg, K.; Jönsson, B.; Kronberg, B.; Lindman, B. (2003) *Surfactants and Polymers in aqueous solutions*; Wiley

[127] Baeckstroem, K.; Lindman, B.; Engstroem, S. (1988) *Langmuir*, 4: 872.

[128] Malmsten, M.; Lindman, B. (1989) *Langmuir*, 5: 1105.

[129] Raghavan, S.R.; Fritz, G.; Kaler, E.W. (2002) *Langmuir*, 18: 3797.

[130] Koehler, R.D.; Raghavan, S.R.; Kaler, E.W. (2000) *Journal of Physical Chemistry Biochemistry*, 104: 11035.

[131] Maurer, E.; Belloni, L.; Zemb, T.; Carrière, D. (2007) *Langmuir*, 23: 6554-6560.

[132] Dubois, M.; Zemb, T. (2000) *Current Opinion in Colloid & Interface Science*, 5: 27.

[133] Lozano, N.; Pinazo, A.; La Mesa, C.; Perez, L.; Andreozzi, P.; Pons, R. (2009) *The Journal of Physical Chemistry B*, 113: 6321-6327.

[134] Michina, Y.; Carrière, D.; Mariet, C.; Moskura, M.l.; Berthault, P.; Belloni, L.; Zemb, T. (2008) *Langmuir*, 25: 698-706.

[135] Kaler, E.W.; Murthy, A.K.; Rodriguez, B.E.; Zasadzinski, J. (1989) *Science*, 245: 1371.

[136] Kaler, E.; Herrington, K.L.; Murthy, A.K.; Zasadzinski, J. (1992) *J. Phys. Chem.*, 96: 6698.

[137] Herrington, K.L.; Kaler, E.W.; Miller, D.D.; Zasadzinski, J.A.; Chiruvolu, S. (1993) *J. Phys. Chem.*, 97: 13792.

[138] Kondo, Y.; Uchiyama, H.; Yoshino, N.; Nishiyama, K.; Abe, M. (1995) *Langmuir*, 1: 2380.

[139] Regev, O.; Khan, A. (1996) *J. Colloid Interface Sci.*, 182: 95.

[140] Yatcilla, M.T.; Herrington, K.L.; Brasher, L.L.; Kaler, E.W.; Chiruvolu, S.; Zasadzinski, J.A. (1996) *J. Phys. Chem.*, 100: 5874.

[141] Brasher, L.L.; Kaler, E.W. (1996) *Langmuir*, 12: 6270.

[142] Jokela, P.; Jonsson, B.; Khan, A. (1987) *J. Phys. Chem.*, 91: 3291.

[143] Fukuda, H.; Kawata, K.; Okuda, H.; Regen, S.L. (1990) *J. Am. Chem. Soc.*, 112: 1635.

[144] Jokela, P.; Joensson, B.; Eichmueller, B.; Fontell, K. (1988) *Langmuir*, 4: 187.

[145] Joensson, B.; Jokela, P.; Khan, A.; Lindman, B.; Sadaghiani, A. (1991) *Langmuir*, 7: 889.

[146] Khan, A. (1996) *Current Opinion in Colloid & Interface Science*, 1: 614.

[147] Horbaschek, K.; Hoffmann, H.; Hao, J. (2000) *Journal of Physical Chemistry B*, 104: 2781.

[148] Chen, L.; Xiao, J.-X.; Ruan, K.; Ma, J.-M. (2002) *Langmuir*, 18: 7250.

[149] Hao, J.; Liu, W.; Xu, G.; Zheng, L. (2003) *Langmuir*, 19: 10635.

[150] Bergstrom, M. (1996) *Langmuir*, 12: 2454.

[151] Yuet, P.K.; Blankschtein, D. (1996) *Langmuir*, 12: 3802.

[152] Safran, S.A.; MacKintosh, F.C.; Pincus, P.A.; Andelman, D.A. (1991) *Progr. Colloid Polym. Sci.*, 84: 3.

[153] Renoncourt, A. Study of supra-aggregates in catanionic surfactant systems. University of Regensburg: Regensburg, 2005.

[154] Chung, Y.C.; Lee, H.J.; Park, J.Y. (1998) *Bull. Korean Chem. Soc.*, 19: 1249.

[155] Bhattacharya, S.; De, S. (1999) *Langmuir*, 15: 3400.

[156] Blanzat, M.; Perez, E.; Rico-Lattes, I.; Lattes, A. (1999) *New J. Chem.*, 23: 1063.

[157] Dubois, M.; Lizunov, V.; Meister, A.; Gulik-Krzywicki, T.; Verbavatz, J.M.; Perez, E.; Zimmerberg, J.; Zemb, T. (2004) *PNAS*, 101: 15082.

[158] Song, A.; Dong, S.; Jia, X.; Hao, J.; Liu, W.; Liu, T. (2005) *Angewandte Chemie*, 117: 4086-4089.

[159] Dubois, M.; Gulik-Krzywicki, T.; Deme, B.; Zemb, T. (1998) *Comptes Rendus de l'Academie des Sciences, Serie IIc: Chimie*, 1: 567.

[160] Zemb, T.; Dubois, M.; Demé, B.; Gulik-Krzywicki, T. (1999) *Science*, 283: 816.

[161] Dubois, M.; Demé, B.; Gulik-Krzywicki, T.; Dedieu, J.C.; Vautrin, C.; Desert, S.; Perez, E.; Zemb, T. (2001) *Nature*, 411: 672.

[162] Zemb, T.; Carrière, D.; Glinel, K.; Hartman, M.; Meister, A.; Vautrin, C.; Delorme, N.; Fery, A.; Dubois, M. (2007) *Colloids and Surfaces A: Physicochemical and Engineering Aspects*, 303: 37-45.

[163] Marques, E.F.; Khan, A.; Miguel, M.G.; Lindman, B. (1993) *J. Phys. Chem.*, 97: 4729.

[164] Filipovic-Vincekovic, N.; Pucic, I.; Popovic, S.; Tomašic, V.; Tezak, D. (1997) *J. Colloid Interface Sci.*, 188: 396.

[165] Tomasic, V.; Popovic, S.; Filipovic-Vincekovic, N. (1999) *J. Colloid Interface Sci.*, 215: 280.

[166] Silva, B.F.B.; Marques, E.F. (2005) *J. Colloid Interface Sci.*, 290: 267.

[167] Small, D.M.; The Physical Chemistry of Lipids: New York, 1988.

[168] Zerbi, G.; Conti, G.; Minoni, G.; Pison, S.; Bigotto, A. (1987) *J. Phys. Chem.*, 91: 2386.

[169] Mizushima, H.; Fukasawa, J.; Suzuki, T. (1995) *Lipids*, 30: 327.

[170] Drummond, C.J.; Wells, D. (1998) *Colloids Surf. A*, 1998: 131.

[171] Crowley, K.J.; Forbes, R.T.; York, P.; Apperley, D.C.; H. Nyqvist; Camber, O. (2000) *J. Pharm. Sci.*, 89: 1286.

[172] Boyd, B.; Krodkiewska, I.; Drummond, J.; Grieser, F. (2002) *Langmuir*, 18: 597.

[173] Akanni, M.S.; Okoh, E.O.; Burrows, H.D.; Ellis, H.A. (1992) *Thermochim. Acta*, 208: 1.

[174] Marques, E.F.; Burrows, H.D.; Miguel, M.G. (1998) *J. Chem. Soc. Faraday Trans.*, 94: 1729.

[175] Mathevet, F.; Masson, P.; Nicoud, J.F.; Skoulios, A. (2002) *Chem. Eur. J.*: 2248.

[176] Wunderlich, B. (1999) *Thermochim. Acta*, 340: 37.

[177] Goltner, C.G.; Antonietti, M. (1997) *Advanced Materials*, 9: 431.

[178] McKelvey, C.A.; Kaler, E.W.; Zasadzinski, J.A.; Coldren, B.; Jung, H.-T. (2000) *Langmuir*, 16: 8285.

[179] Hentze, H.; Raghavan, S.R.; McKelvey, C.A.; Kaler, E.W. (2003) *Langmuir*, 19: 1069.

[180]   Carrière, D.; Michina, Y.; Kopetzki, D. Catanionic vesicles, process for preparing same and applications thereof. alternatives, C.a.l.e.a.e.a.e., Ed.: France, 2010.

[181]   Rosa, M.; Miguel, M.d.G.; Lindman, B. (2007) *Journal of Colloid and Interface Science*, 312: 87-97.

[182]   Tondre, C.; Caillet, C. (2001) *Advances in Colloid and Interface Science*, 931: 115.

[183]   Bauer, K.; Frömming, K.-H.; Führer, C. (1991) *Pharmazeutische Technologie.*; Georg Thieme Verlag

[184]   Kennah, E.; Hignet, H.S.; Laux, P.E.; Dorko, J.D.; Barrow, C.S. (1989) *Fundam. Appl. Toxicol.*, 12: 258.

[185]   Swanston, D.W. (1985) *Food. Chem. Toxicol.*, 23: 169.

[186]   Grant, R.L.; Yao, C.; Gabaldon, D.; Acosta, D. (1992) *Toxicol. Pathol.*, 76: 153.

[187]   Jiang, T.; Acosta, D. (1993) *Fund. Appl. Toxicol. Pathol.*, 20: 486.

[188]   Künstler, K. (1988) *Alternative Methoden in der Industrie am Beispiel der Haut- und Schleimhautverträglichkeitsprüfung*; Gustav Fischer Verlag

[189]   Loprieno, N.; Boncristiani, G.; Bosco, E.; Nieri, M.; Loprieno, G. (1994) 22: 82.

[190]   Osborne, R.; Perkins, M.A. (1994) *Food Chem. Toxicol.*, 32: 133.

[191]   Renzi, D.; Valtolina, M.; Forster, R. (1993) *ATLA*, 21: 89.

[192]   Yamashoji, S. (1996) *Anal. Biochem.*, 240: 310.

[193]   Babich, H.; Babich, J.P. (1997) *Toxicol. Lett.*, 91: 189.

[194]   Bigliardi, P.; Herron, M.J.; Nelson, R.D.; Dahl, M.V. (1994) *Exp. Dermatol.*, 3: 89.

[195]   Pels, E.; Nuyts, R.; Breebaart, A.C.; Hartmann, C. (1993) *Cornea*, 12: 289.

[196]   Groth, T.; Falck, P.; Miethke, R.-R. (1995) *ATLA*, 23: 790.

[197]   Pham, X.T.; Huff, J.W. (1999) *CLAO J.* , 25: 28.

[198]   Barile, F.A.; Dierickx, P.J.; Kristen, U. (1994) *Cell Biol. Toxicol.*, 10: 155.

[199]   Buche, P.; Violin, L.; Girard, P. (1994) *Cell Biol. Toxicol.*, 10: 381.

[200]   Bettley, F.R. (1968) *Br. J. Derm.*, 80: 635.

[201]   Macian, M.; Seguer, J.; Infante, M.R.; Selve, C.; Vinardell, M.P. (1996) *Toxicology* 106: 1.

[202]   Goldberg, A. (1991) *Alternative Methods in Toxicology: In Vitro Toxicol.*; Mary Ann Liebert

[203]   Gueniche, A.; Ponec, M. (1993) *Toxicol. in Vitro*, 7: 15.

[204]   Maurer, J.K.; Parker, R.D.; Carr, G.J. (1998) *Toxicol. Pathol.* , 26: 226.

[205]   Herzinger, T.; Korting, H.C. (1991) *Dermatosen*, 39: 117.

[206]   Schwarz, L.R. (1996) *Toxikologie - Cytotoxizität*

Weinheim: VCH Verlagsgesellschaft GmbH

[207]   Rockstroh, T.; Zapf, K. (1967) *Naturwissenschaften*, 54: 568.

[208]   Partearroyo, M.A.; Ostolaza, H.; Goni, F.M.; Barbera-Guillem, E. (1990) *Biochem. Pharmacol.*, 40: 1323.

[209]   Gloxhuber, C. (1974) *Arch. Toxicol.* , 32: 245.

[210]   Helenius, A.; Simons, K. (1975) *Biochim. Biophys. Acta*, 415: 29.

[211]   Yang, W.; Acosta, D. (1995) *In Vitro Cell. Dev. Biol. – Animal*, 31: 499.

[212]   Borner, M.M.; Schneider, E.; Pirnia, F.; Sartor, O.; Trepel, J.B.; Myers, C.E. (1994) *FEBS Lett.* , 353: 129.

[213]   Bloom, E.; Sznitowaska, M.; Polansky, J.; Ma, Z.; Maibach, H.I. (1994) *Dermatology*, 188: 263.

[214]   Csúcs, G.; Ramsden, J.J. (1998) *Biochimica et Biophysica Acta*, 1369: 304.

[215]   De la Maza, A.; Parra, J.L. (1996) *Arch. Biochem. Biophys.*, 329: 1.

[216]   Rosen, M.J.; Fei, L.; Morrall, S.W. (1999) *J. Surfactants Detgts.* , 2: 343.

[217]   Rosen, M.J.; Fei, L.; Morrall, S.W.; Versteeg, D.J. (2001) *Environ. Sci. Technol.*, 35: 54.

[218]   Scott Hall, W.; Patoczka, J.B.; Mirenda, R.J.; Porter, B.A.; Miller, E. (1989) *Arch Environ Contam Toxicol*, 18: 765.

[219]   Wildish, D.J. (1974) *Wat Res*, 8: 433.

[220]   Dominguez, J.G.; Balaguer, F.; Parra, J.L.; Pelejero, C.M. (1981) *Int. J. Cosmet. Sci.* , 3: 57.

[221]   Lomax, E. (1993) *Speciality Chemicals*, 13: 223.

[222]   Jelinek, A. In-vitro-Toxizität grenzflächenaktiver Substanzen: Wirk,ung auf Zellmembran, mitochondriale Funktion und Apoptose. Martin-Luther-Universität Halle Wittenberg: Halle, 2001.

[223]   Hall-Manning, T.J.; Holland, G.H.; Rennie, G.; Revell, P.; Hines, J.; Barratt, M.D.; Basketter, D.A. (1998) *Food Chem. Toxicol.* , 36: 233.

[224]   Prottey, C.; Ferguson, T. (1975) *J. Soc. Cosmet. Chem.*, 26: 29.

[225]   Brenner-Henaff, C.; Valdor, J.F.; Plusquellec, D.; Wroblewski, H. (1993) *Anal Biochem* 212: 117.

[226]   Shao, Z.; Li, Y.; Krishnamoorthy, R.; Chermak, T.; Mitra, A.K. (1993) *Pharm Res*, 10: 243.

[227]   Knepper, T.P.; Barcelo, D.; Voogt, P.D. (2003) *Analysis and fate of surfactants in the aquatic environment*; Elsevier Science B.V.

[228]   Cserhati, T. (1995) *Environmental Health Perspectives*, 103: 358.

[229]   Jakobi, G.; Löhr, A. Detergent ingredients. In Ullmann's encyclopedia of industrial chemistry; Gerhartz, W., Ed.; VCH: Weinheim, 1987.

[230]   Schulze, K. (1996) *Tenside Surfactants Deterg.* , 33: 94.

[231]   Swisher, R.D. (1987) *Surfactant biodegradation*; Marcel Dekker: New York.

[232]   Schöberl, P. (1989) *Tenside Surfactants Deterg.* , 26: 86.

[233]   Ratledge, C. (1994) *Biochemistry of microbial degradation*; Kluwer: Dordrecht.

[234]   Schramm, L.L. (2005) *Emulsions, Foams, and Suspensions - Fundamentals and Applications*; Wiley-VCH

[235]   Müller-Goymann, C. (1991) *Emulsionen und Microemulsionen, Hager´s Handbuch der Pharmazeutischen Praxis*; Springer Verlag: Heidelberg.

[236]   Müller-Goymann, C. (1984) *Seifen-Öle-Fette-Wachse*, 110: 395.

[237]   (1972) *Manuals of symbols and Terminology for Physicochemical Quantities and Units, Appendix II, Part I*; IUPAC (International Union for Pure and Applied Chemistry) division of physical Chemistry

[238]   Bancroft, W.D. (1913) *J. Phys. Chem.*, 17: 501.

[239]   Bancroft, W.D. (1915) *J. Phys. Chem.*, 19: 275.

[240]   Rincker, R. (1980) *Physikalische Grundlagen zur Stabilisierung von Cremes und Emulsionen, Entwicklung von Emulsionen und Cremes*; APV: Mainz.

[241]   Salager, J.-L. (2000) *Emulsion properties and related Know-how - Pharmaceutical Emulsions and Suspensions*; Marcel Dekker: New York.

[242]   Griffin, W.C. (1949) *J. Soc. Cosmet. Chem.*, 1: 311.

[243]   Griffin, W.C. (1954) 5: 249.

[244]   Davies, J.T.; Rideal, E.K. (1963) *Interfacial Phenomena*; Academic: New York-San Francisco-London.

[245]   Davies, J.T. (1964) *Progress in Surface Science*; Academic: New York.

[246]   Shinoda, K.; Arai, H. (1964) *J. Phys. Chem.*, 68: 3485.

[247]   Aveyard, R.; Binks, B.P.; Clint, J.H. (2003) *Advances in Colloid Interface Sci.*, 100-102: 503.

[248]   Friberg, S. (1971) *J. Colloid Interface Sci.* , 37.

[249] Melzer, E. Herstellung und physikochemische Charakterisierung von w/o Emulsionen unter Verwendung von Ethylcellulose als nichtionischer Polymeremulgator. University of Braunschweig, 2000.

[250] May-Alert, G.; List, P. (1986) *Pharmazie in unserer Zeit* 15: 1.

[251] Schwuger, M.J. (1971) *Kolloid-Z. und Z. Polymere*, 243: 129.

[252] Sacanna, S.; Kegel, W.K.; Philipse, A.P. (2007) *Physical Review Letters*, 98: 1.

[253] Wang, J.; Yang, F.; Tan, J.; Liu, G.; Xu, J.; Sun, D. (2009) *Langmuir*, 26: 5397-5404.

[254] Amalvy, J.I.; Armes, S.P.; Binks, B.P.; Rodrigues, J.A.; Unali, G.-F. (2003) *Chemical Communications*: 1826-1827.

[255] Binks, B.P.; Lumsdon, S.O. (2001) *Langmuir*, 17: 4540-4547.

[256] Wang, S.; He, Y.; Zou, Y. (2010) *Particuology*, 8: 390-393.

[257] (2007) *Optical imaging and microscopy - Techniques and advanced systems*; Springer: Berlin.

[258] Rosevear, F.B. (1968) *J. Soc. Cosmetic Chemists*, 19: 581.

[259] Dunmur, D.A. (2002) *Liquid Crystals Fundamentals*; World Scientific

[260] Clarke, A.R.; Eberhardt, C.N. (2002) *Microscopy Techniques for Materials Science*; CRC

[261] Stegemeyer, H. (1994) *Liquid Crystals*; Steinkopff Springer: Darmstadt New York.

[262] Scharf, T. (2007) *Polarized Light in Liquid Crystals and Polymers*; Wiley-Interscience

[263] Dierking, I. (2003) *Textures of Liquid Crystals*. Wiley-VCH.

[264] Blinov, L.M. (2011) *Structure and Properties of Liquid Crystals*; Springer

[265] Kumar, S. (2001) *Liquid Crystals - Experimental Study of Physical Properties and Phase Transitions*; Cambridge

[266] Khoo, I.C. (1995) *Liquid Crystals Physical Properties and Nonlinear Optical Phenomena*; Wiley: New York.

[267] Chandrasekhar, S. (1977) *Liquid Crystals*; Cambridge

[268] Demus, D. (1999) *Physical properties of liquid Crystals*; Wiley

[269] Atkins, P.W. (1996) *Physikalische Chemie*; VCH

[270] Newnham, R.E. (2005) *Properties of materials - anisotropy, symmetry, structure*; Oxford

[271] Nelson, S.A. Uniaxial Ninerals, Uniaxial Indicatrix, Optic Sign & Ray Path. Tulane University, 2010.

[272] Abramowitz, M.; Davidson, M.W. Microscopy Resource Centre. Olympus America Inc., 2010.

[273] Murphy, D.B. (2001) *Fundamentals of Light Microscopy and Electronic Imaging*; John Wiley & Sons, Inc.

[274] Stoiber, R.E.; Morse, S.A. (1994) *Crystal Identification with the Polarizing Microscope*; Chapman & Hall

[275] Goodby, J.W. Liquid Crystal Phase Transitions - Differential Scanning Calorimetry and Optical Microscopy. The York Liquid Crystal Group.

[276] esa. Impress - Supporting Education Across Europe. www.spaceflight.esa.int.

[277] Kelly, A.; Groves, G.W.; Kidd, P. (2000) *Crystallography and Crystal Defects*; Wiley

[278] Lawrence, A.S.C. (1969) *Molecular Crystals and Liquid Crystals*, 7: 1.

[279] Pinnock, C.; Lin, T.; Smith, T. (2003) *Fundamentals of Anaesthesia*; GMM

[280] Aitkenhead, A.R.; Smith, G.; Rowbotham, D.J. (2007) *Textbook of Anaesthesia*; Elsevier

[281] Bueger, A.; Wachter, H. (1993) *Hunnius´ pharmazeutisches Wörterbuch,*; Walter de Gruyter: New York.

[282] Powell, M.F. (1987) *Pharm. Res*, 4: 42.

[283] Butterworth, J.F. (1990) *Anaesthesiology*, 72: 711.

[284] Strichartz, G.R.; Sanchez, V.; Arthur, G.R.; Chafetz, R.; Martin, D. (1990) *Anaesth Analg*, 71: 158.

[285] Arias, H.R. (1999) *Neurosci. Biobehav. R.*, 23: 817.

[286] Steinhaus, J.E. (1969) *Acta Anaesthesiol. Scand.*, Supplementum XXXVI: 71.

[287] Kubo, K.; Mayumi, T. (1998) *Fragrance Journal*, 9: 71.

[288] Mohammadi-Samani, S.; Jamshizadeh, A.; Montaseri, H.; Rangbar-Zahedani, M.; Kianrad, R. (2010) *Pak. J. Pharm. Sci*, 23: 83.

[289] Fang, L. (2002) *Biol. Pharm. Bull.*, 25: 1339.

[290] Jun, H.; Kang; Lisheng. Enhanced transdermal anesthesia of local anesthetic agents. The University of Georgia Research Foundation: USA, 1999.

[291] Müller, M.; Mackeben, S.; Müller-Goymann, C.C. (2004) *Int. J. Pharm.* , 274: 139.

[292] Müller, M. Liposomale Verkapselung von Lidocain-HCl und Prilocain-HCl zur intravenösen Anwendung. In Fakultät für Lebenswissenschaften; Carolo-Wilhelmina Universität: Braunschweig, 2008.

[293] Yamaguchi, T.; Kawai, K.; Yamanaka, K.; Tatsumi, N. External Preparation composition comprising fatty acid-based ionic liquid as active ingredient. Medrx 2009.

[294] Olofsson, G. (1984) *The Journal of Chemical Thermodynamics*, 16: 39-44.

[295] Kanicky, J.R.; Shah, D.O. (2003) *Langmuir*, 19: 2034.

[296] Kanicky, J.R.; Shah, D.O. (2002) *Journal of Colloid and Interface Science*, 256: 201.

[297] Kanicky, J.R.; Poniatowski, A.F.; Mehta, N.R.; Shah, D.O. (2000) *Langmuir*, 16: 172.

[298] Angell, C.A.; Byrne, N.; Belieres, J.-P. (2007) *Accounts of Chemical Research*, 40: 1228-1236.

[299] Eckert, T.; Müller, J. (1978) *Arch. Pharm.*, 311: 31.

[300] Laughlin, R.G. (1994) *The Aqueous Phase Behavior of Surfactants*; Academic Press: San Diego.

[301] Wang, K.; Yin, H.; Sha, W.; Huang, J.; Fu, H. (2007) *J. Phys. Chem. B*, 111: 12997.

[302] Klaus, A.; Tiddy, G.J.T.; Touraud, D.; Schramm, A.; Stühler, G.; Drechsler, M.; Kunz, W. (2009) *Langmuir*, 26: 5435-5443.

[303] Klein, R.; Touraud, D.; Kunz, W. (2008) *Green Chemistry*, 10: 433.

[304] McBain, J.W.; Lee, W.W. (1943) *Oil Soap*, 20: 17.

[305] Madelmont, C.; Perron, R. (1976) *Colloid Polym. Sci.*, 254: 581.

[306] Lin, B.; McCormick, A.V.; Davis, H.T.; Strey, R. (2005) *J. Colloid Interface Sci.*, 291: 543.

[307] Shinoda, K.; Kunieda, H. (1976) *J. Phys. Chem.*, 80: 2468.

[308] Jansson, M.; Joensson, A.; Li, P.; Stilbs, P. (1991) *Colloids Surf.*, 59: 387.

[309] McBain, J.W.; Sierichs, W.C. (1948) *J. Am Oil Chem. Soc.*, 25: 221.

[310] Kunz, W. (2010) *Specific Ion Effects*; World Scientific Publishing

[311] Ninham, B.W.; Persegian, V.A. (1971) *J. Theor. Biol.*, 31: 405.

[312] Sadler, P.J.; Thompson, H.M.; Maslowski, P.; Liddle, A.; Rowbotham, D.J. (1999) *Br. J. Anaesth.*, 82: 432.

[313] Picard, P.; Tramer, M.R. (2000) *Anesth. Analg.*, 90: 263.

[314] Nathanson, M.H.; Gajraj, N.M.; Rusell, J.A. (1996) *Anesth. Analg.*, 82: 469.

[315] Gajraj, N.M.; Nathanson, M.H. (1996) *J. Clin. Anesth.* , 8: 575.

[316] Kaufke, S.; Krauel, K. (2000) *Krankenhauspharmazie*, 21: 284.

[317] Marsh, K.N.; Boxall, J.A.; Lichtenthaler, R. (2004) *Fluid Phase Equilibria*, 219: 93-98.

[318] Bicak, N. (2005) *J. Mol. Liq.*, 116: 15.

[319] Iglesias, M.; Torres, A.; Gonzalez-Olmos, R.; Salvatierra, D. (2008) *J. Chem. Thermodyn.*, 40: 119.

[320] Alvarez, V.H.; Mattedi, S.; Martin-Pastor, M.; Aznar, M.; Iglesias, M. (2010) *Fluid Phase Equilibria*, 299: 42.

[321] Kunz, W.; Thomaier, S.; Maurer, E.; Zech, O.; Kellermeier, M.; Klein, R. Onium salts of carboxyalkyl-terminated polyoxyalkylenes for use as high-polar solvents and electrolytes. 2008.

[322] Zech, O.; Hunger, J.; Sangoro, J.R.; Iacob, C.; Kremer, F.; Kunz, W.; Buchner, R. (2010) *Physical Chemistry Chemical Physics*, 12: 14341-14350.

[323] Meijer, H. (1995) *Anionic surfactants*; Marcel Dekker

[324] Denzer, H. Compositions comprising hydrophobic silicone oils and alkyl ether carboxylates. Kao Chemicals Europe, 2000.

[325] Meijer, H. (1990) *SÖFW*, 116: 251.

[326] Denzer, H.; Michaelsen, M.; Meijer, H.; Abe, H. Foam-enhancing agent for surfactant mixtures. Kao Chemicals GmbH, 2004.

[327] Felletschin, G. (1964) *Journal of the Society of Cosmetic Chemists*, 15: 245.

[328] Aalbers, J.G. (1966) *Lauryl(Poly-1-Oxapropen)OxaäthanCarbonsäuren*; Drukkerij Wed. G. van Soest: Amsterdam.

[329] Vlachy, N.; Merle, C.; Touraud, D.; Schmidt, J.; Talmon, Y.; Heilmann, J.; Kunz, W. (2008) *Langmuir*, 24: 9983-9988.

[330] Marques, E.F.; Brito, R.O.; Wang, Y.; Silva, B.F.B. (2006) *Journal of Colloid and Interface Science*, 294: 240.

[331] Vautrin, C.; Dubois, M.; Zemb, T.; Schmölzer, S.; Hoffmann, H.; Gradzielski, M. (2003) *Colloids and Surfaces A: Physicochem. Eng. Aspects*, 217: 165.

[332] Marques, E.; Khan, A.; Lindman, B. (2002) *Thermocimica Acta*, 394: 31.

[333] Vautrin, C.; Zemb, T.; Schneider, M.; Tanaka, M. (2004) *The Journal of Physical Chemistry B*, 108: 7986-7991.

[334] Shen, Y.; Hao, J.; Hoffmann, H.; Wu, Z. (2008) *Soft Matter*, 4: 805-810.

[335] Li, H.; Wieczorek, S.A.; Xin, X.; Kalwarczyk, T.; Ziebacz, N.; Szymborski, T.; Hołyst, R.; Hao, J.; Gorecka, E.; Pociecha, D. (2009) *Langmuir*, 26: 34-40.

[336] Fredlake, C.P.; Crosthwaite, J.M.; Hert, D.G.; Aki, S.N.V.K.; Brennecke, J.F. (2004) *J. Chem. Eng. Data* 49.

[337] Fukaya, Y.; Iizuka, Y.; Sekikawa, K.; Ohno, H. (2007) *Green Chem.*, 9: 1155.

[338] Xu, W.; Cooper, E.I.; Angell, C.A. (2003) *J. Phys. Chem. B*, 107: 6170.

[339] Zhou, Z.; Matsumoto, H.; Tatsumi, K. (2005) *Chem. Eur. J.*, 11: 752.

[340] Klein, R.; Dutton, H.; Diat, O.; Tiddy, G.J.T.; Kunz, W. *in preparation*.

[341] Jiang, Y.-Y.; Wang, G.-N.; Zhou, Z.; Wu, Y.-T.; Geng, J.; Zhang, Z.-B. (2008) *Chem. Commun.*: 505.

[342] Zech, O.; Kellermeier, M.; Thomaier, S.; Maurer, E.; Klein, R.; Schreiner, C.; Kunz, W. (2009) *Chem. Eur. J.*, 15: 1341.

[343] Crosthwaite, J.M.; Muldoon, M.J.; Dixon, J.K.; Anderson, J.L.; Brennecke, J.F. (2005) *J. Chem. Thermodyn.*

[344] Crosthwaite, J.M.; Muldoon, M.J.; Dixon, J.K.; Anderson, J.L.; Brennecke, J.F. (2005) *J. Chem. Thermodyn.*: 559.

[345] Ge, R.; Hardacre, C.; jacquemin, J.; Nancarrow, P.; Rooney, D.W. (2008) *J. Chem. Eng. Data*, 53: 2148.

[346] Garcı´a-Miaja, G.; Troncoso, J.; Romanı´, L. (2007) *J. Chem. Eng. Data*, 52: 2261.

[347] Jacquemin, J.; Ge, R.; Nancarrow, P.; Rooney, D.W.; CostaGomes, M.F.; Padua, A.A.H.; Hardacre, C. (2008) *J. Chem. Eng. Data*, 53: 716.

[348] Liu, W.; Cheng, L.; Zhang, Y.; H.Wang; Yu, M. (2008) *J. Mol. Liq.*, 140: 68.

[349] Vila, J.; Ginés, P.; Rilo, E.; Cabeza, O.; Varela, L.M. (2006) *Fluid Phase Equil.*, 247.

[350] Cuadrado-Prado, S.; Dominguez-Perez, M.; Rilo, E.; Garcia-Garabal, S.; Segade, L.; Franjo, C.; Cabeza, O. (2009) *Fluid Phase Equil.*, 278: 36.

[351] Ikeda, S.; Ozeki, S.; Tsunoda, M.-A. (1980) *Journal of Colloid and Interface Science*, 73: 27-37.

[352] Klein, R.; Touraud, D.; Kunz, W. (2008) *Green Chemistry*, 10: 433-435.

[353] Eastoe, J.; Rogueda, P.; Shariatmadari, D.; Heenan, R. (1996) *Colloids and Surfaces A: Physicochemical and Engineering Aspects*, 117: 215-225.

[354] Warr, G.G.; Zemb, T.N.; Drifford, M. (1990) *J. Phys. Chem.*, 94: 3086.

[355] Zana, R.; Benrraou, M.; Bales, B.L. (2004) *J. Phys. Chem. B*, 108: 18195.

[356] (2011) *Specification Triethanolamine Calbiochem*; Merck

[357] Currier, S.; Mautner, H. (1974) *Proc. Nat. Acad. Sci. USA*, 71: 3355.

[358] OECS. (2001) *SIDS Initial Assessment Report - N,N-Dimethyldodecylamine*; UNEP Publications: Orlando.

[359] Bradley, A.E.; Hardacre, C.; Holbrey, J.D.; Johnston, S.; McMath, S.E.J.; Nieuwenhuyzen, M. (2002) *Chem. Mater.*, 14: 629.

[360] Firestone, M.A.; Dzielawa, J.A.; Zapol, P.; Curtiss, L.A.; Seifert, S.; Dietz, M.L. (2002) *Langmuir*, 18: 7258.

[361] Goodchild, I.; Collier, L.; Millar, S.L.; Prokeš, I.; Lord, J.C.D.; Butts, C.P.; Bowers, J.; Webster, J.R.P.; Heenan, R.K. (2007) *J. Colloid Interf. Sci.*, 307: 455.

[362] Singh, T.; Kumar, A. (2007) *J. Phys. Chem. B*, 111: 7843.

[363] Jastorff, B.; Stoermann, R.; Ranke, J. (2007) *Clean: Soil, Air, Water*, 35: 399.

[364] Stock, F.; Hoffmann, J.; Ranke, J.; Stoermann, R.; Ondruschka, B.; Jastorff, B. (2004) *Green Chem*, 6: 286.

[365] Stolte; Arning, J.; Bottin-Weber, U.; Matzke, M.; Stock, F.; Thiele, K.; Uerdingen, M.; Welz-Biermann, U.; Jastorff, B.; Ranke, J. (2006) *Green Chem*, 8: 621.

[366] Klein, R.; Zech, O.; Maurer, E.; Kellermeier, M.; Kunz, W. (2011) *submitted*.

[367] Barthel, J.; Wachter, R.; Gores, H.J. (1979) *Mod. Aspects Electrochem.* , 13: 1.

[368] Barthel, J.; Feuerlein, F.; Neueder, R.; Wachter, R.J. (1980) *Solution Chem.* , 9: 209.

[369] Mosmann, T. (1983) *J Immunol Methods*, 65: 55.

[370] Vlachy, N.; Touraud, D.; Heilmann, J.; Kunz, W. (2009) *Colloids and Surfaces B: Biointerfaces*, 70: 278-280.

[371] Mirgorodskaya, A.; Kudryavtseva, L.; Zakharova, L.; Bel'skii, V. (1998) *Russian Chemical Bulletin*, 47: 1296-1301.

[372] Tomasic, V.; Tsek-Bozic, L.; Visnjevac, A.; Kojic-Prodic, B.; Filipovic-Vincekovic, N. (2000) *J. Coll. Interface Sci.*, 277: 427.

[373] Busico, V.; Castaldo, D.; Vacatello, M. (1981) *Molecular Crystals and Liquid Crystals*, 78: 221 - 226.

[374] Rademeyer, M.; Kruger, G.; Billing, D. (2009) *Cryst. Eng. Comm.*, 11: 1926.

[375] Kong, Y.-X.; Di, Y.-Y.; Zhang, Y.-Q.; Yang, W.-W.; Tan, Z.-C. (2009) *Int. J. Thermophys.*, 30: 1960.

[376] Grandjean, A.; Malki, M.; Simonnet, C.; Manara, D.; Penelon, B., 75. (2007) *Phys. Rev. B: Condens. Matter Mater. Phys.*, 75: 054112/054111-054112/054117.

[377] Zhang, S.; Sun, N.; He, X.; Lu, X.; Zhang, X. (2006) *J. Phys. Chem. Ref. Data*, 35.

[378] Sugihara, G.; Arakawa, Y.; Tanaka, K.; Lee, S.; Moroi, Y. (1995) *J. Coll. Interface Sci.*, 170: 399.

[379] Kale, K.; Zana, R. (1976) *J. Coll. Interface Sci.*, 61: 312.

[380] Evans, D.; Ninham, B. (1963) *J. Phys. Chem.*, 87: 5025.

[381] Evans, H. (1956) *J. Chem. Soc.*: 579.

[382] Skoulios, A.; Luzzati, V. (1959) *Nature*, 183: 1310.

[383] Karlsson, S.; Friman, R.; Björkqvist, M.; Lindström, B.; Backlund, S. (2001) *Langmuir*, 17: 3573.

[384] EC No 684/2004. European Parliament Regulation (EC) No 648/2004 of the European Parliament and of the Council of 31 March 2004 on detergents 2004.

[385] Liang, C.H.; Chou, T.H. (2009) *Chemistry and Physics of Lipids*, 158: 81.

[386] Garcia-Lorenzo, A.; Tojo, E.; Tojo, J.; Teijeira, M.; Rodriguez-Berrocal, F.J.; Gonzalez, M.P.; Martinez-Zorzano, V.S. (2008) *Green Chemistry*, 10: 508-516.

[387] Karanth, H.; Murthy, R.S.R. (2007) *J. Pharm. Pharmacol.*, 59: 469.

[388] Lasic, D.D. (1993) *Liposomes: from Physics to Applications*; Elsevier: Amsterdam.

[389] Floch, V.; Bolch, G.L.; Gable-Guillaume, C.; Bris, N.L.; Yaouanc, J.J.; H. des Abbayes; Ferec, C.; Clement, J.C. (1998) *Eur. J. Med. Chem.*, 33: 923.

[390] Rosa, M.; Moran, M.d.C.; Miguel, M.d.G.; Lindman, B. (2007) *Colloids and Surfaces A: Physicochem. Eng. Aspects*, 301: 361.

[391] Borges, M.; Messeder, J.C.; Figueroa-Villar, J.D. (2004) *Eur. J. Med. Chem.* , 39: 925.

[392] D.D. Lasic; R. Joannic; B.C. Keller; P.M. Frederik; Auvray, L. (2001) *Adv. Colloid Interface Sci.* , 89-90: 337.

[393] E.F.Marques; Regev, O.; Khan, A.; Miguel, M.d.G.; Lindman, B. (1998) *J. Phys. Chem. B*, 102: 6746.

[394] Boudiera, A.; Castagnosa, P.; Soussana, E.; Beauneb, G.; Belkhelfac, H.; Ménagerb, C.; Cabuilb, V.; Haddiouic, L.; Roquesd, C.; Rico-Lattesa, I.; Blanzat, M. (2011) *Int. J. Pharm.*, 403: 230.

[395] Consola, S.; Blanzat, M.; Perez, E.; Garrigues, J.-C.; Bordat, P.; Rico-Lattes, I. (2007) *Chem. Eur. J.*, 13: 3039.

[396] Boudier, A.; Castagnos, P.; Soussan, E.; Beaune, G.; Belkhelf, H.; Ménager, C.; Cabuil, V.; Haddioui, L.; Roques, C.; Rico-Lattes, I.; Blanzat, M. (2011) *Int. J. Pharm.*, 403: 230.

[397] Kuo, J.-H.S.; Jan, M.-S.; Chang, C.-H.; Chiu, H.-W.; Li, C.-T. (2005) *Colloids and Surfaces B: Biointerfaces*, 41: 189.

[398] Brito, R.O.; Marques, E.F.; Silva, S.G.; Vale, M.L.d.; Gomes, P.; Araújo, M.J.; Rodriguez-Borges, J.E.; Infante, M.R.; Garcia, M.T.; Ribosa, I.; Vinardell, M.P.; Mitjansc, M. (2009) *Colloids and Surfaces B: Biointerfaces*, 72: 80.

[399] Weihs, D.; Danino, D.; Pinazo-Gassol, A.; Perez, L.; Franses, E.; Talmon, Y. (2005) *Colloids Surf. A: Physicochem. Eng. Asp.* , 255: 73.

[400] Goursaud, F.; Berchel, M.; Guilbot, J.; Legros, N.; Lemiegre, L.; Marcilloux, J.; Plusquelleca, D.; Benvegnu, T. (2008) *Green Chem*, 10: 310.

[401] Tehrani-Bagha, A.; Oskarsson, H.; Ginkel, C.v.; Holmberg, K. (2007) *Journal of Colloid and Interface Science*, 312: 444.

[402] Tehrani-Bagha, A.R.; Holmberg, K. (2010) *Langmuir*, 26: 9276-9282.

[403] Lippet, K.; Galinski, E. (1991) *Appl Microbiol Biotechnol*, 37: 61.

[404] Howard, M.; Rudolph, T.; Pitner, W. Salts comprising a pyrimidine carboxylic acid derivative for cosmetic use. Merck Patant GmbH, 2010.

[405] Tanaka, M.; . US, 1992.

[406] Storzer, U.; Glauner, U. Verfahren zur Acylierung von Cholinchlorid; Fettsäurecholinsalze und deren Verwendung. Schill + Seilacher Aktiengesellschaft: Germany, 2007.

[407] Huibers, P.D.T. (1999) *Langmuir* 15: 7546.

[408] Berr, S.; Jones, R.R.M.; Johnson, J.S. (1992) *J. Phys. Chem.*, 96: 5611.

[409] Mandru, I. (1972) *Journal of Colloid and Interface Science*, 41: 430-436.

[410] Roelants, E.; De Schryver, F.C. (1987) *Langmuir*, 3: 209-214.

[411] Mata, J.; Varade, D.; Bahadur, P. (2005) *Thermochim. Acta*, 428: 147.

[412] Suenobu, K.; Nagaoka, M.; Yamabe, T.; Nagata, S. (1998) *The Journal of Physical Chemistry A*, 102: 7505-7511.

[413] La Mesa, C.; Ranieri, G.A.; Terenzi, M. (1988) *Thermochimica Acta*, 137: 143-150.

[414] Appell, J.; Porte, G. (1983) *J. Phys. Lett.* , 44: 689.

[415] Jung, H.T.; Lee, S.Y.; Kalter, E.W.; Coldren, B.; Zasadzinski, J.A. (2002) *PNAS*, 99: 15318.

[416] Safran, S.A. (1994) *Statistical Thermodynamics of Surfaces, Interfaces, and Membranes*; Addison–Wesley

[417] Dubois, M.; Zemb, T. (2000) *Current Opinion in Colloid & Interface Science*, 5.

[418] Heimburg, T. (2000) *Biophysical journal*, 78: 1154.

[419] Merrettig-Bruns, U.; Jelen, E. (2009) *Materials*, 2: 181.

[420] Hillaireau, H.; Couvreur, P. (2009) *Cell. Mol. Life Sci.*, 66: 2873.

[421] Binks, B.P.; Clint, J.H. (2002) *Langmuir* 18: 1073.

[422] Binks, B.P. (2002) *Curr. Opin. Colloid Interface Sci.* , 7: 21.

[423]   Tarmala, S.; Dai, L.L. (2004) *Langmuir*, 20: 3492.

[424]   Sadaghiani, A.S.; Khan, A. (1991) *Journal of Colloid and Interface Science*, 146: 69.

[425]   Silva, B.F.B.; Marques, E.F.; Olsson, U.; Linse, P. (2009) *J. Phys. Chem. B*, 113: 10230.

[426]   Schelero, N. Catanionics for stabilisation of emulsions. In Faculty IV; University of Regensburg: Regensburg, 2006.

[427]   Brandenburg, K.; Seydel, U. (1990) *Eur. J. Biochem.*, 191: 229.

[428]   Schneider, M.; Marsh, D.; Jahn, W.; Kloesgen, B.; Heimburg, T. (1999) *PNAS*, 96: 25.

[429]   Casal, H.; McElhany, R. (1990) *Biochemistry*, 29: 5423.

[430]   Wang, Y.; Marques, E. (2010) *J. Therm. Anal. Calorim.*, 100: 501.

[431]   Dörfler, H.-D.; Pietschmann, N. (1990) *Coll. Poly. Sci.*, 268: 559.

[432]   Filipivic-Vincekovic, N.; Bujan, M.; Smit, I.; Tusek-Bozic, L.; Stephanic, I. (1998) *J. Coll. Interface Sci.*, 201: 59.

VII. Appendix

VII. Appendix

VII.1 Scientific Contributions

Poster Presentations:

W. Kunz, E. Maurer, M. Kellermeier, R. Klein, S. Thomaier, O. Zech: *From Ionics to Non-ionics*; **ECIS** Geneva 2007

E. Maurer, M. Kellermeier, R. Klein, S. Thomaier, O. Zech, W. Kunz: *From Ionics to Non-ionics*; **Formula V** Potsdam 2007

E. Maurer, R. Klein, M. Kellermeier, O. Zech, S. Thomaier, W. Kunz: *Liquid Ion Pair Amphiphiles*; **Liquid Matter Conference** Lund 2008

E. Maurer, O. Zech, D. Touraud, J. Heilmann, W. Kunz: *Selfassembling Ionic Liquids – Not really a "Green" Alternative*; **Green Chemistry** Munich 2008

E. Maurer, R. Klein, M. Kellermeier, O. Zech, W. Kunz: *Liquid Ion Pair Amphiphiles (LIPAs)*; **COIL** Cairns 2009

E. Maurer, R. Klein, M. Kellermeier, O. Zech, W. Kunz: *Liquid Ion Pair Amphiphiles (LIPAs)*; **ECIS** Antalya 2009

Oral Contributions:

E. Maurer: Complexation – A Concept to Ionic Liquid Like Surfactants; **SEPAWA** Würzburg 2008

E. Maurer: Liquid Ion Pair Amphiphiles – Catanionics / Ionic Liquids; **Zsigmondy Colloquium** Bayreuth 2009

Eva Maurer, Regina Klein, and <u>Werner Kunz:</u> *New ways towards low toxic and even liquid catanionics*; **Formula VI** Stockholm 2010

Confidential Reports:

E. Maurer: Synthese und physikochemische Charakterisierung von Cholinester- und Cholinethertensiden; **Novatis** 2009

E. Maurer: Physicochemical Characterisation of Cationic/Non-ionic Surfactants and Hydrotropes Based on a New TAMINCO Building-Block (Diquats); **TAMINCO** 2010

E. Maurer: Alkylethercarboxylate Based Ionic Liquids; **Kao Chemicals** 2010

Publications:

O. Zech, M. Kellermeier, S. Thomaier, E. Maurer, R. Klein, C. Schreiner, W. Kunz: Alkali Oligoether Carboxylates – A New Class of Ionic Liquids; (2009) *Chemistry a European Journal*; 15; 6; 1341.

Klaus, G. J. T. Tiddy, R. Rachel, A. P. Trinh, E. Maurer, D. Touraud, W. Kunz, *Hydrotrope Induced Inversion of Salt Effects on the Cloud Point of an Extended Surfactant*, (2010) Langmuir, submitted.

Klaus, G. J. T. Tiddy, I. Grillo, M. Tomsic, H. Garcia, A. Harrar, E. Maurer, D. Touraud, W. Kunz, *Solubility of High Amounts of Triglycerides in Water Using an Extended Surfactant*, (2010) Langmuir, submitted.

Regina Klein, Eva Maurer, Birgit Kraus, Gabriele Brunner, Boris Estrine, Didier Touraud, Joerg Heilmann and Werner Kunz, *Biodegradability and*

cytotoxicty on human cell lines of choline carboxylate surfactants compared to simple soaps (2010) Green Chemistry, submitted.

Regina Klein, Gordon J. T. Tiddy, Eva Maurer, Didier Touraud, Jordi Esquena, Olivier Taché, Werner Kunz, *Aqueous Phase Behaviour of Choline Carboxylate Surfactants – Exceptional Variety and Extent of Cubic Phases*, (2010), J. Phys. Chem., submitted.

Regina Klein, Oliver Zech, Eva Maurer, Matthias Kellermeier, Werner Kunz, *Quaternary Ammonium Oligoether Carboxylates – Room-Temperature Ionic Liquids*, (2011), submitted.

Eva Maurer, Angelika Klaus, Werner Kunz, *Lidocaine Carboxylates – A New Class of Pharmaceutically Active, Surfactant-Like Ionic Liquids,* in preparation.

Eva Maurer, Oliver Zech, Regina Klein, J. Heilmann, Werner Kunz, *New, Cationic Surfactant-Like Ionic Liquids with Oligoether Carboxylate Counterions – Physico-Chemical Properties in Pure Form and Binary Mixtures wit Water,* in preparation.

Eva Maurer, M. Drechsler, Regina Klein, Didier Touraud, J. Heilmann, Werner Kunz, *Physico-Chemical and Toxicological Properties of Novel Choline- and Ectoine-Based Cationic Surfactants and Spontaneously Formed Low-Toxic Vesicles Thereof,* in preparation.

Eva Maurer, Agnes Harrar, Werner Kunz, *Evaluation of Novel, Low Toxic, True Catanionics as Emulsion Stabilizing Agents,* in preparation.

Eva Maurer, H. Denzer, H. Bender, Werner Kunz, *Physico-Chemical Properties of Longchain Alkylether Carboxylate Based Ionic Liquids,* in preparation.

Eva Maurer, H. Denzer, H. Bender, Werner Kunz, *Industrially Relevant Physico-Chemical Properties of Longchain Alkylether Carboxylate Based Surfactants,* in preparation.

Patents:

Werner Kunz, Stefan Thomaier, Eva Maurer, Oliver Zech, Matthias Kellermeier, and Regina Klein, **Onium salts of carboxyalkyl-terminated polyoxyalkylenes for use as high-polar solvents and electrolytes.** PCT Int. Appl. (2008), 19pp. CODEN: PIXXD2 WO 2008135482 A2 20081113.

Kunz Werner, Kellermeier Matthias, Klein Regina, Maurer Eva, Touraud Didier, **Biologically acceptable choline compounds and their use as tensides.** Eur. Pat. Appl. (2010), 10pp. CODEN: EPXXDW EP 2216326 A2 20100811 CAN 153:317887 AN 2010:992673.

VII.2 List of Figures

VII.3 List of Tables

VII.4 Data of Analysis

VII.4.1   Chapter IV.2

2-(2-(dodecyloxy)ethoxy)ethanol

δ *^{1}H-NMR* (300 MHz, CDCl3): 0.8 ppm (t, 3H), 1.2 ppm (s, 18H), 1.5 ppm (m, 2H), 3.0 ppm (s, 1H), 3.4 ppm (t, 2H), 3.5 – 3.7 ppm (m, 8H)

m/z (+c) ESI-Q1MS: 274.3 (80%, MH$^+$), 292.4 (100%, MNH4$^+$)

2-(2-(2-(dodecyloxy)ethoxy)ethoxy)acetic acid (C12EO2COOH)

δ *^{1}H-NMR* (300 MHz, CDCl3): 0.8 ppm (t, 3H), 1.2 ppm (s, 18H), 1.5 ppm (m, 2H), 3.4 ppm (t, 2H), 3.6 – 3.8 ppm (m, 8H), 4.2 (s, 2H)

m/z (+c) ESI-Q1MS: 274.3 (80%, MH$^+$), 292.4 (100%, MNH4$^+$)

3,6,9,12-tetraoxatetracosan-1-ol

δ *^{1}H-NMR* (300 MHz, CDCl3): 0.8 ppm (t, 3H), 1.2 ppm (s, 18H), 1.5 ppm (m, 2H), 3.0 ppm (s, 1H), 3.4 ppm (t, 2H), 3.5 – 3.7 ppm (m, 16H)

m/z (+c) ESI-Q1MS: 363.5 (80%, MH$^+$), 381.7 (100%, MNH4$^+$)

3,6,9,12,15-pentaoxaheptacosan-1-oic acid (C12EO4COOH)

δ ^{1}H-NMR (300 MHz, CDCl3): 0.8 ppm (t, 3H), 1.2 ppm (s, 18H), 1.5 ppm (m, 2H), 3.4 ppm (t, 2H), 3.6 – 3.8 ppm (m, 16H), 4.2 (s, 2H)

m/z (+c) ESI-Q1MS: 421.1 (80%, MH$^+$), 438.2 (100%, MNH4$^+$)

VII.4.2   Chapter IV.3

2,5,8,11-Tetraoxatridecan-13-oic acid (TOTOA)

δ ^{1}H-NMR (300 MHz, CDCl3): 3.3 ppm (t, 3H), 3.5 – 3.6 ppm (m, 12H), 4.1 (s, 2H), 9.82 ppm (s, 1H)

m/z (+p) ES-MS (H_2O / MeOH, NH$_4$Ac): 102.9 (21 %), 176.8 (12 %), 222.9 (57 %), 240,0 (100 %); m/z (-p):221.0 (100%), 443.2 (10%), 476.2 (100%)

Elemental analysis: 47.56% C, 8.39% H

VII.4.3   Chapter IV.4

2-(Dodecanoyloxy)-N,N,N-trimethylethanaminium methylsulfonate (C12OOCh MeSulf)

δ ^{1}H-NMR (300 MHz, CDCl3): 0.8 ppm (t, 3H), 1.2 ppm (s, 18H), 1.5 ppm (m, 2H), 2.3 ppm (t, 2H), 2.8 ppm (s, 3H), 3.3 ppm (s, 9H), 3.8 ppm (t, 2H), 4.5 ppm (t, 2H)

m/z (+p) ES-MS (MeCN, H_2O): 286.1 (100%); m/z (-p):95.1 (75%), 199 (50%), 476.2 (100%)

Elemental analysis: 56.1% C, 10.9% H

2-(Tetradecanoyloxy)-N,N,N-trimethylethanaminium methylsulfonate (C14OOCh MeSulf)

δ^1H-NMR (300 MHz, CDCl3): 0.8 ppm (t, 3H), 1.2 ppm (s, 22H), 1.5 ppm (m, 2H), 2.3 ppm (t, 2H), 2.8 ppm (s, 3H), 3.3 ppm (s, 9H), 3.8 ppm (t, 2H), 4.5 ppm (t, 2H)

m/z (+p) ES-MS (MeCN, H_2O): 314.3 (100%); *m/z (-p)*:95.1 (73%), 199 (51%), 476.2 (100%)

Elemental analysis: 72.0% C, 13.1% H

2-(Hexadecanoyloxy)-N,N,N-trimethylethanaminium methylsulfonate (C16OOCh MeSulf)

δ^1H-NMR (300 MHz, CDCl3): 0.8 ppm (t, 3H), 1.2 ppm (s, 26H), 1.5 ppm (m, 2H), 2.3 ppm (t, 2H), 2.8 ppm (s, 3H), 3.3 ppm (s, 9H), 3.8 ppm (t, 2H), 4.5 ppm (t, 2H)

m/z (+p) ES-MS (MeCN, H_2O): 342.1 (100%)

Elemental analysis: 60.0% C, 11.1% H

2-(Dodecanoyloxy)-N,N,N-trimethylethanaminiumiodide (C12OOCh I)

δ^1H-NMR (300 MHz, CDCl3): 0.8 ppm (t, 3H), 1.2 ppm (s, 18H), 1.5 ppm (m, 2H), 2.3 ppm (t, 2H), 3.3 ppm (s, 9H), 3.8 ppm (t, 2H), 4.5 ppm (t, 2H)

m/z (+p) ES-MS (MeCN, H_2O): 286.1 (100%); *m/z (-p)*: 129.6 (100%), 199 (11 %), 380.6 (30%), 540 (27%)

Elemental analysis: 49.3% C, 9.3% H

2-(Dodecyloxy)-N,N,N-trimethylethanaminium iodide (C12OCh I)

δ^{1}H-NMR (300 MHz, CDCl3): 0.8 ppm (t, 3H), 1.2 ppm (m, 18H), 1.7 ppm (m, 2H), 1.9 ppm (m, 2H), 3.3 ppm (m, 11H), 3.9 ppm (t, 2H)

m/z (+p) ES-MS (MeCN, H$_2$O): 272.2 (100%); ***m/z (-p)***: 129.6 (100%), 380.6 (36%), 526.1 (33%)

Elemental analysis: 50.9% C, 9.9% H

2-(Dodecyloxy)-N,N,N-trimethylethanaminium iodide (C12OCh I)

δ^{1}H-NMR (300 MHz, CDCl3): 0.8 ppm (t, 3H), 1.2 ppm (m, 18H), 1.6 ppm (m, 2H), 2.0 ppm (m, 2H), 2.8 ppm (s, 3), 3.3 ppm (m, 9H), 3.6 ppm (t, 2H), 3.9 ppm (t, 2H)

m/z (+p) ES-MS (MeCN, H$_2$O): 272.2 (100%)

Elemental analysis: 58.0% C, 11.4% H

4-(Decyloxycarbonyl)-2-methyl-3,4,5,6-tetrahydropyrimidin-1-ium chloride (Ecto C10)

δ^{1}H-NMR (300 MHz, CDCl3): 0.8 ppm (t, 3H), 1.2 ppm (s, 14H), 1.6 ppm (m, 2H), 2.1 ppm (m, 2H), 2.4 ppm (s, 3H), 3.2 ppm (m, 1H), 3.5 ppm (t, 1H), 4.0 ppm (t, 1H), 4.1 ppm (m, 2H), 4.3 ppm (m, 2H), 9.3 ppm (s, 1H), 9.7 ppm (s, 1H)

m/z (+p) ES-MS (MeCN, H$_2$O): 283.2 (100%)

Elemental analysis: 60.7% C, 9.7% H

4-(Dodecyloxycarbonyl)-2-methyl-3,4,5,6-tetrahydropyrimidin-1-ium chloride (Ecto C12)

$\delta\,^{1}$*H-NMR* (300 MHz, CDCl3): 0.8 ppm (t, 3H), 1.2 ppm (s, 18H), 1.6 ppm (m, 2H), 2.1 ppm (m, 2H), 2.4 ppm (s, 3), 3.2 ppm (m, 1H), 3.5 ppm (t, 1H), 4.0 ppm (t, 1H), 4.1 ppm (m, 2H), 4.3 ppm (m, 2H), 9.3 ppm (s, 1H), 9.7 ppm (s, 1H)

m/z (+p) ES-MS (MeCN, H_2O): 311.1 (100%)

Elemental analysis: 62.0% C, 10.5% H

4-(Tetradecyloxycarbonyl)-2-methyl-3,4,5,6-tetrahydropyrimidin-1-ium chloride (Ecto C14)

$\delta\,^{1}$*H-NMR* (300 MHz, CDCl3): 0.8 ppm (t, 3H), 1.2 ppm (s, 22H), 1.6 ppm (m, 2H), 2.1 ppm (m, 2H), 2.4 ppm (s, 3), 3.2 ppm (m, 1H), 3.5 ppm (t, 1H), 4.0 ppm (t, 1H), 4.1 ppm (m, 2H), 4.3 ppm (m, 2H), 9.3 ppm (s, 1H), 9.7 ppm (s, 1H)

m/z (+p) ES-MS (MeCN, H_2O): 339.2 (100%)

Elemental analysis: 65.5% C, 11.3% H

4-(Dodecyloxycarbonyl)-2-methyl-3,4,5,6-tetrahydropyrimidin-1-ium methylsulfonate (Ecto C12 Mesulf)

$\delta\,^{1}$*H-NMR* (300 MHz, CDCl3): 0.8 ppm (t, 3H), 1.2 ppm (s, 22H), 1.6 ppm (m, 2H), 2.1 ppm (m, 2H), 2.4 ppm (s, 3), 2.7 (s, 3H), 3.2 ppm (m, 1H), 3.5 ppm (t, 1H), 4.0 ppm (t, 1H), 4.1 ppm (m, 2H), 4.3 ppm (m, 2H), 9.9 ppm (s, 2H)

m/z (+p) ES-MS (MeCN, H_2O): 311.1 (100%); *m/z (-p)*: 94.8 (43%), 501.2 (100%)

Elemental analysis: 65.5% C, 11.3% H

VII.4.4   Chapter IV.5

2-(Dodecanoyloxy)-N,N,N-trimethylethanaminium   dodecanoate (C12C12)

δ *^{1}H-NMR* (300 MHz, CDCl3): 0.8 ppm (t, 6H), 1.2 ppm (s, 32H), 1.6 ppm (m, 4H), 2.3 ppm (m, 4H), 3.5 ppm (s, 9H), 4.1 ppm (2H), 4.5 ppm (2H)

m/z (+c) ESI-Q1MS: 286.1 (100%)

2-(Tetradecanoyloxy)-N,N,N-trimethylethanaminium tetradecanoate (C14C14)

δ *^{1}H-NMR* (300 MHz, CDCl3): 0.8 ppm (t, 6H), 1.2 ppm (s, 36H), 1.6 ppm (m, 4H), 2.3 ppm (m, 4H), 3.5 ppm (s, 9H), 4.1 ppm (2H), 4.5 ppm (2H)

m/z (+c) ESI-Q1MS: 314.7 (100%)

2-(Hexadecanoyloxy)-N,N,N-trimethylethanaminium hexadecanoate (C16C16)

δ *^{1}H-NMR* (300 MHz, CDCl3): 0.8 ppm (t, 6H), 1.2 ppm (s, 40H), 1.6 ppm (m, 4H), 2.3 ppm (m, 4H), 3.5 ppm (s, 9H), 4.1 ppm (2H), 4.5 ppm (2H)

m/z (+c) ESI-Q1MS: 342.2 (100%)

VII.5 Declaration

Herewith I declare that I have made this existing work single-handedly. I have used nothing but the stated utilities.

Regensburg, February 2011-02-28

_____

Eva Maurer